The B cell response to Plasmodium chabaudi chabaudi malaria in the mouse model

Thesis

UNRESTRICTED

The B cell response to *Plasmodium chabaudi chabaudi* malaria in the mouse model

submitted by

Ariel H. Achtman

Dipl. rer. nat.

August 2003

for the degree

Doctor of Philosophy

Division of Parasitology
National Institute for Medical Research
The Ridgeway, Mill Hill
London NW7 1AA
United Kingdom

Submission date: 11 August 2003
Award date: 19 January 2004

Abstract

This thesis characterises the B cell response of C57BL/6 mice after infection with *Plasmodium chabaudi chabaudi* (AS) with regard to plasma cell longevity, B cell memory and the specific response to part of the merozoite surface protein-1 (MSP-1_{21}), an antigen involved in protection against malaria. Infected spleens showed massive but reversible disruption of the white pulp architecture around the peak of infection. Nevertheless, strong plasma cell and germinal centre responses were detected along with atypical plasma cell location and apparent involvement of marginal zone B cells. The MSP-1_{21}-specific B cell response to primary infection did not display any obvious abnormalities at the cellular level. The longevity of protection was assessed in the presence and absence of parasites. *P. c. chabaudi* parasites persisted for 2-3 months after infection. A single infection mediated protection in form of reduced parasitaemias for up to 9 months. When mice were reinfected after 2.5 months but not later, the presence of parasites from the primary infection led to an additional reduction. This can be attributed to cooperation between effector and memory cells.

MSP-1_{21}-specific IgG levels were measured in primary and secondary infections and during the intervening period. Plasma levels of IgG against MSP-1_{21} and crude malarial extract drop significantly between 1 and 2.5 months post infection and then remain constant, suggesting that *Plasmodium*-specific plasma IgG levels are maintained by long-lived plasma cells independent of parasite presence or absence after day 30. However, MSP-1_{21}-specific memory B cell generation, maintenance or reactivation appears to be reduced in the presence of parasites albeit with increased affinity maturation. Primary and secondary antibody responses to MSP-1_{21} develop more slowly than antibody responses observed in other infections, suggesting that despite the strong B cell response during primary infection with malaria, there is an impairment of the B cell response at some level.

I wish to acknowledge the following people for allowing me to include data from shared experiments in my thesis:

Dr. Jean Langhorne for counting the parasitaemias shown in Fig. 5.2b.

Dr. Robin Stephens for performing and analysing some of the ELISA measurements shown in Fig. 6.2 and 6.3.

Emma Cadman for counting the parasitaemias shown in Fig. 5.2c and for the majority of the data shown in Table 5.2.

Acknowledgements

I would like to thank my supervisor, Dr. Jean Langhorne, for her time, advice and choice of an intriguing project. I found our discussions and brainstorming sessions very stimulating and feel that I could not have found a better supervisor for my PhD. I would also like to thank my second supervisor, Dr. Brigitta Stockinger, for her time and suggestions. All the members of my own laboratory have been of assistance in practical and theoretical matters and have helped to make the Langhorne lab a fun place to work: Dr. Ching Li deserves my deepest gratitude for her generous practical assistance and unflagging good cheer, which made the long hours in Laidlaw Yellow pass more quickly. I also appreciate the time Drs. Robin Stephens, Meike Hensmann and Latifu Sanni have spent batting ideas and data interpretations around with me. I am obliged to Dr. Stuart Quin, Dr. Elsa Seixas, Luis Fonseca, Dr. Catherine Allsopp and Dr. Pearline Benjamin for introducing me to new parasitological and immunological methods when I first started in the lab. I appreciate the help that Cecilia Waller, Jane Blythe, Dr. Frank Albano, Dr. Deirdre Cunningham and Sandra Körnig have given me on numerous occasions to manage the temporal complications created by long-term experiments. I would also like to thank Vicky Harrison, Emma Cadman and Dr. Anne-Marit Sponaas for their assistance with my monster affinity ELISAs at the end of the thesis. In that vein, I would like to tender my thanks to Dr. Jean Langhorne and Emma Cadman for counting the parasitaemias of some of my endless numbers of thin blood smears. I am also grateful to Drs. Jean Langhorne, Ching Li, Robin Stephens, Bill Jarra and Meike Hensmann for reading parts of this thesis and making comments.

Furthermore, I owe a lot to Prof. Ian MacLennan at the Medical School of the University of Birmingham for allowing me to work in his laboratory for 2 months to learn the cryosectioning and immunohistology techniques. I also value highly his continuing

support long after my visit had finished. All members of his laboratory were extremely accomodating and I would particularly like to thank Mahmood Khan for technical assistance and Dr. Kai Toellner for discussions and keeping the lines of communication open. At the Deutsches Rheumaforschungszentrum in Berlin, Dr. Rudi Manz and Anja Hauser helped me address the problems involved in plasma cell detection.

Back at the National Institute for Medical Research, Drs. Mike Blackman and Tony Holder of Parasitology have given me advice on protein purification and I made frequent use of Dr. Bill Jarra's impressive pool of knowledge of all aspects of malaria. I would also like to thank Dr. Jeff Babon for taking the gel filtration column off my hands when I couldn't stand the sight of it anymore. I have profited from practical advice offered by various members of the Division of Protein Structure and Dr. Ian Harrigan in Histology. I spent a lot of time chewing the fat with members of Rose Zamoyska's, Gitta Stockinger's and Anne O'Garra's laboratories and usually returned to my own floor with useful pointers or the odd reagent. Dr. Alexandre Potocnik was very generous with his time and advice on issues of haematopoesis. On a more practical note, I would like to thank the staff of Biological Services for the day-to-day care of my experimental animals.

I am deeply indebted to Hannah Polson and Sandra Körnig for supplying me with a bed on the many nights where another 45 minutes on the bicycle and the same journey back the next morning would have been unbearable. At the same time, I would like to thank Stuart Lucas for using his courtly manner and tabletop football skills to lighten long days and to the climbing crew for giving me a reason to leave work and occupy my mind with something totally different. Last but not least, I am very grateful to my family and Philipp for their patience and emotional support.

Table of Contents

Abbreviations

α-NE	α-napthyl acetate esterase
7-AAD	7-aminoactinomycin D
aa	amino acid
Ab	antibody
Ag	antigen
AI	affinity index
AP	alkaline phosphatase
APC	allophycocyanin
AMA-1	apical merozoite antigen-1
BCA	bicinchinonic acid
BCR	B cell receptor
BrdU	bromodeoxyuridine
BSA	bovine serum albumin
CD	cluster of determination
CD40L	CD40 ligand
CGG	chicken gamma globulin
d	day
DAB	diaminobenzidine tetrahydrochloride
E. coli	*Escherichia coli*
EDTA	ethylene diamine tetraacetate
EGF	epidermal growth factor
ELISA	enzyme-linked immunosorbent assay
ep	erythroid precursors
FACS	fluorescence-activated cell sorting
Fc	constant component immunoglobulin
FcR	receptor for the Fc component
FCS	foetal calf serum
FITC	fluorescein isothiocyanate
FSC	forward scatter

GC	germinal centre
GPI	glycosylphosphatidylinositol
H&E	haematoxylin and eosin
His	six histidine tag
HRP	horse radish peroxidase
i.p.	intraperitoneal
IFN-γ	interferon-γ
Ig	immunoglobulin
IL	interleukin
IPTG	isopropyl-β-D-thiogalactopyranoside
iso.con.	isotype control
kDa	kilodalton
KLH	kehyhole limpet cyanine
LPS	lipopolysaccharide
LT- α	lymphotoxin-α
MBP	maltose binding protein
Meg	megakaryoycte
MHC	major histocompatibility complex
MSP-1	merozoite surface protein-1
$MSP\text{-}1_{19}$	C-terminal fragment of *P. falciparum* MSP-1
$MSP\text{-}1_{21}$	C-terminal fragment of *Pc. chabaudi* MSP-1
MZ	marginal zone
NP	normal plasma
OD	optical density
p	probability
P.	*Plasmodium*
P. c. chabaudi	*Plasmodium chabaudi chabaudi*
PALS	periarteriolar lymphatic sheath
PBS	phosphate-buffered saline
PE	phycoerythrin
PfEMP-1	*P. falciparum* erythrocyte membrane protein-1

PI	propidium iodide
PNA	peanut agglutinin
PNPP	nitrophenylphospate-sodium salt
pRBC	parasitised red blood cells
RAG-2	recombination activation gene-2
RAP1	rhoptry associated protein 1
RBC	red blood cells
RESA	ring-infected erythrocyte surface antigen
rpm	rounds per minute
SCID	severe combined immunodeficiency
SDS	sodium dodecyl sulphate
SDS-PAGE	sodium dodecyl sulphate polyacrylamide gel electrophoresis
SEM	standard error of the mean
SPF	specific pathogen free
TBS	Tris-HCl-buffered saline
TCR	T cell receptor
TI	Thymus independent
TNF-α	tumour necrosis factor-α
TUNEL	TdT-mediated dUTP-biotin nick end-labeling

1 Introduction

1.1 The relevance of malaria for immunological studies

Malaria is a major health issue in much of the developing world and because of increased tourism and global warming it is also becoming more important to inhabitants of other countries. Insecticide- and medication-based eradication campaigns have been successful in some parts of the world, but frequently, these efforts have only controlled the level of infections temporarily. In parallel, parasite resistance to anti-malarial drugs is on the rise and can complicate treatment. Despite detailed knowledge of the transmission mode and life cycle of the parasite, no vaccine against malaria has been developed yet. Most of the effective vaccines in existence are against diseases like measles to which survivors acquire long-term immunity after one encounter or diseases which would naturally progress so rapidly that death occurs before natural immunity can develop, e.g. tetanus. By contrast, malaria is contracted repeatedly and parasitaemia can persist over long periods of time. This indicates that vaccine design is not a simple case of pre-exposure to a single parasite protein. Therefore, it is very important to understand precisely how the parasite interacts with the host's immune system in order to create an effective vaccine.

Malaria is also an intriguing object of study from an immunological point of view. Many of the basic concepts in immunology have been established by studying the immune response to non-replicating antigens. However, important aspects of the immune system, such as the link between the innate and adaptive branches of the immune system or the existence of long-lived antibody-producing cells, were discovered by studying the immune response to replicating pathogens. Infections differ from immunisations in the kinetics, location and immunological context of antigenic exposure with a much higher possibility of synergy or antagonism between different branches of the immune system. The immune response to malaria is of particular interest because of the exposure of the host to very

high doses of antigen followed by diminished but chronic parasitaemia. In addition, the parasites evolved a number of immune evasion mechanisms in their adaptation to the host and careful analysis of these processes is likely to reveal strengths and weaknesses in immune responses.

1.2 Background on malaria

1.2.1 The *Plasmodium* parasite

Malaria is caused by protozoans of the subgenus *Plasmodium*, which belong to the family Plasmodiidae and the order Apicomplexa. The species which occur naturally in humans and those adapted to laboratory mice are listed in Table 1.1. *Plasmodium* is an obligatory parasite requiring two hosts. Species of *Plasmodium* are closely adapted to particular hosts with mammals, avians and reptiles serving as the vertebrate hosts. The invertebrate host must belong to either the *Anopheles* or *Culex* genus of mosquitos, with *Culex* restricted as a vector of avian malarias. Asexual reproduction occurs in the vertebrate host in two stages and sexual reproduction in the mosquito host. An overview of the *Plasmodium* life cycle is given in Fig. 1.1, with the emphasis on the stages in the vertebrate host. A detailed review can be found in (Garnham, 1988). The mosquito injects saliva containing a small number of sporozoites into the vertebrate host. The sporozoites travel quickly from the injection site to the liver via the blood stream. They initiate the hepatocytic (also known as the pre-erythrocytic or exo-erythrocytic) stage of the life cycle by invading hepatocytes where they develop into hepatic trophozoites. Nuclear division creates a hepatic schizont containing thousands of merozoites which are released into the blood stream by hepatocyte rupture. In most *Plasmodium* species, the hepatocytic stage takes place only once in each infection, but in *P. vivax*, *P. ovale* and the simian parasite *P. knowlesi* the parasite can persist in the liver in form of hypnozoites.

Table 1.1 Different *Plasmodium* species

Species	**Other designations**	**Host**
P. falciparum	malignant tertian, subtertian, aesotivo-autumnal, tropical, pernicious	Man
P. vivax	benign tertian, simple tertian, tertian	Man
P. ovale	ovale tertian	Man
P. malariae	quartan	Mouse
P. chabaudi		Mouse
P. yoelii		Mouse
P. berghei	*P. yoelii berghei*	Mouse
P. vinckei		Mouse

Table 1.2 Species-specific characteristics of the life cycle of parasites with human and mouse hosts

	Exo-erythrocytic stage		**Erythrocytic stage**		
Parasite species	Duration of cycle	Number of merozoites / schizont	Duration of one cycle	Number of merozoites / schizont	Preferred type of invaded erythrocyte
P. falciparum	5.5-6 days	40 000	48 h	8-24	all
P. malariae	13 days	2000	72 h	8-12	mature
P. ovale	9 days	15 000	49-50 h	16	reticulocytes
P. vivax	8 days	> 10 000	48 h	12-18	reticulocytes
P. berghei	50 h	4000-20 000	24	8-18	reticulocytes
P. chabaudi	53-58 h		24 h	4-10	mature
P. vinckei	60-68 h		24 h	6-12	mature
P. yoelii	50 h		24 h	12-18	reticulocytes

This table was adapted from (Li, 1999).

Figure 1.1 The *Plasmodium* life cycle

Adapted from (Godson, 1985) by Dr. Jean Langhorne.

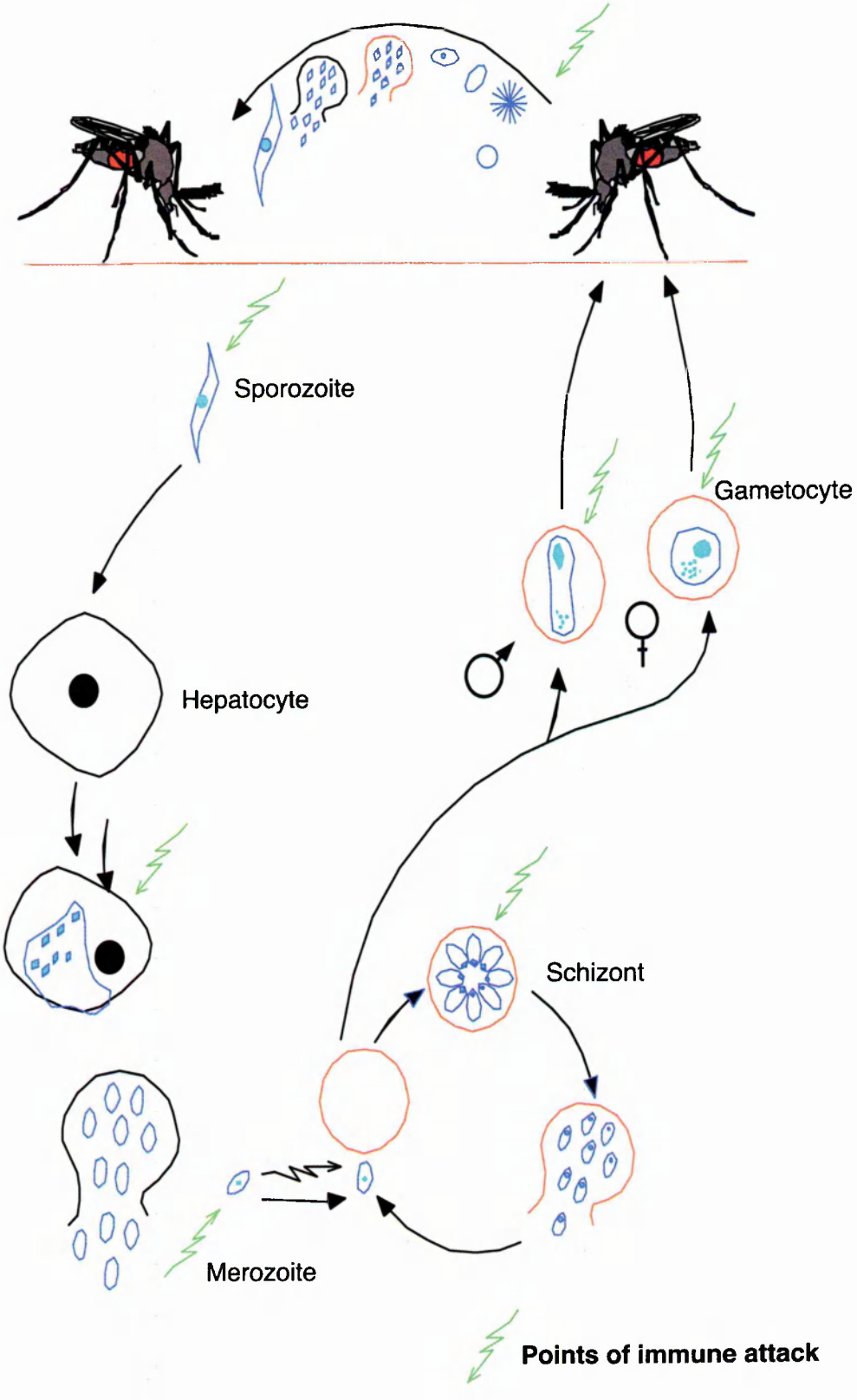
Sporozoite
Hepatocyte
Gametocyte
Schizont
Merozoite
Points of immune attack

The merozoites from liver schizonts initiate the erythrocytic stage of the parasite life cycle, which then repeats itself every 24-72 h, dependent on the parasite species, and is responsible for all of the symptoms of malaria. Merozoites invade erythrocytes rapidly and are enclosed by a parasitophorous vacuole formed by the erthrocyte outer membrane. The parasites develop through the ring stage, trophozoite and schizont stages. Mature schizonts cause the erythrocytes to rupture and release between 6 and 24 merozoites, depending on the species of parasite, for reinvasion of new erythrocytes. This cycle of erythrocytic schizogony is repeated until the increasing parasitaemia is controlled by immune mechanisms or chemotherapy. After a minimum of two erythrocytic schizogony cycles (in most species), some merozoites differentiate into sexual forms, the female macrogametocyte and the male microgametocyte. Gametocytes are taken up by mosquitoes with the blood meal and undergo sporogony in this host: In the midgut, the gametocytes differentiate into macro- and microgametes which combine to zygotes. The zygotes transform into motile ookinetes, which penetrate the midgut epithelium and there form oocysts. The oocysts undergo nuclear division into as many as 10 000 sporozoites. The sporozoites travel to the mosquito's salivary gland and are finally transmitted to a new vertebrate host.

This life cycle is common to the nearly 200 different species of *Plasmodium*. Individual characteristics of the life cycles for the species infecting humans and mice are illustrated in Table 1.2. As mentioned earlier, *P. vivax and P. ovale* possess a unique life stage not shared by the other human malaria parasites, where parasites can survive in the liver as hypnozoites for periods of up to 5 years before initiating blood stage infections. These renewed manifestations of infection arising from the survival of hypnozoites are called relapses whereas the reemergence of infection from low levels of surviving erythrocytic parasites is called a recrudescence.

1.2.2 Malaria disease in humans

There are four *Plasmodium* species which cause malaria in humans: *P. vivax*, *P. ovale*, *P. malariae* and *P. falciparum*. Occasional episodes of zoonosis occur with species which normally infect monkeys, but these are uncommon. Malaria is widespread in Africa, South-East Asia and South America, with about 40% of the world's population at risk. The *Plasmodium* parasite caused an estimated 856 000 deaths in 1990 (Murray and Lopez, 1997) and is generally assumed to cause 100-200 million infections annually. This makes malaria the largest health problem caused by a single infectious agent, with the possible exception of tuberculosis. Most of the deaths occur in children up to 5 years of age, with pregnant women, immigrants to endemic areas and travellers representing further high risk groups. Malaria is typically accompanied by periodic fevers elicited by erythroctye rupture. Further symptoms include severe anaemia and cerebral malaria (the main causes of death), pulmonary oedema, renal complications from deposited immune complexes, hypoglycaemia, thrombocytopenia, splenomegaly, hepatomegaly, renal damage and immunodepression.

Plasmodium parasites and their hosts have adapted to each other over the long course of their co-existence. Selective pressure has led to high prevalence of a number of genetic factors offering partial protection in malaria-endemic areas. Frequently, these are erythrocytic defects which are lethal or disadvantageous to the host in their homozygous form, whereas the heterozygous form offers a degree of protection against malaria. These include sickle cell anaemia, thallassaemias and glucose-6-phosphate dehydrogenase deficiency. Less detrimental adaptations include resistance *to P. vivax* infection due to a lack of Duffy blood group antigen on erythrocytes and biased occurence of certain major histocompatibility complex (MHC) genotypes which results in a more effective immune response against the parasite (reviewed in (Miller, 1988; Riley, 1996)).

1.2.3 Malaria distribution patterns

The terminology describing the epidemiology of malaria is somewhat complex, as several different factors need to be considered. Endemic areas are defined as regions where there is a measurable incidence both of cases and of natural transmission over a succession of years. Endemicity is further divided into four categories proposed by the World Health Organisation (WHO): holoendemic, mesoendemic, hyperendemic and hypoendemic. Table 1.3 outlines two standard ways of defining these categories. In general, the level of endemicity decreases with increasing latitudes and malaria epidemics occur chiefly at the borders of the endemic distribution range. Malaria distribution is further differentiated into perennial and seasonal transmission and often referred to as stable or unstable, depending on the resistance of the situation to change. Endemicity must be established individually for each species. A further way of characterising the situation is to measure the number of infective mosquito bites experienced during a particular time period, usually a year (reviewed in (Molineaux *et al.*, 1988)).

Table 1.3 Definitions of malaria endemicity [a)]

Degree of endemicity	**Definition by spleen rate**	**Definition by parasite rate**
Hypoendemic	0-10% in children of 2-9 years	as a rule < 10% in children of 2-9 years; may be higher during part of the year
Mesoendemic	11-50% in children of 2-9 years	as a rule 11-50% in children of 2-9 years; may be higher during part of the year
Hyperendemic	constantly over 50% in children of 2-9 years, adult spleen rate also high	constantly over 50 %
Holoendemic	constantly over 75% in children of 2-9 years, adult spleen rate low, adult tolerance high	constantly over 75% in infants, spleen rate high (New Guinea type) or low (African type); parasite density declining rapidly between 2nd and 5th year of life and then more slowly

a) Definitions are standard definitions as outlined in (Molineaux *et al.*, 1988).

1.2.4 Animal models for malaria

1.2.4.1 Rodent models

Four species of *Plasmodium* which were isolated from the African thicket rat *Thamnomys rutilans* are capable of infecting mice and rats. The well characterised immune system of the mouse along with the availability of different strains with defined genetic defects make the mouse the preferred animal model for most studies. It is necessary to choose the appropriate parasite species on the basis of similarities to the life cycle of the human parasites. Genetic similarity is not a useful criterion, as all of the *Plasmodium* species diverged in the range of tens of millions to hundreds of millions years ago, making even the human species genetically very diverse (reviewed in (Ayala *et al.*, 1998)). *P. chabaudi chabaudi* is considered a good model for *P. falciparum*, because these species share a preference for mature red blood cells, antigenic variation (del Portillo *et al.*, 2001; McLean *et al.*, 1982) and parasite sequestration (Cox *et al.*, 1987; Gilks *et al.*, 1990). Synchronicity of the blood stage and maturation of gametocytes late in infection make it easier to pinpoint the parasite stage responsible for any identified phenomena. The typical pattern of *P. chabaudi chabaudi* parasitaemia, consisting of exponential multiplication followed by strong reduction and a brief low recrudescence, can be observed in the wild-type curve shown in Fig. 1.2.

The other three species of rodent malaria are used for models with a different focus. Different strains of *P. berghei* are used to model cerebral malaria and anaemia. *P. yoelii* has adapted *in vitro* into clearly defined lethal and nonlethal strains and is therefore useful for questions centring on the virulence of the parasite. The lethal strains are also preferred for vaccine studies as animal survival can be defined as a measure of protection. A number of the earlier studies in rats, especially chemotherapy studies, were performed with *P. vinckei*, but this species is not commonly used anymore (reviewed in (Langhorne *et al.*, 2002; Li *et al.*, 2001).

The mouse strain is also important for the course of infection, with the same strain of *Plasmodium* causing different outcomes of infection in different strains of mice. For the long-term studies of B cell responses in this thesis, the C57BL/6 strain of mice is most suitable, because mice are fairly resistant to *P. chabaudi* infection and therefore usually survive for the duration of the experiments. In addition, many genetically deficient mice are available on the C57BL/6 background, making it easy to test assumptions in other systems afterwards and a lot of data has been published with mice from this genetic background.

1.2.4.2 Simian models

There are 20 species of *Plasmodium* which infect lemurs, monkeys and higher apes and the four species of human malaria pathogens can also infect some of these animals (reviewed in (Collins, 1988)). Many of these species are not suitable for animal models due to limited availability of hosts for experiments. In addition, it is often necessary to perform splenectomy to increase the degree of parasitaemia or to make chimpanzees susceptible to the *P. falciparum* and *P. vivax* species, which make it difficult to assess immunological function in these model systems. However, simian models are sometimes used as a final step in vaccine and anti-malarial drug studies, for example *P. cynomolgi* as a model for *P. vivax* and *P. fragile* for *P. falciparum*. The simian parasite *P. knowlesi* has been used to study antigenic variation, but does not correspond well with the species affecting humans because of its 24-hour life cycle. The most commonly used monkey genera are *Macaca*, *Saimiri* and *Aotus*.

1.3 The immune system

1.3.1 Innate versus adaptive immunity

The immune system contains an innate and an adaptive component. The innate immune system is the first level of defense against many common pathogens. Macrophages,

neutrophils and dendritic cells respond to universal components found on pathogens by phagocytosis, release of inflammatory mediators and activation of the alternative complement pathway. The innate response is important as a defense mechanism in the first days of infection while the adaptive immune response develops to full potency, but it also involved in both activation of and modulation of the adaptive immune response.

The adaptive branch of the immune system allows the host to respond specifically to antigenic challenge and improve the quality of the immune response during the course of exposure to pathogens. The antigen-specific cells are T and B lymphocytes, which are generated as naive cells in the primary lymphoid organs thymus and bone marrow, respectively. These cells migrate into the secondary lymphoid organs via the blood and the lymphatic system. The secondary lymphoid organs include lymph nodes, the spleen, Peyer's patches, tonsils and the appendix. They represent specialised environments where lymphocytes can encounter antigens and are aided in their development into effector and memory cells. Many of the different cells and developmental stages found in the immune system are identified by specifically expressed surface molecules. The nomenclature is to use the name of the molecule followed by the raised signs + and - to refer to the presence or absence of that surface molecule (e.g. $CD4^{+}CD8^{-}$ cells). When the level at which the molecule is expressed is important, the terms high, low and int (intermediate) are used instead.

The specificity of the lymphocytes is determined by the T and B cell receptors. As the lymphocyte matures, inherited sets of gene segments are rearranged and random nucleotides are included at the joins of the segments to form the variable region of the B or T cell receptor. The variable region, which is responsible for the receptors' unique antigenic specificity, is combined with a constant region which is important for the receptors' function. The protein products of all successfully rearranged genes are expressed at the surface of the naive T and B cells, thus creating a very large pool of cells

with different receptor specificities. When the host encounters a new antigen, cells with appropriate receptors are activated, proliferate and differentiate, resulting in groups of genetically identical cells capable of responding to the antigen. This process is known as clonal selection.

1.3.2 T cell development

The T cell receptor recognises proteolytically processed antigenic peptides presented in the context of MHC molecules. T cells can bear either αβ or γδ T cell receptors. γδ T cells have a reduced range of genetic receptor diversity and are sometimes counted as part of the innate immune system (reviewed in (Hayday and Tigelaar, 2003)). A further class of lymphocytes with limited T cell receptor diversity and tissue-specific segregation are the natural killer (NK) T cells. These cells are a class of lymphocytes which express the NK1.1 marker on the cell surface and recognise antigen in the context of the MHC class I-like CD1d molecule (reviewed in (Schmieg *et al.*, 2003)). However, the following explanations will deal only with αβ T cells. T cells with the CD8 coreceptor interact with major histocompatibility complex (MHC) class I, which is expressed on almost all cell types and is the main presentation pathway for antigens located in the cytosolic compartment. T cells carrying the CD4 coreceptor recognise antigen in the context of MHC class II, which presents peptides generated in the exocytotic processing pathway and is found only on specialised antigen-presenting cells. These include dendritic cells, macrophages and activated B cells. As the T cells develop in the thymus, they are positively selected to ensure that they have sufficient affinity for MHC molecules and negatively selected and eliminated if they have high affinity for self antigens. This is one of the most important steps for creating tolerance of the adaptive immune system to self antigens.

Cytotoxic T cells, which are usually $CD8^+$ T cells, kill cells by targeted release of molecules causing penetration of the cell membrane and induction of apoptosis

(programmed cell death). This is an important mechanism for elimination of cells expressing tumour-specific antigens or viral proteins. The $CD4^+$ T cells are subdivided into three subclasses, the inflammatory or T_H1, the helper or T_H2 cells (Bottomly, 1988; Mosmann *et al.*, 1986) (more recent reviews in (Murphy, 2003; O Gor *et al.*, 2003)) as well as regulatory T cells (sometimes also known as T_H3 or suppressor cells) (reviewed in (Bluestone and Abbas, 2003; Francois Bach, 2003)). Cells from the three subclasses express different sets of the intercellular signalling molecules called cytokines - interleukin (IL)-2, interferon (IFN)-γ, and lymphotoxin are characteristic of T_H1 cells, IL-4, IL-5, IL-6 and IL-10 are typical for T_H2 cells and IL-10 and TGF-β are also expressed by regulatory T cells which are further defined by their $CD4^+CD25^+$ phenotype (reviewed in (O'Garra and Barrat, 2003)). The inflammatory T cells activate macrophages to kill intracellular pathogens and recruit phagocytic cells to sites of infection. Helper T cells are responsible for B cell activation and this interaction will be discussed in more detail in Section 1.3.5. Regulatory cells mediate tolerance by down-regulating other T cells which have escaped auto-immune screening mechanisms.

1.3.3 B cells as antibody producers

The main role of B cells is the secretion of antibody, which is the basis of humoral immunity and allows the immune system to deal with pathogens in several different ways. Neutralisation is the simple process of coating a pathogen or toxin and thereby preventing adherence to host cells or blocking access to critical molecular binding sites. Opsonisation involves coating of the surface of the pathogen with antibody. The constant or Fc portion of the antibodies binds to Fc receptors on macrophages and facilitates phagocytic uptake of the pathogen. Antibodies bound to a pathogen can also activate complement, which enhances opsonisation and can also lead to lysis of certain bacteria. Immunoglobulins are generated in different isotypes, as determined by the Fc portion, and antibody function is dependent on the immunoglobulin isotype. This is shown in

Table 1.4 for human antibodies. The human antibody isotypes are IgA1, IgA2, IgD, IgE, IgG1, IgG2, IgG3, IgG4 and IgM. The mouse isotypes are called IgA, IgD, IgE, IgG1, IgG2a, IgG2b, IgG3 and IgM. In general, the function of the isotypes correlates between species, but at the IgG subclass level, this no longer holds true and Table 1.5 shows how the subclasses are thought to correspond between species. (The data on antibody structure and function is reviewed in depth in (Shakib, 1990) and (Hamilton and Mohan, 1998)).

1.3.4 Early B cell development

B cells are generated in the bone marrow, where they undergo a process of maturation driven by bone marrow stromal cells. Productive rearrangement of the immunoglobulin (Ig) heavy and light chain genes leads to the formation of immature B cells, which express B cell receptors of the IgM isotype on the cell surface. If a B cell recognises self antigen at the immature stage, it is eliminated or inactivated. Some self-reactive B cells escape elimination by further immunoglobulin gene rearrangement or receptor editing. B cells which do not recognise any antigen found in the bone marrow environment differentiate into mature B cells bearing both IgM and IgD on the cell surface and circulate through the periphery and secondary lymphoid organs as naive B cells (reviewed in (MacLennan *et al.*, 1997; MacLennan *et al.*, 2000)). In parallel to the γδ T cells, B cells also contain a subpopulation using a reduced selection of rearranged receptors. These cells are called B1 cells and are found mainly in the peritoneal and pleural cavities. Along with the marginal zone B cells (described in Section 3.1.6), B1 cells are the source of natural antibody which recognises frequent pathogenic determinants. B1 cells are subdivided into the $CD5^+$ B1a and the $CD5^-$ B1b cells (reviewed in (Martin and Kearney, 2001)).

Table 1.4 Functions of human immunoglobulin isotypes

	IgM	IgG1	IgG2	IgG3	IgG4	IgA1	IgGA2	IgD	IgE
Transport across placenta	-	+	+	+	+	-	-	-	-
Transport across mucosa	+	-	-	-	-	+++	+++	-	-
Activates classical complement pathway	+++	++	+	++	-	-	-	-	-
Activates alternative complement pathway	-	-	-	-	-	+	-	-	-
Binds macrophage FcR	-	+	-	+	-	-	-	-	-
Binds mast cell and basophil FcR	-	-	-	-	-	-	-	-	+
Present on membrane of naive B cells	+	-	-	--	-	-	-	+	-
Binds staphylococcal protein A	-	+	+	-	+	-	-	-	-

This table was adapted from (Janeway *et al.*, 2001; Knight, 1996).

Table 1.5 Correlation between human and mouse immunoglobulin isotypes [a)]

Human isotype	Mouse isotype	Points of similarity
IgG2	IgG3	• respond to carbohydrate antigens (however, human IgG2 does not autoaggregate)
IgG4	IgG1	• elevated in association with high IgE levels • regulation via IL-4
IgG1 & IgG3	IgG2a & IgG2b	• complement fixation • binding to FcγR • mediate antibody-dependent cellular cytotoxicity (ADCC)

a) This table is based on information found in (Knight, 1996; Snapper, 1990; Snapper and Finkelman, 1993).

1.3.5 B cell activation

Naive B cells are activated by cross-linking of the B cell receptor in the right context. For thymus-dependent antigens, this requires input from T helper cells. Extensive B cell receptor binding through monovalent soluble antigens in the absence of T cell help leads to anergy (an activation refractory state) or deletion of the B cells (reviewed in (MacLennan, 1998; Nossal, 1996)). Immature B cells are especially sensitive to elimination in this manner, which represents a tolerance-inducing mechanism against self reactivity. As a rule, B cell tolerance to self is not as carefully controlled as T cell tolerance and must therefore be governed through the requirement for B cell help. However, B cells can also be activated in the absence of T cell help by two types of thymus-independent antigens. Thymus-independent type I (TI-1) antigens are intrinsically able to induce B cell proliferation and in high doses even cause polyclonal B cell activation. TI-2 antigens cause extensive B cell receptor cross-linking through highly

repetitive structures such as bacterial cell wall polysaccharides. TI-2 but not TI-1 responses can be augmented by T cell help (reviewed in (García de Vinuesa *et al.*, 1999)). Unless stated otherwise, the mechanisms discussed in the following sections involve thymus-dependent antigens.

Activation of B cells in response to thymus-dependent antigens requires help from a T cell recognising an antigenic determinant or epitope from the same pathogen or antigen. The epitopes recognised by the B and T cell do not have to be identical, which is important for immune responses against epitopes which are not processed very well. Antigens binding to the B cell receptor are internalised and degraded, following which, processed peptides will be presented to T cells via MHC class II. Binding of the B cell receptor represents a first activating signal and a T cell responding to any of the peptide / MHC class II complexes supplies the second activating signal in form of secreted IL-4 and membrane-bound CD40 ligand (CD40L). TI-1 and TI-2 antigens also transmit a second signal of a different type, but cells which bind to antigen in the absence of any second activating signal undergo apoptosis (Gray *et al.*, 1997; Noelle *et al.*, 1992; Wykes *et al.*, 1998).

The activation and ensuing development of B cells takes place in specialised microenvironments in the secondary lymphoid organs (described in more detail for the spleen in Section 3 and reviewed in (MacLennan *et al.*, 1997)). The B cells pass through areas packed with T cells such as the T cell zones in the spleen or the paracortex in the lymph nodes. Some B cells can then differentiate into plasma cells which secrete antibody. In the spleen, these cells are found in the extrafollicular foci outside of the white pulp. The antibody produced by these plasma cells tends to be of lower affinity than that seen later in the immune response (Smith *et al.*, 1997; Tarlinton and Smith, 2000). Other activated B cells migrate into the primary follicles in the B cell areas. The primary follicles consist of naive recirculating B cells clustered around the follicular dendritic cells. When activated B cells enter the primary lymphoid follicles, they begin

dividing and thereby form germinal centres. The whole germinal centre along with the surrounding mantle of naive recirculating B cells is now called a secondary lymphoid follicle.

1.3.6 The germinal centre reaction

In general, only thymus-dependent antigens cause germinal centre formation, whereas TI antibody responses are not associated with functional germinal centers or memory formation (Jacob *et al.*, 1991b; MacLennan *et al.*, 1990; Maizels and Bothwell, 1985). Under exceptional conditions, T cell-independent germinal centres can form, but do not complete their development (García de Vinuesa *et al.*, 2000). Several important events take place in the germinal centres: somatic hypermutation of the immunoglobulin genes, isotype switching and generation of memory B cells (reviewed in (Camacho *et al.*, 1998; Kosco-Vilbois *et al.*, 1997; Kosco-Vilbois *et al.*, 1997)). With the partial exception of isotype switching, these events are all dependent on the environment of the germinal centre. Polymerase chain reaction (PCR) analysis of the immunoglobulin genes at the single cell level has shown that all of the B cells in a germinal centre can be traced back to only one or a few founder cells (Jacob *et al.*, 1991a; Jacob *et al.*, 1993; Ziegner *et al.*, 1994). These cells divide about once every 6 h and rapidly fill the germinal centres. These proliferating B cells are called centroblasts and they give rise to the non-proliferating centrocytes. By the 7^{th} day, germinal centres develop two distinguishable regions - the dark zone which consists mainly of closely packed centroblasts and the light zone where the centrocytes and the majority of the follicular dendritic cells are located (reviewed in (Camacho *et al.*, 1998; Kosco-Vilbois *et al.*, 1997)).

During centroblast division, the rearranged immunoglobulin genes undergo somatic hypermutation, which can lead to changes in antibody affinity and specificity. The hypermutation is directed at the areas of the immunoglobulin gene which were encoded by the variable regions and form the antigen-binding site (Jacob *et al.*, 1993). The centrocytes then compete for binding to antigen presented on the processes of the

follicular dendritic cells. Cells whose B cell receptor binds antigen well receive survival signals resulting in the internal expression of the *bcl-2* gene (Smith *et al.*, 2000). The definitive survival signal is CD40-mediated signalling delivered by T cells which recognise antigen internalised during the interaction with the follicular dendritic cells (Gray *et al.*, 1997). B cells with poor or altered recognition of their antigen undergo apoptosis and are phagocytosed by the tingible body macrophages (Han *et al.*, 1995). The average antibody affinity increases slowly at the beginning of a primary immune response, because most of the cells start with low antibody affinities. However, the selection pressure is increased later in the primary and in the secondary immune responses and B cells can cycle between the centroblast and centrocyte compartments several times to increase antibody affinity (reviewed in (Neuberger *et al.*, 2000)). The germinal centre reaction is the source of two major populations of B cells, memory B cells and long-lived plasma cells.

Isotype switching is usually linked to the germinal centres but can also occur in the extrafollicular pathway (Toellner *et al.*, 1996; Toellner *et al.*, 1998). Irreversible genetic splicing allows combination of different Fc components with any given rearranged variable region. Isotype switching is not directly linked to affinity maturation or memory B cell generation, but because they usually occur around the same time in the germinal centres, these phenomena are often referred to as a logical unit and isotype switching to IgG (or affinity maturation) is often used as a surrogate marker for memory B cell generation.

1.3.7 Plasma cells

Plasma cells are terminally differentiated B cells whose function is the secretion of antibody. A large proportion of the activated B cells develops into plasmablasts, which proliferate and thereby increase the production potential for each selected antibody specificity. (Plasma cells and plasmablasts will sometimes be referred to collectively as antibody-containing cells within this thesis). When the plasmablasts differentiate into plasma cells, they develop an enlarged cytoplasm with a prominent rough endoplasmic

reticulum required for the production of secreted immunoglobulins, allowing them to secrete over 5000 immuglobulin molecules per second (reviewed in (Slifka and Ahmed, 1996)). Plasma cells can no longer alter the specificity or isotype of their immunoglobulins and no longer have strong expression of the B cell receptor or MHC class II on the cell surface. This means that they can no longer interact with helper T cells, making antibody production independent of T cell help or the presence of antigen. The majority of plasma cells are short-lived and die after 8 h to 3 days (Jacob *et al.*, 1991a; Sze *et al.*, 2000)). These cells are located in extrafollicular foci. Single cell analysis of the rearranged immunoglobulin genes has revealed that cells found in the germinal centres and the extrafollicular foci can be of the same clonal origin (Jacob and Kelsoe, 1992), demonstrating that the antibody specificity and affinity do not determine whether an activated B cell enters the follicular (or germinal centre) or the extrafollicular pathway. Nevertheless, the cells in the extrafollicular foci generally produce antibody of lower affinity than those emerging from the germinal centres. The antibodies produced by these plasma cells are critical for controlling pathogens while B cells with higher affinity are being selected in the germinal centres. Many of the short-lived plasma cells are of the IgM isotype and the higher avidity of the pentameric IgM (as compared to monomeric IgG) can partially compensate for the poorer affinity. Secreted antibody has a limited life span in serum, which in humans ranges from 2 days for IgA through 7 days for IgG3 to 21 days for IgG1 (reviewed in Shakib, 1990).Thus, the effector molecules survive their short-lived plasma cell source temporarily but do not remain in the serum indefinitely. Recently, it has been discovered that some plasma cells have a much longer life span of at least 2 years in the mouse (Manz *et al.*, 1997; Slifka *et al.*, 1998; Slifka *et al.*, 1995). These cells persist in the bone marrow and to a smaller extent in the spleen and are thought to be responsible for the maintenance of serum antibody levels after the termination of infection (Slifka and Ahmed, 1996; Slifka *et al.*, 1998). Chronically inflamed tissues seem to represent an additional survival niche for long-lived plasma cells

(reviewed in (Manz and Radbruch, 2002)). Many open questions still remain concerning these cells, such as the signals and selection processes governing plasma cell survival.

1.3.8 Memory B cells

Memory B cells are resting cells which can be reactivated rapidly to proliferate and differentiate into antibody-secreting cells (reviewed in (Ahmed and Gray, 1996; MacLennan *et al.*, 2000). Memory B cells have altered homing patterns leading to accumulation in particular locations - the epithelium of the tonsilar crypts, the sub-epithelial part of the dome in Peyer's patches and the inner surface of the subcapsular sinus in lymph nodes (reviewed in (MacLennan *et al.*, 2000)). They are responsible for secondary antibody responses which are more rapid, generally generate antibodies of higher affinity and show a preponderance of the IgG, IgA and IgE isotypes. (However, evidence exists for a large compartment of IgM-expressing memory B cells in humans and mice as well (Ho *et al.*, 1986; Klein *et al.*, 1997)) The rapidity of the secondary response is based on the higher frequency of antigen-specific B cells, the availability of T cells with corresponding antigenic specificities and irreversible molecular changes of the B cell receptor which lead to increased proliferative burst capacity (Martin and Goodnow, 2002). The memory B cell response is limited to T-dependent antigens. This is due to the requirement for CD40-mediated signalling in allowing germinal centre B cells to enter the memory pathway (Gray *et al.*, 1994; Siepmann *et al.*, 2001).

In humans, memory B cells can by identified by expression of CD27 on cells in the periphery or of either CD27 or CD148 on cells in the spleen (Klein *et al.*, 1998; Tangye *et al.*, 1998). In mice, no unique marker for memory B cells has been identified as of yet. Mouse memory B cells express high levels of CD38, but this marker only serves to distinguish the population from their germinal centre B precursors and from antibody-forming cells, as CD38 is also expressed by naive B cells (Ridderstad and Tarlinton, 1998). Therefore, studies on murine B cell memory are forced to rely on circumstantial detection methods. In immunisation studies, the most common method is to define any

antigen-specific, isotype-switched B cells detected after an interval long enough for the elimination of activated non-memory B cells as memory B cells. Sometimes, just the presence of IgG^+ B cells after a given time period is taken as an indication of B cell memory, but that is a very simplified way of addressing the problem. Another way of detecting memory B cells is in a functional assay where the rapidity and affinity of a secondary antibody response is used as a readout for B cell memory.

There is considerable debate about the mechanisms involved in the persistence of memory B cells (reviewed in (Martin and Goodnow, 2000)). One theory is that the memory B cells must be restimulated occasionally by the appropriate antigen or a cross-reactive facsimile. This idea is supported by experiments where memory B cells were transferred into sublethally irradiated congenic rats. If the cells were transferred without the activating antigen, memory B cells had a half life of 2-3 weeks and were undetectable by 12 weeks post transfer (Gray and Skarvall, 1988). The other theory is that memory B cells can persist in a resting state without further stimulation. This idea is supported by findings that B cell memory persists in mice lacking follicular dendritic cells and in mice deprived of helper T cells (Karrer *et al.*, 2000; Vieira and Rajewsky, 1990). An elegant study with a mouse strain carrying two rearranged immunoglobulin alleles showed that memory cells which were generated after exposure to one of the recognised antigens persisted after the immunoglobulin gene had been replaced by the gene whose specific antigen was not present in the mouse, supporting the hypothesis that B cell memory can persist in the absence of the activating antigen (Maruyama *et al.*, 2000). However, the evidence is not conclusive, as the mice were only studied for 15 weeks after the gene switch.

Figure 1.2 Influence of the presence of various lymphocyte types on the course of parasitaemia.

The course of parasitaemia is shown for wild-type mice and mice deficient for various lymphocyte populations.

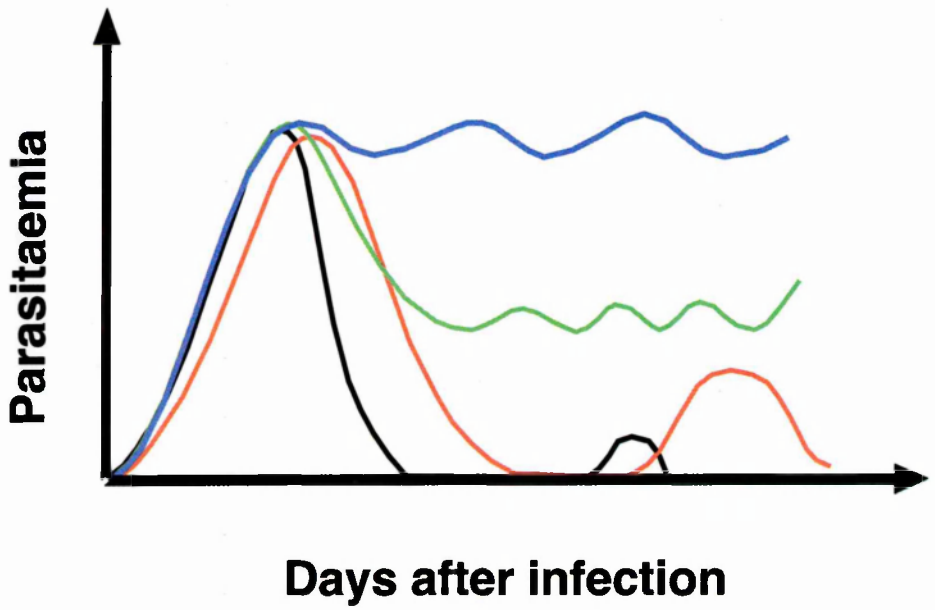
Parasitaemia
Days after infection
Wild type
μMT
αβ-/-
γδ-/-

1.3.9 Interactions of immune cells in protective humoral responses

The mechanisms involved in protective immunity against infections with live pathogens are similar to those which are elicited by immunisation with non-replicating antigens. However, repeated immunisations are usually necessary for the development of comparable immunity and therefore, this section will focus on infections. If the reinfection occurs very soon after the first exposure, effector B and T cells will still be present and can counter the infection. Otherwise, the first line of protection are serum antibodies produced by long-lived plasma cells. Studies of viral infections in isolated populations have shown that serum antibodies are produced for decades after a single infection (reviewed in (Ahmed and Gray, 1996; Slifka and Ahmed, 1996)). In some of the classic cases (reviewed in (Ahmed and Gray, 1996; Slifka and Ahmed, 1996)), such as the measles outbreaks on the Faroe islands with an intervening interval of 75 years, only protection was shown, not presence of antibodies. However, the presence of neutralising antibodies 75 years after an outbreak of yellow fever was demonstrated by passive antibody transfer to monkeys and the maintenance of polio- and vaccinia-specific antibodies over 40 and 15 years, respectively, in the absence of re-exposure to antigen was shown by enzyme-linked immunosorbent assay (ELISA).

It seems that protection lasts longer for systemic than for mucosal infections, which may be due to the anatomical location of the long-lived plasma cells. If neutralisation and opsonisation via pre-existing antibody are not sufficient to control the spread of the pathogen, a secondary immune response is triggered which relies on the presence of memory T cells as well as memory B cells. The presence of both cell types increases the speed of the secondary response, as one of the main delaying factors in the primary response is the necessity for two consecutive activation steps.

1.4 Immune responses to malaria infection

1.4.1 Relevance of immune responses against different stages of *Plasmodium*

The different stages in the *Plasmodium* life cycle result in an immune response taking place at several non-related levels. The three areas of interest are the immune responses against the sporozoite and liver stage, against the blood stage and against the gametocytes. This introduction focuses on the immune mechanisms dealing with the blood stage of the parasite; the other two stages will be mentioned only briefly. Sporozoites are only accessible to the immune system for a very limited time period and are injected in small numbers, so sporozoite-specific immunity develops slowly even in highly endemic areas and is of low magnitude. Anti-sporozoite immunity can be induced in humans with multiple exposures to attenuated but not killed sporozoites injected intravenously or by irradiated malaria-infected mosquitoes. The immune response against sporozoites and infected hepatocytes includes $CD8^+$ and $CD4^+$ T cell-mediated release of IFN-γ and induction of nitric oxide synthesis, but apparently no role for direct killing of infected hepatocytes via the perforin or Fas pathways. Antibodies to sporozoites are probably important and antibodies against liver-stage antigens, NK T cells (a special group of T cells expressing the NK1.1 marker and a semi-invariant TCR) and γδ T cells also seem to be involved to some extent (reviewed in (Hollingdale and Krzych, 2002; Sinnis and Nardin, 2002)).

Immune responses against the sexual form of the parasite are of little benefit to the current host, but are important in blocking parasite transmission. This area of research has concentrated on antibodies which can be effective either in the vertebrate or the mosquito host (reviewed in (Kaslow, 2002)). Therefore, vaccines are being designed to include B cell epitopes eliciting an immune response against the gametocytes. In fact, vaccines which contain epitopes against all stages of the *Plasmodium* life cycle are a popular idea, since a single parasite slipping through the stage controlled by the vaccine-

generated immune response can multiply in the next stage of the parasite life cycle and nullify the effect of the vaccine.

1.4.2 The role of T cells in the rodent malaria model

Early experiments in naturally occurring mutant mouse strains have shown that T cells are essential for the development of anti-malarial immunity in rodents. T cell-deficient *nude* mice which were infected with the normally nonlethal parasite species *P. c. chabaudi*, *P. c. adami* or *P. vinckei petteri* could not control the parasitaemia and eventually died (Cavacini *et al.*, 1986). However, nude mice could be rescued from the lethal effects of *P. c. chabaudi* or *P. c. adami* infection by adoptive transfer of immune T cells (Meding and Langhorne, 1991) Adoptive transfer of parasite-specific T cell clones was also able to protect nude mice from lethal infection with *P. yoelii* (Brake *et al.*, 1988; Brinkman *et al.*, 1985; Jayawardena *et al.*, 1975).

Genetically engineered mice where a single gene has been "knocked out", thereby preventing the development of particular cell populations, have proven extremely useful in determining the effects of different cell types on anti-malarial immunity. *P. c. chabaudi* infection has been tracked in mice where either the αβ and the γδ TCR had been knocked out or γδ T cells had been depleted by antibody administration (Langhorne *et al.*, 1995) and Fig. 1.2 shows the course of parasitaemia in these and other knock-out mice. Mice lacking the αβ TCR are incapable of clearing infection with *P. c. chabaudi* or even of reducing the parasitaemia after the peak. The absence of T cells expressing the γδ TCR has less pronounced effects, with only a slight delay in reduction of the peak of parasitaemia and a slightly increased level of parasite recrudescence as compared to wild-type mice.

The αβ TCR-positive T cells can be further split into $CD4^+$ and $CD8^+$ T cells, whose relevance has been examined in knock-out mice or mice depleted of the appropriate T cells by repeated injection of anti-CD4 or anti-CD8 antibodies from birth. Mice lacking

$CD8^+$ T cells - either through antibody treatment or because the CD8 or β_2-microglobulin gene was knocked out - exhibit only a slight delay in the clearance of the acute parasitaemia (Süss *et al.*, 1988). However, antibody depletion of $CD4^+$ T cells results in a similar course of parasitaemia as that seen in αβ TCR knock-out mice (Kumar *et al.*, 1989; Podoba and Stevenson, 1991; Simon-Haarhaus *et al.*, 1991; Süss *et al.*, 1988). This shows that $CD4^+$ T cells are the main T cell population involved in protection against the erythrocytic stages of malaria infection.

The role of NK T cell in malaria is still under debate. One study demonstrated a role for NK T cells both *in vivo* and *in vitro* in the humoral response against the pre-erythrocytic stages of malaria (Schofield *et al.*, 1999). However, two other groups were unable to confirm these results (reviewed in (Schmieg *et al.*, 2003)). NK T cells were able to enhance protective immunity induced by protective malaria vaccines if the NK T cell ligand α-galactosylceramide was injected along with the vaccine, but this may not mimic a natural role for these cells (Gonzalez-Aseguinolaza *et al.*, 2002). An interesting study has shown that NK T cells are involved in murine cerebral malaria pathogenesis with differential outcome in C57BL/6 and BALB/c mice by regulation of the Th1 / Th2 switch via inflammatory cytokines (Hansen *et al.*, 2003).

1.4.3 The Th1 to Th2 switch during infection

During *P. c. chabaudi* infection, the T cell response switches from a Th1 response during the acute phase to a Th2 response in the chronic phase (Langhorne *et al.*, 1989; Langhorne and Simon, 1989; Stevenson and Tam, 1993). The Th1 cells release IFN-γ with peak production preceding the peak of parasitaemia by 2 or 3 days (Meding *et al.*, 1990; Slade and Langhorne, 1989). The IFN-γ does not act directly on the parasites. Instead, it mediates an inflammatory response by activating macrophages which are responsible for reducing the parasitaemia in the acute phase (reviewed in (Li *et al.*, 2001)). As the infection progresses, the cytokines produced by splenic $CD4^+$ cells shifts to Th2-type

pattern and antibody help can be demonstrated (Langhorne *et al.*, 1989; Langhorne and Simon, 1989; Stevenson and Tam, 1993). Interestingly, this switch to a Th2 response is dependent on the presence of B cells (Langhorne *et al.*, 1998).

1.4.4 The role of B cells in the rodent malaria model

Transfer of immune serum into naïve humans or mice can diminish or prevent infection in the recipient (Cohen *et al.*, 1961; Jarra *et al.*, 1986). At the cellular level, it has been shown that mice with severe combined immunodeficiency (SCID), i.e. lacking both B and T cells, could only control and clear parasites when B cells were transferred with the T cells (Meding and Langhorne, 1991). The importance of B cells is also revealed by infections of B-cell deficient mice like the μ-MT or J_HD mouse. In these mice, the parasitaemia is partially controlled in the acute phase but then continues as a fluctuating visible chronic infection which can rise as high as 50% parasitised red blood cells in male μ-MT mice (van der Heyde *et al.*, 1994; von der Weid *et al.*, 1996). The control of chronic parasitaemia is effected by antibodies, as repeated passive immunisation with immune serum during the chronic phase of the infection enables the B cell-deficient mice to clear their parasites (Langhorne *et al.*, 1998; von der Weid *et al.*, 1996). Mice which are depleted of $CD4^+$ T cells during the chronic phase of their infection are able to control their parasitaemia as long as the specific antibody titres remained high (Langhorne *et al.*, 1990). Together, these results show that B cells or parasite-specific antibody is necessary for the final reduction step in the rodent malaria *P. c. chabaudi*, although they do not appear to play a strong role during the acute phase of infection. B1 cells are known to be involved in the immune response against other protozoan parasites such as *Trypanosoma cruzi* and it has been hypothesised that they play a role during malaria infection, but no conclusive evidence exists yet for this theory (Minoprio *et al.*, 1989).

Malaria infection with *P. c. chabaudi* is accompanied by changes in the antibody isotype. Malaria-specific IgG2a could be measured 2 weeks after infection. This was followed by

IgG3 and IgG2b production, whereas IgG1 could only be measured during late infection (Falanga *et al.*, 1987; Langhorne *et al.*, 1984). This pattern is seen for the total parasite-specific response, but has also been shown for separate fragments of the merozoite surface protein-(MSP)-1, with the exception that the IgG2b response precedes the IgG2a response in some cases (Quin and Langhorne, 2001a). The switch to IgG1 production could be attributed to the production of IL-4, IL-5 and IL-6 by Th2 T cells, although suppression of IgG1 production has been seen in severe malaria infections (Falanga *et al.*, 1987; Langhorne *et al.*, 1984).

Malaria infection is accompanied by hypergammaglobulinaemia in both mice and humans (Greenwood, 1974; Wyler, 1974). It has been shown in mice that polyclonal B cell activation occurs (Langhorne *et al.*, 1985; Rosenberg, 1978). This type of response is suggestive of a large thymus-independent response. There has been some debate about the role of a B cell mitogen in malaria, which would elicit a TI-2 response, but there has been no conclusive decision on the matter (Greenwood, 1974; Wyler, 1974; Wyler *et al.*, 1979). Newer studies have presented evidence for thymus-independent responses to the repeat sequences of the 70-kDa *P. falciparum* heat shock protein and the repetitive surface protein of sporozoites (Kumar and Zheng, 1998; Schofield and Uadia, 1990). Considering the high degree of repetitive epitopes found in *Plasmodium* antigens, one would expect more TI-2 responses against malaria, but this issue has not been addressed thoroughly yet.

1.4.5 Theories on the antibody mechanisms involved in malaria

The effector mechanisms by which antibodies act on the *Plasmodium* parasite are still not clear. Evidence exists for several theories and the most likely explanation is that several mechanisms are acting simultaneously. Antibodies directed against variant antigens on the surface of infected erythrocytes can cause erythrocyte agglutination and thereby target the erythrocytes for phagocytic destruction (Bull *et al.*, 1998). Neutralising antibodies

can act at several levels, such as preventing binding of the 235-kDa rhoptry protein to infected red blood cells and thereby preventing erythrocyte invasion (Ogun *et al.*, 2000), preventing the pre-invasion processing of merozoite surface protein-1 (MSP-1) (discussed in Section 4.1.1) or interfering with the sexual development stage of the parasite in the mosquito midgut after ingestion of the blood meal and thereby preventing parasite transmission (discussed in (Gozar *et al.*, 1998)).

Although human studies suggest that there may be a role for the interaction of antibodies and the classical complement pathway in the immune response to malaria infection (reviewed in (Taylor *et al.*, 2001)), this was not confirmed in mouse studies. Mice deficient in either the classical complement pathway or both the classical and alternative pathways showed only minor delays in the control of primary infections (Taylor *et al.*, 2001). However, a larger role was identified for the classical complement pathway during reinfection. As a further mechanism, sera from clinically immune individuals can opsonise *P. falciparum*-parasitised *Saimiri* red blood cells and this effect is mediated by the IgG1 and IgG3 subclasses (Groux and Gysin, 1990). Sera taken from *P. c. chabaudi* (AS)-infected CBA/Ca mice 1-2 days after the peak of infection also bind to parasitised red blood cells in a strain-specific manner and mediate phagocytosis *in vitro* (Mota *et al.*, 1998) The link between opsonisation and phagocytosis can also be assumed for early studies showing that macrophages of the liver, bone marrow, spleen and peripheral blood contained infected erythrocytes (reviewed in (Arese *et al.*, 1991)).

A possible antibody effector mechanism termed antibody-dependent cytotoxic inhibition (ADCI), a variation on antibody-mediated cell cytoxicity (ADCC), has been studied in considerable detail for *P. falciparum* (reviewed in (Druilhe and Pérignon, 1997)). *In vitro* experiments have shown that cytophilic antibodies (antibodies of the IgG1 and IgG3 isotypes in humans) crosslink surface antigens (such as MSP-3) on free merozoites with the FcRγII on monocytes (Bouharoun-Tayoun *et al.*, 1990; Bouharoun-Tayoun *et al.*,

1995; Oeuvray *et al.*, 1994). The monocytes release soluble mediators such as TNF-α which cause parasites located in nearby erythrocytes to remain at the one-nucleus stage of schizogony. This parasitistatic effect is seen for sera taken from residents of endemic areas who are in a state of premunition, but not for sera from non-exposed individuals or sera taken after a single malaria attack (Bouharoun-Tayoun *et al.*, 1995).

Support for this hypothesis is drawn from human field studies showing that the isotype distribution differs between protected and non-protected individuals. In clinically immune subjects from the Ivory Coast, IgG1 and IgG3 were the predominant antibodies, whereas children or adults experiencing their first malaria attack tended to display different isotype distributions (Bouharoun-Tayoun and Druilhe, 1992). It has also been shown in Dielmo, an area of seasonal holoendemic malaria transmission, that increases in IgG3 levels during the high transmission season were associated with protection from clinical malaria, with the strongest effects seen in children 3-6 years of age (Aribot *et al.*, 1996). A protective role for human IgG1 has been suggested for an area of unstable malaria transmission in Brazil (Braga *et al.*, 2002). In mice, a protective role has also been shown for the cytophilic IgG2a subclass in lethal and non-lethal *P. yoelii* infection (White *et al.*, 1991). Passive antibody transfer of different IgG subclasses showed that only IgG2a (but not IgG2b, which is also a cytophilic antibody) could impede the development of parasitaemia in a fashion similar to passively transferred hyperimmune serum. This difference between subclasses did not appear to be caused by different antigen specificities.

However, further studies in the mouse model raise the question how relevant ADCI is *in vivo*. The course of parasitaemia was not changed in mice made deficient for FcR and infected with *P. yoelii* or *P. c. chabaudi* while simultaneously receiving parasite-specific antibody, although these mice do not have the capability to perform ADCI ((Rotman *et al.*, 1998; unpublished data by Dr. J. Langhorne). There are several possible explanations

for the discrepancies between the *in vitro* results with *P. falciparum* and the *in vivo* mouse studies. One is that the ADCI effect is unique to either *P. falciparum* or humans and could therefore not be detected in the animal model. Another possibility is that the effect is supplanted by other protective antibody-mediated mechanisms at the high antibody concentrations used in the mouse studies. Another consideration is that the epidemiological studies showing temporal concurrence between the presence of cytophilic antibodies and clinical protection do not necessarily represent a causal link for the importance of ADCI. Several malarial antigens preferentially or exclusively induce antibodies of a particular subclass, such as a predominant IgG3 response to MSP-2 (Taylor *et al.*, 1995). The antibody response to MSP-1, which plays a role in clinical protection (discussed in Section 4.1.2) is also limited to IgG1 and IgG3,with a bias of IgG1 for the C-terminal portion and IgG3 for the N-terminal part observed in Sudan, the Gambia and Kenya but not in Senegal (Cavanagh *et al.*, 2001; Diallo *et al.*, 2002; Egan *et al.*, 1995; Garraud *et al.*, 1999). Thus, it is possible that the link between clinical protection and the presence of cytophilic antibodies is based on the antibody specificity rather than the effector mechanism. Alternatively, the milieu in which B cells are activated could be the reason for the occurrence of cytophilic antibodies as locally secreted cytokines and the type of antigen-presenting cell can direct isotype switching.

1.4.6 Immunopathology

In addition to controlling parasitaemia, the immune system can also contribute to the aetiology of malaria. This is a large field of malarial research and shall only be outlined briefly here. The cytokine theory of malarial disease states that many of the disease symptoms of malaria can be attributed to inflammatory mediators released by the host in response to schizogonic erythrocyte rupture. The foremost of these inflammatory cytokines is TNF-α and locally high levels of this molecule are involved in cerebral malaria and anaemia. Further components of the inflammatory response are IL-1, IFN-γ

and lymphotoxin. Some of the effects previously attributed to TNF-α may actually be caused by lymphotoxin, as the two ligands share a receptor (e.g.(Engwerda *et al.*, 2002)). These cytokines lead to up-regulation of inducible nitric oxide synthase, resulting in high levels of nitric oxide in tissues which are normally only exposed to low levels of this cellular messenger (reviewed in (Clark *et al.*, 1997; Clark and Schofield, 2000; Jakobsen *et al.*, 1995).

1.4.7 Immune evasion mechanisms

The *Plasmodium* parasite employs several mechanisms of immune evasion: The replication cycles in the liver and the blood are immunologically independent in many respects (discussed in (Urban and Roberts, 2003). Once merozoites enter the erythrocytes, they occupy an immunologically privileged site lacking antigen presenting or processing capability. Furthermore, many surface molecules on the parasite are polymorphic, making immune recognition of new strains more difficult. In addition, several of the antigens expressed on the surface of the parasite or the infected red blood cell undergo antigenic variation. Different variant antigen families have been discovered on *P. falciparum*, *P. vivax*, *P. knowlesi*, *P. chabaudi* and *P. yoelii* (reviewed in (Snounou *et al.*, 2000)). The families can contain up to several hundred variants and it has been shown for the the *var* gene family of *P. falciparum* that even without immune pressure, 2% of the population switch the expressed gene per generation *in vitro* (Roberts *et al.*, 1992). The members the *var* family also function as adhesion molecules, allowing the infected red blood cells to sequester in various tissues and avoid erythrocyte elimination by the splenic red pulp macrophages (Su *et al.*, 1995).

It has also been suggested that many malarial antigens elicit cross-reactive immune responses to a high degree, both at the intra- and intermolecular level (Anders, 1986). Another possible way of interfering with the B cell response lies in the shedding of large quantities of soluble antigen which occurs during merozoite invasion. This can interfere

with the B cell response by causing anergy of immature B cells (reviewed in (Nossal, 1996)) or deletion of B cells leaving the germinal centres (MacLennan, 1995; Pulendran *et al.*, 1995; Shokat and Goodnow, 1995). At an even earlier stage, *P. falciparum* and *P. yoelii* parasites have been shown to inhibit dendritic cell maturation and thereby affect both $CD4^+$ and $CD8^+$ T cell responses (Ocaña-Morgner *et al.*, 2003; Urban *et al.*, 1999; Urban and Roberts, 2003). However, no comparable effect has been observed for *P. c. chabaudi* parasites (Seixas *et al.*, 2001).

1.5 Protection against malarial reinfection

1.5.1 Types of protection

For many pathogens, a single infection suffices to enable the immune system to protect the host from disease for the rest of the host's life span. However, malaria is contracted repeatedly both under endemic and epidemic conditions. Instead of developing classic immunity, people living in malaria-endemic areas reach a steady state level termed premunition, where the host is protected from disease as long as exposure to the parasite continues. Premunition is not a sterilising form of immunity and is maintained by the persistence of low-grade chronic parasitaemia. The phenomenon is peculiar to holo- or hyperendemic areas, mainly in Africa and protection is lost within 1 year without rechallenge (reviewed in (Druilhe and Pérignon, 1994)).

One very basic problem in evaluating studies on protection against malaria is that there are two different levels of protection involved. Protection against the parasite and protection against disease are both seen in semi-immune individuals, as the hosts show both resistance to the inflammatory effects of the anti-parasite immune response and reduced levels of parasitaemia. The two forms of protection develop at different rates (Gupta *et al.*, 1999). The studies on malaria infection often do not differentiate between these different types of protection and field studies usually only measure protection against disease, with parasitaemias only being measured in people entering the hospital

with symptoms of malaria. An additional problem is that it is usually not possible to determine how many infections someone living in an endemic area has experienced by the time they develop premunition. Some information on this aspect can be gleaned from studies in the 1930's, when malaria infection was used to treat neurosyphilis. One such study summarises data from 2061 Roumanian patients who were infected several times with malaria for syphilis treatment (Ciuca *et al.*, 1934). This study showed that after one treatment with *P. falciparum*, 29% of patients did not develop measurable parasitaemia upon reinfection, with the number of protected patients rising gradually to 97% after nine infections. Protection developed more rapidly against *P. malariae* and *P. vivax*, but even for *P. vivax* infection, four mosquito incoculations were required for protection to reach 100%. No species cross-protectivity was observed and the cross-protection between different strains of *P. vivax* was also low.

1.5.2 The cumulative exposure and age-dependent hypotheses of protection

The general view of resistance to malaria infection is that it takes 10-15 years of continuous exposure in a holo- or hyperendemic area for the host to be protected from morbidity and mortality. Most of the mortality occurs in children under 5 years of age and pregnant women. Several hypotheses exist to explain this slow development of immunity (reviewed in (Baird, 1998)). One theory is that immunity develops slowly because antigenic variation by the parasite make it necessary for the host to develop immune responses to each of the prevalent parasite strains and many of the variants of their surface molecules (Bull *et al.*, 1999; Bull *et al.*, 1998).

In contrast to this cumulative exposure theory Baird also puts forward the hypothesis that the slow onset of immunity to *P. falciparum* is linked to changes in immune functions determined by normal host development and maturation (age-dependent hypothesis). This is based on observations that children acquire protection from death rapidly if exposed to high levels of malaria, but still suffer from a high degree of

morbidity. The slow development of premunition in endemic areas is attributed to the fact that the first infections occur before the immune system of the host is capable of an adequate response. This hypothesis is supported by data from Indonesia, where inhabitants of Java, a low malaria transmission area, were encouraged to migrate to Irian Jaya which has high malaria transmission. Comparison of malaria incidence between the immigrants and the natives after 19 months showed a comparable distribution of disease prevalence and other linked parameters such as spleen rate and parasite density among the age groups, irrespective of the individual's origin (Baird *et al.*, 1991). Subsequent studies in six further transmigration villages confirmed these results (Baird *et al.*, 1993).

Both of the hypotheses discussed above deal with the development of resistance to malaria under continuous exposure. However, even under hyperendemic conditions, it took an estimated three to six infections for the morbidity rate to drop and the age-dependent prevalence pattern to establish itself in the Indonesion transmigrants (Baird, 1998; Baird *et al.*, 1993). In addition, as stated previously, immune individuals who leave the endemic area lose their immunity without the continued exposure to parasite. This is in sharp contrast to the situation seen with many viral infections which render the host immune after a single exposure. Therefore, irrespective of whether the cumulative exposure or the age-dependent hypothesis is a better description of the development of anti-malarial immunity, standard immune mechanisms are not functioning as fully in malaria as they do in other infections. This issue needs to be examined in greater detail and main candidates for disturbed immune mechanisms are faulty generation or maintenance of B or T cell memory or of long-lived plasma cells. T cell memory will not be examined here, but the next two subsections present the confusing array of data on B cell memory and long-lived plasma cells in malaria.

1.5.3 B cell memory after malaria infection

The presence of activated B cells or memory B cells has been detected in both human and rodent malaria long after the initial infection. Spleen cells derived from mice infected with *P. chabaudi* can be stimulated *in vitro* by parasitised red blood cells to produce parasite-specific antibody 369 days after infection (Pearson *et al.*, 1983). However, the levels are fourfold lower than those produced by spleen cells taken 96 days after infection, indicating a decay of memory. In human infections, peripheral B cells from malaria-exposed donors can be activated *in vitro* by combinations of cytokines and costimulatory signals to secrete *Plasmodium*-specific antibodies (Garraud *et al.*, 2002). In this, study, antibody production was seen for peripheral B cells from individuals living in holendemic or mesoendemic areas, but rarely for individuals from a hypoendemic area and not at all in Europeans with no history of *P. falciparum* infection. Limiting dilution assays showed that *Plasmodium*-specific B cells could be activated from the blood of individuals from a hyperendemic area in Cameroon as well as in Madagascans who had probably last encountered malaria parasites 8 years previously, with the latter generally found in lower numbers (Migot *et al.*, 1995). These different studies share the weakness that one cannot be sure that the reactivated cells are truly memory B cells, as there were no definite controls for the absence of recent infections. In addition, the use of total parasite antigen increases the risk that cross-reactive B cells are restimulated in these systems. Therefore, it is necessary to examine memory B cell generation in malaria in a more stringent system with exact knowledge of the host's infection history.

1.5.4 Plasma cell longevity after malaria infection

Information concerning the persistence of plasma cells can be derived from longitudinal studies of malaria-exposed human populations where exposure to the parasite is reduced or terminated in some fashion. Several studies have shown that in areas of seasonal

malaria transmission antibody levels to malarial proteins drop during the dry season: In an area of low intensity malaria transmission, the levels of variant-specific antibodies directed against the malarial antigen *P. falciparum* erythrocyte membrane protein-1 (PfEMP-1) drop within months of clinical malaria attacks (Giha *et al.*, 1999). Antibody responses to the non-polymorphic rhoptry-associated protein 1 (RAP1) measured in the same area showed that these were even more short-lived and closely linked to clinical infection (Fonjungo *et al.*, 1999).

A meticulous 4-year longitudinal study relating antibody levels against components of the MSP-1 protein to clinical malaria infection showed that antibodies against the C-terminal MSP-1_{19} fragment were found in 61%-73% of individuals with clinical malaria and only in 11-14% of individuals without clinical malaria in any given transmission season. For the polymorphic Block 2 antigens of MSP-1, 39-47% of clinical malaria patients had antibodies against one of the nine variants tested but only 0-6% non-symptomatic individuals had detectable antibodies. Since 96% of the cohort experienced clinical malaria during the observation period, this speaks for a rapid decay of antibody levels. This is also shown explicitly for 20 individuals who experienced clinical malaria and were drug treated. Their antibody levels drop by 45% for MSP-1_{19} and by 40% for Block 2 in the 8-9 months of the following transmission season (Cavanagh *et al.*, 1998).

This rapid drop in MSP-1-specific antibody levels was also observed in a study of *P. vivax* infections in Bélem, Brazil where exposure to the parasite occurs only on visits to the surrounding countryside (Soares *et al.*, 1999). Further evidence can be found in a research project involving a total of about 3000 people in the Garki District of Nigeria. A large-scale serological study was performed from 1970-1975 before, during and after a period of intense insecticide- and drug-mediated malaria control. Several different serological tests showed that *P. falciparum*- and *P. malariae*-specific antibody levels dropped after the intervention (Brögger *et al.*, 1978). Taken together, these data show

that antibodies against malarial antigens drop after parasite exposure ends, often reaching undetectable levels. This contrast with antibody responses to non-renewable protein antigens that can be sustained for years (Askonas *et al.*, 1970; Maple *et al.*, 2000). However, data also exist showing that only the children experienced fluctuations in antibody levels between the dry and rainy seasons whereas antibody levels remained constant in adults (over 16 years of age). This was shown in a longitudinal study in comparing antibody levels against MSP-1, MSP-2 and SP360 (a gametocyte antigen) in children and adults (Taylor *et al.*, 1996).

There are difficulties in evaluating these longitudinal field studies where rough trends have to be dissected from the background of individual variation. It is likely that the parasitaemic status of the study participants exerts a strong influence in form of chronic infections or individual treatment regimes. One study showed that a third of the subjects from an area of seasonal transmission actually had detectable parasitaemia right before the start of the transmission season (Ferreira and Katzin, 1995). There are no comparable studies made in an animal model although this offers the possibility of directly linking antibody levels to the infection history and the presence or absence of parasites.

However, a few studies do exist where the parasitaemic status of the participants is somewhat more defined and which show that after the initial drop in antibody levels, antimalarial antibodies can persist in the absence of infection. In a small study group, antibodies against sporozoite antigens were shown to persist 6-10 years after the hosts had left the malaria-endemic area (Druilhe *et al.*, 1986). Even more surprisingly, a single 50-day outbreak of *P. vivax* (with very thorough controls for parasitaemia infection afterwards) resulted in antibodies against circumsporozoite protein and MSP-1 which could still be detected in some individuals 7 years later (Braga *et al.*, 1998).

On the island of Aneityum in the Vanuatu archipelago of Melanesia, malaria was mesoendemic until 1991 when a thorough eradication campaign involving multiple drug

administration, pesticide-treated bed nets and distribution of mosquito-larvicidal fish was initiated (Kaneko *et al.*, 2000). The parasitological status of the roughly 700 islanders was monitored over the next 7 years. *P. falciparum* infection was practically eliminated within the first year of the programme and the last cases of *P. vivax* (probably relapses rather than reinfections) were detected in 1996. When malaria-specific IgG titres were measured 7 years after the start of the intervention, 37% of 6-15-year-olds and 80% of 16-30-year-olds had titres higher than the cut-off point. However, part of this antibody is likely to be caused by cross-reactivity with non-malarial antigen, as 19% and 29%, respectively, of the inhabitants of an island without malaria had positive IgG titres too (Kaneko, 1999). Therefore, further studies, preferably focusing on single antigens, are required.

1.6 Aims of the thesis

In summary, the introduction has shown that despite the importance of antibody and B cells for protection against the erythrocytic stages of the *Plasmodium* parasite, relatively little is known about the development of the B cell response during malaria infection. Therefore, this thesis aims to characterise the B cell response in the *P. c. chabaudi* (AS) model system. This can be accomplished by the following means:

1. Analysis of the primary B cell response during *P. c. chabaudi* infection
2. Determination of the longevity of protection against reinfection in this model
3. Assessment of memory B cell generation in malaria infection
4. Evaluation of plasma cell longevity following malaria infection

The primary B cell response to malaria infection is dealt with in the first two results chapters. Section 3 analyses the total splenic B cell response irrespective of antigenic specificity using immunohistology and flow cytometry to identify and quantify the B cell populations of the spleen. Section 4 focuses on the proportion of that response which is

specific for one particular malarial antigen, the merozoite surface protein-1 (MSP-1). The next two results chapters focus on the development of the immune response after the acute phase of primary infection and during secondary infection. In Section 5, secondary infections with the same strain of parasite are used to elucidate the quality of protection and how this is influenced by parasite persistence. Section 6 deals with the long-lived plasma cell and memory B cell responses by using ELISA to determine changes in MSP-1-specific IgG levels and affinity in the period after primary infection and during reinfection.

2 Materials and Methods

2.1 Buffers

This section lists all the buffers used in the Materials and Methods section. All chemicals whose source is not stated were purchased from Sigma (Poole, UK) or BDH (Poole, UK). Unless specified otherwise, dH_20 refers to water from the NanoPure system.

Parasites and infections (Section 2.4)

Glycerol freezing buffer	glycerol	40% v/v
	sodium lactate	0.14 M
	potassium chloride	0.005 M
	pH to 7.4	

Staining of thin blood films (Section 2.5)

Giemsa 10x buffer	NaCl	0.9% w/v
	KH_2PO_4	0.2 mM
	K_2HPO_4	0.8 mM
	pH to 7.0-7.2	
Giemsa stain	improved R66 solution 'Gurr'	20% v/v
	(#35086 5P, BDH))	
	Giemsa 10x buffer	10% v/v
	dH_2O	70% v/v

Whole blood transfer (Section 2.10)

Heparanised Krebs phosphate saline buffer with glucose, pH 7.2

NaCl	6.67 g
KCl	0.341 g
MgSO4 x 7 H_2O	0.284 g
NaH_2PO_4	3.094 g
1 M HCl	4.36 mL
make up to 1 L with dH_2O	
heparin	25 U/mL
(# 9860, Leo Laboratories Ltd., Aylesbury, UK)	
add the heparin directly before use	

MSP-1 / MBP fusion proteins (Section 2.12)

Rich medium	tryptone	10 g/L
	yeast extract	5 g/L
	NaCl	5 g/L
	glucose	2 g/L
	ampicillin	50 mg/L

Affinity purification of MBP fusion proteins (Section 2.13)

Loading buffer	Tris HCl pH 7.4	10 mM
	NaCl	200 mM
	EDTA	1mM
	sodium azide	0.05% w/v
Elution buffer	Loading buffer	
	maltose (M-5885, Sigma)	10 mM

Reducing SDS-PAGE (Section 2.15)

Sample buffer, reducing	1 M Tris/HCl pH 6.8	8 mL
	10 % (w/v) SDS	20 mL
	20 mM dithiotreitol (DTT)	154.2 mg
	glycerol	10 mL
	0.2% w/v bromphenol in ethanol	0.6 mL
	fill up to 50 mL with d H_2O	
Running buffer (5x)	Tris base	25 mM
	glycine	250 mM.
	SDS	0.1% w/v
	fill up to 2 L with dH_2O	

Coomassie staining of SDS-PAGE gels (Section 2.16)

Coomassie stain	Coomassie Brilliant Blue R250	0.25 % w/v
	(# B-0149, Sigma)	
	ethanol	45 % v/v
	acetic acid	10 % v/v
	(AnalR, # 10001CU, Merck, internal order)	
	dH_2O	45 % v/v
Coomassie destain	ethanol	45 % v/v
	acetic acid	10 % v/v
	dH_2O	45 % v/v

Silver staining of SDS-PAGE gels (Section 2.17)

Fixative	formaldehyde	0.05% v/v
	(# F 1635, Sigma)	
	methanol	50% v/v
	deionised H_2O	49.95% v/v

DTT stock	dithiothreitol (DTT)	5 mg/mL
	(D-9779, Sigma)	
	deionised H_2O	
	store at -20°C	
Silver nitrate solution	$AgNO_3$ (AnalR quality)	0.1% w/v
	deionised H_2O	
Developer	Na_2CO_3 (GPR quality)	3% w/v
	formaldehyde	0.05% w/v
	deionised H_2O	

Immunohistology (Section 2.21)

Tris stock (0.2 M)	Trizma base	121.14 g
	fill up to 5 L with deionised water	
Saline stock	NaCl	42.5 g
	fill up to 5 L with deionised water	
Tris-buffered saline pH 7.6	Tris stock	1 L
(0.05 M)	saline stock	1.6 L
(TBS)	concentrated HCl	14 mL
	deionised H_2O	1.386 L
Tris-buffered saline pH 9.2	Tris stock	500 mL
(0.1 M)	pH to 9.2 with 1 N HCl	
	fill up to 1 L with saline stock	

Nonspecific esterase staining (Section 2.24)

Buffered formol sucrose solution, pH 6.8	$NaH_2PO_4.H_2O$	2 g
	Na_2HPO_4	3.25 g
	sucrose	37.5 g
	formaldehyde (40%)	50 mL
	dH_2O	450 mL
	store at 4°C	
Gum sucrose	gum arabicum (gum acacia)	1% w/v
	sucrose	30% w/v
	dH_2O	
	filter through thick paper and store at 4°C	
Fixative	citrate solution (kit)	12.5 mL
	acetone	32.5 mL
	formaldehyde (37%)	4 mL
α-NE staining solution	(all ingredients from Sigma kit 91-A)	
	Fast Blue BB base	1 mL
	sodium nitrite solution	1 mL
	mix Fast Blue and sodium nitrite and wait 2 min	
	Trizmal concentrate	5 mL
	α-naphthyl acetate	1 mL
	deionised water, 37°C	40 mL

Flow cytometry (Section 2.26)

Erylysis buffer	0.16 M NH_4Cl-Tris buffer, pH 7.2	
	1 part 0.16 M NH_4Cl	
	50 parts 0.17 M Tris base	

FACS buffer	BSA	1% w/v
	EDTA	5 mM
	sodium azide	0.01% w/v
	PBS	
Supplemented HBSS	Hepes	12 mM
	(#15630-056, Gibcco BRL, Paisley, Scotland)	
	FCS	5% v/v
	(#S-0001a, batch 6010826, Harlan Sera-Lab Ltd, Crowley Down, UK)	
	Hank's balanced salt solution(HBSS, #24020-291-091,Gibco BRL)	

Annexin V staining in flow cytometry (Section 2.28)

Binding buffer	Hepes / NaOH, pH 7.4	10 mM
	sodium chloride	140 mM
	$CaCl_2$	2.5 mM
	sterile filter and store at 4°C	

Enzyme-linked immunosorbent assay (ELISA) for MSP-1-specific IgG (Section 2.29)

Carbonate buffer (pH 9.5)	NaH_2CO_3	15 mM
	$NaHCO_3$	35 mM
	pH to 9.5	
Blocking buffer	BSA	1% w/v
	Tween 20	0.3% v/v
	sodium azide	0.05% w/v
	PBS	
	store at 4°C	
Wash buffer	sodium chloride	0.9% w/v

	K_2HPO_4	5 mM
	KH_2PO_4	5 mM
	Tween 20	0.025% v/v
	pH to 7.0-7.2	
Diluent buffer	BSA	0.1% w/v
	Tween 20	0.3% v/v
	sodium azide	0.05% w/v
	PBS	
Diethanolamine buffer	diethanolamine	48.5 mL
	$MgCl_2 \cdot 6\ H_2O$	400 mg
	sodium azide	450 mL
	dH_2O (autoclaved)	450 mL
	stir overnight at 4°C in dark to dissolve diethanolamine	
	adjust pH to 9.8	
	fill up to 1 L with autoclaved dH_2O	

Enzyme-linked immunosorbent assay (ELISA) with crude malarial extract (Section 2.30)

Parasite lysis buffer	Tris HCl, pH 7.5	50 mM
	EDTA	1 mM
	SDS, pH 8.0	0.5% w/v

2.2 Antibodies

Primary antibodies used for immunhistology are listed in Table 2.1, secondary antibodies for immunohistology in Table 2.2, antibodies for flow cytometry in Table 2.3 and isotype controls for flow cytometry in Table 2.4. For ELISA, the only commercial antibody was AP-labelled goat anti-mouse IgG H +L (# 1031-04, lot G770-W990E, Serotec).

Table 2.1 Primary antibodies and reagents for immunohistology [a)]

Antibody	Source	Dilution ⇒	Concentration	Order no.	Batch
rat anti-mouse CD3	Serotec	1:200	1.25 µg/mL	MCA5006	0399
rat anti-mouse IgM heavy chain	Serotec	1:600	0.42 µg/mL	MCA 199	301199
sheep anti-mouse IgD H chain [b)]	The Binding Site	1:100	120 µg /mL	PC 283	039123
rat anti-mouse IgG H chain	Serotec	1:400	?	MCA424	010801
anti-mouse CD138 (syndecan-1) [c)]	Pharmingen	1:300	0.17 µg/mL	09342D	MO40221
biotinylated peanut agglutinin	Vector Laboratories Inc.	1:100	5 mg/mL	B-1075	J0730
$MSP\text{-}1_{21}$ / MBP [b)]	see Section 2.12		370 µg/mL	---	---
rabbit anti-MBP	New England Biolabs	1:150	?	800-30S	77, 73
hamster anti-CD11c	Ian MacLennan	1:2000	0.9 µg/mL	clone N418	22.12.93
rat anti-F4/80 [b)]	Siamon Gordon	1:50	?	?	?
rat anti-CD169 [b)]	Siamon Gordon	1:50	?	clone 3D6	?

a) All dilutions were determined by titration.

b) Polyclonal antibodies.

c) The anti-CD138 antibody was biotin-labelled, but the biotin reactivity was so poor that a biotin-labelled secondary antibody was used as well.

d) Company locations: Serotec, Oxford, UK; The Binding Site, Birmingham, UK; Pharmingen, San Diego, CA; USA; Vector Laboratories, Burlingame, CA, USA; New England Biolabs, Hertfordshire, UK.

Table 2.2. Secondary antibodies used in immunohistology [a)]

Antibody	Label	Source [b)]	Dilution ⇒	Concentration	Order no.	Batch
donkey anti-sheep/goat Ig	HRP	The Binding Site	1:100	10 µg/mL	AP360	100435
rabbit anti-rat Ig	biotin	DAKO	1:600	1 g /L	E0468	099(101)
rabbit anti-rat Ig	HRP	DAKO	1:50	?	P0450	?
swine anti-rabbit Ig	biotin	DAKO	1:400	0.56 g/L	E0353	028(301)
sheep anti-rat Ig	HRP	The Binding Site	1:200	?	AP331	089(101)
goat anti-hamster Ig H&L [c)]	biotin	Vector	1:50	?	AI916	?

a) All dilutions were determined by titration.

b) Company location: DAKO, Cambridgeshire, UK.

c)The rabbit anti-rat Ig-HRP and goat anti-hamster IgG-biotin antibodies must be pre-incubated separately with normal mouse serum and then mixed right before application to the sections to prevent cross-reactivity between the secondary antibodies.

Table 2.3 Antibodies and reagents used in flow cytometry

Antibody specificity	Label	Clone	Isotype	Source [c]	Dilution	Concentration	Order no.	Batch
FcR (CD16) [a]	none	2.4G2		hybridoma	1:40	***		
CD19	biotin	1D3		Pharmingen	1:200	62.5 ng / 5x10^5 cells	553784	MO51892
CD21 /35 [b]	FITC	7G6	rat IgG2b,κ	Pharmingen	1:200	62.5 ng / 5x10^5 cells	553818	MO52001
CD23 (FcεR)	PE	B3B4	rat IgG2a, κ	Pharmingen	1:20	250 ng / 5x10^5 cells	553139	MO54018
CD23	bio	B3B4	rat IgG2a, κ	Pharmingen	1:50	250 ng / 5x10^5 cells	553137	MO68588
CD138 (syndecan-1)	PE	281-2	rat IgG2a, κ	Pharmingen	1:200	25 ng / 5x10^5 cells	09345B	MO51030
CD138 (syndecan-1)	none	281-2		Pharmingen	1:100	125 ng / 5x10^5 cells	553712	MO73516
GL7/Ly77	FITC	GL7	rat IgM, κ	Pharmingen	1:100	125 ng / 5x10^5 cells	553666	MO54871
B220 (CD45R) [a]	biotin	RA3 3A1		hybridoma	1:35	***		
B220 (CD45R)	biotin	RA3-6B2	rat IgG2a, κ	Pharmingen	***	***	***	***
Streptavidin	FITC			Pharmingen				
Streptavidin	Tricolor			Caltag	1:100	50 ng / 5x10^5 cells	SA1006	

a) Rat anti-mouse B220 (RA3 3A1) (van Essen *et al.*, 1995) and rat anti-mouse Fc receptor (2.4G2) antibodies (Unkeless *et al.*, 1979) were purified from hybridoma supernatants.

b) In mice, CD21 and CD35 are altenate splice forms of complement receptors 2 and 1. This antibody will be referred to solely as anti-CD21 in the text.

c) Company locations: Caltag Laboratories, Burlingame, CA, USA.

Table 2.4 Isotype controls for flow cytometry [a)]

Isotype	Label	Source	Order no.	Batch
rat IgG2b,κ	FITC	Pharmingen	11184C	MO40705
rat IgG2a, κ	PE	Pharmingen	553930	MO73097
rat IgM, κ	FITC	Pharmingen	11054C	?
rat IgM, κ	biotin	Pharmingen	11052C	MO27261
rat IgG2a, κ	FITC	Pharmingen	110224C	MO34036
rat IgG1, κ	biotin	Pharmingen	11012C	MO28793

a) All antibodies were diluted to the same concentration as the antibody whose control they represented.

2.3 Animals

Female C57BL/6 mice bred in the SPF unit at the National Institute for Medical Research (London) were used at 6-12 weeks of age. Recombination activation gene (RAG)-2-deficient mice on a BALB/c background were used at 2-5.5 months of age and were kindly provided by Anton Rolink (Basel Institute for Immunology, Basel, Switzerland) (Young *et al.*, 1994). All mice were conventionally housed on sterile bedding, food and water. The food was autoclaved 41B rodent diet (Harlan) until May 2001 and was then changed to autoclaved CRM rodent diet (Harlan). For short-term experiments, animals were identified by tail marking with a waterproof Edding pen. In long-term experiments, 12-mm microchips (Avid, Uckfield, UK) were implanted for identification. The light cycle in the animal unit consisted of 12 h light and 12 h dark to mimic conditions in malaria-endemic regions. Mice were checked daily to identify gross health problems and cages were cleaned once a week.

Mice were usually killed by cervical dislocation. When large quantities of blood were required, mice were lethally anaesthetised by i.p. injection of 0.1-0.15 mL Sagatal Pentobarbitone sodium BP (#7SA005, Rhône-Mérieux). After 2-3 min, the effectivity of the anaesthesia was confirmed by absence of reaction to placing a finger on the mouse's eye or pinching between the toes. All injections were performed with sterile 1 mL syringes and 27G x _ " needles.

2.4 Parasites and infections

P. c. chabaudi clone (AS) was originally isolated from an African thicket rat (*Thamnomys rutilans*) by Dr. D. Walliker and cloned *in vivo* by passaging in mice (Carter and Walliker, 1975; Ladel *et al.*, 1995). The orginal frozen stabilate obtained from Dr. K.N. Brown (National Institute for Medical Research, London) had only been passaged five or six times in mice. In order to keep mutation and genetic drift to a minimum, frozen stocks were passaged once and then amplified by infection of large numbers of mice (e.g. 16 mice

for the present stock). Mice were lethally anaesthetised mice and bled out when the parasitaemia had reached 10-15%. The blood was centrifuged 10 min at 4°C and 500 x g and plasma removed without disturbing the erythrocyte pellet. Two pellet volumes of glycerol freezing medium (Section 2.1) were added dropwise. The solution was aliquoted into cryotubes, frozen rapidly at -80°C and then stored in liquid nitrogen until use. One batch of frozen stock was sufficient to initiate all infection series for 3-5 years before it became necessary to amplify another vial from the previous stock. This ensures genetic comparability between experiments performed at different times and makes the parasites as similar to the original stock as possible. Frozen stocks were negative for mycoplasma contamination and for common mouse pathogens such as hepatitis, pasteurella and lactate dehydrogenase virus.

Infections were initiated from frozen stocks by thawing the stock rapidly at room temperature by addition of 200µL of 0.9% sodium chloride (#S8776, Sigma) and injecting this i.p. into two to three mice. The erythrocytic stages of the parasites were passaged up to four times by i.p. injection of 100 µL of 0.9% sodium chloride containing 10^5 or 10^6 parasitised red blood cells obtained from infected mice before the peak of parasitaemia. Inoculum sizes were calculated by determining the percentage of parasitaemia in the infected mice and assuming an erythrocyte density of 6×10^9 / mL blood.

Taking blood before the peak of parasitaemia ensures that parasites are healthier and less likely to undergo antigenic variation in response to immune pressure. Keeping the number of passages low also reduces the amount of time in which antigenic variation can occur and prevents the increase of virulence seen when the erythrocytic stage of parasites is passaged for long periods (e.g. (Stevenson and Kraal, 1989)). An inoculum size of 10^5 *P. c. chabaudi* (AS) pRBC was chosen for all infections.

For drug-mediated elimination of parasites, mice were treated with three i.p. injections of 25 mg chloroquine / kg body weight in 0.9% saline solution at 48-h intervals, starting between days 30 and 35 of infection (Taylor *et al.*, 2001).

2.5 Staining of thin blood films

Thin blood films were made from tail blood and fixed with 100% methanol. For fast results, the blood films were stained with the LAMB/034-K (Raymond A. Lamb) by dipping six times each in first the acid dye and then the basic dye. For better quality staining the Giemsa stain was used (Section 2.1). Giemsa stain was made up fresh each day and could only be reused (for a maximum of three lots of slides) if the Coplin jar was wrapped in aluminium foil and covered with a lid to prevent oxidisation. Slides were immersed in the stain for 20 min and then rinsed thoroughly under running tap water. Slides were left to air dry and could then be stored indefinitely.

2.6 Counting parasitaemias

The parasitaemia was counted under oil immersion on the Zeiss Axioskop with a 100x objective (1200x final magnification). The grid in the eye piece was used to define fields for counting and the percentage of pRBC was calculated according to this formula:

$$\text{Parasitaemia [\%]} = \frac{\text{Total number of infected erythrocytes in } n \text{ fields}}{(\text{Total number of erythrocytes in a representative field}) \times n} \times 100\%$$

The number of fields counted varied, depending on the density of pRBC. Ten fields were counted for high parasitaemia (≥1%) and 50-100 fields for low parasitaemias (0.01%-0.1%), with twenty to thirty fields for intermediate levels of pRBC.

To calculate average parasitaemias, it is necessary to use geometric means, because variation in parasitaemias from the same day of infection does not follow a Gaussian

distribution in non-transformed mode due to the exponential expansion of parasites. The positive and negative standard error of a geometric mean differ when shown on a linear scale and the error is only shown in one direction in figures for clarity. The geometric mean is calculated by taking the average of the decadic logarithm of the parasitaemias and unlogging that result. The positive error is calculated by taking the SEM of the logged parasitaemias, unlogging the result and then multiplying that with the geometric mean.

2.7 Crude malarial extract

Crude malarial extract (preparation #38) was taken from laboratory stock. It was prepared in the following manner: Synchronously infected mice kept in reverse light cycle were bled out under lethal anasthaesia (Section 2.2) when the parasitaemia had exceeded 15%. Blood was taken at the late trophozoite stage and collected in heparinised syringes. CF11 columns were prepared for leukocyte removal by layering dry CF11 powder (Whatman International Ltd., Maidstone, UK) onto a thin bed of nylon wool (NEN Products) in a 5-mL syringe. The column was pre-washed with cold PBS and then loaded with the blood. The eluted erythrocytes were centrifuged 10 min at 500 x g and 4°C. The supernatant was removed carefully with a sterile glass pipette and the erythrocyte pellet washed twice in PBS. The erythrocyte membranes were lysed by addition of one to two drops of 10% saponin (BDH). Lysis took about 5 min and was complete when the solution had turned dark brown. The parastite pellet was washed three times in PBS and centrifuged 10 min at 750 x g and 4°C. The protease inhibitor aprotinin (Sigma) was added and the pellet was aliquoted and stored at -20°C until use.

2.8 Preparation of plasma

Syringes were filled with approximately 0.1 mL heparin (500 U) and used to take blood from the chest cavity after cutting the artery leading from the heart. For smaller quantities, a drop of heparin (about 3 µL or 15 U) was put in an Eppendorf tube and the pipette tip left coated with heparin. The mouse's tail was nicked with a scalpel blade and

blood flow encouraged by massaging gently from the base to the tip of the tail until 50 or 100 µL had been collected. The blood was centrifuged twice at 8500 x g and 4°C and the plasma removed. Samples were stored at -20°C.

2.9 Normal mouse plasma and hyperimmune plasm

Normal mouse plasma was prepared from uninfected mice as described in Section 2.8. Hyperimmune plasma was prepared from mice who had been infected six to eight times in 2-4-week intervals. Starting with the the fourth infection, titres of antibodies specific for crude malarial extract (see Section 2.7) were tested by ELISA (Section 2.29) 1 week after reinfection. If the levels of IgM, IgG1, IgG2a, IgG2b and IgG3 were sufficiently high, plasma was taken as described in Section 2.8.

2.10 Whole blood transfer

Blood donor mice which had been infected the stated number of months previously were lethally anaesthetised (Section 2.3) and after opening up the chest cavity, the artery under the heart was cut. A glass Pasteur pipette was used to transfer 200-250 µL heparinised Krebs saline buffer into the body cavity and then the blood buffer mixture was transferred to a sterile Eppendorf tube. The blood was taken up in a syringe, avoiding air bubbles and clots and two RAG-2-deficient mice injected i.p.with 300 µL, using two injection sites.

2.11 Immunisation with chicken gamma globulin (CGG)

Chicken gamma globulin (#003-000-002; Jackson Immunoresearch Inc., Bar Harbor, ME, USA) was diluted to a concentration of 1 mg/mL and then mixed with an equal volume of 9% potassium aluminium sulphate. Sodium hydroxide (1 M) was added dropwise until the maximum precipitate had formed. The precipitate was washed twice in 5 mL PBS by centrifuging 5 min at 300x g and then resuspended in 0.9% saline solution. Mice were injected i.p. with the precipitated equivalent of 25 µg CGG in a volume of 100 µL.

2.12 MSP-1 / MBP fusion proteins

The approximate equivalent of the C-terminal portion of MSP-1 is expressed in *E. coli* as a fusion protein with maltose binding protein (MBP) in the pMCK129 protein (amino acids 1640-1729; see Fig. 4.1). by a modified pMAL-CRI plasmid (McKean *et al.*, 1993a; McKean *et al.*, 1993b).

Plasmid-containing *E. coli* were grown overnight from glycerol stocks in 20 mL of rich medium (Section 2.1). This volume was then expanded to 1600 mL with rich medium. The bacteria were incubated at 37°C, shaking at 120 rpm until the OD_{600} reached 0.5. IPTG was added at 0.3 mM to induce protein expression and the culture incubated another 2 h. Bacteria were centrifuged 20 min at 4500 x g and 4°C. The pellet was resuspended in 120 mL amylose resin loading buffer (Section 2.1) with CompleteTM proteinase inhibitor (#1697498, Roche Diagnostics Ltd., Lewes, UK). The bacteria were lysed at 10 000 pounds per square inch with the cell disruption device in the large scale cell culture lab at the NIMR and the debris cleared by centrifuging 30 min at 4°C and 17 400 x g, followed by a 2-h centrifugation in an ultracentrifuge at 40 000 rpm and 4°C. The supernatant was snap-frozen and stored at -70°C or passed directly over an amylose resin column for affinity purification.

2.13 Affinity purification of MBP fusion protein

An Amersham Pharmacia XK 16 column (Amersham Pharmacia, Little Chalfont, UK) was packed with the MBP-binding amylose resin (# 800-21L, New England Biolabs, Hitchin, UK) according to the instructions supplied by New England Biolabs. The ultracentrifuged bacterial supernatant from the previous section was filtered through a 0.22-µm filter (GV type filter, # GVWP04700, Millipore, Watford, UK) in a Reusable Bottle Top Filter (# 0320-5033, Nalgene, Milton Keynes, UK) and diluted fourfold in loading buffer. The sample was run over the prepared amylose resin column at 1 mL/min or less at 4°C and the OD_{280} of the effluent monitored to detect the presence of protein.

For large quantities of protein, the amylose resin was loaded by batch binding, in which the resin was transferred into 50-mL tubes containing the supernatant. These were placed for 2 h on an end-over-end roller at 4°C and after that time the column was repacked.

The column was washed with at least three to five column volumes of loading buffer until the OD_{280} had returned to the baseline. Bound protein was eluted with elution buffer (Section 2.1). The eluted protein was detected by the change in the OD_{280}. The column was regenerated by washing with three column volumes dH_2O, three column volumes 0.1 % w/v SDS (at room temperature), three column volumes dH_2O and three column volumes loading buffer.

Samples were taken before loading, from the effluent during loading and during elution to determine the efficacy of the affinity binding. This was done by measurement of the protein concentration (Section 2.14) and SDS-PAGE followed by Coomassie Brilliant Blue or silver staining (Sections 2.15-2.17). The gels also showed whether the protein had been contaminated or degraded. The eluted protein was concentrated in an Amicon concentrator with a 10 kDa cutoff ultrafiltration membrane (#13622, Millipore) and stored at -70°C.

2.14 Measuring protein concentrations

Protein concentrations were measured with the BCA protein assay (#23223, Pierce, Rockford, IL) according to the manufacturer's instructions. Components A and B were mixed in a ratio of 50 parts to 1 part. The reaction was carried out in flat-bottom 96-well plates and each well contained 200 µL of the pre-mixed BCA reagents and 25 µL of the protein. Concentrations of BSA (diluted in the same buffer as the protein samples) ranging from 0-2 mg / mL were included as a standard. The plate was covered with an acetate plate sealer (#76-401-05, ICN Biomedicals, Aurora, OH, USA) and incubated at 37°C for 30 min. The optical density at 565 nm was measured on the ELISA reader and the protein concentration calculated by comparison with BSA the standard curve.

2.15 Reducing SDS-PAGE

Denaturing, discontinuous SDS-PAGE under reducing conditions was performed according to the Laemmli method as described in Current Protocols in Immunology (John Wiley and Sons Inc., 1995). SDS-PAGE gels were cast and run in the BIO-RAD Mini Protean II system. The gels were made up according to the following recipes:

Separating gel (for 2 gels)

Stock solutions	Final acrylamide concentration		
	7.5%	10%	12.5%
Ultra pure protogel	2.5 mL	3.3 mL	4.16 mL
1 M Tris pH8.8	3.75 mL	3.75 mL	3.75 mL
10% w/v SDS	0.1 mL	0.1 mL	0.1 mL
dH_2O (ml)	3.6 mL	2.8 mL	1.94 mL
10% w/v APS	50 µL	50 µL	50 µL
TEMED	5 µL	5 µL	5 µL

Stacking gel (for 2 gels)

Stock solutions	Final acrylamide concentration 4%
Ultra pure protogel	1.3 mL
1M Tris pH 6.8	1.25 mL
10% w/v SDS	0.1 mL
dH_2O (ml)	7.3 mL:
10% w/v APS	100 µL
TEMED	30 µL

The reagents were procured from the following suppliers: Ultra pure Protogel (30 % acrylamide, 0.8 % bisacrylamide, premixed solution; # EC-890 (1 L), National Diagnostics), TEMED (N, N, N', N'-Tetramethylethylenediamine, #15524-010, GibcoBRL), APS (ammonium persulphate, #15523-012, GibcoBRL) and Trizma Base (#T-8524, Sigma).

The gel constituents were mixed immediately before use, with APS and TEMED being added before casting. The separating gel was poured first, overlayed with dH_2O and left to polymerise. Then the separating gel was poured with a plastic comb creating pockets. Once this layer had polymerised as well, the gel was transferred to the electrophoresis chamber which was filled with running buffer (diluted down to 1x concentration from the buffer in Section 2.1).

Samples were diluted with an equal volume of reducing loading buffer (Section 2.1) and heated for 5 min at 95°C to denature the proteins. Protein samples were loaded into the pockets of the stacking gel and a prestained protein medium molecular weight standard with a range of approximately 14-200 kDa (#26041-020, GIBCO/BRL) was included. A constant voltage of 120 V was applied to the gel and progress of the proteins was monitored by the location of the bromphenol blue band. (For better resolution, the voltage could be kept at 80-100 V until the blue band had exited the stacking gel.) Proteins were revealed by Coomassie or silver staining (described below).

2.16 Coomassie staining of SDS-PAGE gels

Coomassie staining was used as the standard method for protein visualisation in SDS-PAGE gels (detection limit:about 1 μg protein). Buffers were prepared as described in Section 2.1. The gel was covered with Coomassie staining solution and placed on shaker for 1 h at room temperature or until the gel had absorbed the blue colour. After this, the staining solution was poured off and the gel rinsed in deionised water followed by incubation with destain solution. A piece of tissue paper was included in the staining tray to aborb the blue colour and speed up the destaining process. The gel was placed on a shaker until the protein bands became visible in blue and the background was clear or only moderately stained. The destaining solution was replaced by deionised water. Gels were stored that way for photography or dried onto Whatman filter paper with a Scie-Plas gel drier (model GD4534). The Coomassie staining solution was reused up to ten times by

pouring the used solution through Whatman filter paper (e.g. No. 1, 15 cm diameter, internal orders).

2.17 Silver staining of SDS-PAGE gels

For greater sensitivity, SDS-PAGE gels were silver stained (detection limit 2-5 ng of protein). All buffers except for DTT stock were made up fresh (Section 2.1). Gels were washed in fixative for 15 min and washed thoroughly at least twice in deionised H_2O. Then they were incubated for 15 min in 25 mL DTT at 5 µg/mL (diluted 1:1000 from stock in Section 2.1) and the solution was poured off without rinsing. The next incuabation was for 15 min in 25 mL silver nitrate solution, which had to be removed in a swirling fashion to ensure even staining. Gels were rinsed once in a small volume of deionised H_2O and twice in 25 mL developer. Finally the gel was incubated 25 mL developer until brown- or silver-coloured bands became visible and the reaction was stopped by several washes in deionised H_2O.

2.18 Expression of MSP-1 in *Pichia pastoris*

Dr. Meike Hensmann, Dr. Ching Li and Dr. Robin Stephens (Division of Parasitology, NIMR) kindly supplied the purified recombinant MSP-1_{21} fragment expressed by *Pichia pastoris*. The methods basically followed those outlined in the Invitrogen manuals. In brief, the Hxa vector was produced by Dr. Bill Morgan (NIMR) by addition of an N-terminal six-histidine (His) tag to the Invitrogen pIC9K vector (Morgan *et al.*, 1999). The MSP-1_{21} fragment was inserted into a blunt-ended *PmlI* site and the vector cloned into competent *Escherichia coli (E. coli)* cells, which were selected on kanamycin. The vector was then transfected into competent SD1168 *Pichia pastoris* cells by electroporation and clones with multiple inserts selected by high concentrations of G418. The yeast cells were expanded with glycerol as a carbon source and protein expression via the AOX promoters was induced by switching to methanol, which was added in 24-h intervals over

3-4 days. The protein was purified via the His tag with the aid of a nickel column and then passed over a gel filtration column to remove further contaminants.

2.19 Tissue preparation for immunohistology

The methods in sections 2.19-2.22 were performed according to standard protocols from the laboratory of Prof. Ian MacLennan (Division of Infection and Immunity, University of Birmingham, Birmingham, UK) and are partially described in (Luther *et al.*, 1997). Spleens were removed after cervical dislocation. The ends were cut off and the spleen was placed on a rectangle of aluminium foil. The enlarged spleens from later stages of infection were halved before freezing. The spleens were snap frozen by repeated dipping in liquid nitrogen, which prevents tissue cracking. They were placed in gripseal plastic bags and stored at -70°C

2.20 Cryosectioning

Cold OCT compound (# 4583, Sakura, Zoeterwede, The Netherlands) was placed on a cryostat chuck and the frozen spleen gently pressed into the embedding compound with the widest flat plan facing upwards. The freezing process was started with Quickfreeze spray (#1950, Histological Equipment Ltd., Nottingham, UK) and spleens were left 20 min to freeze. Sections were cut either in a Bright cryostat at the Medical School in Birmingham or a Jung 2000 cryostat at the National Institute for Medical Research in London. In the latter, the chamber temperature was set at -23°C and the object temperature at -19°C. The top layers of the spleen were trimmed off and the cutting surface shaped with a scalpel so that the hardened OCT compound formed a supporting structure without being cut itself and the splenic capsule was trimmed off to prevent jerky cutting on account of different hardnesses. Serial 5-µm cryosections were mounted on four-spot glass slides (#PH-005, Hendley Essex, Loughton, UK). Slides were allowed to air dry at room temperature with a fan for at least 1 h. They were fixed in 90% acetone at 4°C for 20 min, air dried and stored in gripseal bags at -20°C until use.

2.21 Immunohistology

Slides were allowed to adjust completely to room temperature before opening the gripseal bags and then washed for 5 min in 0.05 M TBS pH 7.6 (see Section 2.1). All antibodies were diluted in 0.05 M TBS pH 7.6 (dilutions see Tables 2.1 and 2.2) and mixtures of antibodies applied at 75 µL per section. The sections were incubated with the primary antibodies for 1 h at room temperature in a moist chamber. Sections were washed twice in 0.05 M TBS pH 7.6, followed by a 45 min incubation with secondary HRP- or AP-labelled antibodies. All secondary antibodies had been preincubated for 30 min with 10% normal mouse plasma (see Section 2.9) in a volume of 50-100 µL to minimise binding to mouse tissues. AP- or HRP-labelled StreptABC complex (#K0391 and #K0377, DAKO, Cambridgeshire, UK) was prepared by mixing 45 µL each of components A and B in 5 mL 0.05 M TBS pH 7.6 and waiting at least 30 min before use. After two 5-min washes, StreptABC complex was added to the sections for 30 min to bind to biotin-labelled antibodies. This was followed by two more washes.

Sections were developed first for HRP activity with freshly prepared diaminobenzidine tetrahydrochloride (DAB;#D-5905, Sigma) solution. One tablet (10 mg) was dissolved in 15 mL 0.05 M TBS pH 7.6 buffer and the solution filtered through Whatman No. 1 filter paper. One drop of H_2O_2 was added to 10 mL of the filtrate to inhibit endogenous peroxidases. Sections were incubated with the solution until the brown stain was sufficiently developed and then washed twice in 0.05 M TBS pH 7.6. AP activity was detected using the substrate Naphthol AS-MX phosphate (0.4 mg/mL, #N-4875, Sigma) and the chromogen Fast Blue BB salt (1 mg/mL, #F-3378, Sigma) in 0.1 M TBS pH 9.2, containing .0.8 mg/mL levamisole (#L-9756, Sigma), which inhibits endogenous phosphatases, and 3.8% v/v N,N-dimethylformamide (#D-4254, Sigma). The solution was filtered through Whatman paper and applied to the sections. Sections were developed until the blue stain was sufficiently strong and then washed twice in 0.05 M

TBS pH 7.6 and once in distilled water for 5 min each. The slides were then mounted in Immuno-Mount (#999 0402, Shandon, Pittsburgh, PA) with 23x65 mm^2 coverslips (BDH).

2.22 Size measurements in histological sections

The size of the germinal centers (PNA^+ areas in the follicular mantle) and of total spleen sections was determined by systematic perusal of the entire section through the grid of the microscope ocular while counting the number of grid intersections that fell within the area of interest. This measurement was converted into mm^2 by comparison with the grid of a Neubauer counting chamber at the same magnification. Where spleens had to be halved for cryosectioning, germinal center numbers were extrapolated for whole spleens.

2.23 Haematoxylin and eosin staining of splenic sections

Spleens were fixed 24 h in 10% neutral buffered formalin. They were then given to the Histology Division at the NIMR, where they were embedded in fibrowax (BDH) and sectioned. The sections were stained with Ehrlich's haematoxylin and eosin, dehydrated in graded alcohols, cleared with Histoclear (National Diagnostics, Hull, UK) and mounted in DPX (BDH).

2.24 Nonspecific esterase staining

Spleens were placed in buffered formol sucrose for 24 h and then in gum sucrose for 24 h (Section 2.1) and then frozen by repeated dipping in liquid nitrogen. Cryosections of 5-8 μm thickness were made as described in Section 2.20, except that the slides were dried for 30 min at 37°C and then processed immediately. Nonspecific esterase staining was performed with an α-naphthyl acetate esterase kit (#91-A, Sigma). Slides were placed in the fixative for 30 s and agitated for the last 5 s. They were rinsed in running deionised water for 45-60 s and then immediately placed in foil-wrapped Coplin jars containing the α-NE staining solution. The slides were stained for 30 min and then rinsed under running

deionised water for 2 min. The hematoxilyn supplied with the kit was used to counterstain the slides for 2 min and rinsed off with tap water. After air drying, the slides were mounted in Immunomount.

2.25 Detection of antigen-specific B cells specific by immunohistology

CGG-specific B cells were detected by binding of biotinylated CGG (kindly supplied by Prof. Ian MacLennan) to immunoglobulin. The biotinylated antigen was used at a dilution of 1:150 and detected as described above.

MSP-1_{21}-specific B cells were detected by binding of the MSP-1_{21} / MBP fusion protein pMCK 129 to immunoglobulin. The fusion protein was then detected with rabbit anti-MBP followed by biotin-labelled swine anti-rabbit immunoglobulins (see Tables 2.1 and 2.2). As the MBP binds to a number of sugar residues including starch, all antibodies and the StreptABC were diluted in 0.05 M TBS pH 7.6 supplemented with 10 mM maltose to inhibit binding by MBP. All further steps were performed as described in Section 2.21.

2.26 Flow cytometry

Spleens were collected into 10 mL supplemented HBSS. Single cell suspensions were made by pressing spleens through a fine-meshed sieve into 5 mL supplemented HBSS (Section 2.1). The volume was made up to 30 mL and the splenocytes were washed by centrifuging for 10 min at 4°C and 240 x g. Erythrocytes were lysed by 10 min incubation with 0.16 M NH_4Cl_2-Tris buffer, pH 7.2. The cells were washed again in supplemented HBSS and resuspended in 10 mL FACS buffer (see Section 2.1). Cells were filtered through cell strainer caps to remove clumps and stained with a Trypan blue (#T-8154, Sigma, diluted 1:4) to distinguish dead cells. Cells were counted in a Neubauer chamber and the cells aliquoted into 5-mL FACS tubes (#35202, Falcon) or round-bottom 96-well

PS microplates (#650101, Greiner), depending on the number of samples. Each sample contained $5x10^5$ live cells. Cells were kept in the dark and on ice from now on.

Fluorochrome-labelled antibodies were diluted in FACS buffer (dilutions in Table 2.3), centrifuged 5 min at 8500 x g and 4°C to remove aggregates and added at 25 µL per sample. Anti-Fc receptor antibody (Unkeless, 1979) was added to all samples to prevent non-antigen-specific antibody binding via the Fc component. This was followed immediately by the first antibody. All antibody incubation steps were 15-25 min long. They were followed by two washes in 150 µL or 2 mL FACS buffer, for plates or tubes respectively, for 5 min at 240 x g and 4°C. After the final wash, cells were resuspended in 250-300 µL FACS buffer. If the staining was performed in plates, they were now transferred to 1-2 mL Cluster tubes (#4401, Costar, Corning, NY, USA). Samples were acquired on a FACScalibur® at a maximum speed of 2000 events per second. Cells stained with a single fluorochrome were used to calibrate the flow cytometer so that the emission from each fluorochrome was registered in separate fluorescence channels. The results were analysed with CellQuest Pro 4.0.1 software (BD Biosciences, San José, CA). Gates defining cell populations were set by comparisons with isotype control staining.

Staining plasma cells with the anti-syndecan-1 antibody can be complicated (personal communications by Anja Hauser, Deutsches Rheumaforschungszentrum, Berlin, Germany and Kai Toellner, Division of Infection and Immunity, University of Birmingham, Birmingham, UK). After trying numerous methods, the best results (i.e low background and identifiable populations) were achieved by using FACS buffer without sodium azide and otherwise adhering to the method described above. The results are clear for high numbers of plasma cells, but it is difficult to identify small populations accurately and therefore, the results with low numbers of antibody-containing cells are prone to error.

2.27 Cell death in flow cytometry

The nuclear binding marker 7-aminoactinomycin D (7-AAD; #A-9400, Sigma) was used to detect apoptotic cells, with the necrotic cell marker propidium iodide used in parallel to ascertain that the majority of the 7-AAD$^+$ cells were actually apoptotic. Unfixed, nonpermeabilised splenocytes were stained as described in the previous section. In the final step, either 7-AAD (1 μg/2.5 x 10^5 cells) or propidium iodide (1 μg/2.5 x 10^5 cells; #P-4864, Sigma) was added for 20 or 5 min, respectively. Cells were then analysed on the FACScalibur® without any further washes.

2.28 Annexin V staining

Annexin V binds to the membrane phospholipid phosphatidylserine which is translocated from the inner to the outer leaflet of the plasma membrane in apoptotic cells. Annexin V is therefore used as an early apoptosis marker. Cells (2.5 x 10^5 per well) were prepared and stained as described in Section 2.26, with all steps reduced to the minimal possible times. At the end, the cells were washed twice in cold PBS to remove all EDTA and resuspended in 200 μL binding buffer. The samples were transferred to the final tubes and 2 μL of allophycocyanin (APC)-labelled annexin V (#209-252-T100, lot L08625, Alexis Biochemicals, Lausen, Switzerland) added per tube. The samples were incubate 10 min at room temperature in the dark and the acquisition performed within the next hour.

2.29 Enzyme-linked immunosorbent assay (ELISA) for MSP-1 specific IgG

The *Pichia*-produced MSP-1_{21} was diluted to a concentration of 5 μg/mL in carbonate buffer pH 9.5 (Section 2.1). Flat-bottom 96-well polysorb plates (Nunc,) were coated overnight at 37°C with 50 μL/well of the antigen. All incubation steps were performed in a moist chamber in the dark. Plates were flicked out and incubated for 2 h at 37°C with 200 μL blocking buffer (Section 2.1) per well to prevent nonspecific binding to the plastic. Plates were washed by hand with a 12-channel washer (Nunc). The test sera and hyperimmune serum (Section 2.9) and normal serum (Section 2.9) - all from C57BL/6 mice - were diluted in blocking buffer in a two-fold titration starting with a 1:50 dilution

and applied at 50 µL per well. Each ELISA plate also contained two controls: C57BL/6 normal mouse plasma to assess background reactivity and C57BL/6 hyperrimmune plasma as a standard (preparation described in Section 2.9). The controls were titrated in the same fashion as the samples, except that there was only one row of each control per plate since the inclusion on all plates provided replicates. Background staining by normal mouse plasma was consistently low for all plates. The plates were incubated 1 h at 37°C and then washed. AP-labelled goat anti-mouse IgG (Section 2.2) was diluted 1:1000 in PBS, added at 50 µL per well and incubated for 1 h at 37°C.

The substrate for the alkaline phosphatase was made up by diluting PNPP capsules (nitrophenylphospate-sodium salt, #N-9389, Sigma) at 1 mg/mL in diethanolamine buffer (Section 2.1). Another particularly thorough wash followed and then 50 µL of PNPP substrate were added per well. The plates were kept in the dark at room temperature while monitoring the change in optical density. Once the optical density at 405 nm reached the range of 0.5-1.0 for the 1:50 dilutions of the test sera, measurements were taken with the ELISA reader (Vmax Kinetic Microplate Reader, Molecular Device Corporation, Sunnyvale, CA, USA). Data was analysed with the Revelation 3.0 program.

The OD values were converted into arbitrary units by designating the binding of hyperimmune plasma as 1 Unit. Plasma IgG titres were calculated from all measurements where the titration resulted in a linear decrease in OD and these values were averaged arithmetically. IgG titres from different mice were averaged geometrically.

2.30 Enzyme-linked immunosorbent assay (ELISA) with crude malarial extract

Crude malarial extract was prepared as described in Section 2.7. A 50-µL aliquot was thawed and diluted in 200 µl parasite lysis buffer (Section 2.1). A portion of this sample was then diluted 1:100 in PBS so that the OD_{280} was between 0.1 and 0.2. Plates were coated with 50 µL per well and after that, the ELISA was carried out as described in Section 2.29.

2.31 Chaotropic ion dissociation in ELISA

In this assay, the concentrations of plasma, coating antigen and detecting antibody are kept constant and the variant factor is the concentration of sodium thiocyanate (S-7757, Sigma) (Kang *et al.*, 1998). The coating and blocking steps were performed as descibed in Section 2.29. For the next step, two different serum concentrations were chosen, which were from the linear portions of the respective IgG titration curves. For sera taken during secondary infections and hyperimmune serum, which would have high MSP-1_{21}-specific IgG titres, a dilution of 1:800 was chosen. All other sera were diluted in 1:100. Dilutions were in ELISA diluent buffer. This incubation step was again 1 h at 37°C. Sodium thiocyanate titrations ranging from 0-3 M salt concentrations were made in PBS and were applied to the plates for exactly 15 min, after which the reaction was stopped by flicking out the plates and covering the wells with wash buffer. For sera diluted 1:800, there were 11 salt concentrations for sera diluted 1:100 only 7 salt concentrations due to limited amounts of serum. Hyperimmune serum was applied in a single row per plate, all other sera were in duplicate rows. All further steps were performed as described in Section 2.29.

2.32 Statistics

Data were analysed with a two-tailed Mann-Whitney test with a 95% confidence interval, because this does not assume a Gaussian distribution of values. Probabilities of less than 0.05 were considered statistically significant. All statistical analyses were performed with Prism Graphpad, version 3.0c (Graphpad Software, Inc., San Diego, CA).

3. Splenic responses to primary infection with malaria

3.1 Introduction

3.1.1 The spleen as the main lymphoid organ for malaria infection

This section deals with the analysis of the microstructure of the spleen and the population dynamics of the splenic lymphocyte subsets during primary infection with *P. c. chabaudi*. Immunohistology and flow cytometry are used to analyse the splenic B cell populations and thereby assess the potential for long-lived malaria-specific B cell responses.

The spleen is separated into the red and white pulp. Macrophages filter the blood and phagocytose defective erythrocytes in filtration beds in the red pulp whereas the white pulp is a major site of immune effector cell development. This combination makes the spleen the main lymphoid organ dealing with blood-borne infections (reviewed in (Kraal, 1992)). This holds true for malaria, as numerous studies have shown that the spleen improves the ability of human, monkey and rodent hosts to control parasitaemia (e.g. (Butcher *et al.*, 1978; Favila-Castillo *et al.*, 1996; Israeli *et al.*, 1987; Petersen *et al.*, 1992; Spitalny *et al.*, 1976; Wyler *et al.*, 1977)). It has also been shown that an intact splenic microarchitecture is required for effective immune responses against malaria infections, including *P. c. chabaudi* infection (Yap and Stevenson, 1994).

3.1.2 Blood flow within the spleen

The current model of blood flow in the rodent spleen is as follows (reviewed in (Kraal, 1992; Steiniger and Barth, 2000)): Several branches of the splenic artery enter the main body of the spleen and give rise to the central arterioles. Capillaries leave the central arterioles at right angles to empty into the marginal sinus, which is formed by a series of vascular spaces but is not classed as a true blood vessel because it lacks high endothelial venules. Larger branches of the central arterioles traverse the red pulp as „marginal zone bridging channels“ or „terminal arterioles“ ending in the splenic cords (also known as

cords of Billroth). The splenic cords contain large number of mature macrophages, as well as B and T lymphocytes, erythrocytes, thrombocytes, granulocytes, some plasma cells and haematopoietic cells in a network of fibroblasts. Blood passes from the splenic cords into the splenic sinuses (or sinusoids) of the red pulp, which are vessels lined by endothelia with intercellular slits. These vessels carry the blood out of the spleen. The splenic cords and the marginal sinus constitute the open component of splenic circulation and the closed component is formed by the arteries and capillaries. Most of the work elucidating these connections has been done on rat spleens and there is still debate about the relative extents of open and closed circulation.

3.1.3 White pulp architecture

The structure of the splenic white pulp is schematically depicted in Fig. 3.1 and is reviewed in (Steiniger and Barth, 2000). In rodents, the white pulp is organised concentrically around the central arterioles and consists of three compartments: the T zone or periarteriolar lymphatic sheath (PALS), the follicular mantle and the marginal zone. The T zone surrounds the central arteriole and is in turn enveloped by the follicular mantle, which consists of individual follicles. Primary follicles contain a uniform population of naive recirculating B cells (also known as follicular B cells), which are characterised by surface IgD and IgM and have a short life span unless they become activated by antigen encounter. Secondary follicles contain a germinal centre and the recirculating cells are displaced to the outer edge of the follicle. The T zone and B cell follicles are girdled by the marginal zone, whose border is demarcated by the marginal sinus.

3.1.4 Differences between human and mouse spleens

Human spleens differ from rodent spleens in a number of aspects (reviewed in (Steiniger and Barth, 2000)). In the white pulp, T cell areas are more dispersed, with many sections of the central arterioles surrounded only by B cell follicles, which consist of four rather

Figure. 3.1 Overview of white pulp structure and cell populations.

(a) Schematic representation of the separation of the spleen into red and white pulp areas.

(b) Division of the white pulp into different functional areas. An extrafollicular focus of antibody-containing cells is also shown as an element of the red pulp, which lies at the edge of marginal zone bridging channels.

(c) Detailed structure of the marginal zone which also shows central arteriole branches terminating in the marginal sinus and red pulp. This panel is a colored reproduction of a figure in (Kraal, 1992).

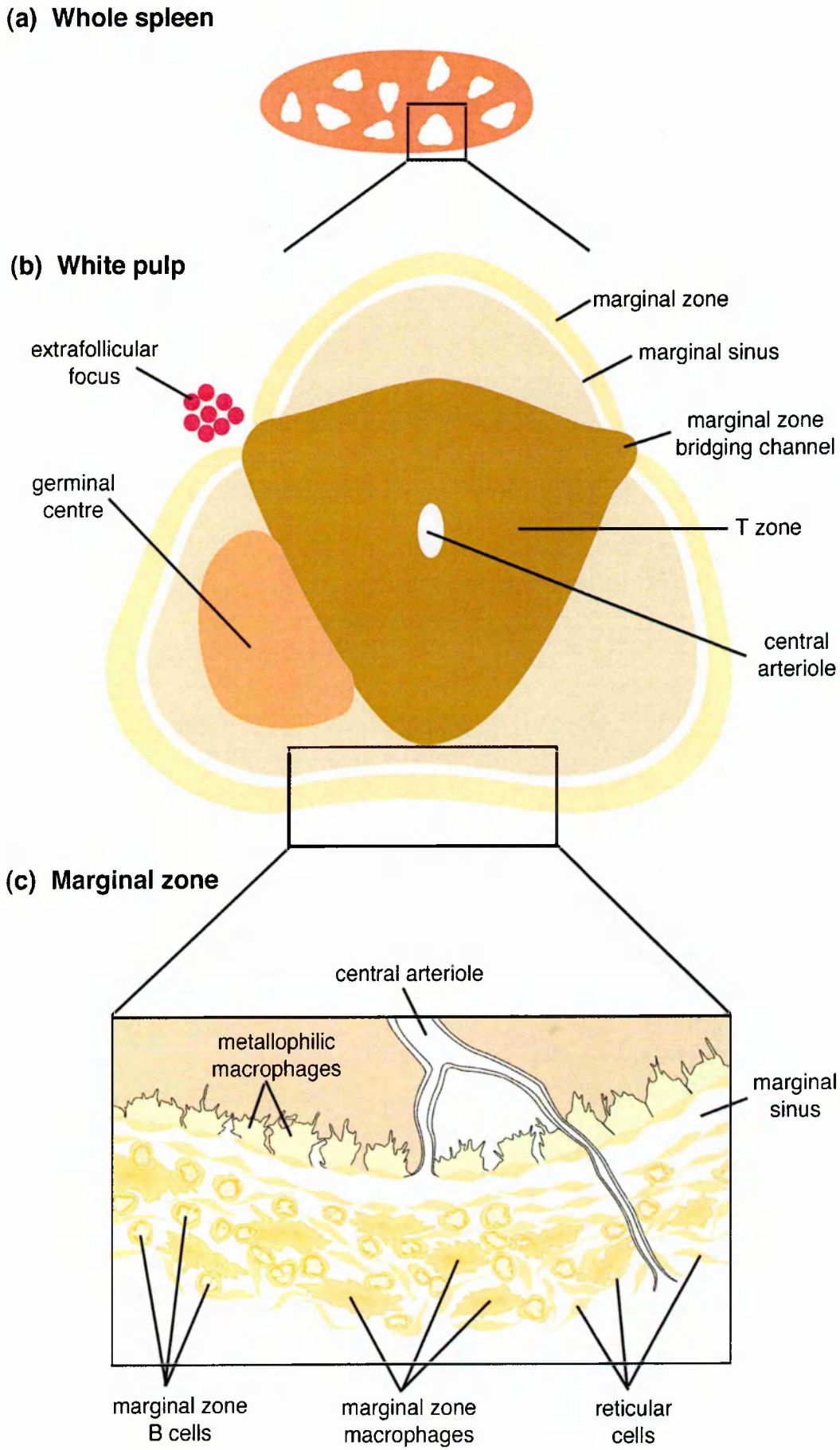
(a) Whole spleen
(b) White pulp
marginal zone
marginal sinus
extrafollicular focus
marginal zone bridging channel
germinal centre
T zone
central arteriole
(c) Marginal zone
central arteriole
metallophilic macrophages
marginal sinus
marginal zone B cells
marginal zone macrophages
reticular cells

than three distinct areas - the germinal centre, the corona (which corresponds to the follicular mantle of rodent spleens), the marginal zone and the perifollicular zone, which is sometimes viewed as part of the red pulp. The overall shape of these follicles tends to be globular rather than hemispheric. Marginal sinuses and marginal zone metallophilic macrophages (described below) are absent, but a unique form of macrophage-sheathed blood vessel, the sheathed capillary, can be found in the perifollicular zone. Despite the differences in structure and possibly in blood circulation, the spleen appears to function similarly to its rodent counterparts, with one exception. Human spleens do not become additional sites of haematopoiesis in times of haematological stress, a phenomenon common in rodent spleens (e.g. (Nikcevich *et al.*, 1986)).

3.1.5 B cell populations of the spleen

This chapter studies the cells generated in the spleen in the follicular and extra-follicular B cell responses. This differentiation is performed by studying the four major B cell populations of the spleen: naïve recirculating B cells, germinal centre B cells as the source of memory B cells and long-lived plasma cells, plasma cells and their plasmablast precursors (grouped as antibody-containing cells) and the marginal zone B cells. Naïve recirculating B cells have already been discussed in Sections 1.3.4 and 3.1.3 and germinal centres and antibody-containing cells in Sections 1.3.6 and 1.3.7.

3.1.6 The marginal zone

The marginal zone contains three unique cell populations: metallophilic macrophages, marginal zone macrophages and marginal zone B cells (Fig. 3.1c). The marginal zone metallophilic macrophages have a characteristic appearance, especially in small rodents, with slender cell processes extending into the white pulp. Located on the white pulp side of the marginal sinus, they are well situated for degradation of foreign material and interaction with both stationary and migrating lymphocytes, but their actual functions are

still unknown. Marginal zone macrophages are distributed between the marginal sinus and the red pulp and appear to be in close contact with marginal zone B cells. They are highly phagocytic and specialise in the uptake of neutral polysaccharides, which are classed as thymus-independent type 2 (TI-2) antigens (reviewed in (Kraal, 1992)).

The marginal zone is also enriched in a population of B cells differing from the adjacent follicular B cells. They are IgM^{high} IgD^{low} $CD21^{high}$ $CD23^{low}$ as opposed to the mainly IgM^{low} IgD^{high} $CD21^{int}$ $CD23^{high}$ phenotype in the follicles (Oliver *et al.*, 1997). They are also larger than the follicular B cells and do not recirculate but display high motility in response to stimuli such as heat-killed *E. coli* (Gray *et al.*, 1984; Gray *et al.*, 1982). Marginal zone B cells can be generated in a thymus-independent manner (Kumararatne and MacLennan, 1981; Kumararatne and MacLennan, 1982) and are preferentially selected into this pathway by weak signals through the B cell receptor (Cariappa *et al.*, 2001), leading to a clonally restricted repertoire. This cell type is only found in the spleen, although attempts have been made to define equivalents in the lymph nodes.

The function of these cells has been studied in mice lacking the tyrosine kinase Pyk-2 which do not produce marginal zone B cells. They are deficient in thymus-independent type II responses and to a lesser extent in thymus-independent type I responses (Guinamard *et al.*, 2000) suggesting a role for MZ B cells in these responses. There is also a smaller group of marginal zone B cells which responds to thymus-dependent antigens. Marginal zone B cells are particularly responsive to blood-borne particulate antigens (Martin *et al.*, 2001) and polysaccharide antigens are specifically targeted to marginal zone B cells via complement, creating a link between the innate and adaptive immune systems (Guinamard *et al.*, 2000). Therefore, along with B1 cells, marginal zone B cells are often described as the source of „natural memory“ and „natural antibody“ and are very important in the early immune response.

In VH81X_Ig heavy chain transgenic mice, which have a higher proportion of marginal zone B cells, it was shown that marginal zone cells are not activated *per se*, because they do not express increased levels of the activation markers CD69, CD25, MHC class I, MHC class II and CD95 as compared to follicular B cells (Oliver *et al.*, 1999). However, their surface antigens indicate a memory phenotype characteristic of previous antigen encounter, i.e. decreased levels of CD62L and IgD and increased levels of CD44, B7.1 and B7.2. In addition, they have lower thresholds for activation, proliferation and differentiation into antibody-secreting cells and are more sensitive to apoptosis than the recirculating follicular B cells (Kumararatne *et al.*, 1980; Martin *et al.*, 2001; Oliver *et al.*, 1997; Oliver *et al.*, 1999). Therefore, these cells are sometimes classed as a particular subtype of memory B cells (first suggested by (Liu *et al.*, 1988)) or as a mixture of memory and virgin cells.

3.1.7 Aims and strategy

In this chapter, immunohistology was used to analyse the four splenic B cell populations during a primary infection with *P. c. chabaudi* in comparison with a classic immunisation model. The following aspects were studied:

(i) the respective distribution of T cells and recirculating naive B cells by staining for CD3 and IgD,

(ii) the extrafollicular antibody response by staining cells committed to plasma cell differentiation with syndecan-1 (CD138),

(iii) the development and persistence of germinal centres by staining for PNA binding,

(iv) the involvement of marginal zone B cells by IgM staining in the marginal zones.

Flow-cytometric analysis was used to validate these data with quantitative evaluations and to assess the extent of apoptosis in the different B cell populations.

3.2 Results

3.2.1 Experimental design

C57BL/6 mice were infected with 10^5 *P. c. chabaudi* (AS) parasitised red blood cells (pRBC) and spleens were taken at various time points afterwards for analysis. Days 3-8 represent the stage of ascending parasitaemia, days 9-12 the peak, days 16-30 the late stages and recrudescence and days 40 and 60 the phase when parasitaemia is no longer detectable by thin blood smear.

The main methods of analysis in this section are immunohistology and flow cytometry (Fig. 3.2). Two series of infected spleens with three mice per time point were frozen for cryosectioning and immunohistology. The first series encompassed days 0, 4, 8, 10, 16, 20, and 40 of infection and the second supplied additional information for the peak and late stages of infection with days 7-12, 20, 30 and 60. Cryosections of 5 μm thickness were made so that approximately one layer of cells would appear in the sections. The aim was to have four consecutive sections on each microscope slide so that four different stain combinations could be applied to spatially close areas in the spleens. Often, anti-IgD was used in several consecutive stain combinations to allow orientation in the spleen and make comparison between sections easier. However, most of the malarial spleens were difficult to cut because of their increased size and fragility. Therefore, some sections had to be discarded and a slide did not always contain absolutely consecutive sections.

All of the primary and secondary antibodies used for immunohistology in these experiments have been carefully tested for cross-reactivity and have been used extensively in the laboratory of Prof. Ian MacLennan (University of Birmingham, UK). In addition, most of the primary antibodies share the same labelled secondary reagent and can thus act as controls for each other. Each of the antibodies causes a unique staining pattern, demonstrating that there is no nonspecific binding by the secondary antibody.

Figure 3.2 Experimental design for Section 3.

The left-hand side depicts the use of immunohistology to determine the relative location of splenic cell populations. The right-hand side shows the use of flow cytometry to quantify splenic B cell populations. It also shows how the live cell gate is defined in a profile graphing the side scatter (which is a marker of cell granularity) against the forward scatter (which is a marker of cell size) of unstained cell populations. Only cells from the live cell gate were then used for the further analyses. The examples are from a naive and a day-20 infected mouse and are representative of the live cell gates on which the flow cytometry plots in Figs. 3.4, 3.5, 3.8, 3.9, 3.10, 3.12 and 3.13 are based.

pRBC (*P. c. chabaudi*): erythrocytes infected with *P. c. chabaudi* (AS)

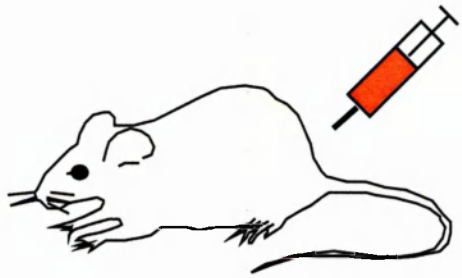

10^5 pRBC (*P. c. chabaudi* (AS))

OR

25 µg alum-precipitated CGG

IMMUNOHISTOLOGY

FLOW CYTOMETRY

spleens

Cryosections (5 µm thick)

count live cells / spleen

set live cell gate

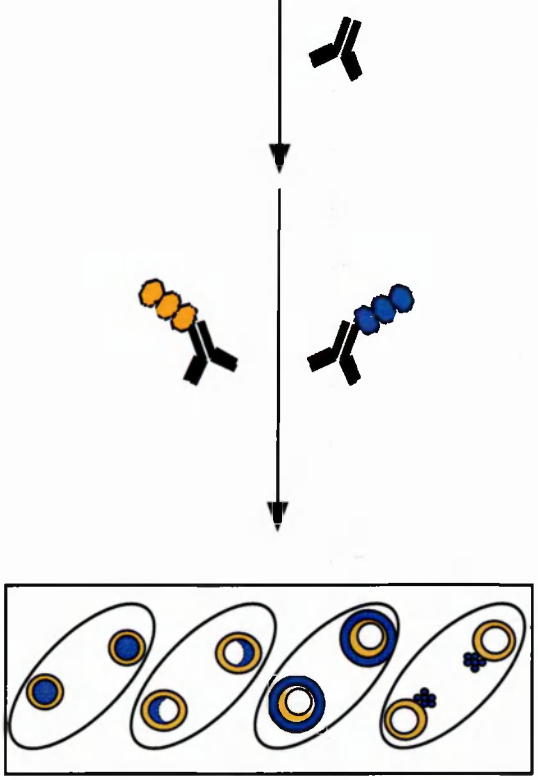

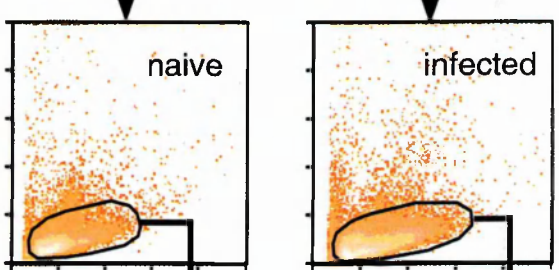

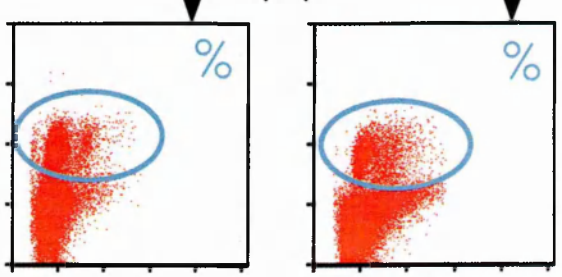

4 consecutive spleen sections showing different cell populations

% X live cell number

= total cell number / spleen

Localisation of splenic cell populations

Quantification of splenic B cell populations

Immunohistology is the ideal method for studying relative locations of cell populations and can normally be used for rough quantification as well. In the malaria infection, this is not possible, because there is marked splenomegaly with spleen weights increasing more than tenfold (e.g. (Sanchez-Torres *et al.*, 2001)) in *P. chabaudi* infection. Fig. 3.3a shows the increase of spleen size with cryosections from different stages of infection, with the increased gaps between the stained areas showing that most of the increase is due to red pulp expansion. In Fig. 3.3b, the number of nucleated splenocytes (after erythrocyte lysis of a single cell spleen suspension) is compared with the level of parasitaemia in Fig. 3.3c. Peak numbers of nucleated splenocytes on day 16 of infection are eightfold higher than in uninfected mice.

A two-dimensional section will give a skewed picture of how cell population sizes are changing, because the cells are also spread out in the third dimension. Therefore, it was essential to perform quantification of cell populations by flow cytometry which takes the whole spleen into account and allows population definition with up to four fluorochromes exciting and emitting at different wavelengths. Spleens were analysed from days 0, 3-8, 10, 12, 16, 20, 30 and 40 of infection. After making single cell suspensions of the spleens, a sample was counted and the number of live cells per spleen calculated. During acquisition on the FACScalibur®, all population definitions were based on a gate which represented the live cells of the spleen (Fig. 3.2). Relative percentages were then transformed into absolute numbers with the aid of the original live cell count. A spleen from a naive mouse was included in every experiment as a control for normal staining. The splenic B cell response to an antigen frequently used in immunisation studies was examined by immunohistology and flow cytometry for comparison. Spleens were analysed 10 days after immunisation with 25μg alum-precipitated chicken gamma globulin (CGG), when the humoral response against the antigen is fully developed.

Figure 3.3 Splenic size increase during *P. c. chabaudi* infection.

(a) Sections of spleens from days 0, 16 and 40 of infection were stained with antibodies against CD3 (blue), IgD (brown) and BrdU (pink). All sections were photographed at the same magnification (25x). At day 16, the section was larger than the microscope's field of view. The increased gaps between the areas of white pulp show that most of the size increase is due to red pulp expansion. Each image is representative of 3-6 mice.

(b) Numbers of nucleated splenocytes were counted after generation of a single cell suspension and erythrocyte lysis (as described in Sect. 2.26). Each data point represents 3-6 mice for all times except for day 10 (9 mice) and day 0 (15 mice). Error bars represent the SEM.

(c) A course of parasitaemia from 5 mice is shown on the same time scale for comparison. The geometric mean is shown and error bars represent the SEM.

(a) Spleen overviews

CD3 / IgD (BrdU)

d0

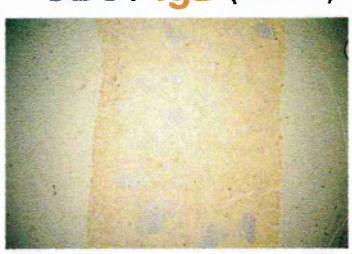

d16

d60

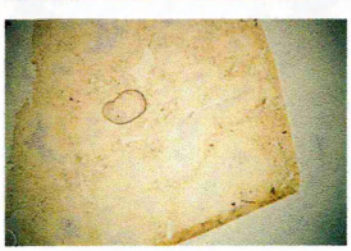

(b) Nucleated splenocyte numbers

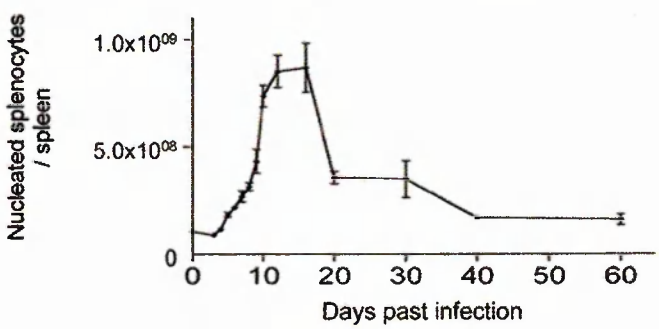

(c) Course of infection

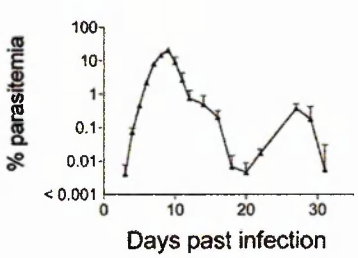

3.2.2 Total B cell numbers

Splenic B cells are identified by the markers B220 (CD45R) and CD19. Antibodies against both markers were compared for quantifying B cell numbers after *P. c. chabaudi* infection (Fig. 3.4). Two clones of anti-B220 were tested: The commercially produced RA36B2 clone (Fig. 3.4 b) produced greater resolution between positive and negative populations than the RA33A1 antibody purified from hybridoma supernatant (data not shown). The numbers of $CD19^+$ and $B220^+$ cells were comparable (Fig. 3.4f), but the anti-CD19 antibody was used in further experiments, as B220 expression is reported to be more variable, undergoing down-regulation on plasma cells and mature germinal centre B cells (Calame, 2001; Han *et al.*, 1997). $CD19^+$ B cell numbers are greatest at day 8 of infection when there are roughly twice as many B cells as in uninfected mice (Fig. 3.4e). After that, numbers drop slightly and fluctuate around a value that is still higher than that in uninfected or day-10 CGG-immunised mice.

3.2.3 Basic changes in the white pulp structure and the naive recirculating B cell population

The basic structure of the white pulp is defined by the location of T cells ($CD3^+$) in the T zone and naive recirculating B cells (IgD^+) in the follicular mantle. Marked changes occur in the distribution of splenic lymphocytes during the rise of parasitaemia. By day 7 to 8 of infection, the outlines of the T zone and the follicular mantle lose definition with concomitant blurring of the boundary between the two areas (d8 in Fig. 3.5a) and an apparent loss of cells. At the peak of parasitaemia, the white pulp structure is so strongly disorganised that it can be impossible to identify these regions. By 10 days of infection, only few T cells are detected in the T zone and the indistinct follicular mantle consists mainly of some IgD^+ recirculating small B cells at the outer surface of the newly formed germinal centres (Fig. 3.5a, d10). The extraordinary white pulp disorganisation reverses with the waning of the parasitaemia. Between days 10 and 40, the cuff of T cells

Figure 3.4 Total B cell numbers during *P. c. chabaudi* infection.

Total numbers of splenic B cells were determined by flow-cytometric analysis. Representative time points are shown for staining with biotin-labelled anti-CD19 (a) and anti-B220 (clone RA36B2). Isotype controls (rat IgG2a, κ) were always negative and examples from day 20 are shown in (c). CD19 staining is shown 10 days after immunisation with CGG as a positive control (d). Forward scatter is plotted on a linear scale and antibody staining on a logarithmic scale. The absolute numbers of $CD19^+$ B cells calculated from the live cell gate are shown in panel (e) with a comparison between CD19 and B220 staining shown for selected time points in (f). Each bar represents the arithmetic mean and SEM from 3-9 mice for the infected groups and 15 mice for day 0.

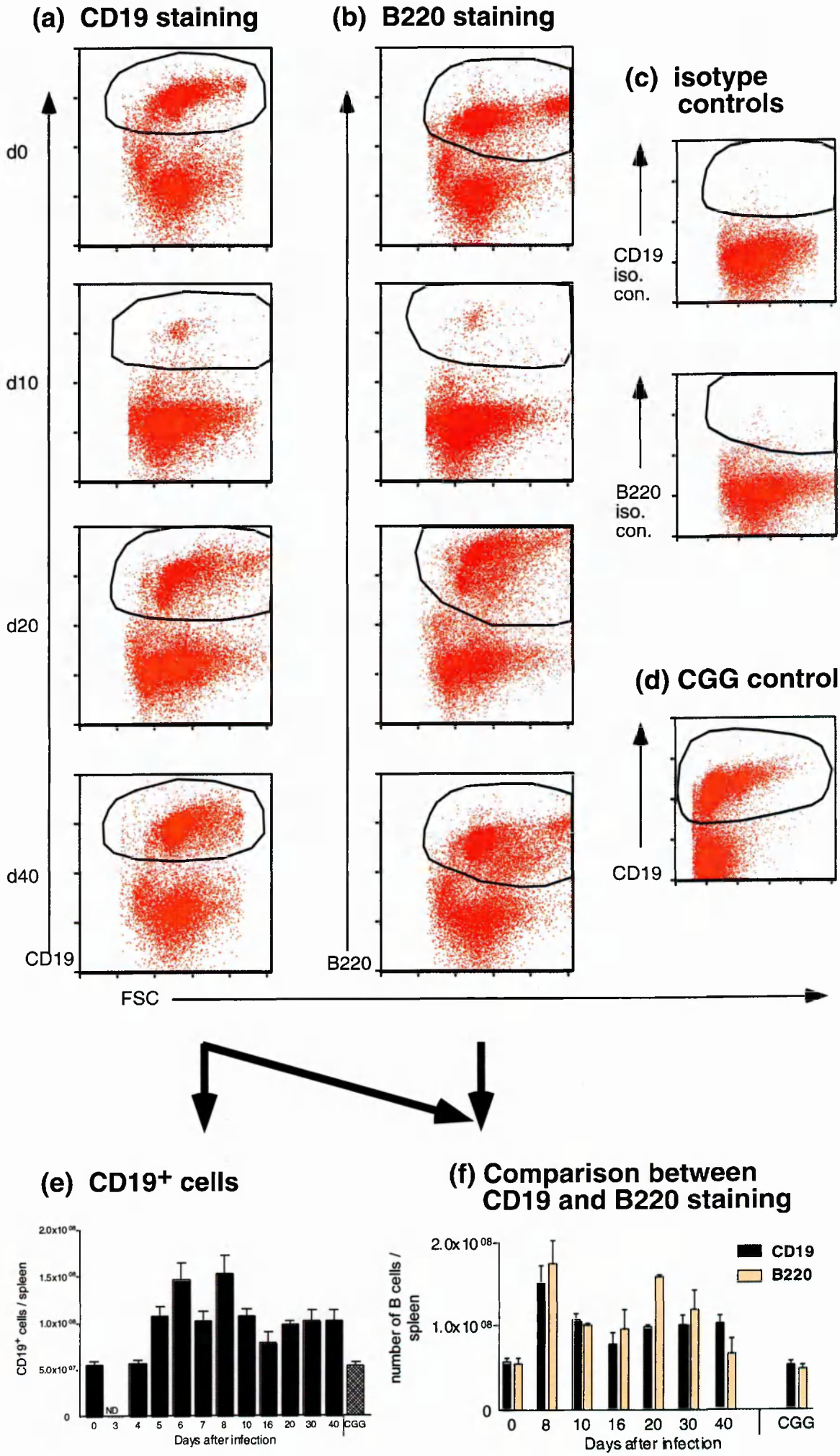
(a) CD19 staining
(b) B220 staining
(c) isotype controls
d0
d10
d20
d40
CD19
B220
CD19 iso. con.
B220 iso. con.
(d) CGG control
CD19
FSC
(e) CD19+ cells
CD19+ cells / spleen
2.0x10 08
1.5x10 08
1.0x10 08
5.0x10 07
0
ND
0 3 4 5 6 7 8 10 16 20 30 40 CGG
Days after infection
(f) Comparison between CD19 and B220 staining
number of B cells / spleen
2.0x10 08
1.0x10 08
0
CD19
B220
0 8 10 16 20 30 40 CGG
Days after infection

Figure 3.5 Basic white pulp structure and naive recirculating B cells during *P. c. chabaudi* infection.

(a) The basic division of the white pulp into the T zone and the follicular mantle basic structure of the white pulp is defined by antibodies against T cells (CD3, blue) and naïve recirculating B cells (IgD, brown). Dark spots at late time points are caused by the malarial pigment hemozoin. Spleens from days 0, 8, 10, 20 and 60 of infection were chosen to portray the different stages during infection. Each image is representative of three to six mice. The size bar corresponds to 100 μm.

GC: germinal centre, FM: follicular mantle, T: T zone.

(b) Flow-cytometric profiles of the live nucleated splenocyte fraction are shown for representative time points The naive recirculating B cell population which corresponds to the IgD^+ cells in panel a is defined as $CD21^{int}CD23^+$. All plots are based on a logarithmic scale. Gates were set by comparison with the isotype control staining and in relation to the marginal zone B cell gate shown in Fig. 4.12b. The same gate was used for all samples in each experiment.

(c) Isotype controls for the anti-CD21 (FITC-labelled rat IgG2b,κ) and anti-CD23 (PE-labelled rat IgG2a, κ) antibodies were used as negative controls. A representative example from day 20 of infection is shown.

(d) Flow-cytometric and immunohistological analysis 10 days after immunisation with alum-precipitated CGG was used as a positive control.

(e) The percentages of the $CD21^{int}CD23^+$ live cells shown in panel b were used to calculate total number of naive recirculating B cell numbers after subtraction of percentage of cells which was positive for the CD21 isotype control. Each bars represents the arithmetic mean from 3 to 6 spleens, with up to 15 spleens for time point 0, as an uninfected control was included in each experiment. Error bars show the SEM.

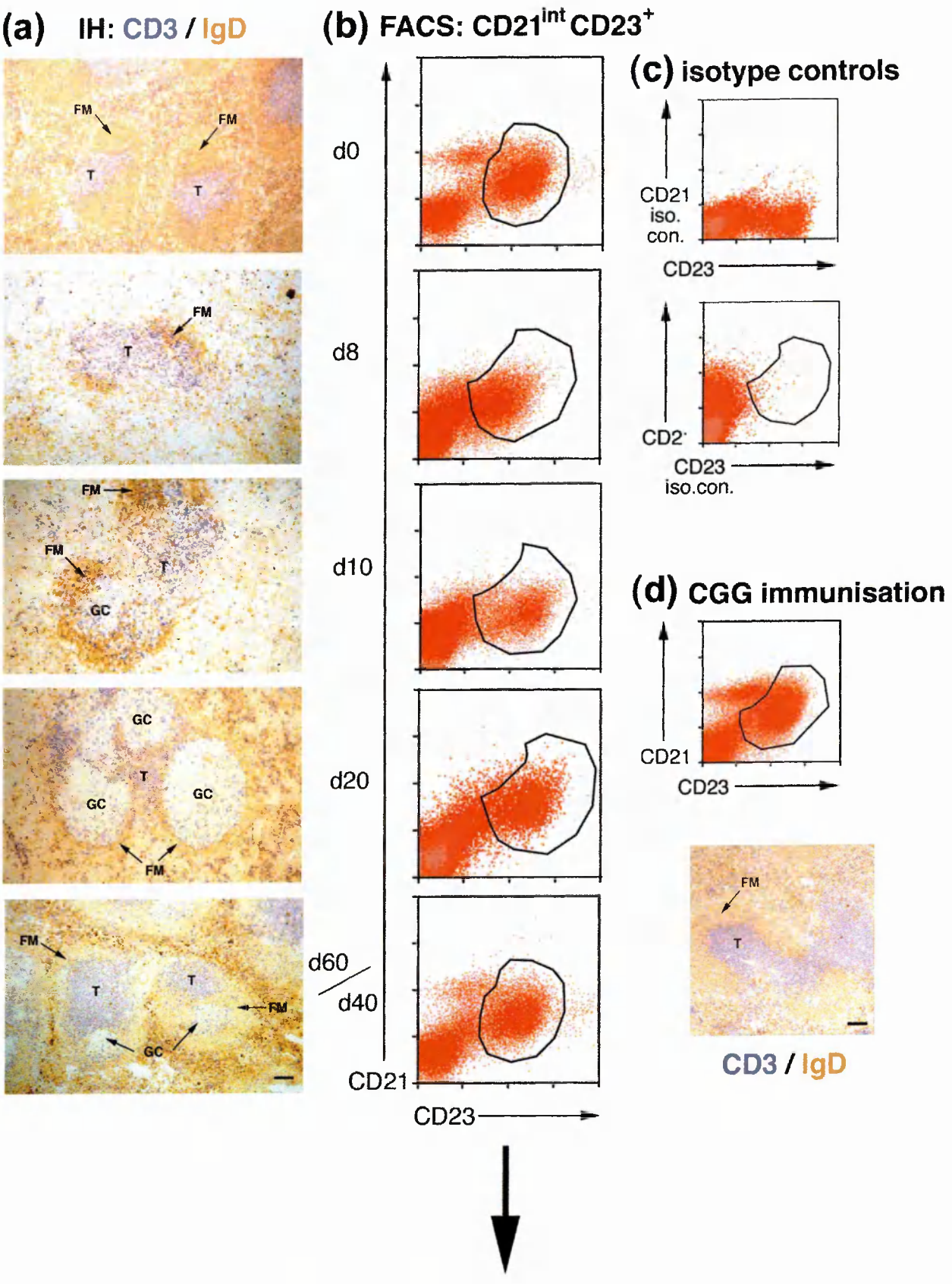
(a) IH: CD3 / IgD
FM
T
GC
(b) FACS: CD21int CD23+
d0
d8
d10
d20
d60
d40
CD21
CD23
(c) isotype controls
CD21 iso. con.
CD23
CD2·
CD23 iso.con.
(d) CGG immunisation
CD21
CD23
CD3 / IgD

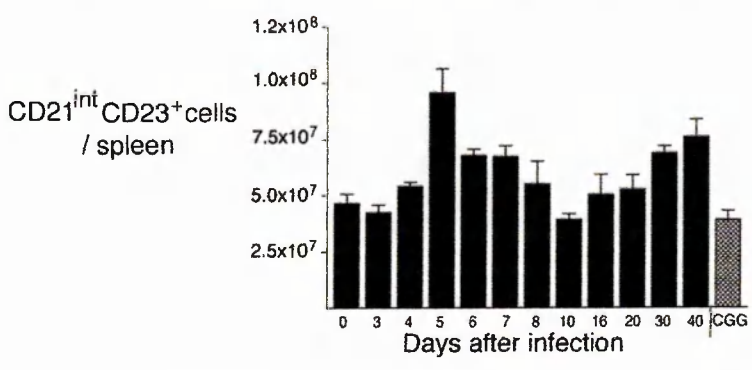
(e)
Naive recirculating B cell numbers
CD21int CD23+ cells / spleen
1.2x10^8
1.0x10^8
7.5x10^7
5.0x10^7
2.5x10^7
0 3 4 5 6 7 8 10 16 20 30 40 CGG
Days after infection

in the periarteriolar region reforms and the follicular mantle extends fully around the white pulp again (Fig. 3.5, d20-60). By day 40-60 of infection, the white pulp has regained fairly normal appearance albeit with somewhat less sharp outlines and the addition of germinal centres and red pulp granules of haemozoin, a degradation product of haemoglobin produced by the parasite (Fig. 3.5a, d60).

In flow-cytometric analysis, the naive recirculating B cell population is best defined as $CD21^{int}CD23^{+}$ ((Oliver *et al.*, 1997)) (Fig. 3.5b). The use of this marker combination has the added advantage that marginal zone B cells can be identified at the same time as $CD21^{+}CD23^{-}$ (Fig. 3.12b). There was no major size difference between the $CD19^{+}CD21^{int}CD23^{+}$ and the $CD21^{int}CD23^{+}$ populations (data not shown), so the marginal zone B cells were defined without the antibody against CD19. Representative flow-cytometric dot plots were chosen to represent different stages of infection. (Fig. 3.5b) and results for isotype controls and a 10-day CGG immunisation time point are included as negative and positive controls, respectively. Flow-cytometric analyses are shown only up to day 40 of infection after several experiments showed that results looked very similar on days 40 and 60 of infection.

Between days 10 and 20 of infection, the red pulp appears almost devoid of IgD^{+} and $CD3^{+}$ lymphocytes in immunohistological staining (Fig. 3.5a, d10 and d20). Along with the marked transient reduction of these cells in the follicular mantles and T zones observed between days 8 and 12, one might assume that the population sizes of follicular B cells and T cells would be reduced in the malarial spleens around and after the peak of infection. On the contrary, flow-cytometric analyses show that IgD^{+} B cell (Fig. 3.5b) and T cell (Helmby *et al.*, 2000) numbers are only minimally lower than in naïve mice at the peak (Fig. 3.5e) and even increase in the early and late stages of infection. This suggests that the effect observed in immunohistology is a dilution effect, where the lymphocytes are just spread out further in the vastly enlarged spleens.

3.2.4 Cellularity of the red pulp

The previous section has shown how the increase in spleen size can influence distribution of splenocytes. This wider spacing might influence their interactions with other cells. Therefore, it is necessary to identify which types of cells occupy the expanded red pulp. For a basic overview, hematoxylin and eosin staining was performed on paraffin sections of spleens from days 0, 8, 10, 12 and 14 of infection (Fig. 3.6a), when the spleen is increasing rapidly in size. This shows that the red pulp becomes the site of extensive but transient haematopoiesis involving large islands of erythroid precursors and abundant megakaryocytes. On day 10 of infection, the erythroid precursors are so numerous that they compress splenic cords and red pulp sinuses (Fig. 3.6a, d10). However, by day 12 of infection, the red pulp sinuses and cords of Billroth are seen to open up again (Fig. 3.6a, d12 and d14), indicating that the strong haematopoietic burst is a response to the high loss of erythrocytes at the peak of parasitaemia.

Macrophages are one of the main cell groups in the red pulp and their numbers could be expected to increase to cope with the mass of defective erythrocytes. Nonspecific esterase activity and the MHC class II and F4/80 markers were used to identify macrophage populations of the red pulp. Activated macrophages show increased nonspecific esterase activity. The density of these cells in the red pulp decreased as the infection progressed (Fig. 3.6b). The MHC class II stain was concentrated in the white pulp with particular emphasis on the follicular mantle (data not shown), suggesting that it was also detecting B cells and therefore not specific enough for statements about the changes in macrophage populations. The $F4/80^{+}$ macrophages remained confined to the red pulp throughout infection, with their numbers but not their density increasing steadily as the red pulp distended (Fig,. 3.7b). Together these stains show that there may be more macrophages in the enlarged red pulp, but that they do not exclude other cells from this area.

Figure 3.6 Cellularity of the red pulp

(a) Paraffin-embedded spleens from days 0, 10, 12 and 14 were stained with H& E.

(b) Nonspecific esterase activity was revealed with α-naphthyl esterase activity (in black) with a haematoxylin counterstain (green).

(c) In more detailed images of H & E stained spleens, examples of erythroid precursors islands are circled and some megakaryocytes are pointed out. In the righthand panel, the splenic capsule can be seen at the bottom of the picture.

Spleens were cut in half and one half each used for H & E and nonspecific esterase staining. Each panel is representative of three spleens.

RP: red pulp, WP: white pulp, ep: erythroid precursors, Meg: megakaryocyte

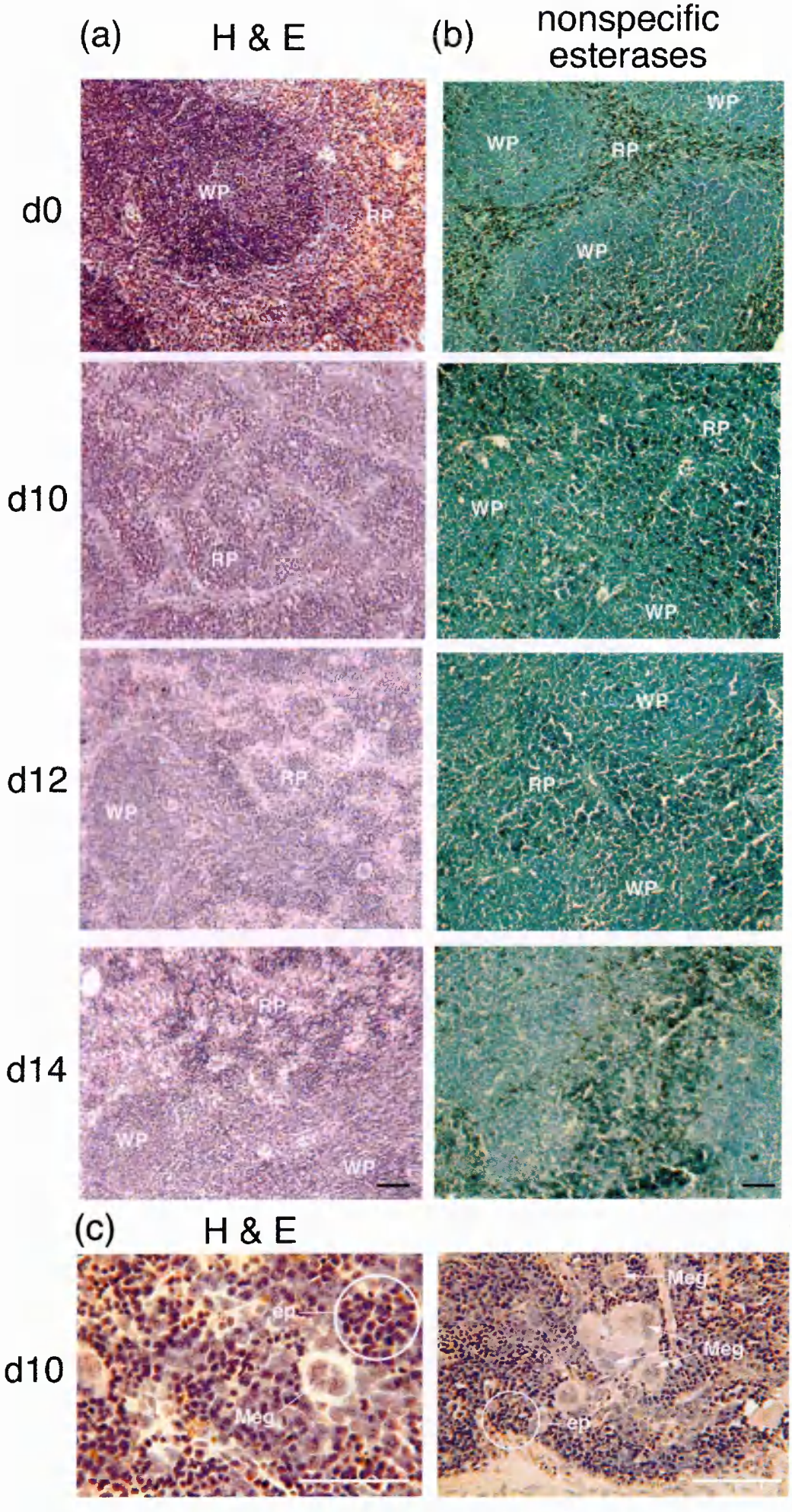
(a)
H & E
(b)
nonspecific esterases
d0
WP
RP
WP
RP
WP
d10
RP
WP
RP
WP
d12
RP
WP
WP
RP
WP
d14
RP
WP
WP
(c)
H & E
d10
ep
Meg
Meg
Meg
ep

Figure 3.7 Dendritic cells and macrophages during *P. c. chabaudi* infection.

(a) $CD11c^+$ dendritic cells were stained in blue and the metallophilic macrophage population was identified by staining for CD169 (brown). On day 0, the metallophilic macrophages were not stained. Days 8, 16 and 40 also show traces of an irrelevant red stain for BrdU.

MZ: marginal zone, T: T zone

(b) $F4/80^+$ macrophages were stained in brown.

All panels are representative of three spleens.

RP: red pulp, WP: white pulp

Dendritic cells and macrophages

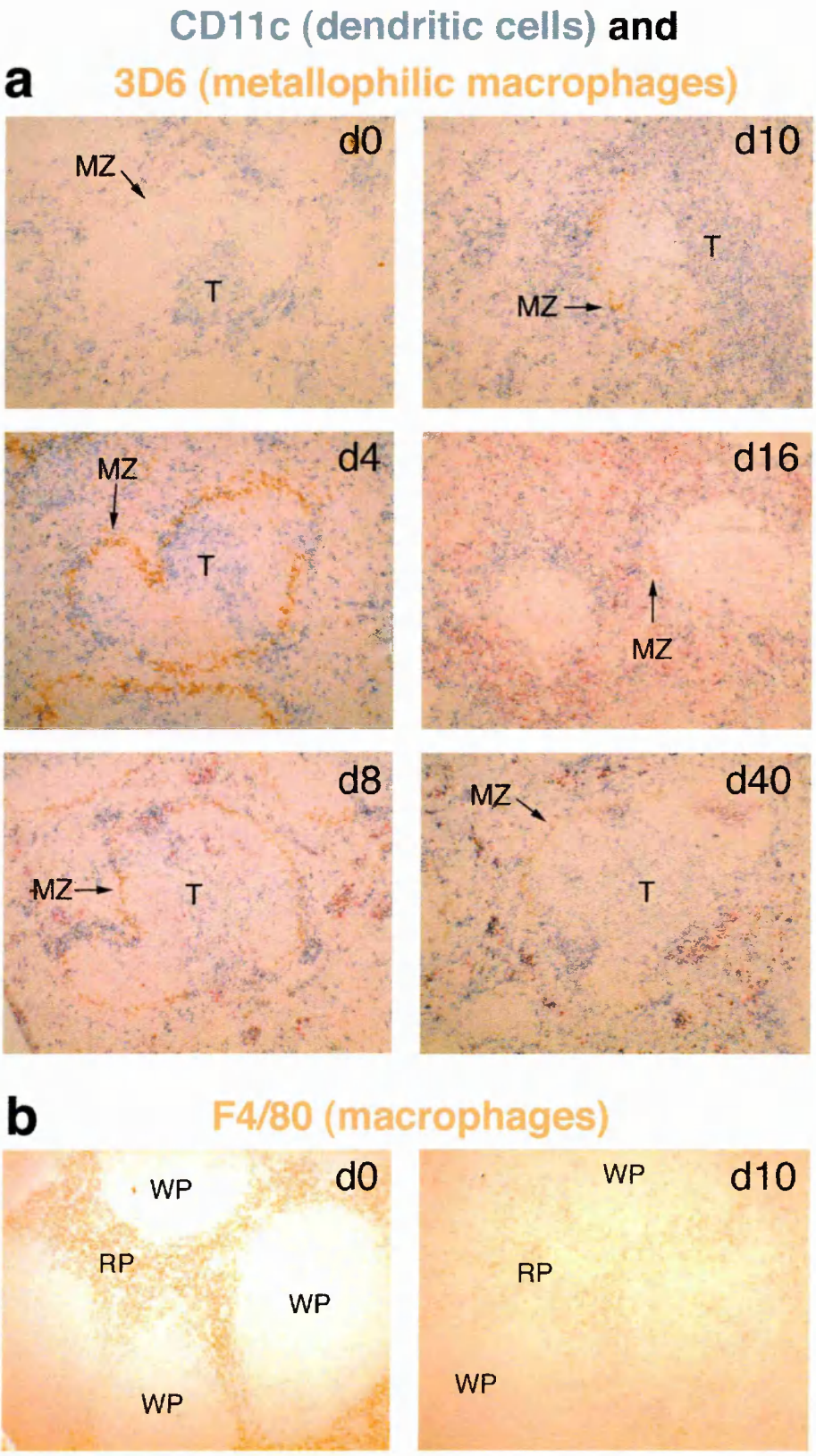

More dramatic changes can be seen in a group of macrophages which are confined to the marginal zones, the metallophilic macrophages, which are $CD169^+$ and have a typical appearance that makes the marginal zone look like a crown of thorns. By day 8 of infection, the ring formed by these cells becomes slightly discontinuous (Fig. 3.7a, d8) and between days 10 and 16, it is reduced to individual cells usually located at the edge of secondary follicles (Fig. 3.7a, d10 and d16). By day 40, some of the marginal zones contain metallophilic macrophages again (Fig. 3.7a, d40), but there are still no continuous rings.

The same figure shows the $CD11c^+$ dendritic cells, which first become more numerous in the red pulp and the T zone (Fig. 3.7a, d10). By day 16 they are concentrated in the T zone and at the edges of the follicular mantle (Fig. 3.7a, d16). By day 40, the number and distribution of $CD11c^+$ cells is approaching that of naïve spleens again (Fig. 10, d40). Together, the increase in macrophages and dendritic cells at the peak of infection shows that there is a large antigen presenting potential at this time point.

3.2.5 Germinal centre B cells

Germinal centres are detected specifically in immunohistology by binding of the lectin PNA (Fig. 3.8a) and they are also recognisable as typical round unstained structures in the follicular mantle when using the IgD / CD3 stain combination (Fig. 3.5a). Small numbers of PNA-positive germinal centres are present in the spleens of uninfected control mice, which is consistent with housing in a non-sterile environment (Table 3.1). Slightly increased numbers of small germinal centres are seen on days 7-9 of infection and by day 10, the germinal centre response is firmly established (Figs. 3.5 and 3.8, Table 3.1). The germinal centres continue to increase in size and number up to day 20. Normal germinal centres are present up to day 40 and still visible on day 60, in a more weakly stained form.

Figure 3.8 Germinal centre B cells during *P. c. chabaudi* infection.

(a) Germinal centres are revealed with the lectin PNA (blue) along with naïve reciculating B cells (IgD, brown) for orientation. Dark spots at late time points are caused by the malarial pigment hemozoin. Random isolated cells in the red pulp and some epithelial cells are also stained by PNA, but can easily be distinguished from germinal centre B cells by form or location. Spleens from days 0, 8, 10, 20 and 60 of infection were chosen to portray the different stages during infection. Each image is representative of three to six mice. The size bar corresponds to 100 μm.

GC: germinal centre

(b) Flow-cytometric profiles of the live nucleated splenocyte fraction are shown for representative time points. The germinal centre B cell population which corresponds to the PNA^+ cells in panel a is defined as $GL7^+CD19^+$. All plots are shown on a logarithmic scale. Gates were set by comparison with the anti-GL7 isotype control and by choosing obviously distinct cell populations. Therefore, gates often needed to be chosen individually for different samples in the same experiment.

(c) The isotype controls for the anti-GL7 antibody (FITC-labelled rat IgG2a,κ) was used as a negative control. A representative example from day 20 of infection is shown.

(d) Flow-cytometric and immunohistological analysis 10 days after immunisation with alum-precipitated CGG was used as a positive control.

(e) The percentages of the $GL7^+CD19^+$ live cells shown in panel b were used to calculate total number of germinal centre B cell numbers after subtraction of the percentage of cells which were positive for the GL7 isotype control. Each bar represents the arithmetic mean from 3 to 6 spleens, with up to 15 spleens for time point 0, as an uninfected control was included in each experiment. Error bars show the SEM.

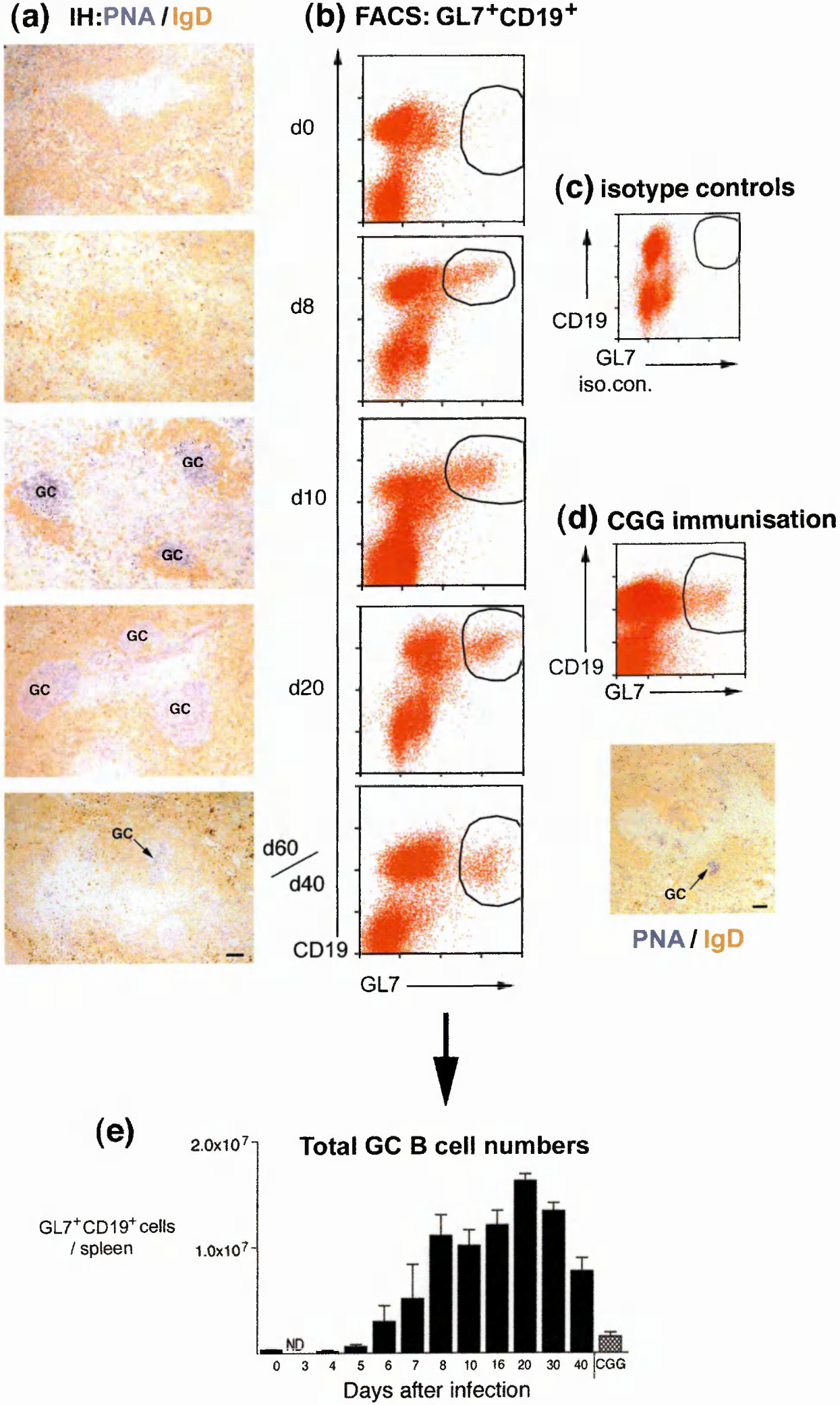
(a) IH:PNA / IgD
GC
GC
GC
GC
GC
GC
GC
(b) FACS: GL7+CD19+
d0
d8
d10
d20
d60
d40
CD19
GL7
(c) isotype controls
CD19
GL7
iso.con.
(d) CGG immunisation
CD19
GL7
GC
PNA / IgD
(e)
Total GC B cell numbers
GL7+CD19+ cells / spleen
2.0x10^7
1.0x10^7
ND
0 3 4 5 6 7 8 10 16 20 30 40 CGG
Days after infection

Table 3.1. Germinal centre growth after *Plasmodium chabaudi chabaudi* infection [a)]

Day	No. [b)]	Average size [c)] [mm^2]	Area of spleen [d)] [%]
0	1.5	0.002	0.01
8	21.2	0.004	0.28
9	47.0	0.009	0.57
10	70.0	0.016	1.29
11	77.7	0.010	0.91
12	78.0	0.021	1.93
20	152.0	0.040	9.20
30	110.0	0.028	4.6
60	35.2	0.013	2.0
CGG [e)]	51.7	0.013	2.5

a) All values are arithmetic means of germinal centres in single cryosections from two to three spleens.

b) Germinal centres were counted as described in Section 2.22.

c) Areas were determined as described in Section 2.22.

d) The percentage of the spleen covered by germinal centers was calculated by measuring the area of the combined germinal centres and dividing this by the total area of the cryosection.

e) Spleens were taken 10 days after immunisation with alum-precipitated CGG.

The germinal centres in splenic sections from day 10 of malaria infection are slightly larger and more frequent than those seen 10 days after immunisation with a conventional antigen, chicken gamma globulin (Table 3.1). At the peak of the malaria-induced germinal centre response, day 20 of infection the germinal centres and sizes are about threefold higher than those seen on day 10 of CGG immunisation and this difference is statistically significant ($p<0.05$) Germinal centre appearance is normal in that a light and dark zone can be distinguished by H& E staining (data not shown) and by the outer ring of T cells (Fig. 3.5a, d20) in the older germinal centres. There is not much variation in the staining intensity of germinal centres on day 60, suggesting that they are of a similar age.

In flow cytometry, germinal centre B cells were identified by positive staining with antibodies against GL7 and CD19 (Fig. 3.8b), as PNA bound quite unspecifically (Fig. 3.9) GL7 is a protein found on germinal centre B cells in the spleen and on activated thymocytes (but not splenic T cells) (Laszlo *et al.*, 1993). The relative location of the different populations in the dot plot shifts slightly during infection, but the germinal centre population is always readily recognisable.

The kinetics of germinal centre B cell development revealed by flow cytometry agree well with the immunohistological observations. Total numbers of germinal centre B cells rise gradually in the early days of infection, with greater increases on days 6 and 8 (Fig. 3.8e) and the peak at day 20. The $GL7^{+}CD19^{+}$ cells are still present in large numbers by day 40 of infection and even at this late stage, levels are five times higher than at day 10 of chicken gamma globulin immunisation.

3.2.6 Antibody-containing cells

Antibody-containing cells, which comprise the differentiating plasmablasts and the immunoglobulin-secreting plasma cells, can be recognised in both immunohistology and flow cytrometry by antibodies against the proteoglycan syndecan-1. Immunohistology shows that on both days 0 (Fig. 3.10a, d0) and 4 of infection (data not shown), small foci

Figure 3.9 Comparison of germinal centre staining by PNA and anti-GL7 in FACS analysis.

The panels on the left show attempts to identify the germinal centre population with the lectin PNA in three spleens from different time points of infection. On the right, cells from the same spleens are stained with anti-CD19 and anti-GL7. Comparison with the GL7 isotype control (shown in Fig. 4.8c) allows populations to be identified clearly.

All analyses were performed on the live nucleated splenocyte fraction. Forward scatter is on a linear scale. All antibody and reagent stains are on a logarithmic scale.

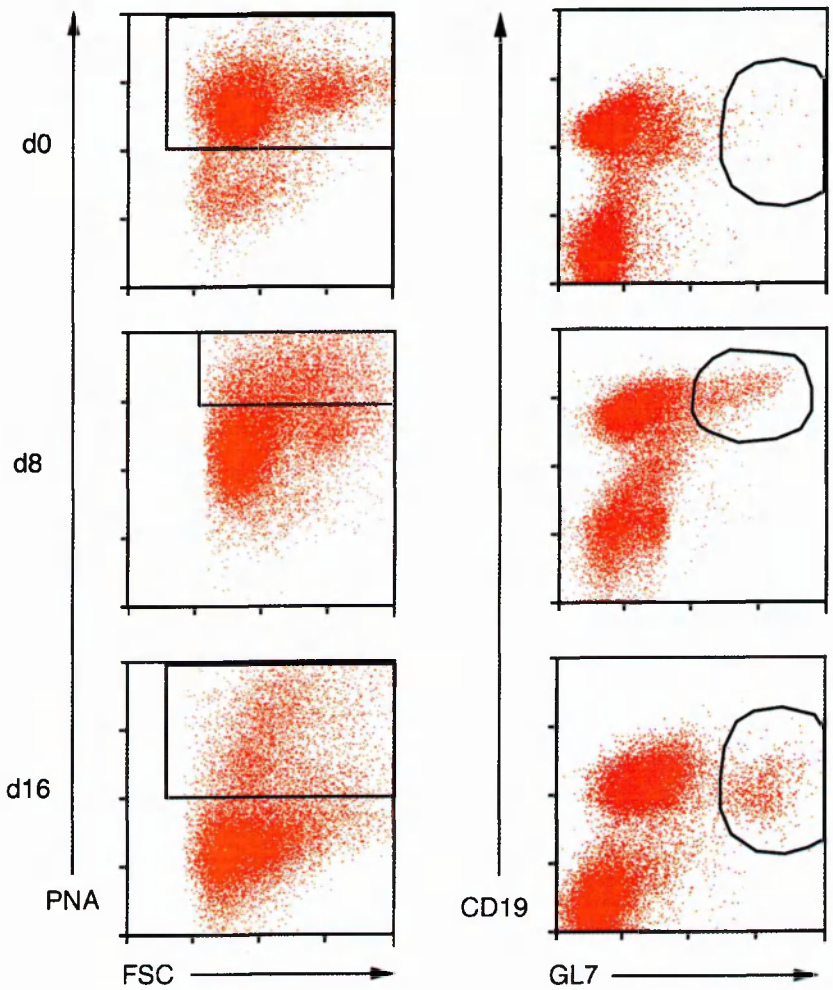
d0
d8
d16
PNA
FSC
CD19
GL7

of antibody-containing are present in the typical red pulp location. The numbers of antibody-containing cells increase rapidly, reaching peak density at day 9 or 10 of infection (Fig. 3.10a, d8 and d10) followed by an equally rapid decline (Fig. 3.10a, d20 and d60). In the rapid expansion period between days 7 and 10, many IgD^+ antibody-containing cells are seen among the syndecan-1^+ cells in the red pulp (Fig. 3.11a). Between days 8 and 10 of infection, the location of the majority of the syndecan-1^+ cells shifts from the extrafollicular foci to the T zone of the white pulp (Fig. 3.10a, d8 and d10). Antibody-containing cells are found in this location up to day 20 of infection (Fig. 3.10a, d20) and from day 30 are again located in the red pulp (data not shown) with numerous foci still visible at day 60 (Fig. 3.10a, d60).

Between days 12 and 20 of infection (Fig. 3.5; d10 and d20, Fig. 3.10, d10 and d20), as the number of syndecan-1^+ cells begins to decrease and more T cells are again seen in the T zone, it becomes possible to compare the relative locations of these two populations. The sections used for anti-CD3 and anti-syndecan-1 staining were part of a consecutive series with at least two other 5-μm sections in between. Nonetheless, the distances between the relevant sections are very small, making it possible to match up corresponding areas of the spleen accurately. This shows that between days 12 and 20 of the infection, T cells and antibody-containing cells occupy non-overlapping areas of the T zone (Fig. 3.11b and c).

The syndecan-1 staining was difficult to use in flow cytometry: With the protocol used for the other marker combinations, populations of syndecan-1^+CD19^+ cells could not be defined by comparison with the syndecan-1 isotype control or the uninfected mice. Intracellular staining resulted in clearly identifiable populations, but the background of the isotype control was unacceptably high (up to 50%, data not shown). Finally, an extracellular staining protocol using FACS buffer without sodium azide proved successful.

Figure 3.10 Antibody-containing cells during *P. c. chabaudi* infection.

(a) The location of antibody-containing cells (syndecan-1, blue), i.e. plasma cells and plasmablasts, is shown along with naïve recirculating B cells (IgD, brown) for orientation. Dark spots at the late time points are caused by the malarial pigment hemozoin. Spleens from days 0, 8, 10, 20 and 60 of infection were chosen to portray the different stages during infection. Each image is representative of three to six mice. The size bar corresponds to 100 μm.

T: T zone, ex foc: extrafollicular focus.

(b) Flow-cytometric profiles of the live nucleated splenocyte fraction are shown for representative time points The antibody-containing B cell is defined as syndecan-1^+CD19^+. All plots are based on a logarithmic scale. Gates were set by comparison with the negative controls from part c and by choosing obviously distinct cell populations. Therefore, gates often needed to be chosen individually for different samples in the same experiment.

(c) The isotype control for the anti-syndecan-1 (PE-labelled rat IgG2a,κ) is shown on top. The bottom panel shows that syndecan-1 staining could be blocked by prior incubation with unlabelled antibody in fivefold excess. As explained in Section 4.2.6 this proves that the syndecan-1 staining was specific. These examples are from day 20 of infection.

(d) Flow-cytometric and immunohistological analysis 10 days after immunisation with alum-precipitated CGG was used as a positive control.

(e) The percentages of the syndecan$^+$CD19$^+$ live cells shown in panel b were used to calculate total number of antibody-containing B cell numbers after subtraction of the percentage of cells which were positive for the syndecan-1 isotype control. Each bars represents the arithmetic mean from 3 to 6 spleens, with up to 15 spleens for time point 0, as an uninfected control was included in each experiment. Error bars show the SEM.

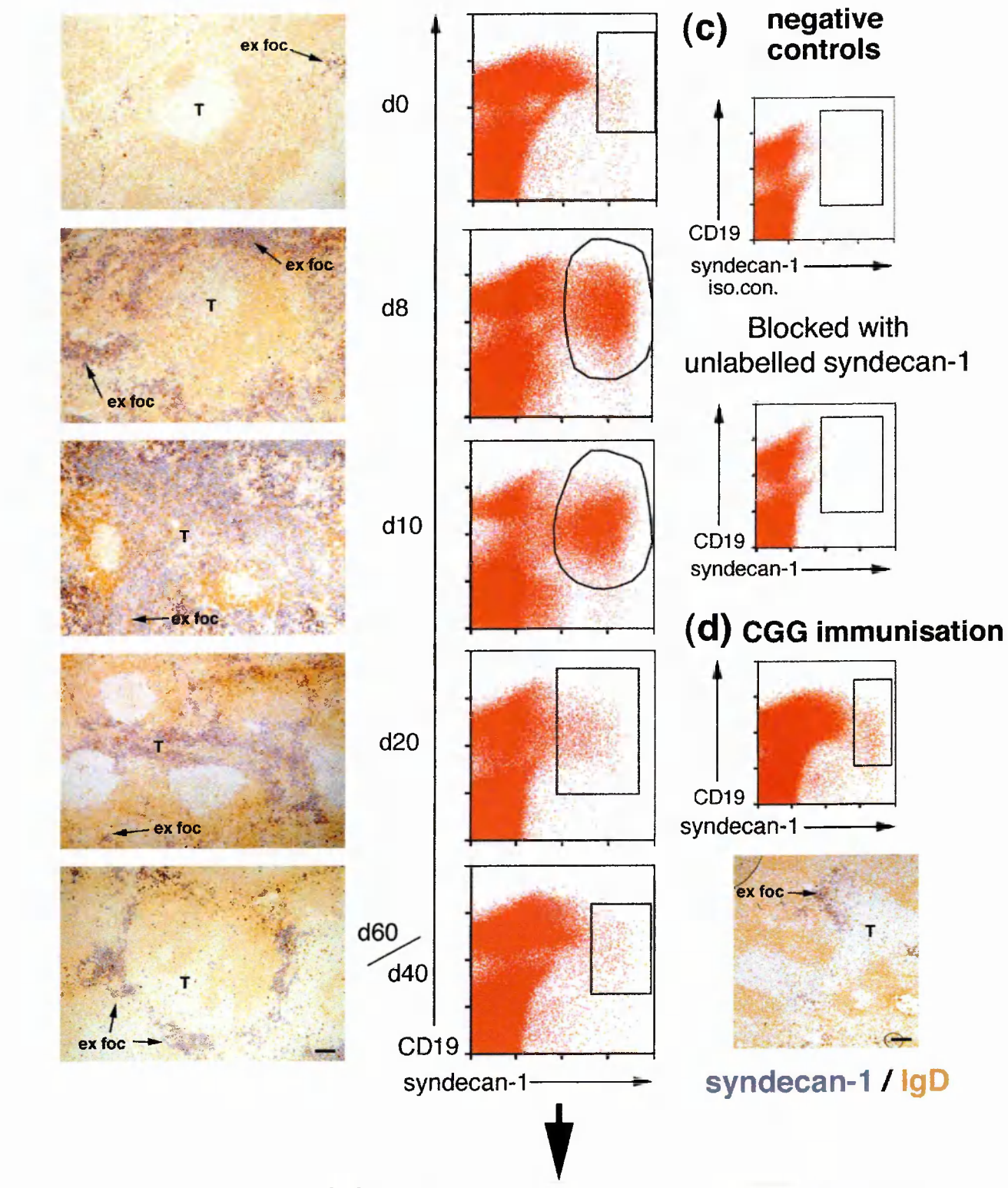
(a) IH:syndecan-1 / IgD
(b) FACS: syndecan-1+CD19+
(c) negative controls
(d) CGG immunisation
(e) Total antibody-containing cell numbers
ex foc
T
d0
d8
d10
d20
d60
d40
CD19
syndecan-1
syndecan-1 iso.con.
Blocked with unlabelled syndecan-1
syndecan-1 / IgD
syndecan-1+ cells / spleen
7.0x10^7
6.0x10^7
5.0x10^7
4.0x10^7
3.0x10^7
2.0x10^7
1.0x10^7
ND
0 3 4 5 6 7 8 10 12 20 30 40 CGG
Days after infection

Figure 3.11 Details of antibody-containing cells in infection.

(a) Numerous large IgD^+ cells (brown) are visible in the red pulp on day 7 of infection. Arrowheads point out some of the cells were the grey-black colour indicates that there is double staining with anti-syndecan-1 (blue), demonstrating that these are plasmablasts.

(b and c) T cells ($CD3^+$) or antibody-containing cells (syndecan-1^+) were stained in blue with recirculating naive B cells (IgD^+) in brown in nearly consecutive sections from the same spleens. Arrows point out the areas of the T zone occupied by T cells but not by antibody-containing cells. Examples are shown for days 12 (a) and 16 (b) of infection. The red stain in panel c is from anti-BrdU and is irrelevant in this context.

Each panel is representative of three mice.

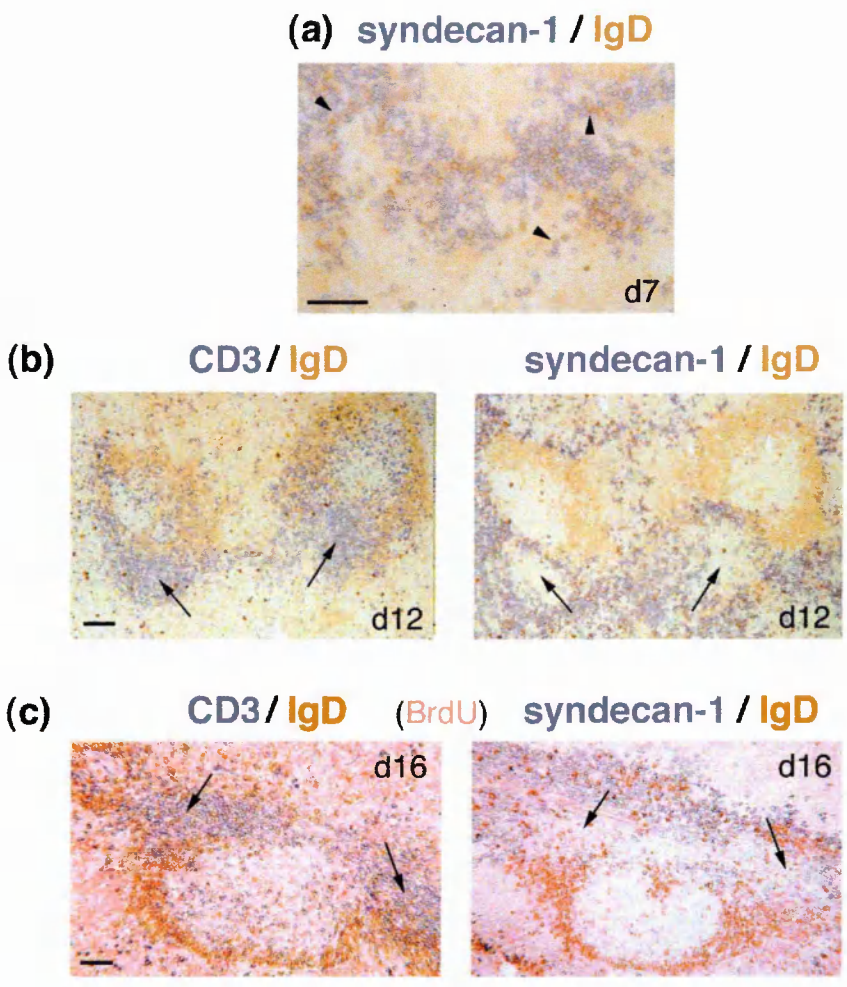
(a) syndecan-1 / IgD
d7
(b)
CD3 / IgD
syndecan-1 / IgD
d12
d12
(c)
CD3 / IgD
(BrdU)
syndecan-1 / IgD
d16
d16

An additional control was included because of the difficulties with this stain. Samples were incubated for 30 min with a fivefold excess of unlabelled anti-syndecan-1 before addition of the labelled antibody (Fig. 3.10c, lower panel). The assumption is that if the antibody binds nonspecifically, even a tenfold excess of the unlabelled antibody would not be sufficient to competitively block all potential binding sites. The controls were convincingly negative and for high numbers of antibody-containing cells, the borders of the syndecan-1^+CD19^+ population were very clear (e.g. Fig. 3.10b, d10). At lower cell numbers, the population outlines are harder to define. This may explain why only 2.5-fold higher levels of antibody-containing cells 10 days after CGG immunisation than in naive mice (Fig. 3.10e), less of a difference than the extrafollicular foci in the immunised mice observed by immunohistology would lead one to expect (Fig. 3.10d).

The flow-cytometric analysis can be used to confirm the kinetics observed by immunohistology: Antibody-containing cell (syndecan-1^+CD19^+) numbers increase sharply (Fig. 3.10b) with the peak levels at day 10 of infection about 300-fold higher than uninfected levels ($p<0.01$ comparing day 0 with day 8-12 of infection). After that, levels drop quite rapidly, but are still significantly higher than uninfected levels 40 days after infection (fourfold higher, $p<0.01$). Although the numeric values may be inaccurate in the low range, as discussed above, the kinetics of the plasma cell response determined by flow cytometry agree well with the histological results.

3.2.7 Marginal zone B cells

Marginal zone B cells are identified in immunohistology as IgM^+IgD^- cells at the edge of the white pulp, as can be seen in the spleens from uninfected mice (Fig. 3.12a, d0). After infection, the marginal zones become depleted of B cells and by day 10, no IgM^+ IgD^- cells can be detected in the marginal zones (Fig. 3.12a, d10). The cells may have migrated to other parts of the spleen or to other organs or have undergone apoptosis. Immunohistology cannot distinguish between IgM^+ plasma cells and migrated IgM^+

marginal zone B cells without the additional locational indicator, so it is impossible to determine by this method whether the marginal zone B cells are still present in the spleen. By day 40, the marginal zones contain IgM^+ B cells again (data not shown), but even at day 60 they form a less continuous structure than before the infection (Fig. 3.12a, d60). The marginal zone B cell population is defined in flow cytometry as $CD21^+CD23^+$ (Fig. 3.12b), which allows it to be identified at the same time as the $CD21^{int}CD23^-$ naive recirculating B cells (Fig. 3.5b). It is easy to obscure the typical CD21 staining pattern during compensation in flow cytometry, so special care was taken to ensure that the naive control was comparable between experiments. The gate defined for the marginal zone B cells of the naive mouse was then used on the plots from the infected mice, as this population is so small that it is otherwise not possible to locate the population in the enlarged spleens. The marginal zone B cell population exhibits a strong peak at days 5 and 6 of infection ($p<0.01$), followed by a gradual decline up to day 16. After that, the population regains and maintains a level somewhat higher than the uninfected level up to day 40 ($p<0.05$, 0.01 and 0.05 for days 16, 30 and 40 of infection) (Fig. 3.12e). Therefore, marginal zone B cells are still present in the spleen when they are not detectable by immunohistology, implying that the cells have migrated to other parts of the spleen.

Marginal zone B cells are known to be involved in early immune responses and produce plasma cells more quickly than the naïve follicular B cells (Oliver *et al.*, 1999). As early as 24 h after LPS stimulation, the differentiation into plasmablasts can be observed by up-regulation of syndecan-1 and increase in cell size (Martin *et al.*, 2001). The doubling in marginal zone B cells on days 5 and 6 and the rapid development of plasma cells in the spleen following *P. c. chabaudi* infection suggest that marginal zone B cells may be differentiating into plasmablasts. Therefore, the cell size of the marginal zone B cells was analysed by forward scatter in spleens from days 0 and 3-7 of infection (representative examples in Fig. 3.13 and Table 3.2). Attempts to determine the syndecan-1^+ proportion

Figure 3.12 .Marginal zone B cells during *P. c. chabaudi* infection.

(a) Marginal zone B cells are defined immunohistologically by their presence in the marginal zones along with being positive for IgM (blue) and negative for IgD (brown) Arrows point to the marginal zone B cells, arrowheads point out the location of the marginal zone when no marginal zone B cells are visible there. On day 10, the white pulp structure is so poorly defined that it was not possible to say exactly where the marginal zone lies.

Dark spots at the late time points are caused by the malarial pigment hemozoin. Spleens from days 0, 8, 10, 20 and 60 of infection were chosen to portray the different stages during infection. Each image is representative of three to six mice. The size bar corresponds to 100 μm.

MZ: marginal zone B cells.

(b) Flow-cytometric profiles of the live nucleated splenocyte fraction are shown for representative time points The marginal zone B cell population which corresponds to the $IgM^{+}IgD^{-}$ cells in part a is defined as $CD21^{int}CD23^{-}$. All plots are based on a logarithmic scale. Gates were set by comparison with the isotype control staining and in relation to the naive recirculating B cell gate shown in Fig. 4.5b. The same gate was used for all samples in each experiment.

(c) Isotype controls for the anti-CD21 (FITC-labelled rat IgG2b,κ) and anti-CD23 (PE-labelled rat IgG2a, κ) were used as negative controls.Representative examples from day 20 of infection are shown.

(d) Flow-cytometric and immunohistological analysis 10 days after immunisation with alum-precipitated CGG was used as a positive control.

(e) The percentages of the $CD21^{+}CD23^{-}$ live cells shown in panel b were used to calculate total number of marginal zone B cell numbers after subtraction of the percentage of cells which were positive for the CD21 isotype control. Each bar represents the arithmetic mean from 3 to 6 spleens, with up to 15 spleens for time point 0, as an uninfected control was included in each experiment. Error bars show the SEM.

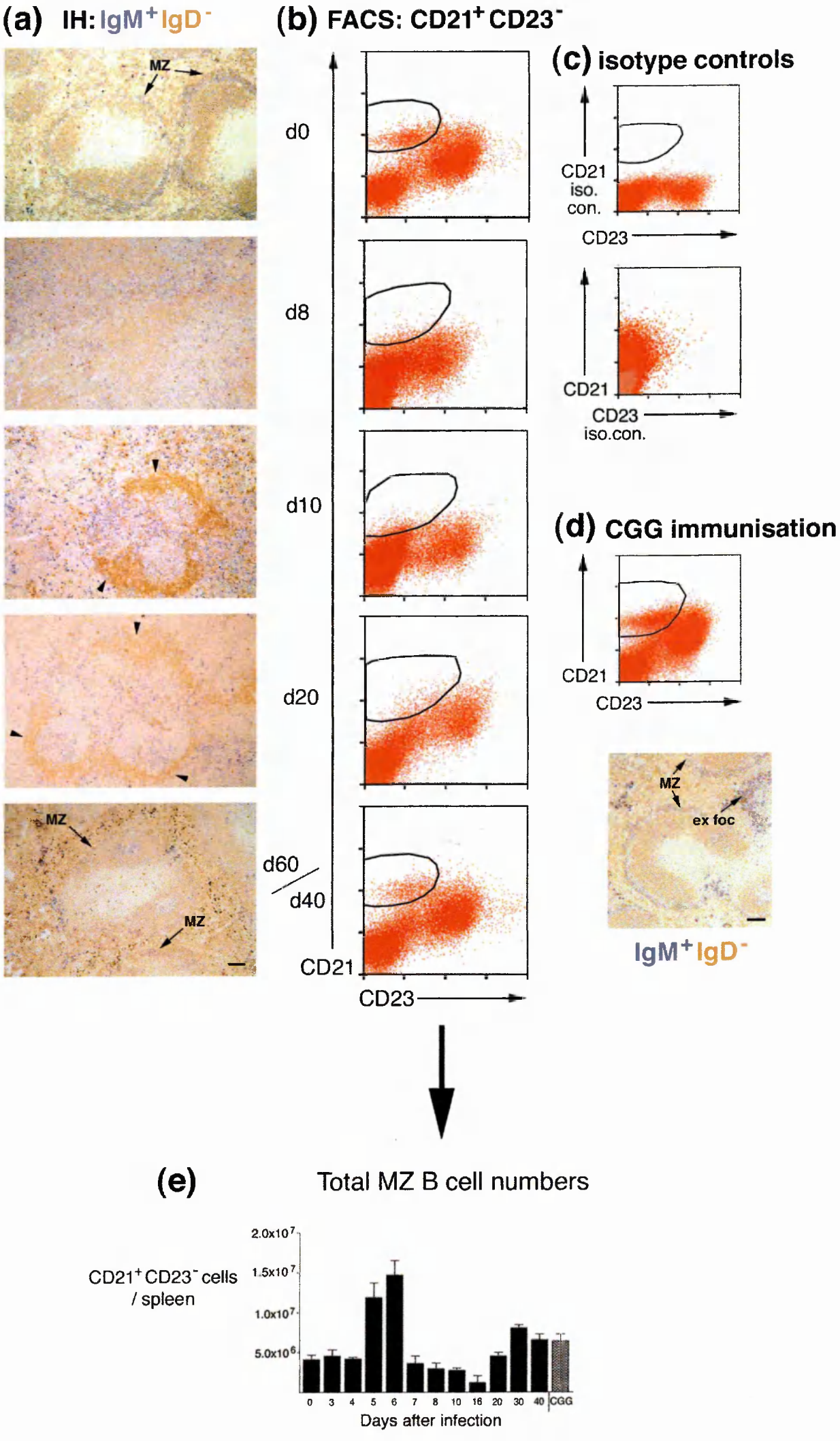
(a) IH: IgM+ IgD-
(b) FACS: CD21+ CD23-
(c) isotype controls
(d) CGG immunisation
MZ
d0
d8
d10
d20
d60
d40
CD21
CD23
CD21 iso. con.
CD23 iso.con.
ex foc
IgM+ IgD-
(e)
Total MZ B cell numbers
CD21+ CD23- cells / spleen
2.0x10^7
1.5x10^7
1.0x10^7
5.0x10^6
0 3 4 5 6 7 8 10 16 20 30 40 CGG
Days after infection

Figure 3.13 Examples of plasmablasts in the marginal zone B cell population during *P. c. chabaudi* infection.

The live marginal zone B cell population is depicted in representative dot plots on the left for days 0 and 3-7 of infection. The cells in the marginal zone B cell gates were then further analysed for cell size by forward scatter in the histograms on the right. The marked region contains marginal zone B cells of plasmablast size and its percentage is given in the corner. The results for all mice are summarised in Table 3.2.

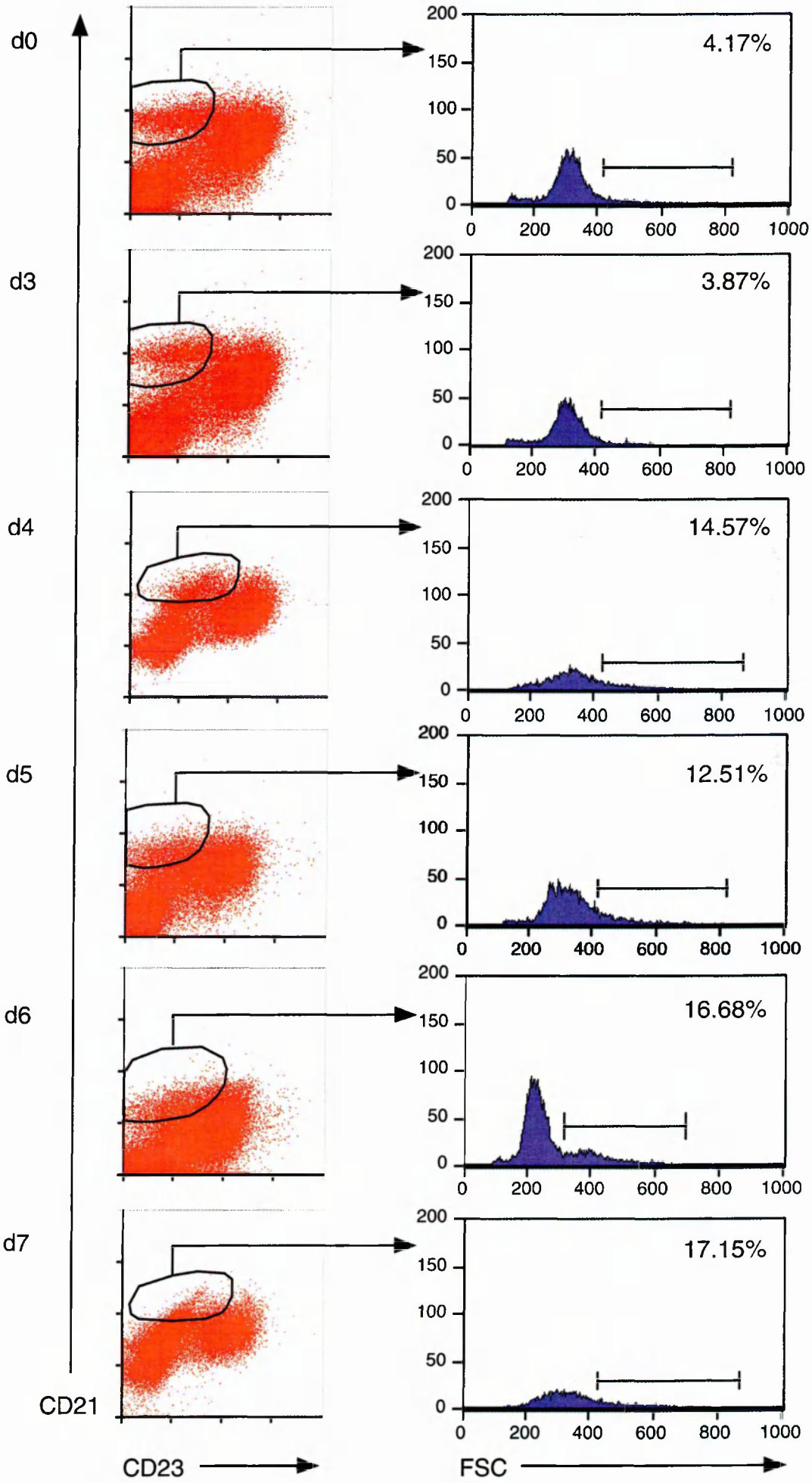
d0
d3
d4
d5
d6
d7
CD21
CD23
FSC
4.17%
3.87%
14.57%
12.51%
16.68%
17.15%
0
50
100
150
200
0
200
400
600
800
1000

Table 3.2 Numbers of plasmablast-sized cells in the marginal zone population [a)]

Day of infection	Percentage of large cells in the marginal zone region[b)]
0	3.19 ± 0.40
3	3.54 ± 0.23
4	14.00 ± 0.96
5	12.17 ± 0.34
6	17.28 ± 1.59
7	15.41 ± 3.59

a) The marginal zone region and the region defining plasmablast-sized cells are shown in Fig. 3.13.

b) The geometric mean and SEM from three mice are shown for each time point, except for day 6 where six mice were used.

of the marginal zone B cells were unsuccessful, but the size measurements give clear results with the percentage of large cells in the marginal zone B cell population increasing from day 4 to a peak at day 6/7, where the percentages are more than fivefold higher than in uninfected mice. This indicates that a part of the marginal zone B cell population is differentiating into plasmablasts early in infection.

3.2.8 Cell death

Previous studies have shown that malarial infection causes large numbers of splenic host cells to undergo apoptosis (Helmby *et al.*, 2000; Sanchez-Torres *et al.*, 2001). To determine whether apoptosis preferentially affects any particular population of B cells, $CD19^+$ B cells, germinal centre B cells and marginal zone B cells from days 8, 9 and 10 of infection were studied. These time points were thought most likely to exhibit apoptosis, as the parasitaemia and splenic disruption are highest during this period. At first, staining with annexin V, an early indicator of apoptosis which binds to phosphatidylcholine in apoptotic membranes, was attempted. The levels of annexin V^+ cells in naive spleens were too high, perhaps because the complex marker combinations in staining made the staining protocol somewhat lengthy, causing many cells to begin the process of apoptosis *in vitro*. Therefore, a later indicator apoptosis was chosen, 7-aminoactinomycin D (7-AAD), a dye which passes through the leaky membranes of apoptotic cells to bind to DNA and whose fluorescence can be detected with the FL3 detector on the FACScalibur® (Fig. 3.14). It is customary to use propidium iodide as an indicator of necrosis in parallel with 7-AAD to show that cells are truly apoptotic and have not just been killed by the staining procedure (Fig. 3.14). Inconveniently, propidium iodide is registered by two of the four fluorescence detectors on the FACScalibur®, thereby limiting the number of fluorochromes that can be used to define the B cell populations. These channel limitations meant that the marginal zone B cells could not be tested for propidium iodide staining and neither apoptosis nor necrosis of antibody-containing cells could be measured.

Figure 3.14 Examples of cell death around the peak of *P. c. chabaudi* infection.

(a) The total B cell population ($CD19^+$) is shown in the top row. The bottom row shows the 7-AAD^+ and propidium $iodide^+$ cells in the gate defined in the top row.

(b) On the top, the germinal centre B cell population is defined as either $GL7^+CD19^+$ (for 7-AAD staining) or $GL7^+$ (for propidium iodide staining). The bottom row shows the 7-AAD^+ and propidium $iodide^+$ cells in the gate defined in the top row.

(c) The marginal zone B cells ($CD21^+CD23^-$) were identified in the top row. This population was then analysed for 7-AAD staining in the bottom row. The marginal zone B cell markers could not be used in combination with propidium iodide, as the latter prevents use of either the second or third laser channels on the FACScalibur.

The complete nucleated splenocyte fraction was used for these analyses, as the apoptotic cells might otherwise be excluded with the dead cells. Forward scatter is on a linear scale. All fluorescence intensities are on a logarithmic scale.

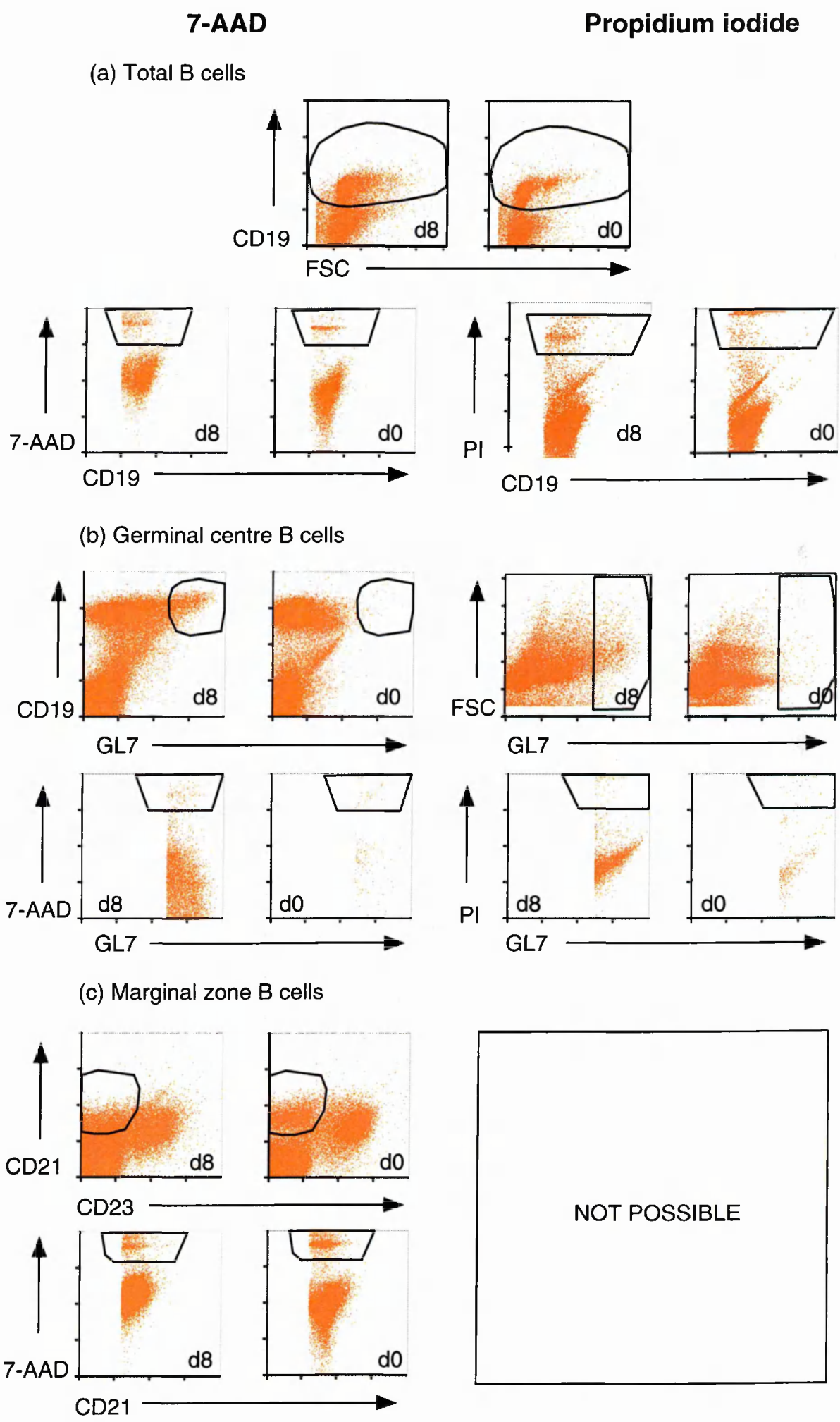
7-AAD
Propidium iodide
(a) Total B cells
CD19
FSC
d8
d0
7-AAD
CD19
PI
(b) Germinal centre B cells
GL7
(c) Marginal zone B cells
CD21
CD23
NOT POSSIBLE

Although the total number of apoptotic $CD19^+$, germinal centre and marginal zone B cells increases up to 5-fold, 23.5-fold and 2.3-fold, respectively, by day 8 or 9 of infection (Table 3.3), the apoptotic percentage of each population remains roughly similar for the $CD19^+$ cells and drops for the germinal centre and marginal zone B cells (5.5-fold and 2.7-fold, respectively). This suggests that the increase in absolute apoptotic B cell numbers is entirely explained by the size increase in these populations during infection (see Fig. 3.3).

Examination of the hematoxylin and eosin-stained sections from days 0. 8, 10, 12 and 14 of infection supports this idea. Apoptotic nuclei can be recognised by their condensed chromatin, but increased clusters of such cells were only observed in the germinal centres, where apoptosis is an integral part of affinity-based B cell selection (Fig. 3.15).

Table 3.3. Levels of cell death in splenic B cells at the peak of *P. c. chabaudi* infection [a)]

Day	$CD19^+$ B cells		Germinal centre B cells		Marginal zone B cells	
	% [b)]	Total no. of cells x 10^7 [c)]	%	Total no. of cells x 10^5	%	Total no. of cells x 10^5
0	10.2 ±1.5	0.4 ± 0.09	24.4 ± 6.4	0.2 ± 0.08	10.7 ± 1.8	8.0 ± 3.5
8	7.7 ± 0.06	1.4 ± 0.36	3.1 ± 0.9	3.3 ± 0.86	4.0 ± 0.3	18 ± 1.3
9	8.7 ± 5.0	2.0 ± 0.35	4.4 ± 2.5	4.7 ± 0.61	5.4 ± 3.1	4.5 ± 0.5
10	14.1 ± 0.9	1.7 ± 0.29	5.6 ± 1.5	3.5 ± 0.24	6.6 ± 0.8	2.6 ± 0.4

a) Each data set represents the arithmetic mean and standard error from a group of three mice.

b) % refers to the percentage of each B cell population which is apoptotic, as determined by the nuclear binding reagent 7-AAD.

c) Total numbers of apoptotic cells of this type in the spleen.

Figure 3.15 Clusters of apoptotic cells in a germinal centre after *P. c. chabaudi* infection.

A germinal centre is shown in a haematoxylin and eosin (H & E)-stained spleen from day 10 of infection. Clusters of apoptotic cells, identifiable by the condensed chromatin of their nuclei, are circled in white. Panel b shows a magnified section from panel a.

RP: red pulp, GC: germinal centre

H & E

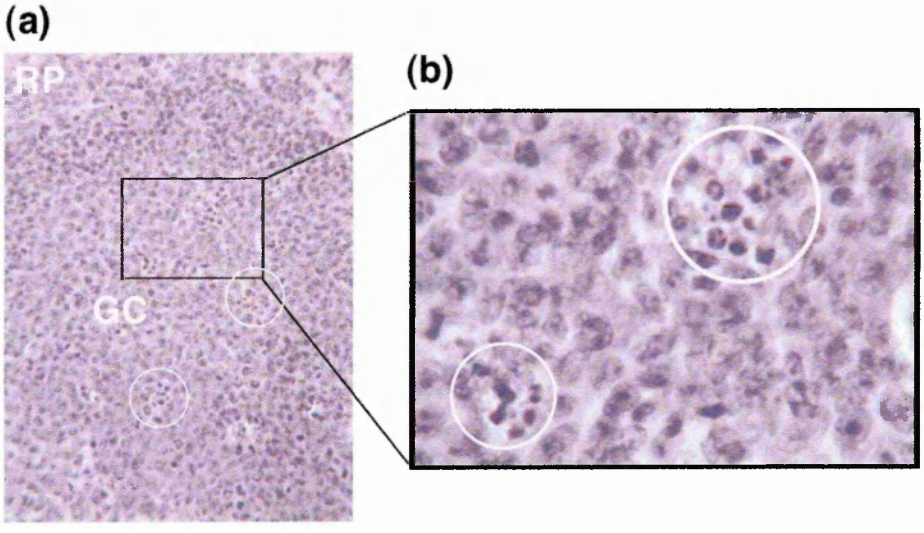

Figure 3.16 Summary of the changes in the white pulp during *P. c. chabaudi* infection.

Marginal zones

- temporary disappearance of metallophilic macrophages and marginal zone B cells from marginal zones
- marginal zone B cells remain in the spleen and probably participate in the early plasma cell response to infection

T zone

- temporary disappearance of T cells coinciding with the peak of infection
- atypical occupation by antibody-containing cells for 10 days after the peak of infection

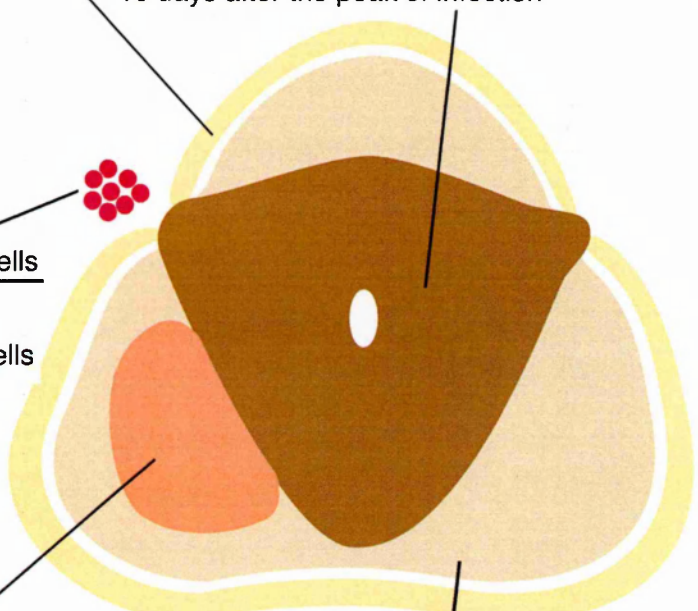

Antibody-containing cells

- very high levels of antibody-containing cells

Germinal centres

- strong, persistent germinal centre response
- no signs of excessive cell death interfering with the generation of memory B cells

Follicular mantle

- temporary disruption coinciding with peak of parasitiaemia
- total number of naive recirculating B cells in the spleen not reduced

3.3 Discussion

Infection of C57BL/6 mice with *P. c. chabaudi* leads to severe but reversible disruption of the splenic white pulp architecture, with transient loss of the follicular mantle and T zone integrity, atypical location of plasma cells and migration of marginal zone B cells (summarised in Fig. 3.16). These observations extend previous studies on *P. chabaudi* and *P. yoelii* infections where less specific histological analysis indicated splenic disruption and partial lymphocyte depletion.

Kumararatne *et al.* observed that in *P. c. chabaudi* (AS) infection of C57BL/6 mice, the white pulp was reduced in size and depleted of lymphocytes between days 10 and 11 of infection (Kumararatne *et al.*, 1987), regaining its normal appearance after day 14 of infection. A partial depletion of T cells at the peak of parasitaemia occurred after infection of outbred CD-1 mice with a more virulent strain of *P. c. chabaudi* (AS) (Stevenson and Kraal, 1989). Stevenson *et al.* also noted an enlargement of the white pulp which was also seen for the parasite *P. yoelii* (reviewed in (Weiss, 1990)). This enlargement can probably be accounted for by the presence of the germinal centres. These studies did not observe the transient depletion of the follicular mantles, the severity of splenic disruption or the completeness of reconstitution. This does not contradict my results, as these other groups were not able to assess the full extent of the changes with the less specific histological methods employed and only examined a few early time points in infection.

The splenic disruption observed in mouse malaria infection is not just a normal consequence of a disease with splenic involvement. There is no parallel in severity in any of the varied clinical samples studied by Prof. Ian MacLennan at the University of Birminingham (personal communication), which include diseases such as hairy cell leukaemia. The one known exception, which is discussed below, is the murine model of visceral leishmaniasis. There is only one published study showing immunohistology in a

human *P. falciparum*-infected spleen (Bordessoule *et al.*, 1990) and that only shows that the white pulp T cells are present and are mainly of the αβ TCR type. As there is no information on the stage of infection and only one spleen was examined, no general conclusions for splenic architecture in human malaria can be made from these data.

An unpublished study by Dr. Britta Urban (John Radcliffe Hospital, Oxford, UK) on 13 spleens from Vietnamese patients with *P. falciparum* malaria allows better comparisons. Similarities with the mouse model include loss of T cells from the white pulp and marginal zone depletion of B cells. The coronas (which correspond to the murine follicular mantle) however remained intact, and surprisingly, there were fewer germinal centres than in a normal adult. The ratio between the red and white pulp remained constant although the spleens almost doubled in weight. It is possible that the rapid red pulp expansion due to extramedullary hematopoesis in mice is responsible for some of the differences. On the other hand, there was also a lot of variation among the human samples, and B cell populations were not analysed in detail (partially because the fixation method made it impossible to use some antibodies). In addition, patients may have died before the full range of disruption seen in the mouse had a chance to occur. More complete analysis of human spleens should be forthcoming from a series of specimens collected in Malawi by Dr. Terri Taylor which includes spleens from patients who died of malaria or other causes.

The disturbance of the B and T cell areas does not appear to inhibit either generation of germinal centres or the production of antibody-containing cells (plasma cells and plasmablasts) in the spleen. This suggests that uninterrupted organisation of naive recirculating cells and T cells into primary B cell follicles and T cell areas is not necessary for the generation of germinal centres. This idea is supported by findings that B cells could co-localise with the follicular dendritic cell network and develop fully functional germinal centres in mice incapable of forming primary splenic B cell follicles (Voigt *et al.*, 2000). Spleens from mice which lack organised follicular dendritic cell networks in

addition to primary B cell follicles do not form germinal centres (Pasparakis *et al.*, 1996). Along with the complete and rapid reconstitution of white pulp structure after disappearance of the original insult, this implies that the follicular dendritic cell network remains intact during malaria infection. In visceral leishmaniasis on the other hand, which resembles malaria in parasite persistence and extent of splenomegaly, germinal centres diminished after 4 weeks of infection in parallel with the destruction of follicular dendritic cells (Smelt *et al.*, 1997). It would be easy to verify the continued presence of these cells during malaria infection by immunohistological staining with antibodies specific for follicular dendritic cells.

The kinetics of germinal centre appearance after infection are similar to those observed after immunisation with classical hapten antigens such as (4-hydroxy-3-nitrophenyl)acetyl (NP), where PNA^+ germinal centres are visible within 8 days of immunisation (Jacob *et al.*, 1991a). The lifespan of germinal centres depends on the duration of antigen exposure and NP-specific germinal centres are present in the spleen for about 3 weeks after immunisation (e.g. Liu *et al.*, 1991). However, germinal centres in the spleens of *P.c.chabaudi*-infected mice can persist for at least 60 days, which is reminiscent of the persistence of germinal centres at least 4 months after murine mammary tumour virus infection (Luther *et al.*, 1997). The germinal centres appear to be functional, as can be inferred from the large amount of isotype switching during malaria infection mentioned in Section 1.4.4 and the clear division of the germinal centres into a dark and light zone. Their persistence also speaks for their functionality, as germinal centres formed without the possibility of productive T and B cell interactions disintegrate about 5 days after formation (García de Vinuesa *et al.*, 2000).

These results indicate that if B cell memory is impaired in malaria infections, this is not due to a deficiency in germinal centre formation or maintenance. It has been shown previously that large amounts of soluble antigen can induce apoptosis of specific B cells in germinal centres and thus affect affinity maturation and B cell memory (Pulendran *et*

al., 1995; Shokat and Goodnow, 1995). Since malaria infections generate circulating soluble antigen (O'Dea *et al.*, 1995), this would be an attractive mechanism of impairing the development of B cell memory in malaria. However, there was no evidence of unduly enhanced apoptosis taking place in germinal centres around the peak of infection when maximal amounts of circulating antigen would be present.

The lack of increased apoptosis in the whole B cell population during *P. c. chabaudi* infection is supported by previous results in (BALB/cXC57BL/6)F_1 hybrids or BALB/c mice (Favila-Castillo *et al.*, 1999). Another study using BALB/c mice states that there is an increase in apoptotic B cells *P. c. chabaudi* infection, but they do not take into account that the B cell population has also increased in size (Helmby *et al.*, 2000). Nevertheless, they see a larger percentage of apoptotic B cells, which could be accounted for by different methodology or the different mouse strain. Sanchez-Torres *et al.* state that increased numbers of apoptotic B cells can be detected in sections by hematoxylin staining and TUNEL, but do not report where they saw the cells, which is likely to be the germinal centre location observed here (Sanchez-Torres *et al.*, 2001). In fact, they only show one picture of apoptotic cells taken on day 38 of infection and the encapsulated apoptotic cells seen in that image have the typical appearance of the tingible body macrophages which are found phagocytosing apoptotic cells in the germinal centres. It would be useful to do more detailed analyses with the TUNEL method in both flow cytometry and histology.

Plasmablast and plasma cell numbers expand greatly up to the peak of the infection and then rapidly disappear. This fits in with a study showing that the spleen has a limited capacity to support plasma cells and always reduces their number to the same level, irrespective of the size of the original response (Sze *et al.*, 2000). Most plasma cells generated during an immune response are short lived, with only a small proportion of long-lived cells remaining in the spleen or migrating to the bone marrow (Slifka *et al.*, 1998; Smith *et al.*, 1996). Apoptotic plasma cells probably account for a large part of the

increase in 7-AAD$^+$ B cells around the peak of infection and may well cause further increases in the period between 10 and 14 days. This could perhaps be analysed with the TUNEL method of detecting apoptosis in immunohistology. Further experiments are essential to determine the balance between the acute short-lived plasma cells in the spleen and the long-lived plasma cells in the bone marrow, as this could provide important information on the longevity of the antibody response in malaria.

Normally, plasma cells move from the edges of the T zone through the marginal zone bridging channels into the extrafollicular foci of the red pulp (Jacob *et al.*, 1991a). In the *P. c. chabaudi* infection, large numbers of antibody-containing cells were detected within the T zone for 10 days after the peak of infection. In nonspecific histology, this atypical location of plasma cells has previously been noted for isolated time points after infection with *P. berghei*, *P. yoelii* (Turk, 1973) and *P. chabaudi adami* (Alves *et al.*, 1996). The T zone location of plasma cells in malaria is similar to very early observations in neonatally thymectomised mice, where the splenic white pulp develops an area corresponding to the T zone, but in place of T cells, most of the cells within are immature plasma cells (Parrott *et al.*, 1966).

This suggests that plasma cells do not migrate into the red pulp if T cells are absent or diminished in number in the periarteriolar region. Stromally produced CCL-13 is thought to play a role in plasma cell migration (Hargreaves *et al.*, 2001), but it is not known whether T cells supply further migration signals via other chemokines or direct cellular interaction. Studies on migration of activated B cells have shown that the relative levels of two chemokines and their receptors can determine cell location (Reif *et al.*, 2002). In TNFRI$^{-/-}$ (p55$^{-/-}$) mice, antibody-containing cells stained by syndecan-1 also localise to the T cell area around the arterioles, rather than the usual location in the outer T zone, bridging channels and the red pulp (Tkachuk *et al.*, 1998). As the TNF signalling pathways are quite active in malaria infection and are also linked to chemokine signalling (reviewed by (Müller and Lipp, 2003)), members of the TNF family could also play a

role in the unusual behaviour of the antibody-containing cells in this infection. With the many drastic changes in the splenic cell populations, a detailed analysis of chemokine production during malaria infection could lead to very interesting discoveries. There could also be important downstream effects, as the signals which cause plasma cells to remain in the periarteriolar region could also affect subsequent migration to the bone marrow.

The marginal zone cell populations seem to be strongly affected by *P. c. chabaudi* infection. The disappearance of marginal zone B cells and a decrease of metallophilic macrophages as well as a complete disappearance of the marginal zone macrophages from their typical location has been noted before (Stevenson and Kraal, 1989). This partially matches the observations in visceral leishmaniasis, where marginal zone macrophages disappear and metallophilic macrophages are unaffected (Engwerda *et al.*, 2002). Unfortunately, B cells were not studied in this article. Transient loss of B cells from marginal zones is thought to be a normal response to antigen and LPS injection stimulates IgD^+ blast formation, which was also observed around the peak of malaria infection (Gray *et al.*, 1984; Groeneveld *et al.*, 1985). A high dose of LPS also causes a decrease of metallophilic macrophages in the marginal zone (reviewed in (Kraal, 1992)). However, malaria-infected spleens do not exhibit the rapid repopulation of the marginal zone seen after injection of non-replicating antigens (Gray *et al.*, 1984) and this might be due to persistent antigen stimulation. The similarity of this response of marginal zone populations to that induced by LPS is reminiscent of the elusive „malaria toxin". There have been several attempts to assign an endotoxin-like role to malarial products, most recently to the glycophosphatidylinositol-anchoured proteins (e.g. (Schofield *et al.*, 2002)).

The GPI-anchoured proteins from the parasite could be stimulating the capability of marginal zone B cells to develop quickly into plasma cells secreting low affinity antibody in response to particulate T-independent antigens (Martin *et al.*, 2001; Oliver *et al.*, 1999). This is supported by the increase in marginal zone B cell numbers on days 5 and 6

of infection with a sizable fraction of the population of plasmablast size. Due to the fact that B cell-deficient mice show impaired clearance of parasites after the peak of infection, it has been assumed that the role of B cells in malaria infection is limited to the later chronic stage (von der Weid *et al.*, 1996). Therefore, it would be interesting to see whether early phases of malaria infection are altered in a mouse lacking marginal zone B cells, such as the Pyk-2-deficient mouse (Guinamard *et al.*, 2000). This could also be important in human malaria infections, as the heightened susceptibility of young children is in part blamed on an immature immune system and the marginal zone takes 1-2 years to develop in infants (reviewed in (Martin and Kearney, 2000)).

Obviously, the earliest stages of the splenic immune response require more detailed study. In light of the visceral leishmaniasis study mentioned above (Engwerda *et al.*, 2002), the metallophilic macrophages and marginal zone macrophages should be studied in more detail. In addition, the antigen-presenting potential in the spleen seems very strong with the increase in $CD11c^+$ dendritic cell and F4/80 macrophage numbers. Especially the dendritic cells in their role as the most specialised antigen-presenting cell need to be studied with more attention to very early events and involvement of different subsets.

In summary, my findings suggest that if there is a poor memory B cell response in malaria infections it is not due to any obvious deficiencies in the follicular or extrafollicular B cell pathways. On the contrary, the B cell response is much stronger than that seen in classical immunisation experiments. Malaria is known to generate a large polyclonal B cell response (Anders, 1986; Langhorne *et al.*, 1985; Rosenberg, 1978) and this could mean that most of the B cell response seen during infection may be due to activation of innate immune mechanisms by pattern receptors. Therefore, the next essential step is to study how the specific response to a malarial antigen with known protectivity is distributed between the splenic B cell compartments and in other organs such as the bone marrow.

4 MSP-1_{21}-specific B cells in a primary infection

4.1 Introduction

This section analyses the primary B cell response to a single malarial antigen, the C-terminal portion of the merozoite surface protein-1 (MSP-1).The main question is how this specific response compares with the large general B cell response described in the previous section and with the specific response observed after immunisation with a non-replicating antigen. The magnitude and development of the response during primary infection with *P. c. chabaudi* are studied. Merozoite surface protein-1 was chosen for study because this protein is expressed during the erythrocytic life cycle of the parasite and is known to elicit protective immune responses. The C-terminal fragment of MSP-1 is very well characterised and was available in the laboratory as a recombinant antigen. In addition, it is one of the main candidates for a malaria vaccine and so a more detailed understanding of the immune response against this molecule is important for clinical applications.

4.1.1 Structure and processing of the MSP-1 molecule

MSP-1 was first characterised in 1982 (Holder and Freeman, 1982) and has also been called the precursor to the major merozoite surface antigen (PMMSA), gp190, gp195 or merozoite surface antigen-1 (MSA-1). It is a polymorphic glycoprotein which is expressed as a precursor protein of 185-250 kDa apparent weight and has been found on all investigated species of *Plasmodium* (Holder *et al.*, 1992). Most studies have used the *P. falciparum* MSP-1 and unless otherwise stated, all sizes refer to this protein. The protein is attached to the parasite membrane via a GPI anchor (Heidrich *et al.*, 1983). Before reaching the parasite membrane, the protein undergoes primary proteolytic processing into fragments of 83, 30, 38 and 42 kDa (referred to as MSP-1_{83}, MSP-1_{30} , MSP-1_{28} and MSP-1_{42}, see Fig. 4.1), which remain associated in a non-covalently bound

complex (Blackman and Holder, 1992; Blackman *et al.*, 1991). The complex also contains the proteins MSP-6 and one MSP-7, which are encoded by separate genes (Pachebat *et al.*, 2001; Trucco *et al.*, 2001), and remains attached to the parasite membrane via the GPI anchor of the MSP-1_{42} fragment.

Expression of MSP-1 begins at the trophozoite stage and the molecule is found on all subsequent stages up to the merozoite. The exact function of the MSP-1 molecule is still unknown, but indirect evidence exists for an involvement in erythrocyte invasion. Shortly before reinvasion of erythrocytes, the 42-kDa fragment undergoes essential secondary processing by a subtilisin-like protease into the C-terminal, membrane-bound 19-kDa fragment (MSP-1_{19}) and a non-covalently associated 33-kDa fragment (MSP-1_{33}) (Blackman *et al.*, 1998). During invasion, all of the MSP-1 fragments except for MSP-1_{19} are shed as a soluble complex (Blackman *et al.*, 1994), leaving the 19-kDa fragment as the only part of MSP-1 detected on the ring stages in newly parasitised erythrocytes (Blackman *et al.*, 1990). The C-terminal fragment is functionally conserved between distantly related *Plasmodium* species, indicating that strong evolutionary selection is preventing changes in this part of the MSP-1 (O'Donnell *et al.*, 2000). Structurally, the MSP-1_{19} fragment is one of the most conserved portions of the molecule with only two sites of polymorphism in *P. falciparum* (Jongwutiwes *et al.*, 1993). It contains 10-12 conserved cysteine residues which form five or six cysteine bonds (depending on the species of *Plasmodium*) which are responsible for the formation of two contiguous epidermal growth factor (EGF)-like domains (Blackman *et al.*, 1991).

In vitro assays have demonstrated the existence of so-called inhibitory antibodies which prevent the secondary processing step and are directed against epitopes in the 19-kDa fragment of *P. falciparum* MSP-1 (Blackman *et al.*, 1994). Another group of antibodies called blocking antibodies competitively interferes with the inhibitory antibodies such that secondary processing progresses without hindrance if both antibody types are

present. Frequently, the epitopes recognised by inhibitory and blocking antibodies are similar or spatially close (Blackman *et al.*, 1994), but some blocking antibodies bind to epitopes in the 83-kDa fragment (Guevara Patiño *et al.*, 1997). Due to the tertiary structure of MSP-1 protein, the blocking antibodies probably act by steric hindrance at both locations. A third class of MSP-1-specific antibodies, the neutral antibodies, exhibit neither inhibitory nor blocking function (Holder *et al.*, 1999). Several monoclonal antibodies have been described which inhibit both the cleavage of the 42-kDa fragment and erythrocyte invasion *in vitro* (Blackman *et al.*, 1994), demonstrating a possible causative link between secondary processing of MSP-1 and erythrocyte invasion. Antibodies of all three types have been shown to occur in natural *P. falciparum* infections (Guevara Patiño *et al.*, 1997; Nwuba *et al.*, 2002). Considering the degree of conservation in the C-terminal fragment of MSP-1, it as assumed that blocking and inhibitory antibodies occur in rodent infection, but this remains to be demonstrated.

In *P. c chabaudi*, the MSP-1 precursor protein has an apparent mass of 250 kDa in SDS-PAGE and a predicted mass of 197 kDa, with the difference being attributed to aberrant migation in SDS-PAGE rather than extensive post-translational modification (McKean *et al.*, 1993a). Primary processing results in fragments with apparent masses of 95 kDa, 52 kDa, 63 or 66 kDa and 45 kDa, with the 95-kDa fragment sometimes splitting further into 35 and 52 kDa (O'Dea *et al.*, 1995). Secondary processing of the 45-kDa fragment results in the C-terminal 21-kDa fragment, which corresponds to MSP-1_{19} of *P. falciparum*, and a 32-kDa fragment. (In this thesis, the term MSP-1_{21} will refer to the *P. c. chabaudi* protein in particular and the term MSP-1_{19} will be used both as a generic term when the *Plasmodium* species is irrelevant and specifically for the *P. falciparum* protein.) The fragments resulting from proteolytic cleavage of the *P. falciparum* and *P. c. chabaudi* MSP-1 molecules are compared in Fig. 4.1 along with the recombinant MSP-1 fragments used in this study.

Figure 4.1 Comparison of the results of MSP-1 processing.

This is a schematic representation of the fragments resulting from primary and secondary proteolytic processing of MSP-1 from *P. falciparum* (a) and *P. chabaudi* (b). The products of primary processing are shown in white and the products of secondary processing in light grey. Molecular weights observed by SDS-PAGE are given for each fragment.

(c) The recombinant constructs of *P. c. chabaudi* MSP-1_{21} used in this thesis are shown in dark grey for comparison. (The MBP fusion protein attached to pMCK129 is not shown.)

(a) *P. falciparum* MSP-1 (195 kDa)

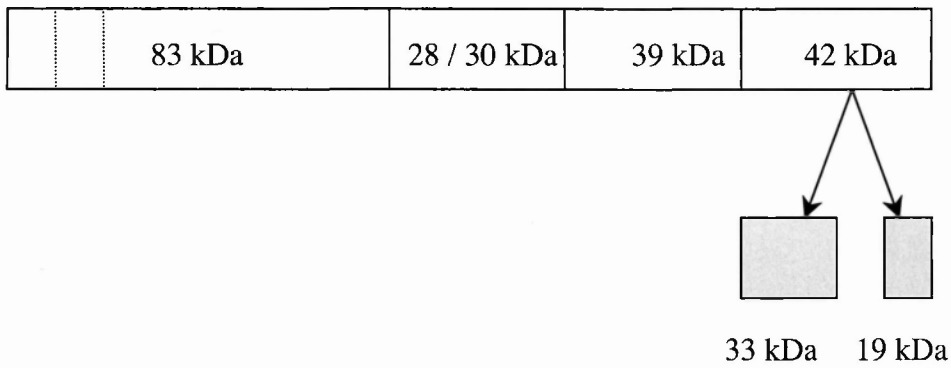

(b) *P. c. chabaudi* (AS) MSP-1 (250 kDa)

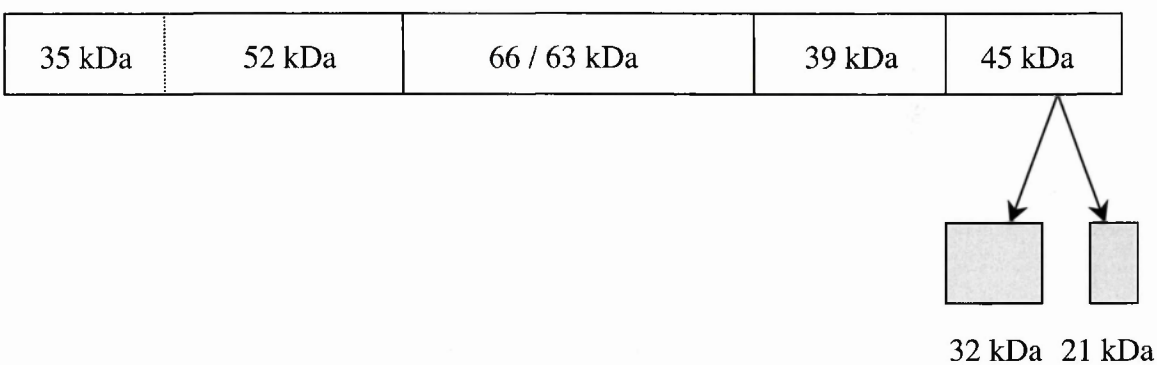

(c) Recombinant constructs for *P.c.chabaudi* MSP-1_{19}

pMCK129

Pichia MSP-1_{19}

4.1.2 Correlation between MSP-1_{19}-specific antibodies and protection

Field studies give contradictory results on the role of MSP-1_{19}-specific antibodies in protection. Protection against infection *per se* cannot be measured, because it cannot be determined whether aparasitaemic individuals were exposed to infection. Therefore, protection against morbidity is measured for example by differentiating between asymptomatic cases and symptomatic cases with parasitaemias ≥ 5000 / µL. A study in an area of seasonal, stable malaria transmission in The Gambia showed that high concentrations of MSP-1_{42}-specific IgG correlated with reduced malaria morbidity (Riley *et al.*, 1992). Corresponding results were seen for a site in Sierra Leone with perennial malaria transmission but not in a seasonally endemic area of The Gambia (Egan *et al.*, 1996). The prevalence of MSP-1_{19}-specific IgG was higher in children with asymptomatic malaria than in children with clinical malaria and was associated with an up to 40% reduced risk of clinical malaria. A further study encompassing sera from different regions of Africa and Southeast Asia indicates that antibody positivity for MSP-1_{19} alone was not associated with protection whereas the antibody levels were, but this data was not shown (Conway *et al.*, 2000).

On the other hand, a study of natural infections in an area of Ghana with perennial transmission did not find a link between prevalence or levels of MSP-1_{19}-specific antibodies and protection (Dodoo *et al.*, 1999). The contradiction with the previously detailed set of studies could have several causes: The studies demonstrating protection looked at children of 3-8 years of age, when immunity to malaria is developing, whereas Dodoo *et al.* chose an age group of 3-15 years. It is possible that MSP-1_{19}-linked protection in the older children is masked by other protective immune responses which take longer to develop, such as the variant antigen-specific immune responses. In addition, geographically determined host genetic factors may influence which malarial antigens are targets of protective immune responses. This could also be a factor controlling the ratio between inhibitory and blocking antibodies, which is another issue that can obscure the presence of protective MSP-1_{19}-specific antibodies.

4.1.3 Effectivity of immunisation with MSP-1_{19}

The results from MSP-1 immunisation studies in monkeys present an equally divided picture. *Aotus* monkeys were completely protected from *P. falciparum* infection after immunisation with antibody-purified MSP-1 (Siddiqui *et al.*, 1987) and partial to complete protection could be induced by immunisation with *Baculovirus*-expressed MSP-1_{42} (Chang *et al.*, 1996). In contrast, an *E.coli*-expressed MSP-1_{19} fusion protein did not induce protection in *Aotus* monkeys (Burghaus *et al.*, 1996). The most likely explanation for these differences is that the first two studies immunised with complete Freund's adjuvant and boosted with incomplete Freund's adjuvant whereas the third study used a milder adjuvant, alum-adsorbed liposomes.

Numerous immunisation studies have been performed in the mouse model with *P. yoelii* MSP-1_{19} and MSP-1_{42}.Complete protection from lethal infection or only low levels of parasitaemia were seen when the recombinant antigen was administered in complete Freund's adjuvant and then boosted with incomplete Freund's adjuvant (Daly and Long, 1995; Hirunpetcharat *et al.*, 1997; Ling *et al.*, 1995). Protection of a lesser degree was seen with the AF adjuvant formulation, which is acceptable for use in humans (De Souza *et al.*, 1996). The RAS, alum and Titermax adjuvants were as successful as Freund's adjuvant if additional T cell epitopes were supplied by the fusion partner GST (glutathione-S-transferase from *Schistosoma japonicum*) (Daly and Long, 1996). Linkage of T cell-activating elements in form of cholera toxin subunit B also improved the effectivity of intranasally administered MSP-1_{19}, but the protection was still inferior to parenteral administration of antigen in Freund's adjuvant (Hirunpetcharat *et al.*, 1998). Thus it appears that MSP-1_{19} requires a strong adjuvant and a potent avenue of administration to induce protection.

4.1.4 Contribution of different components of the immune system to MSP-1_{19}-specific protection

It has been suggested that the C-terminal fragment of MSP-1 has lower immunogenicity than the other portions of the molecule. In blood from residents of a holoendemic area of

Kenya, peptides from the C-terminal portion of MSP-1 induced proliferative T cell responses in only 13.6-36.9% of the samples and the magnitude of these responses was low (Udhayakumar *et al.*, 1995). In the mouse model, it has been shown that the structural complexity of MSP-1_{21} causes it to be processed more slowly than the less complex N-terminal fragments of MSP-1, leading to lower MSP-1_{21}-specific $CD4^+$ T cell responses and a strongly reduced capability to supply T cell help to B cells (Quin and Langhorne, 2001a; Quin *et al.*, 2001b). A role for T cells is also indicated by the influence of the MHC haplotype in mice on the degree of protection, although this has not been confirmed in humans (Taylor *et al.*, 1996; Tian *et al.*, 1996).

Transfer of MSP-1_{19}-specific T cells from infected mice into nude mice does not protect against challenge infection (Wipasa *et al.*, 2002a), indicating that T cells do not exert a protective effect in the absence of antibody. Passive transfer of MSP-1_{19}-specific antibodies from immunised mice or of monoclonal antibodies results in partial protection against *P. yoelii* and *P. chabaudi* infection (Daly and Long, 1995; Spencer Valero *et al.*, 1998; Tian *et al.*, 1996; Hirunpetcharat *et al.*, 1999; Wipasa *et al.*, 2002b; Dr. Ching Li unpublished data).The level of protection is lower than in the originally immunised mice and parasitaemias progress to the lethal stage if the host is B cell deficient or unable to supply T cell help for continued antibody production as the original antibody inoculum is depleted by binding to the parasites (Hirunpetcharat *et al.*, 1999; Wipasa *et al.*, 2002b).

Antibody transfer experiments have shown that no other antibody specificities other than MSP-1_{19} are required for protection as long as the host is immunocompetent and thus able to contribute to that response (Wipasa *et al.*, 2002b). On the other hand, immunisation with the 33-kDa product of secondary processing has no protective effect (Ahlborg *et al.*, 2002). Immunisation with the EGF1 or EGF2 domains of MSP-1_{19} on their own as well as a mixture of the single domains produces inferior results to immunisation with the linked EGF domains (Calvo *et al.*, 1996; Ling *et al.*, 1995). This shows the importance of conformational epitopes which may be a product of both EGF

domains or are only correctly folded if the domains are stabilising each other. The immunity to MSP-1_{21} does not transfer between the species of *P. yoelii*, *P. berghei* ANKA and *P. chabaudi adami* (Rotman *et al.*, 1999), which in light of the strong conservation of MSP-1_{19} (McKean *et al.*, 1993a) suggests that only a limited number of B cell epitopes are involved in protection.

The poor quality of T cell help and the dependence on strong adjuvants as well as the lack of MSP-1_{19}-specific antibodies in large percentages of malaria-exposed humans suggest that MSP-1_{19} is not very immunogenic. Strong adjuvants such as Freund's and the more protective parenteral administration methods are not acceptable for use in humans. The immunisation protocols leading to protection in mice involve up to four boosts after the initial immunisation, which would also be impractical for human vaccination. A better idea of the type of B cell response elicited by MSP-1_{19} would be helpful for understanding the poor immunogenicity of the antigen and could assist in improving immunisation protocols.

4.1.5 Aims

The aims of this section are to characterise the splenic B cell response to the *P. c. chabaudi* MSP-1_{21} fragment for the following aspects:

(i) size of the specific B cell response as compared to a classic immunisation with a non-replicating antigen,

(ii) distribution of the specific response between the extrafollicular and follicular compartments,

(iii) degree of isotype switching in MSP-1_{21}-specific B cells.

Together, the results should give an idea of the volume of the MSP-1_{21}-specific B cell response and its potential to generate long-lived cells.

4.2 Results

4.2.1 Experimental design

Cryosections from the second series of spleens described in Section 3.2.1 were examined, i.e. spleens from days 0, 7-12, 20, 30 and 60 of infection. B cells specific for MSP-1_{21} were detected as outlined in Fig. 4.2 by binding of the MSP-1_{21} / MBP fusion protein followed by a polyclonal rabbit anti-MBP antibody, a biotin-labelled swine anti-rabbit antibody and HRP-labelled streptavidin complex. In order to determine the location of the specific B cells, one section on each slide was also stained with anti-IgD antibody. Two sections were stained with anti-IgG or anti-IgM to observe the degree of isotype switching in MSP-1_{21}-specific B cells. The secondary antibodies were AP-labelled donkey anti-sheep antibody (for IgD) or sheep anti-rat antibody (for IgG and IgM).

To control for non-MSP-1_{21}-specific binding by the MBP fusion partner, the fourth section on half of the slides received MBP as the first reagent rather than the MSP-1_{21} / MBP fusion protein. On the other half of the slides, the fourth section was stained with MSP-1_{21} / MBP and its revealing agents but not with the isotype-specific reagents to ensure that the isotype-specific brown stain was not obscuring any MSP-1_{21}-specific binding. A panel of additional controls was performed on spleens from day 9 of infection, when MSP-1_{21}-specific binding was strong, and is detailed in Table 4.1.

4.2.2 Identification of MSP-1_{21}-specific B cells

The detection of MSP-1_{21}-specific B cells with the MSP-1_{21} / MBP fusion protein was a novel approach. The technique was adapted from antibody-based immunohistology. First attempts were unsuccessful, with the entire sections staining blue. This background staining was attributed to binding of the MBP component to sugar residues and was eliminated by adding 10 mM maltose to the TBS buffer (Section 2.25). This concentration of maltose was chosen because it is capable of eluting MBP-containing proteins from amylose resin (Section 2.13).

Figure 4.2 Experimental design for Section 4.

This figure shows how MSP-1_{21}-specific B cells were detected by binding of the MSP-1_{21} / MBP fusion protein to the B cell receptor.

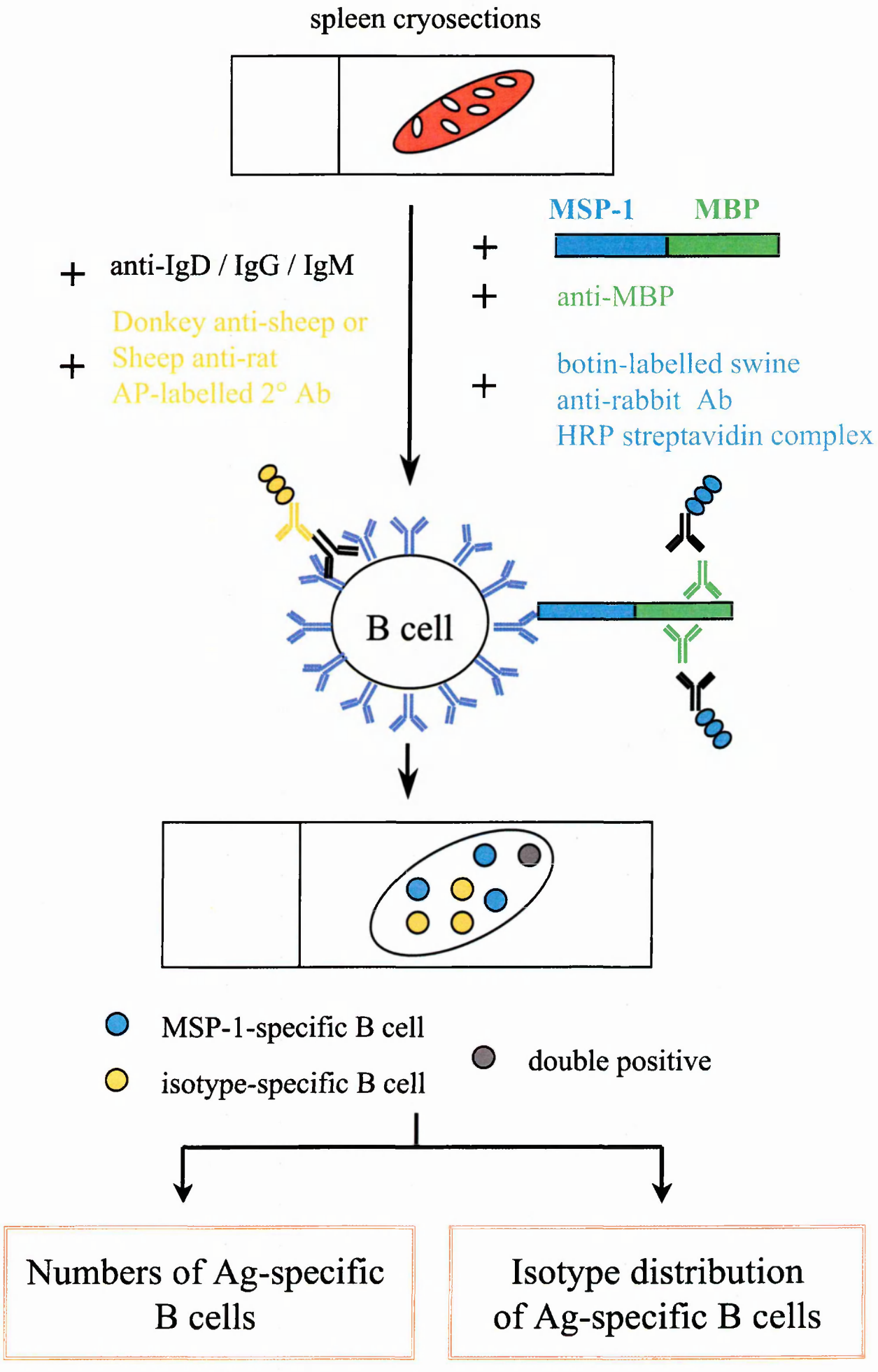
spleen cryosections
MSP-1
MBP
+ anti-IgD / IgG / IgM
+ Donkey anti-sheep or Sheep anti-rat AP-labelled 2° Ab
+
+ anti-MBP
+ botin-labelled swine anti-rabbit Ab HRP streptavidin complex
B cell
MSP-1-specific B cell
isotype-specific B cell
double positive
Numbers of Ag-specific B cells
Isotype distribution of Ag-specific B cells

Table 4.1 Controls for the MSP-1-specific B cell staining [a)]

	Antigen	1° Ab	2° Ab	Conclusion
Stain 1	pMCK 129	rabbit anti-MBP	swine anti-rabbit Ig	Complete stain
		sheep anti-IgD	donkey anti-sheep Ig	
Stain 2	pMCK 129	rabbit anti-MBP	swine anti-rabbit Ig	Complete stain
		rat anti-IgG / IgM	sheep anti-rat Ig	
Control 1	pMCK129	---	swine anti-rabbit Ig	a) No AP labelling without the anti-MBP antibody
		sheep anti-IgD	---	b) Swine anti-rabbit Ab does not cross-react with
Control 2	pMCK129	---	swine anti-rabbit Ig	any of the isotype-specific antibodies
		sheep anti-IgG	---	
Control 3	pMCK129	---	swine anti-rabbit Ig	
		sheep anti-IgM	---	
Control 4	pMCK129	rabbit anti-MBP	swine anti-rabbit Ig	The sheep anti-rat antibody does not interfere with binding in the pMCK129 pathway
		---	sheep anti-rat Ig	
Control 5	pMCK129	rabbit anti-MBP	swine anti-rabbit Ig	The donkey anti-sheep antibody interferes very slightly with binding in the pMCK129 pathway.
		---	donkey anti-sheep Ig	
Control 6	pMCK129	rabbit anti-MBP	swine anti-rabbit Ig	
		---	---	
Control 7	---	rabbit anti-MBP	swine anti-rabbit Ig	Hardly any staining without an antigen
		rat anti IgG	goat anti-rat Ig	

a) All controls were performed in single stains on spleen sections from day 9 of infection, when the MSP-1_{21}-specific B cell response is strong.

In addition to the streptavidin and substrate layers common to all of the immunohistological experiments (Section 2.21), this protocol consists of three staining layers in the MSP-1_{21} / blue branch and two in the isotype / brown branch. This creates many potential sources of false positive and negative results and Table 4.1 shows which controls were performed to test these possibilities. Controls 1-6 show that the isotype branch neither inhibits nor exaggerates staining in the MSP-1_{21} branch. Cell counts for control 6 showed that the numbers of MSP-1_{21}-positive B cells detected in the presence and absence of the isotype-specific antibodies were comparable (data not shown). Controls 1-3 and 7 show that all layers of the MSP-1_{21} branch must be present for B cells to be detected in the blue pathway. B cells are also labelled when MBP rather than the fusion protein is used as the first step reagent and this is discussed below.

It is necessary to define carefully what represents specific B cell staining. Examples of positive cells are marked by squares in the first panel of Fig. 4.3a. Some of the positive cells display a blue halo of secreted MSP-1_{21}-specific immunoglobulin, which can partially cover other cells. Therefore, only cells where both an unstained nucleus and a stained ring of cytoplasm were visible were counted. This also prevented inclusion of nonspecific substrate clumps. It was also necessary to exclude macrophages which exhibit a narrow blue ring caused by specific immunoglobulin bound to the Fc receptor (Fig. 4.3, panel a). These cells can be distinguished by the narrowness of the ring and the fact that they usually contain dark brown granules inside the blue ring. These granules represent either phagocytosed haemozoin or a reaction of incompletely inhibited endegenous peroxidases. This precise definition of what constitutes an MSP-1_{21}-specific B cell probably results in exclusion of some positive cells and is likely to favour plasma cells rather than undifferentiated or memory B cells because of the size of the cytoplasm in the former.

Two examples of MSP-1_{21} / MBP staining are shown in Fig. 4.3b and c with differing magnifications to allow an overview of the location of the specific B cells (Fig. 4.3b) or a

Figure 4.3 Examples of MSP-1_{21} / MBP staining.

(a) The squares in the left panel are placed around cells that were counted as positive for the blue MSP-1_{21}-specific stain. Only cells with a clear nucleus and a fully stained cytoplasmic ring were counted to avoid confusion with FcR-bound antibody or secreted immunoglobulins. The circle in the right panel show macrophages (MΦ) with a light blue stain which were not counted. These were recognised by the dark brown staining in the centre of the blue ring, which is caused by incompletely inhibited endogenous peroxidases.

(b) The panels show four consecutive sections of a spleen with an arteriole marked with X for orientation. The first three panels were stained with MSP-1_{21} (blue) and IgD, IgG or IgM (brown) and the fourth with MBP alone (blue). This overview shows how MSP-1_{21} / MBP^+ cells are located in similar locations in consecutive sections.

(c) The panels show four consecutive sections of a spleen. The first three panels were stained in blue for MSP-1_{21} and in brown for IgD, IgG or IgM. Double positive cells are brown-black in the second panel. The fourth panel was stained with blue for MBP and brown for IgM. This series shows the positive cells at larger magnification and shows an example of the brown / black double-positive cells (second panel) compared with single-positive cells (first and third panels).

Size bars correspond to 50 μm in panel a and 100 μm in panels b and c.

(a) MSP-1_{21} / IgM

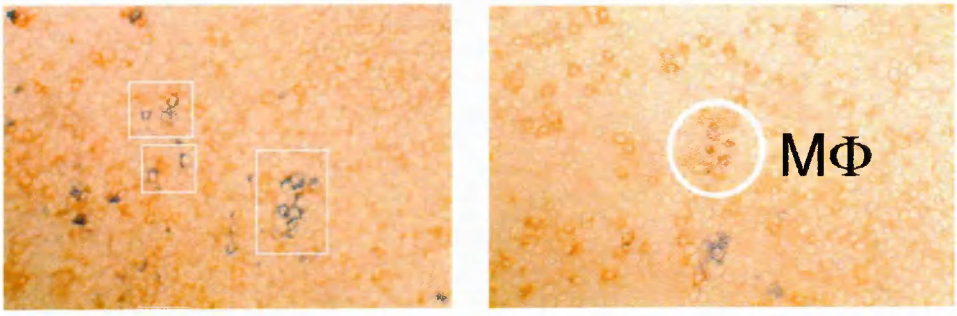

(b) MSP-1_{21} / IgD

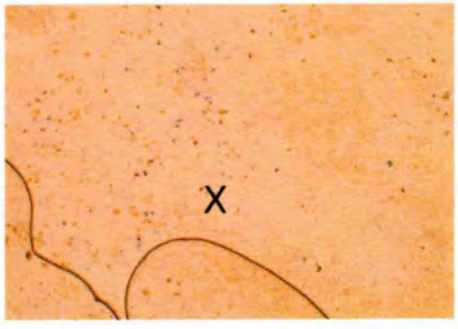

MSP-1_{21} / IgG

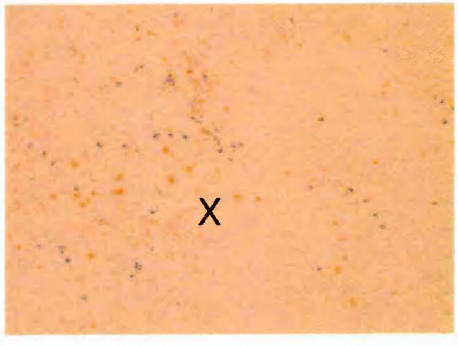

MSP-1_{21} / IgM

MBP

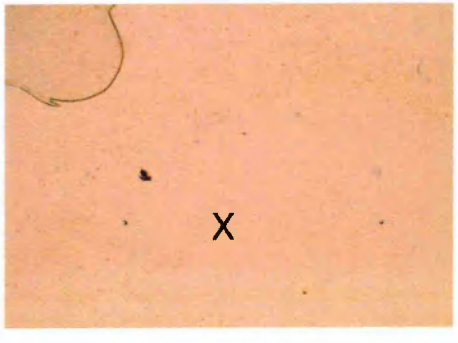

(c) MSP-1_{21} / IgD

MSP-1_{21} / IgG

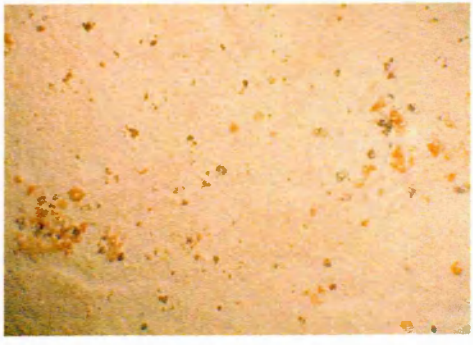

MSP-1_{21} / IgM

MBP / IgM

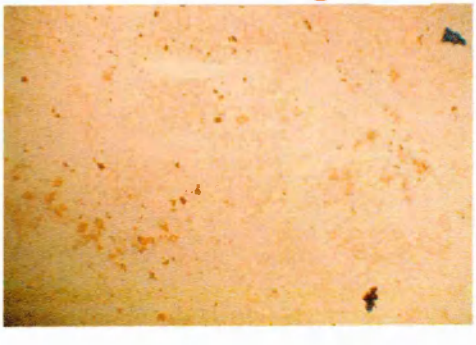

more detailed view of the cells (Fig. 4.3c). The four panels represent MSP-1_{21} / MBP staining in combination with antibodies against IgD, IgG or IgM and staining with MBP as a control. As can be seen in Fig. 4.3b, intensity of blue staining varies and blue-stained cells are still seen when one of the four consecutive sections on a slide was stained with MBP rather than MSP-1_{21} / MBP. The MBP^+ cells were often more weakly stained than those stained with the fusion protein in the other three sections (Fig. 4.3b), so faint blue stains were not counted in any of the sections. However, no clear cut-off level can be defined and there are MBP^+ cells which are stained as strongly as the most intensely stained MSP-1_{21} / MBP^+ cells. Therefore, some of the cells detected by MSP-1_{21} / MBP will be MBP^+ rather than MSP-1_{21}^+ and will inflate the count with false positives. Positive cells are often seen in loose foci, which show up in several consecutive sections (Fig. 4.3b and c). The MBP^+ cells showed up in the same areas as the MSP-1_{21} / MBP^+ part of the time (Fig. 4.3b), but there were also many instances where the locations of the MBP^+ and MSP-1_{21} / MBP^+ cells did not correspond (Fig. 4.3c).

Sections were stained simultaneously with the MSP-1_{21} / MBP fusion protein and an antibody against IgD, IgG or IgM to determine the isotype specificity of the MSP-1_{21}-specific B cells The two colours combine to produce a brown / black stain on cells which are double-positive for MSP-1_{21} and the respective isotype. An example can be seen in the second panel (MSP-1_{21} / IgG) of panel 4.3c).

4.2.3 Quantification of antigen-specific B cells

The number of antigen-specific cells is given as the total number counted per section (absolute number per section), the number of cells per 100 ocular squares (relative number per section) or the extrapolated relative number per spleen. The absolute number and the extrapolated relative number per spleen describe the size of the response. The relative number per section was calculated to describe densities of antigen-specific cells and to allow comparisons with sections with missing portions. The relative number per

spleen was also extrapolated to allow comparison between the absolute size of the specific B cell response to MSP-1_{21} and CGG.

The calculations for determining the relative number of antigen-specific B cells per spleen are described in Fig. 4.4 and this shows how the values in the final column of Table 4.2 were determined. It is not possible to compute absolute numbers of antigen-specific cells in the spleen, but a rough estimate of relative numbers could be made. This is based on the fact that proportion of the spleen occupied by a given compartment is the same in both area and volume measurements (Weibel, 1963). By using the splenocyte numbers measured in the FACS experiments in Section 4 as a measure of spleen volume, it was possible to calculate the proportional number of antigen-specific B cells per spleen. The unit cannot be translated into absolute numbers, but the numbers are comparable between spleens. Therefore, the proportional numbers of MSP-1_{21}-specific B cells were converted into a percentage of the proportional number of antigen-specific cells found in a CGG-immunised spleen and the results were summarised in the final column of Table 4.2.

4.2.4 Antigen-specific B cell after malaria infection and CGG immunisation

The relative numbers per section of MSP-1_{21} / MBP^+ cells are shown in Fig. 4.5 and are compared with relative numbers of MBP^+ cells. The relative numbers of MSP-1_{21} / MBP^+ B cells are highest at day 8 to 9, just before or around the peak of infection, with a second peak around day 30. The absolute numbers have matching peaks at the same time points (Fig. 4.7b, Table 4.2). As explained in Section 4.2.1, the control staining for MBP was only performed on half of the spleens. For the available time points (Fig. 4.5), it can be seen that the difference between the MSP-1_{21} / MBP and the MBP stain is largest around the two peaks, whereas MBP^+ staining was higher than MSP-1_{21} / MBP^+ staining for days 12 and 60 of infection- albeit with large error bars making it possible that the numbers are actually equal. Error bars are generally quite large, which is due to the large variations in positive cells between spleens from the same day of infection. Therefore,

Figure 4.4 Calculation of the size of the MSP-1_{21}-specific B cell response as a proportion of the CGG-specific B cell response.

The proportional number of antigen (Ag)-specific cells per spleen was calculated in the same fashion for *P. c. chabaudi*-infected and CGG-immunised spleens. The number of splenocytes per spleen is the average derived from all appropriate spleens used in the flow-cytometric experiments in Section 3. By relating numbers of splenocytes from treated animals to those from untreated animals via the size factor, the proportion of antigen-specific B cells in the whole spleen is extrapolated. The proportional number of antigen-specific cells is based on arbitrary units, but allows comparisons between spleens of different sizes. The final result is the percentage of MSP-1_{21}-specific B cells in infected spleens when compared to the number of CGG-specific B cells after CGG immunisation (100%). These values are listed in the final column of Table 4.2.

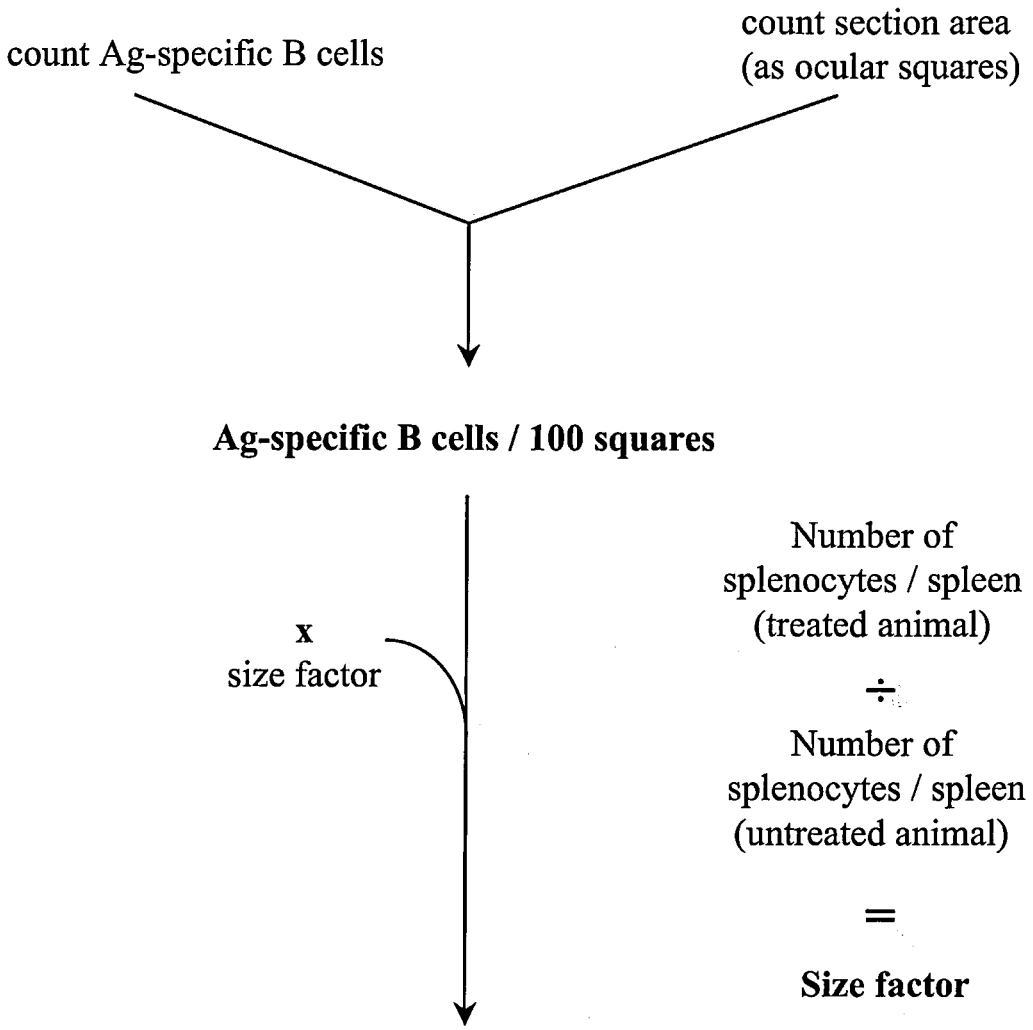

Proportional number of MSP-1-specific B cells / spleen ÷ Proportional number of CGG-specific B cells / spleen

= **% of CGG response in whole spleen**

Table 4.2. Antigen-specific B cells after *P. c. chabaudi* infection or immunisation with CGG [a)]

Days after infection	Ag-specific B cells / section [b)]	Ag-specific B cells / 100 squares [c)]	% of CGG response in whole spleen [d)]
0	2.4	2.4	1.1
7	39.1	14.5	17.0
8	100.4	36.3	50.0
9	73.8	24.6	46.6
10	31.8	8.1	26.2
12	14.7	3.7	13.6
20	33.8	10.5	16.3
30	92.2	20.3	31.0
60	20.0	17.5	12.3
CGG	311.1	238.5	100.0

a) MSP-1-specific B cells were measured at the stated time points after infection with 10^5 *P. c. chabaudi* pRBC. CGG-specific B cell numbers were measured 10 days after immunisation with 25 µg alum-precipitated CGG. MSP-1-specific values represent the arithmetic means of one to three sections each in three spleens. CGG-specific values represent the arithmetic means of one section each from three spleens.

b) These numbers include the false positives demonstrated by MBP-specific staining and are adjusted to represent sections of the whole spleen.

c) The size of the section was counted in numbers of grid squares in the ocular with a 20x objective and a 12x ocular magnification and the number of cells related to this area measurement.

d) The percentage of MSP-1-specific B cells in a whole infected spleen as compared to those in a whole CGG-immunised spleen was calculated as described in Fig. 4.4.

Figure 4.5 Comparison of B cells detected with MSP-1_{21} or MBP.

The number of antigen-specific cells per 100 ocular squares detected by immunohistology is shown for different days of infection. The values for MSP-1_{21} / MBP-specific B cells represent the arithmetic means from one to three consecutive sections from two to three different spleens. The values for MBP-specific B cells represent the arithmetic means from single sections from two to three spleens. Error bars show the SEM.

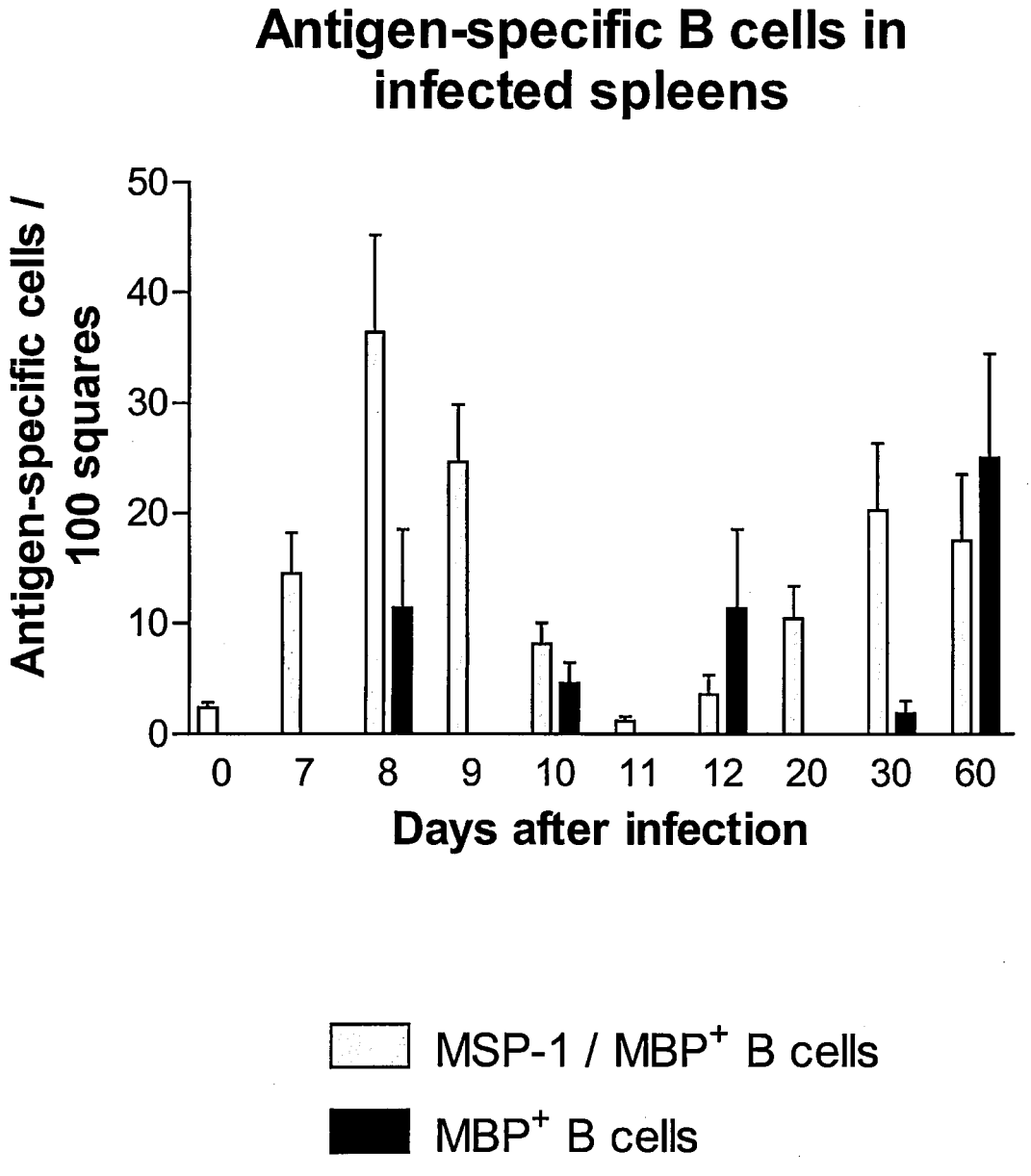
Antigen-specific B cells in infected spleens
Antigen-specific cells / 100 squares
50
40
30
20
10
0
0
7
8
9
10
11
12
20
30
60
Days after infection
MSP-1 / MBP+ B cells
MBP+ B cells

the most reliable results on MSP-1_{21}-specific B cell numbers were obtained at time points corresponding to peaks of parasitaemia.

The number of MSP-1_{21}-specific B cells generated in *P. c. chabaudi* infection was compared with the number of CGG-specific B cells found 10 days after immunisation with CGG with the aid of the calculations described in the previous section (Fig. 4.4). The results are shown in Table 4.2. Even at the peak of infection and at the time of parasitic recrudescence (day 30), there are at most half as many MSP-1_{21}-specific B cells per section in the infected spleens as CGG-specific B cells in immunised spleens. The true percentage is probably even smaller, as the fact that some of the MSP-1_{21} / MBP^+ cells are actually binding to the MBP fragment was disregarded in these estimates. When comparing the number of antigen-specific cells per 100 squares, the MSP-1_{21} / MBP^+ cells are more widely spaced than the CGG-specific B cells. This is not surprising, considering the increase in size of the spleen during malaria infection.

4.2.6 Extrafollicular versus follicular MSP-1_{21}-specific B cell responses

An important aspect of the antigen-specific response is whether any portion of the malaria-specific response is found in the germinal centres and can therefore give rise to long-lived B cells. The majority of the MSP-1_{21}-specific B cell response was found in the extrafollicular spaces. In sections from 27 spleens from different stages of infection, only a single MSP-1_{21}-specific germinal centre was detected in one of the day 20 spleens (Fig. 4.6a). However, only three consecutive sections from each spleen were examined, meaning that further MSP-1_{21}-specific germinal centres may be located outside of this plane of sectioning. The germinal centre is strongly stained with clear cytoplasmic staining, which shows that actual cells are stained rather than just immune complexes on follicular dendritic cells. The cells are all of the IgM isotype.

Figure 4.6 MSP-1_{21}- and CGG-specific germinal centres.

(a) Consecutive sections of a spleen from day 20 of infection with 10^5 *P. c. chabaudi* pRBC are shown. Spleens were stained with MSP-1_{21} / MBP fusion protein (blue) and either IgD, IgG or IgM (brown). In the third panel, cells are positive for both MSP-1_{21} and IgM, resulting in a brown-black stain. The panels show a large germinal centre and some antibody-containing cells located in the surrounding red pulp.

(b) Two different germinal centres are shown from a spleen taken 10 days after CGG immunisation with CGG stained in blue and IgG in brown. The top panel shows the clearest germinal centre seen in five immunised spleens and the bottom panel shows a less clearly defined example.

(a) MSP-1_{21} / IgD

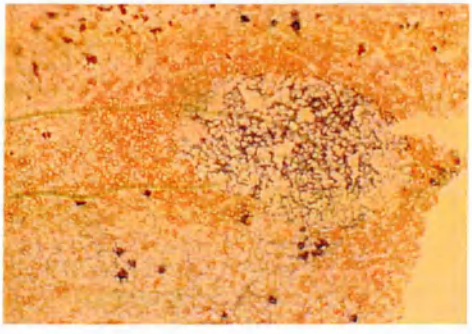

MSP-1_{21} / IgG

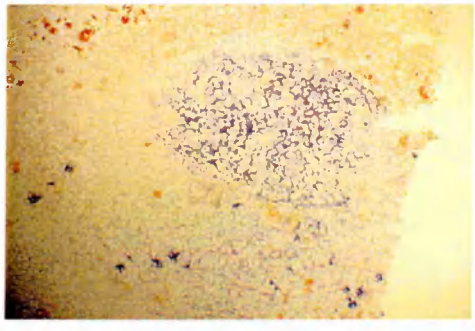

MSP-1_{21} / IgM

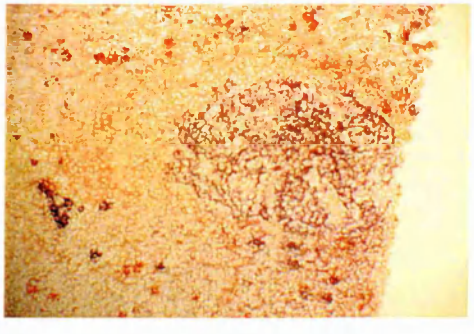

(b) CGG / IgD

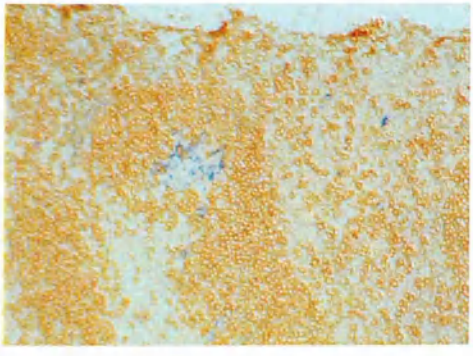

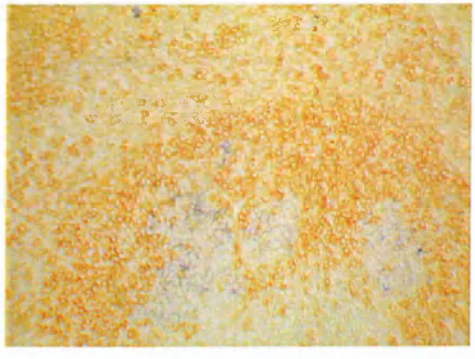

In sections from five spleens from CGG-immunised mice, about five CGG-positive germinal centres could be detected (examples in Fig. 4.6b), but the staining was much weaker than in the MSP-1_{21}-specific germinal centre. Of the CGG-positive germinal centres, the one with the strongest stain is shown in the upper panel of Fig. 4.5b, whereas the others looked more like the bottom panel of Fig. 4.6b, where it is difficult to judge whether the staining represents B cells or or immune complexes. The detection protocol for CGG-specific cells does not stain more weakly *per se*, as plasma cells of both specificities were stained with equal intensity.

4.2.7 Isotype distribution of MSP-1_{21}-specific B cells

The isotype specificity of MSP-1_{21}-specific B cells was determined by double staining with the MSP-1_{21} / MBP fusion protein and antibodies against IgD, IgG and IgM. An example of cells double positive for MSP-1_{21} and IgG is shown in Fig. 4.3c and for MSP-1_{21} and IgM in Fig. 4.6a. In the later stages of infection, the dark haemozoin granules look similar to the brown-black double-positive cells, but the presence of a visible nucleus makes it possible to distinguish the B cells. The percentage of MSP-1_{21}-specific B cells which was positive for each isotype is shown in Fig. 4.7a with the average absolute number of MSP-1_{21}-specific B cells per section for those days plotted in Fig. 4.7b. Percentages on days 0, 11 and 12 could be skewed, as the total mean number of MSP-1_{21} / MBP^+ cells on those days was very low (Table 4.2 and data not shown). As can be seen by the length of the error bars, there is considerable variation between spleens from the same day of infection, but nonetheless, certain trends can be identified.

On day 8 of infection, 33% of the MSP-1-specific B cells are IgD-positive. Double positive cells were mainly located outside of the follicular mantles. As the criteria for MSP-1_{21}-positivity lead to preferential detection of antibody-containing cells (see Section 4.2.2), it seems likely that these cells form part of the extrafollicular IgD^+ plasmablast population seen around the peak of infection (Section 3.2.6). However, the predominant

Figure 4.7 Isotype distribution among MSP-1_{21}-specific B cells.

(a) The graph shows the percentage of MSP-1_{21} / MBP^+ B cells which were also positive for IgD, IgG or IgM at different time points after infection with *P. c. chabaudi,* as detected by immunohistology. Each point represents the arithmetic mean from one to three consecutive sections from two to three different spleens. Error bars show the SEM.

(b) The absolute number of MSP-1_{21} / MBP^+ B cells in single splenic sections is shown for different days of infection. This panel is important for interpretation of panel a, as it gives the percentages a numerical basis. The values represent the arithmetic means from single sections from one to three consecutive sections from two to three different spleens. Error bars show the SEM.

(a) Isotype distribution of MSP-1_{21}^{+} B cells

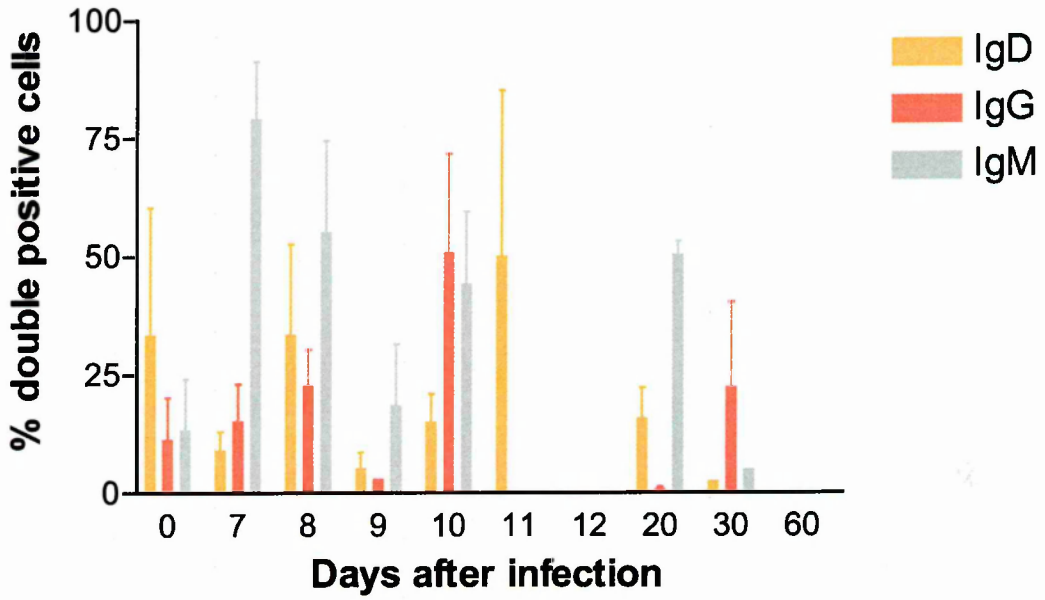

(b) Total MSP-1_{21} / MBP^{+} B cells

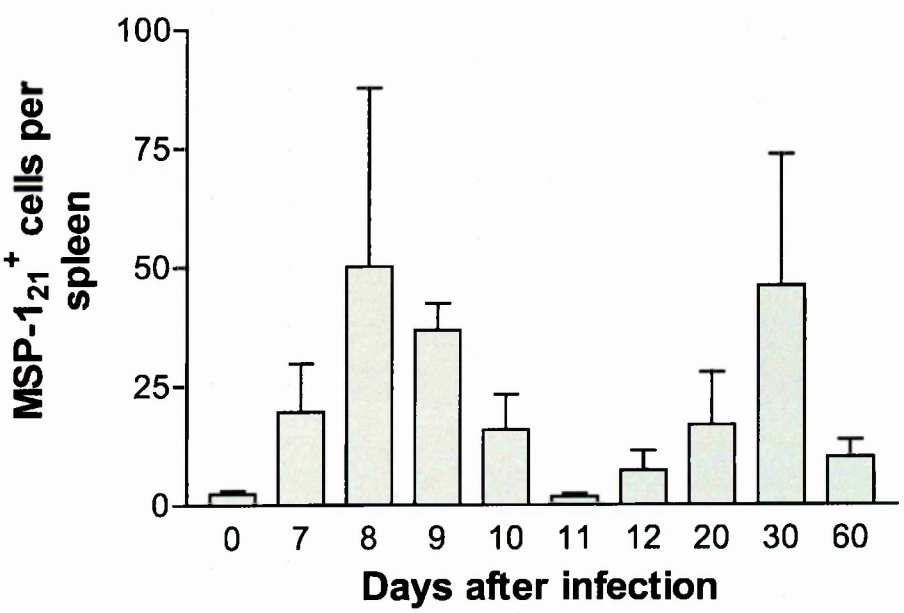

isotype of the MSP-1_{21}-specific B cells is IgM, with the percentage of double-positive cells peaking on day 7 and total numbers on day 8 (Fig. 4.7a and data not shown). IgG double positive cells are present at the earliest measured time point, day 7, showing that isotype switching occurs at an early stage of infection, and represent the dominant isotype on d30 (Fig. 4.6a). Their absolute numbers peak on days 8 and 30 of infection, coinciding with the peaks in MSP-1_{21}-specific cell numbers (data not shown and Fig. 4.7b).

The percentages for the three measured isotypes add up to close to 100% for days 7, 8 and 10 of infection, but the sums are lower on days 20 and 30. (All isotypes were not measured at other time points). IgA and IgE double positive B cells are unlikely to make up the burden of the discrepancies on later days of infection, since they are far less common isotypes. A more plausible candidate is IgG2a. The anti-IgG antibody is made up of a mixture of four monoclonal antibodies directed against the four IgG subclasses, including one against the *Igh-1a* allele of IgG2a. However, the C57BL/6 mice possess the *Igh1-b* allele of IgG2a also known as IgG2c (Martin *et al.*, 1998) which is only poorly stained by this antibody (data not shown), so that this subclass could well be under-represented in immunohistology. Another explanation for the discrepancy could be that the high proportion of cells which are positive in MBP staining are not actually B cells, but perhaps macrophages with a phenotype of different appearance from those in Fig. 2a. These cells would obviously not bind to immunoglobulin-specific antibodies. The results of this section are summarised in Fig. 4.8.

Figure 4.8 Summary of the results from Section 4.

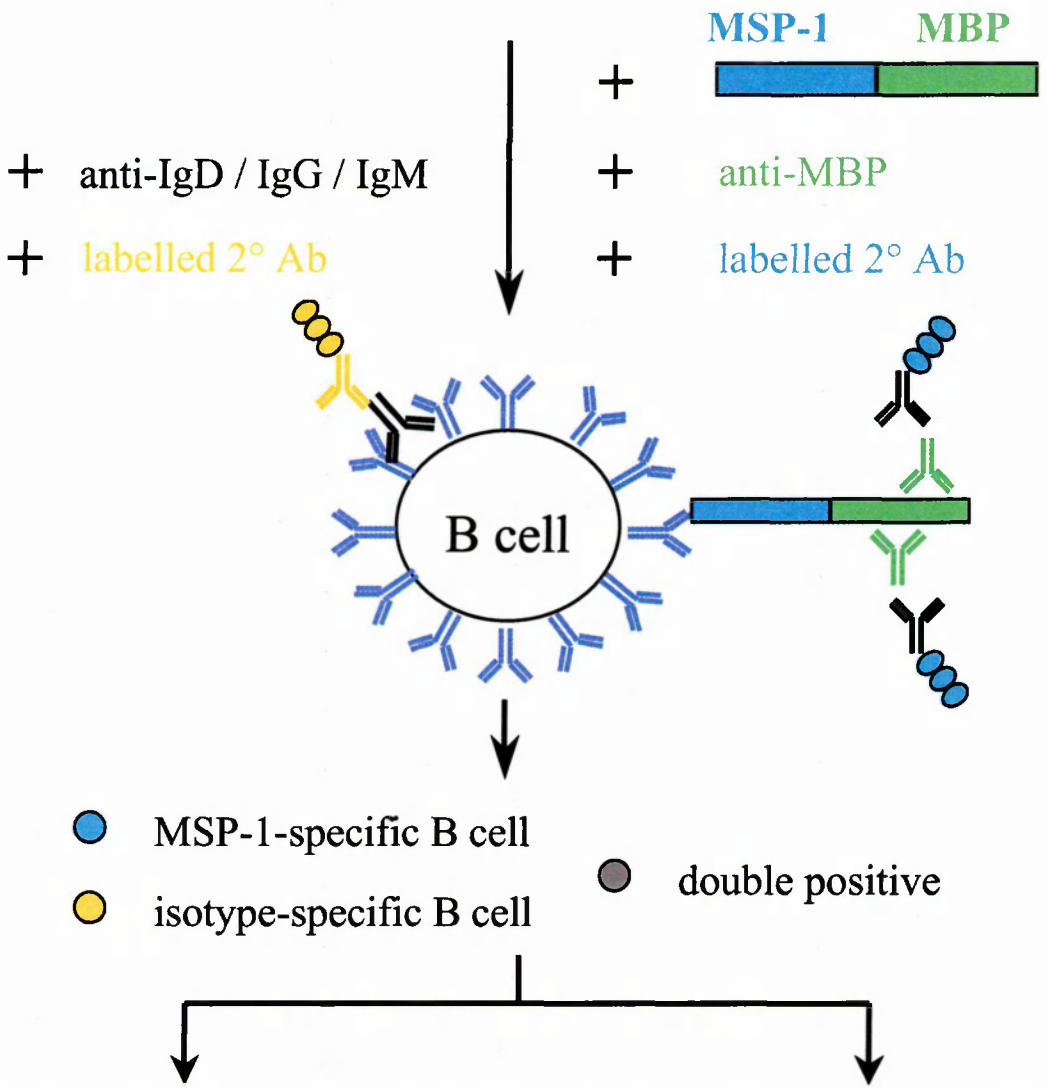

- **Peak numbers at peak of infection**
- **Less Ag-specific B cells than after CGG immunisation**
- **Technique needs refining:**
  - **MSP-1 without MBP**
  - **less layers**
  - **fluorescence**

- **IgM-positive Ag-specific cells most common at all times**
- **IgD-positive Ag-specific cells present ondays 7-11**
- **IgG switching of Ag-specific cells early in infection and peaks at day 30**

4.3 Discussion

The MSP-1_{21}-specific B cell response forms only a small fraction of the malaria-induced extrafollicular and follicular B cell response described in Section 3. MSP-1_{21}-specific B cells were quantified as the total number per section, the number in a given area or the estimated amount in the whole spleen. Irrespective of the representation of data, the peak number of MSP-1_{21}-specific B cells was between two- and tenfold lower than the number of CGG-specific B cells seen 10 days after immunisation. In CGG immunisation, there is only one antigen eliciting an immune response, whereas the B cell response will be directed against different parasitic antigens during malaria infection. In addition, a large pool of plasma cells which is not *Plasmodium*-specific is generated in malaria infection (Langhorne *et al.*, 1985; Rosenberg, 1978). The proportion of the B cell response which can be dedicated to any given antigen is homeostatically regulated by competition with B cells of other specificities for survival signals. Since the CGG-specific response develops without such competition, a response to a single malarial antigen which is half that size in total splenic numbers seems strong.

This contrasts with the evidence listed in Section 4.1.4 which suggested poor immunogenicity for MSP-1_{21}. Those results dealt mainly with immogenicity for T cells. However, MSP-1_{21}-specific B cells can also be activated by T cells recognising other parts of the MSP-1 molecule, so a poor T cell response to MSP-1_{21} does not automatically imply a poor MSP-1_{21}-specific B cell response. Apart from a 1-week delay in the detectability of MSP-1_{21}-specific IgM, the levels of IgG and IgM responses in *P. c. chabaudi* (AS)-infected BALB/c mice are comparable for MSP-1_{21} and other parts of the MSP-1 molecule (Quin and Langhorne, 2001a), suggesting that the B cell response does not exhibit as much variation between different parts of the MSP-1 molecule as the T cell response. An immunohistological comparison of the B cell responses to MSP-1_{21} and one of the N-terminal fragments is essential for answering the question of the relative

immunogenicity of MSP-1_{21} for B cells. Particular attention should be paid to spleens from the first 2 weeks of infection, when the delayed IgM response to MSP-1_{21} takes place. In addition, it would be valuable to compare the B cell response to another malarial antigen such as apical membrane antigen (AMA)-1.

The kinetics of the first half of the MSP-1_{21}-specific response correspond well with the kinetics in previously published immunisation studies: The first peak in MSP-1_{21}-specific B cells is seen on day 8-9 of infection. Day 8-10 also represents the peak B cell response seen in the spleen or draining lymph nodes of NP-CGG-immunised mice (Luther *et al.*, 1997; Toellner *et al.*, 1998) or in the draining lymph nodes after infection with mouse mammary tumour virus (Luther *et al.*, 1997). Immunisation with thymus-independent antigens results in an earlier peak at 5 days, because there is no 72-h delay for T cell priming (García de Vinuesa *et al.*, 1999). The timing of the peak in MSP-1_{21}-specific B cells suggests a predominantly thymus-dependent response which is initiated at the beginning of the infection or a thymus-independent response requiring a certain threshold of parasite antigen. The immediate induction of a thymus-dependent B cell response seems the more probable scenario, since MSP-1_{21} does not contain the kind of repetitive epitopes seen in thymus-independent type 2 antigens and thymus-independent type 1 antigens require an additional stimulus such as LPS for B cell activation.

The possibility that the GPI anchors might exhibit endotoxin-like activities in malaria infection was discussed in Section 3.3 in connection with the unusually large numbers of IgD^+ plasmablasts in the red pulp. The results in this section show that up to 33% of the MSP-1_{21}-specific B cells are also IgD^+, implying that some of these plasmablasts form a part of the *Plasmodium*-specific B cell response. Therefore, the involvement of a thymus-independent portion of the immune response must still be kept under consideration. Immunohistological study of earlier time points in the infection might reveal an earlier peak of specific B cells.

Another interesting facet of the kinetics of the MSP-1_{21}-specific B cell response is that the first peak takes place before or concurrent with the peak of infection, although the antigenic load increases over a period of 9 days and could therefore continue to activate naïve B cells resulting in a later peak or a plateau. Apparently, the smaller dose of antigen at the beginning of infection is sufficient to activate most of the MSP-1_{21}-specific B cells and later activation could be prevented by competition as described earlier.

The second peak of specific B cells at day 30 does not have a parallel in immunisation studies. It could be linked to the recrudescence of parasites, which occurs at the same time. Alternatively, since this peak contains predominantly IgG^+ cells, it is possible that germinal centre B cells play a role in the peak. The only germinal centre detected in the infected spleens was found at day 20 of infection. It is likely that other MSP-1_{21} germinal centres were present but lay outside of the section, since the infected spleens are so large. On the present evidence, it is difficult to judge whether the germinal centre response against CGG or MSP-1_{21} is stronger, as more CGG^+ germinal centres were seen, but these were mainly so weakly stained that the staining could be due to immune complexes. On the other hand, there was only the one MSP-1_{21}-specific germinal centre, but it was large and very clearly stained and had 10 more days to develop than the germinal centres observed in sections from day 10 after CGG immunisation. Spleens from day 20 after CGG immunisation should be examined to determine for a better comparison. Nonetheless, the presence of the germinal centre and the IgG-switched B cells indicate that memory generation against MSP-1_{21} is possible in malaria infection.

Small numbers of IgG^+ antigen-specific B cells are seen on day 7 of infection, increasing on day 8 and peaking after a transient drop on day 11. IgG^+ B cells appear as early as 2 days after immunisation (Jacob *et al.*, 1991a), so the presence of switched MSP-1_{21}-specific B cells on day 7 after infection is not unusual. The peak at day 11 also matches well with the peak in immunoglobulin heavy chain γ1 switch transcripts seen on day 10 after immunisation with NP-CGG (Toellner *et al.*, 1996) or the peak of $IgG1^+$ B cells

seen around day 10 after immunisation with NP-KLH (Smith *et al.*, 1996). The fluctuations before the peak could be due to the problems with the staining method or be caused by the splenic disruption at this time.

Overall, several interesting conclusions can be made about the B cell response to MSP-1_{21} from these data, but the technique used to identify MSP-1_{21}-specific B cells has a number of flaws which need to be addressed before these issues can be studied on more detail. One of the problems is the number of cells stained in the MBP control. If those cells are truly B cells which either recognise the MBP component or themselves contain carbohydrate residues bound by that portion of the fusion protein, then using a recombinant MSP-1_{21} protein which does not contain MBP would eliminate this complication. Direct biotinylation of the antigen is sufficient for detection of CGG-specific B cells and would also reduce the cross-reactivity by decreasing the number of staining steps. If the staining seen in the MBP control is due to macrophages rather than B cells, which is unlikely as there were hardly any positive cells when no antigen was used, then switching from immunohistology to immunofluorescence would avoid the problem of incompletely blocked endogenous peroxidases and phosphatases. The colour combinations in immunoflourescence would also make it easier to identify double-positive cells because the difference between yellow and green is clearer than that between dark blue and grey-black as well as avoiding confusion with haemozoin granules.

In summary, although the immunohistological method needs to be refined, this approach shows that the MSP-1_{21}-specific primary response roughly resembles classical immunisation responses in kinetics and isotype switching. The specific response has a strong extrafollicular component, but the existence of a germinal centre demonstrates the potential for generation of memory B cells and long-lived plasma cells. The persistence of MSP-1_{21}-specific immunity and the development of specific antibody responses during secondary infection will be addressed in Section 6 along with further evidence for the persistence of memory B cells and long-lived plasma cells.

Section 5. Protection against reinfection

5.1 Introduction

The previous two sections have examined the B cell response in a primary response and have shown that the potential for long-lived B cell responses exists. Before adressing the realisation of this potential in terms of the B cell response during secondary infections, it is necessary to establish the degree of protection against reinfection in this malaria model. Therefore, this section deals with the protection against parasites upon reinfection with the homologous strain after increasing periods of time.

Protection against reinfection has been studied in a variety of ways in rodent malaria models, most frequently using a parasite strain which would be lethal to the chosen host without intervention. The degree of parasitaemia and mortality of the initial infection are controlled by methods such as drug treatment, cytokine treatment, diet or blood transfusions (e.g. (Eling and Jerusalem, 1977; Eling, 1980; Falanga and Pereira da Silva, 1989; Mohan *et al.*, 1999)). This gives the host enough time to develop immunity to the parasite and makes host survival an unambiguous measure of protection in challenge infections. Protection measured by host survival and decreased peaks of parasitaemia has been shown for example for drug-controlled *P. chabaudi* (IP-PC1) and *P. vinckei* infections (Cox, 1966; Falanga *et al.*, 1984). In these studies, mice were reinfected 7 or 30 days, respectively, after the first infection became undetectable.

There is a very detailed study demonstrating the longevity of protection against lethal *P. berghei* (K173) in outbred Swiss mice over much longer periods (Eling, 1980). Mice were treated with subcurative doses of sulfathiazole during the first infection, which kept the parasites at subpatent levels while allowing immunity to develop. Mice were challenged with the homologous parasite 2 days after the end of drug treatment. All mice which survived the challenge (84% of the initial group) were declared immune and were reinfected at later time points. The longer the interval between the primary and

reinfection episodes, the fewer mice survived, but even after 304-488 days, about 40% of the mice survived a challenge infection. This shows that protection in this system is long lasting but does decay with time. When non-lethal, self-curing infections - such as *P. yoelii* (17X) in GP mice or *P. c. chabaudi* (AS) in NIH or CBA/Ca mice - are studied, long-lived protection in the form of reduced parasitaemic peaks and diminished duration of parasitaemia can also be seen (Barker, 1971; Jarra and Brown, 1985; Pearson *et al.*, 1983) (discussed in more detail in Section 5.3).

These reinfection studies used many different parasite species and strains, mouse strains, drug treatments, infection regimens and definitions of protection. In addition, most of them will have been performed with uncloned parasite isolates which can contain multiple strains of the parasite. Therefore it is crucial to establish the quality and type of protection for the model used in this thesis before asking questions about the longevity of B cell responses. If C57BL/6 mice are infected with *P. c. chabaudi* (AS) and then rechallenged 1-2 months after the primary infection reaches subpatent levels, the secondary infection shows a reduced peak and duration (shown e.g. in Taylor *et al.*, 2001). However, it is unknown how long this partial immunity lasts and whether it is maintained by long-lived cells of the immune system, serum antibody or by continued effector cell activation by low numbers of persisting parasites.

As discussed above, it has been shown for drug-cured *P. berghei* infection that protection against reinfection (in form of host survival) correlates with parasite persistence (Eling, 1980). However, when CB6F1 mice were infected with *P. c. chabaudi* (AS), drug cured in the early stages of infection and reinfected 7-8 weeks after parasite elimination, parasitaemias are also reduced in the secondary infection (Favila-Castillo *et al.*, 1999), arguing against a role for parasite persistence. It is difficult to compare these studies because the models are very different. Nonetheless, the studies demonstrate that parasite

persistence must be considered when looking at the longevity of protection against *Plasmodium* infection.

Therefore the aims of this chapter are to characterise the *P. c. chabaudi* model of infection in C57BL/6 mice regarding

(i) persistence of parasites

(ii) longevity of protection in the presence and absence of parasites

5.2. Results

5.2.1 Experimental design

The experimental design is outlined in Fig. 5.1. All time points are calculated from the day of injection of parasites in the primary infection. To determine how long C57BL/6 mice retain *P. c. chabaudi* parasites, the parasitaemic status of infected mice was determined for up to 9 months after infection, first by thin blood smear and then by subinoculation into naïve hosts at monthly intervals. For these experiments, mice were infected with 10^5 pRBC. After 1-9 months, the mice were bled out under lethal anaesthesia and the blood from each mouse was injected into one or two RAG-2-deficient mice. Immunodeficient (RAG-2-deficient) mice were used to increase the likelihood of low numbers of transferred parasites establishing an infection without interference from the immune response if the low initial parasite numbers took a long time to establish a patent infection. Thin blood films were taken at intervals of 2-3 days for 2 weeks and the RAG-2-deficient mice were kept under observation for several weeks after that.

A further set of experiments studied the longevity of protection: Two groups of mice were infected with 10^5 *P. c. chabaudi* pRBC while a third age-matched group was kept as controls. To distinguish between protective effects based solely on the existence of long-lived cells and those due to continued effector cell stimulation by low levels of replicating parasites, parasites were completely eliminated by chloroquine treatment after the primary

Figure 5.1. Experimental design for Section 5.

The top half of the figure shows the three types of infection protocols used in this section. The bottom half shows what procedures were performed with these mice after waiting for intervals of 2-9 months.

1°: primary infection, 2°: secondary infection

Three groups:

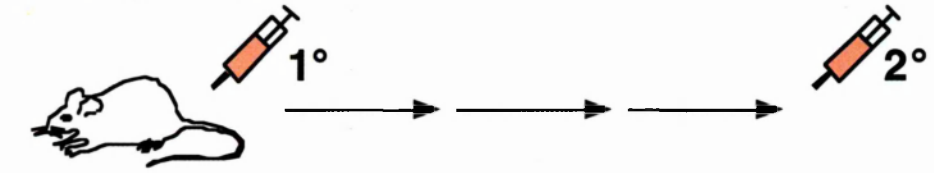

1. reinfected mice

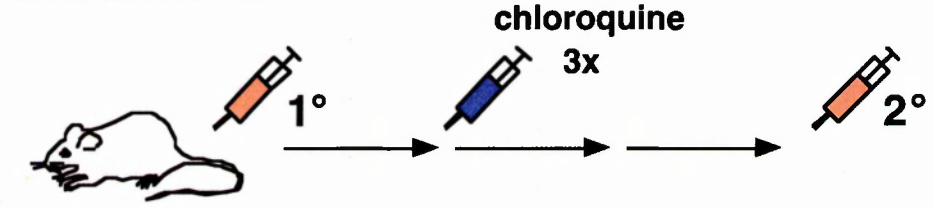

2. reinfected choloroquine-treated mice

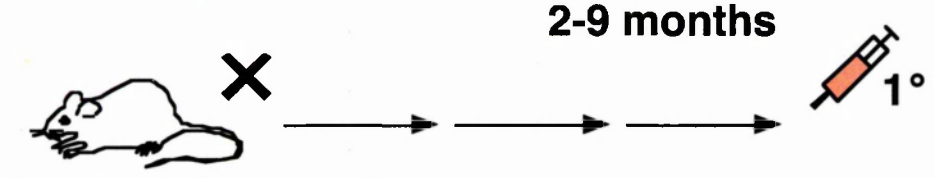

3. age-matched controls

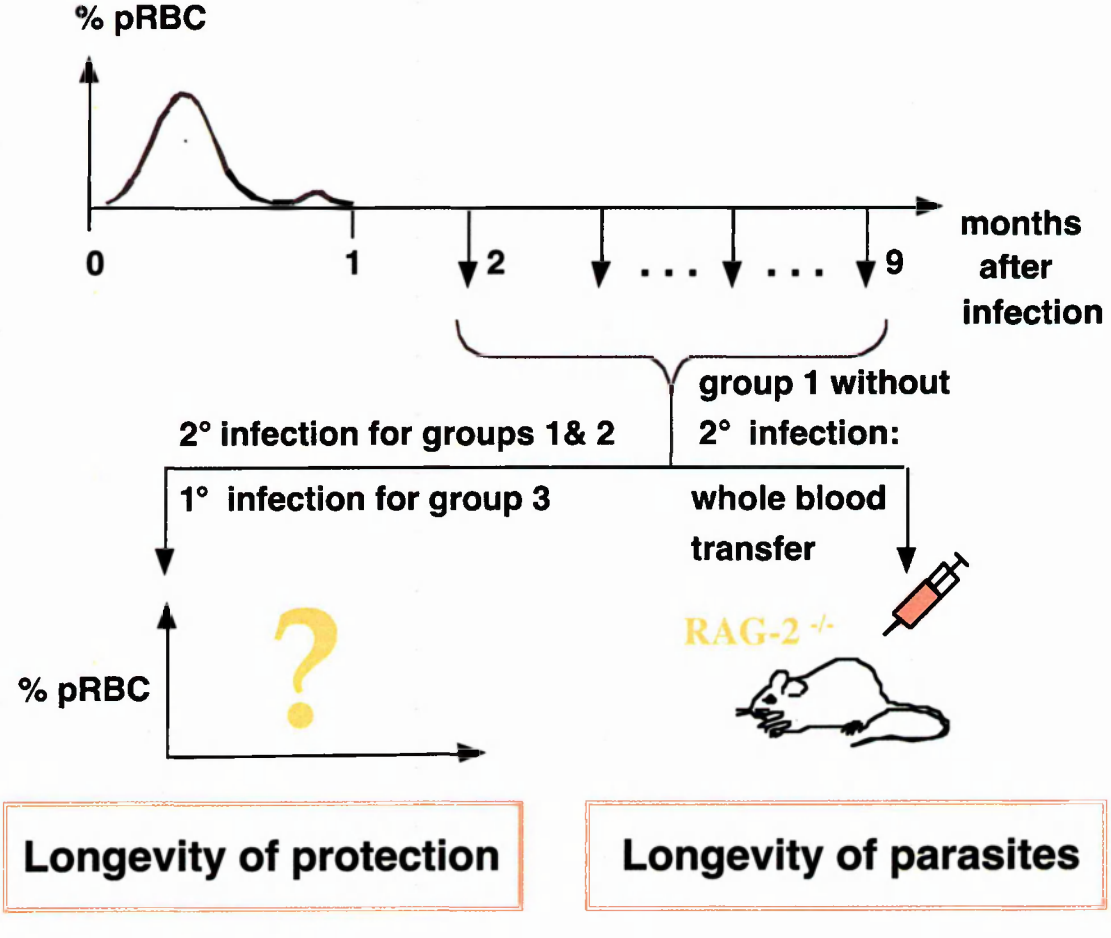

infection in one group of mice. Both groups were then infected a second time between 2 and 9 months later with the same number, species and strain of parasites. At the same time, an age-matched naive control group was infected to ensure that none of the observed effects were due to an abnormal infection or age-dependent changes in either the immune response or susceptibility to parasites.

Thin blood films were taken daily between days 3 and 12 of infection for maximal sensitivity during the rise and peak of parasitaemia and at intervals of 2-3 days thereafter. Protective effects were defined as alterations in parasitaemia in the form of lower amplitudes, delayed onset of patency and delayed peaks during the course of infection.

5.2.2 Persistence of parasites

Mice were infected with *P. c. chabaudi* and the infections were allowed to progress normally. After 2-9 months, mice were bled out and the blood was transferred into RAG-2-deficient mice. The results are summarised in Table 5.1. Parasites were detectable by this method up to 2 months post infection in some but not all of the mice. From 3 months onward, no infections developed in the sub-inoculated RAG-2-deficient mice, suggesting that no viable parasites were transferred or that their numbers were too small to establish an infection. So although parasites persist past the 30-40-day detection limit for thin blood films, they are not likely to play an active role in stimulating immune responses later than 3 months after infection. Parasite antigen will of course be displayed in immune complexes on follicular dendritic cells as would be the case with any non-replicating immunogen, but the additional stimuli supplied by a live parasite are absent.

5.2.3 Longevity of protection

Mice were reinfected after 2.5, 4.5, 6.5, 7 or 9 months. At all time points, protection against the parasite could be seen for both reinfected groups, irrespective of drug treatment. Protection manifested itself in the significantly reduced peaks of parasitaemia as compared to the age-matched controls. This reduction is in the range of 100-fold for

Table 5.1 Persistence of parasites demonstrated by whole blood transfers [a)]

Time after infection	No. of blood donor mice	RAG-2$^{-/-}$ mice with parasites [b)]	Persistence of parasites
1 month	3	33%	**YES**
2 months	2	50%	**YES**
3 months	2	0%	**NO**
4 months	2	0%	**NO**
5 months	2	0%	**NO**
6 months	3	0%	**NO**
7 months	2	0%	**NO**
8 months	2	0%	**NO**
9 months	2	0%	**NO**

a) The whole blood transfers at 1 to 6 months were performed and evaluated by Emma Cadman, NIMR.

b) The blood from each infected mouse was transferred into two RAG-2-deficient mice for the 1-6-month time points and into one mouse for the 7-9 month time points.

the chloroquine-treated group reinfected after 2.5 months (p=0.0079). whereas the peak of parasitaemia is reduced over 10-fold further for the untreated group at this time point (p=0.0025). (Fig. 5.2a),. From 4.5 months onwards, these reductions were in the range of 100-fold for both chloroquine-treated and untreated mice (Figs. 5.2b and c and Fig. 5.3). Other measures of protection, namely delayed patency and a delayed peak of parasitaemia, were only seen clearly for the untreated 2.5-month-reinfected group. For all other reinfected groups, the timing of the peak precedes or matches that of the uninfected group, suggesting that infection progresses at the normal rate but is controlled at an earlier stage. There is a 1-day delay in patency in the reinfected groups from the 7- and 9-month time points, but it is not as definite as the 3-day delay seen for the 2.5-month untreated reinfected group.

Due to circumstances beyond our control, there was an unintentional parasite eradication step about 4 and 6 months after the primary infections of the mice showed in Fig. 5.3a and b, respectively. All mice had been switched to a new diet, which rapidly terminated all current measurable malaria infections. The cause is unknown, but we assume that this batch of food was contaminated with anti-coccidial or antibiotic drugs. Therefore, mice in both the chloroquine-treated and the untreated groups were to all intents and purposes drug treated late in the infection. This should not have had any effect, as parasites were no longer detectable after 3 months after infection (Section 5.2.2) and the reinfections at 7 and 9 months have comparable results to those at 4.5 and 6.5 months.

Figure 5.2. Reinfections after 2.5, 4.5 and 6.5 months.

Chloroquine-treated and untreated mice were infected with 10^5 *Plasmodium chabaudi chabaudi* (AS)-parasitised red blood cells and reinfected 2.5 months (a), 4.5 months (b) or 6.5 months (c) later while the age-matched controls underwent a primary infection at the same time. The parasitaemia was measured by counting in Giemsa-stained thin blood films and is displayed logarithmically as the percentage of parasitised red blood cells. Geometric means were calculated from five to eight mice for the two reinfected groups and from three to five mice in the age-matched control groups. The control mice in panel c were not perfectly age matched with the reinfected groups. Error bars represent the positive SEM.

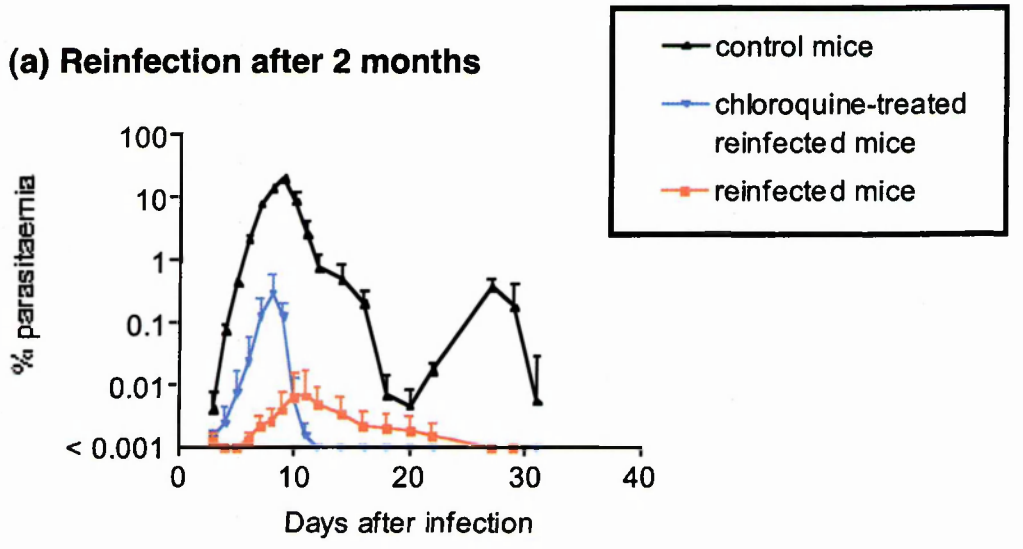
(a) Reinfection after 2 months
control mice
chloroquine-treated reinfected mice
reinfected mice
% parasitaemia
100
10
1
0.1
0.01
< 0.001
0
10
20
30
40
Days after infection

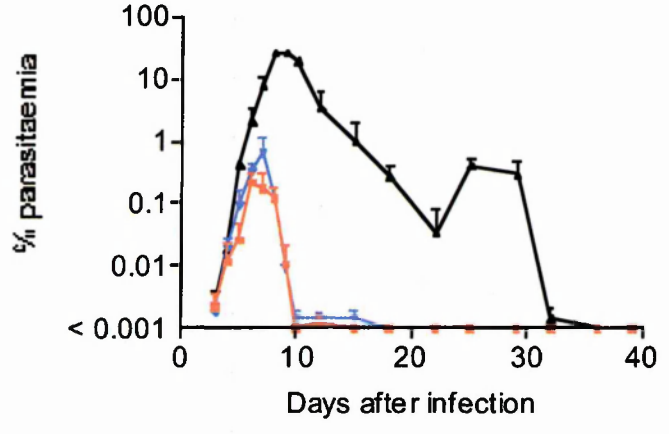
(b) Reinfection after 4.5 months
% parasitaemia
100
10
1
0.1
0.01
< 0.001
0
10
20
30
40
Days after infection

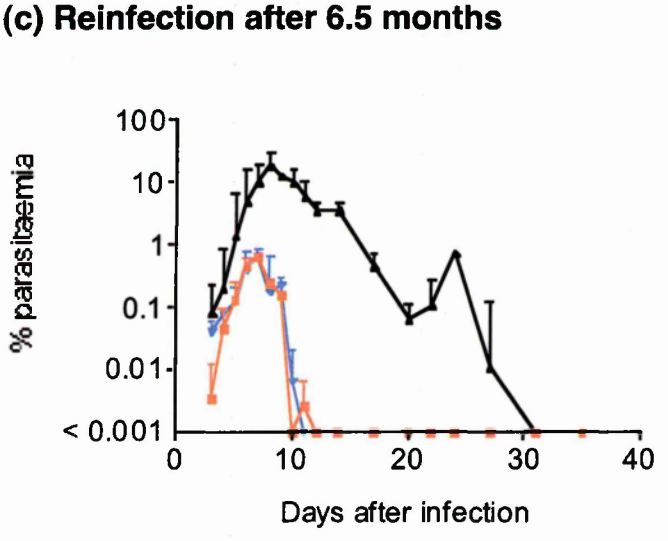
(c) Reinfection after 6.5 months
% parasitaemia
100
10
1
0.1
0.01
< 0.001
0
10
20
30
40
Days after infection

Figure 5.3. Reinfections after 7 and 9 months.

Chloroquine-treated and untreated mice were infected with 10^5 *Plasmodium chabaudi chabaudi* (AS)-parasitised red blood cells and reinfected 7 months (a) or 9 months (b) later while the age-matched controls underwent a primary infection at the same time. The parasitaemia was measured by counting in Giemsa-stained thin blood films and is displayed logarithmically as the percentage of parasitised red blood cells. Geometric means were calculated from three to eight mice per group. Error bars represent the positive SEM.

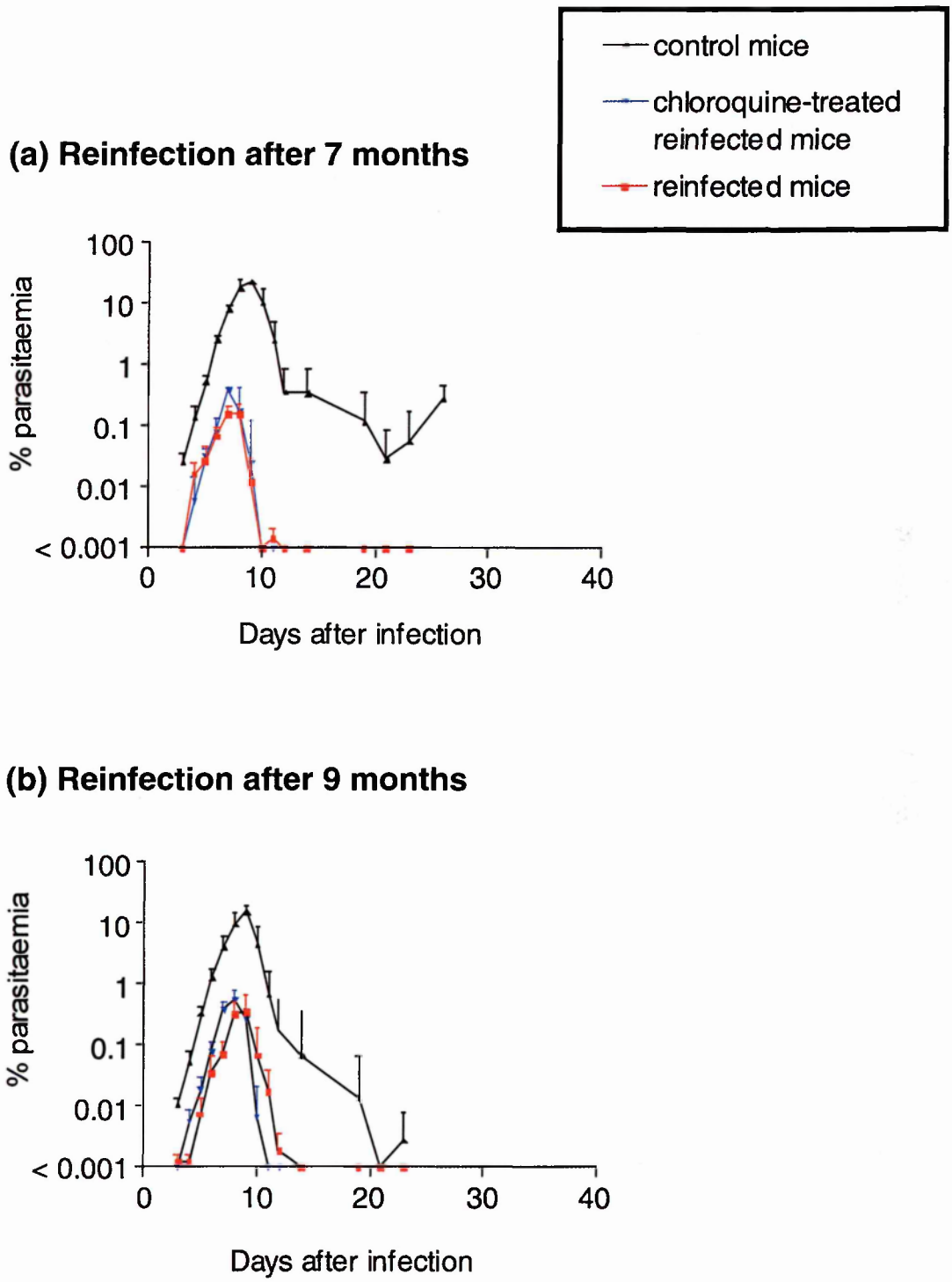
control mice
chloroquine-treated reinfected mice
reinfected mice
(a) Reinfection after 7 months
% parasitaemia
100
10
1
0.1
0.01
< 0.001
0
10
20
30
40
Days after infection
(b) Reinfection after 9 months
% parasitaemia
100
10
1
0.1
0.01
< 0.001
0
10
20
30
40
Days after infection

Figure 5.4. Summary of Section 5.

Three groups:

1. reinfected mice
2. reinfected choloroquine-treated mice
3. age-matched controls

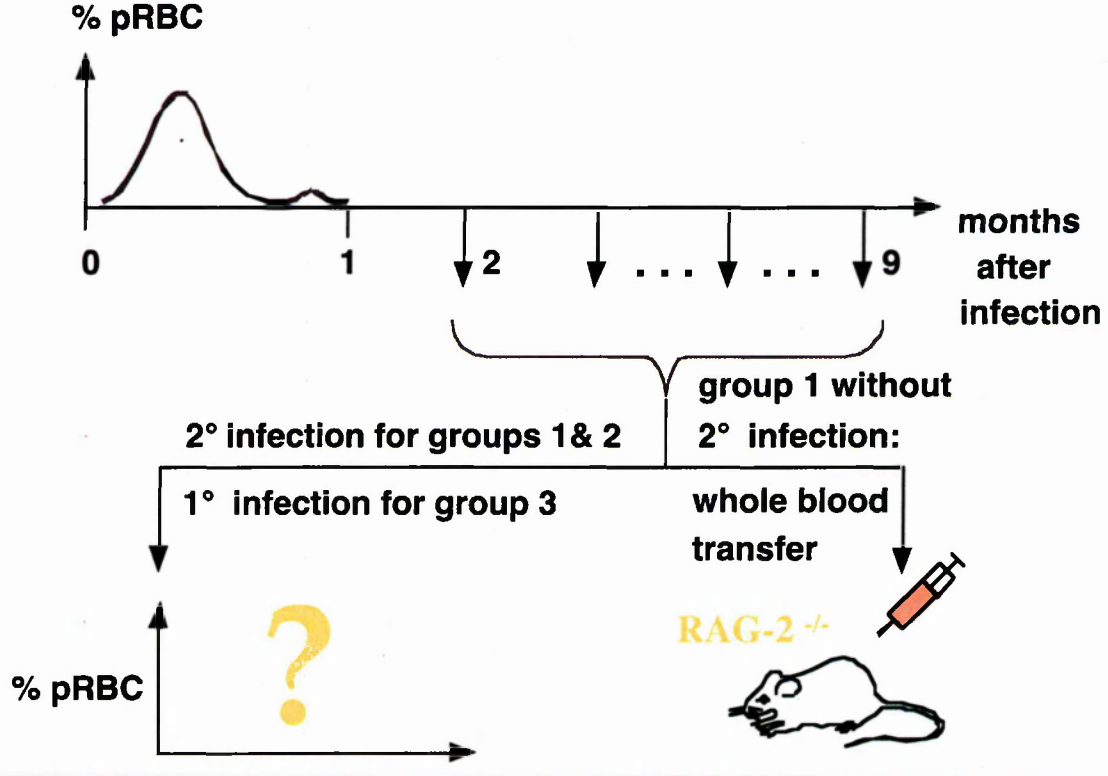

- A single infection causes protective effects for up to 9 months
- Elimination of parasites after 30 days only affects protection during the 2.5-month reinfection
- From 4.5 months, protection is independent of parasite elimination

- Parasite persistence (as detected by subinoculation) ends after 2-3 months

5.3 Discussion

The results are summarised in Figure 5.4 and show that a single infection causes protective effects against the same strain of parasite for periods up to 9 months. Individual observations from other publications match well with these results: Reinfection of NIH mice with *P. c. chabaudi* showed that the peak of parasitaemia was reduced by less than an order of magnitude with a 96-day interval between infections and by about 3 orders of magnitude with a 369-day interval (Pearson *et al.*, 1983). Infection of CBA/Ca mice with *P. c. chabaudi* (AS) also resulted in peaks of parastaemia reduced between one and two orders of magnitude upon reinfection after 98 or 332 days (Jarra and Brown, 1985). These data confirm the longevity of protective effects and that protection may differ in degree depending on the interval after the first infection. Differences in the magnitude can be explained by the use of different mouse strains, parasite doses, infection routes and potentially of animal diet (Gilks *et al.*, 1989).

Protection is also seen in at least one other non-lethal species of *Plasmodium*, as NIH mice infected with *P. berghei yoelii* (now known as *P.yoelii yoelii*), were also protected from reinfection with the same strain (Barker, 1971). When reinfected after 2 months, the protection was complete and after 12 and 17 months, peak parasitaemias were reduced about fivefold. The lesser reduction in parasitaemia may be due to the greater virulence of this species of *Plasmodium* compared to *P. c. chabaudi*. It is more difficult to make comparisons with the studies on lethal infections mentioned in Section 5.1, as the degree of parasitaemia seen in the mice surviving reinfection was normally not reported.

The duration of parasite persistence could also play a role in the different degrees of protection seen between models. Whereas about 50% of mice infected with drug-treated *P. berghei* still had blood-transferable parasites after 126 days and 15% after 186 days

(Eling, 1980), the experiments described above show that the parasites persist less than 3 months in the *P. c. chabaudi* (AS) infection. Although this comparison is quite clear, there are limits to the subinoculation method for analysing parasite persistence. Parasites may sequester in the tissues and therefore not be accessible to transfer in whole blood. In addition, with very low numbers of parasites, uneven distribution of parasites according to Poisson distribution statistics and poor parasite viability in the inoculum may prevent transfer of any infectious parasites. Regarding the Poisson distributions, unpublished data by Emma Cadman (NIMR, London) shows that when the inoculum size is reduced to 100 parasites or less, not all mice are infected. Therefore, a more sensitive method, such as detection of parasite RNA in tissues or peripheral blood by real-time polymerase chain reaction (PCR) is required to definitively determine the duration of parasite persistence.

The importance of subpatent levels of parasites can clearly by seen by comparing the drug-treated and untreated groups reinfected after 2.5 months. The untreated group, which would have had subpatent parasites up to the time of reinfection (or at least a time point later than the 30-day termination induced by chloroquine), experienced an additional level of protection, manifesting as a tenfold lower peak of parasitaemia. Once all parasites from the primary infection have been eliminated, it does not appear to make any difference whether mice had been drug-cured or not, since the courses of parasitaemia were practically identical for treated and untreated mice from 4.5 months onwards. Therefore the presence of parasites must be the deciding factor for the difference between the untreated and drug-treated reinfections at 2.5 months.

The mechanisms responsible for controlling infection in the absence of parasites from a previous infection are based on long-lived lymphocytes. Long-lived plasma cells produce parasite-specific antibodies, which can lead to elimination of the parasites and can also target the parasites for rapid phagocytosis and antigen processing and presentation. Long-

lived memory B and T cells with parasite specificity are present in higher frequencies than naïve parasite-specific B and T cells. Along with their lower activation threshold and high proliferation capacity, this results in faster production of the lymphocyte numbers necessary for controlling the infection. In the mice still harbouring parasites from the previous infection, these resting long-lived cells will be supplemented by short-lived effector cells, such as Th1, Th2 and short-lived plasma cells, which have been activated by the parasites from the primary infection. These cells can respond to the parasites from the second inoculum immediately and can aid the long-lived cells by directing the immune response and supplying more partners for the B and T cell interactions. Higher levels of plasma antibody may also play a role in keeping the secondary parasitaemia lower. Although the exact cells involved in reducing the parasitaemia in a secondary infection in the presence of pre-existing parasites cannot be identified by the parasitological approach used in these experiments, it is very likely that an interaction between activated effector cells and long-lived lymphocytes is the central mechanism.

This mouse model is comparable with human malaria in that a single infection is not sufficient to generate sterile immunity against reinfection. Beyond that, it is difficult to compare the degree of protection between the mouse and human systems, because different parameters are measured in each case. The experiments in this section were looking for protection against the parasite whereas human studies tend to evaluate protection against disease. As discussed in Section 1, levels of parasitaemia and disease often do not correlate. As mice, especially those of the C57BL/6 strain, do not experience severe disease symptoms and it is not possible to document the infection and parasitaemic history of humans in sufficient detail, a direct comparison is not possible.

Another important difference is that the mice were infected with the same strain of parasite, whereas field studies in humans indicate that new episodes of symptomatic

malaria are usually caused by a different strain of parasite (Bull *et al.*, 1999; Eisen *et al.*, 2002). In addition, antigenic variation is thought to play a major role in susceptibility to reinfection (Bull *et al.*, 1998; Marsh *et al.*, 1989). *P. c. chabaudi* does undergo antigenic variation (del Portillo *et al.*, 2001; McLean *et al.*, 1982), but it is still unknown how important this is in immune evasion and the antigenic variation is unlikely to play a large role in these experiments due to the design of the infection (Section 2.4). An additional difference could lie in the duration of exposure to parasite during the acute infection stage. Chloroquine treatment of *P. c. chabaudi*-infected mice at different time points of infection showed that the generation and degree of immunity depend on the duration of the infection (Favila-Castillo *et al.*, 1999). If this is the case in human malaria as well, then the tendency to treat fever immediately with anti-malarial drugs immediately could prolong the time it takes for immunity to develop.

In summary, the experiments from this chapter show clearly that the mouse immune system is capable of partial protection against reinfection with *P. c. chabaudi* (AS), but they cannot give any indication of whether B cells are involved in the protective effects. The role of B cells in the immune response in relation to the presence or absence of parasites will be addressed in more detail in the following section.

Section 6 Development of the antibody response to merozoite surface protein-1

6.1 Introduction

6.1.1 Prevalences and levels of MSP-1_{19}-specific antibodies in human infections

This section shows the development of the IgG response to MSP-1_{21} in relationship to the parasitic status of the host. Plasma cell longevity is studied here via the persistence of antibodies after a primary infection and the presence of memory B cells is assessed by comparing antibody level and affinity development during primary and secondary infections.

The structure and proteolytic processing of MSP-1 as well as its relevance in protection against malaria infection have been discussed in Section 4. This section will review the data pertaining to the development of anti-MSP-1_{21}-specific antibody responses.

Field studies which measured IgG levels against MSP-1_{19} in humans from malaria-endemic areas offer important insights into the quality of this particular antibody response. It has been shown for various conditions of endemicity that the prevalence of these antibodies as well as their levels drop after termination of exposure: In an area of seasonal malaria transmission in The Gambia, prevalences of IgG antibodies to *P. falciparum* MSP-1_{19} or MSP-1_{42} of 25-50% have been measured outside of the transmission season (Egan *et al.*, 1995; Riley *et al.*, 1992). However, even under conditions of moderate perennial exposure to malaria, prevalences between 30% and 72% were measured in Ghana (Dodoo *et al.*, 1999; Riley *et al.*, 2000). The highest prevalences of MSP-1_{19}-specific antibody, namely 82% and 100%, were measured in two areas of perennial transmission in Papua New Guinea (O'Donnell *et al.*, 2001). It is particularly striking that antibodies against MSP-1_{19} were found in 61%-73% of individuals with clinical malaria and only in 11-14% of individuals without clinical malaria in any given

transmission season in a 4-year longitudinal study in an area of unstable malaria transmission in the Sudan although 96% of the cohort experienced clinical malaria during the observation period (Cavanagh *et al.*, 1998). As discussed previously in Section 1.5.4, MSP-1-specific antibody levels can drop rapidly when exposure to the parasite ceases. due to the end of the transmission season or departure from the endemic area (Cavanagh *et al.*, 1998; Soares *et al.*, 1999). However, this fluctuation in antibody levels may only be restricted to children (Taylor *et al.*, 1996).

6.1.2 Evaluation of the presence of long-lived and memory B cells

This rapid decay of antibody levels suggests that the MSP-1_{19}-specific antibody response is generated mainly by short-lived plasma cells. As stated in Section 1.4.5, the antibody response to MSP-1_{19} has been seen in some cases to be predominantly of the IgG1 or IgG3 isotype. The serum half lives of 21-23 days and 8 days, respectively, for these isotypes explains why antibody levels (and thereby prevalence) must drop rapidly once the antigenic stimulus for the generation of short-lived plasma cells is reduced. However, the drops in antibody levels measured in field studies were only trends and it is impossible to link antibody levels to exact infection histories. Therefore, a more detailed analysis of the development of MSP-1_{21}-specific antibody levels in dependence on the recency of infection must be performed in the animal model. By setting an endpoint to the exposure to live parasites, it is possible to use serum antibody levels as a readout for either plasma cell longevity (or continued generation of short-lived plasma cells via antigen complexes on follicular dendritic cells).

The importance of MSP-1_{19} antibodies in protection against clinical malaria was discussed in Section 4.1. However, pre-existing antibodies generated by long-lived plasma cells may not be enough to control the numbers of parasites released from the liver after hepatic schizogony, since MSP-1_{19} is not expressed on accessible parasites before initiation of the erythrocytic stage of the parasite's life cycle. Therefore, it is necessary to

analyse the memory B cell response as well as the long-lived plasma cell response for MSP-1_{21}. One way to do this is to compare the magnitude and speed of the primary and secondary antibody responses as detailed in Section 1. A further test for B cell memory which has been used in establishing rubella or toxoplasma infection history as well as determining the efficacy of vaccination with meningitis or *Haemophilus influenzae* polysaccharide conjugates is the measurement of antibody affinities (Böttiger and Jensen, 1997; Goldblatt *et al.*, 1999; Goldblatt *et al.*, 1998; Jenum *et al.*, 1997).

6.1.3 Aims

The IgG response to malarial antigens, especially to *P. c. chabaudi* MSP-1_{21}, is to be studied to address the following issues:

(i) Determination of plasma cell longevity for MSP-1_{21} and total parasite antigen

(ii) Assessment of the generation of MSP-1_{21}-specific memory B cells

(iii) Evaluation of the role of parasite persistence in the development of MSP-1_{21}-specific long-lived plasma cells and memory B cells

6.2 Results

6.2.1 Experimental design

The basic design for the experiments in this section is outlined in Fig. 6.1. Mice were infected with 10^5 *P. c. chabaudi*-parasitised red blood cells and then either allowed to self cure or were treated with chloroquine 1 month post infection to eliminate parasites. Plasma samples were taken at monthly to bimonthly intervals after the primary infection. The mice were reinfected 2.5 months, 4.5 months or 6.5 months after the first infection at the same time as an age-matched control group underwent a primary infection (as described in Section 5.1 and Fig. 5.1). Plasma samples were taken at weekly intervals during the primary and secondary infections.

Figure 6.1 Experimental design for Section 6.

The three groups listed at the top correspond to the groups detailed in Fig. 5.1. Sera taken 1 month after the primary infection and at roughly bimonthly intervals thereafter were used to determine how MSP-1_{21}-specific IgG levels and affinity develop with increasing distance to the infection. Sera taken weekly during secondary infections were used to compare the MSP-1_{21}-specific antibody response with that of a primary infection in age-matched controls.

Three groups:

1. reinfected mice
2. reinfected choloroquine-treated mice
3. age-matched controls

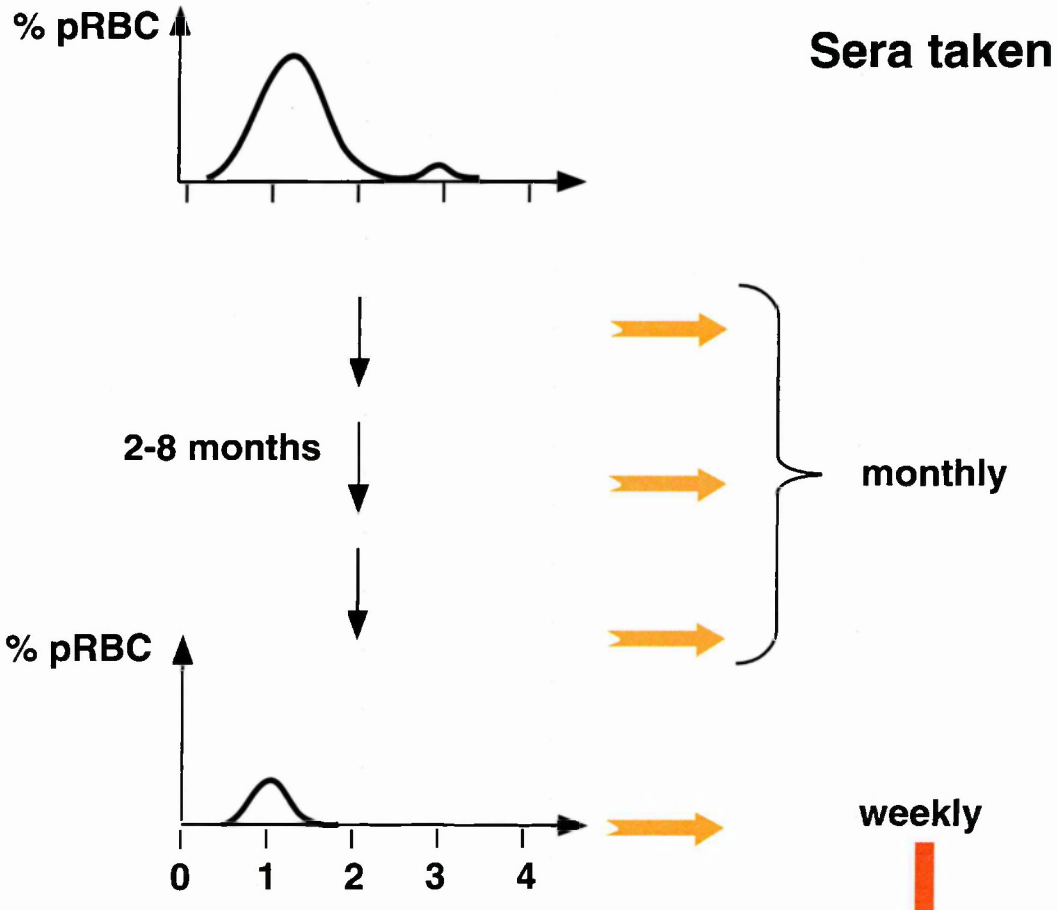

ELISA to determine

Longevity of malaria-specific antibodies:

Changes in antibody titres against MSP-1_{21}

Changes in antibody titres against crude malarial extract

Affinity maturation of malaria-specific antibodies:

Changes in antibody affinity for MSP-1_{21}

The plasma samples taken after the primary infection were used to assess the longevity of the malaria-specific antibody response by measuring the levels of IgG recognising MSP-1_{21} or a crude malarial extract. The affinity of MSP-1_{21}-specific IgG antibodies was also determined for these samples. Affinities against the crude malarial extract were not measured, because the antigen mix is too heterogeneous. To study whether the secondary antibody response to MSP-1 was affected by the interval between primary and secondary infection, the levels and affinities of MSP-1_{21}-specific IgG were determined in reinfections initiated after 2.5, 4.5 or 6.5 months.

6.2.2 IgG levels against MSP-1_{21} and crude malarial extract after primary infection

The relative amounts of IgG specific for either crude malarial extract or *Pichia*-purified recombinant MSP-1_{21} were determined by ELISA, as described in Sections 2.29 and 2.30. Crude malarial extract was prepared from *P. c. chabaudi* parasites according to the protocol in Section 2.7 and is a mixture of parasite antigens present at the late trophozoite stage, including MSP-1. Plasma was collected from groups of four to eight mice at 1, 2.5, 4.5 or 6.5 months after an untreated primary infection or at 2.5, 4.5 and 6.5 months after a drug-treated primary infection. At 1 month, there is no differentiation between chloroquine-treated and untreated mice, as the drug treatment only begins after this time point.

Between 1 and 2.5 months after infection, plasma IgG levels specific for crude malarial extract or for MSP-1_{21} drop and the reductions are statistically significant for the untreated as well as the chloroquine-treated groups: a drop of 4.4-fold for crude malarial extract (p=0.0079 for both the drug-treated and the untreated groups) and 2.3-fold for MSP-1_{21} (p=0.0048) (Fig. 6.2). From 2.5 months on, the levels are similar in untreated and chloroquine-treated mice, suggesting that the drug treatment has little effect on the later persistence of MSP-1_{21}-specific IgG. The slight changes in IgG levels observed between 2.5 and 6.5 months are not statistically significant for either antigen.

Figure 6.2 IgG levels for crude malarial extract and MSP-1_{21} after primary infection.

IgG levels were measured with specificity for crude malarial extract (top panels) or recombinant *Pichia*-expressed MSP-1_{21} (bottom panels). Samples were taken after an untreated primary infection (left side) or a chloroquine-treated primary infection (right side). All levels are given in arbitrary units calculated by defining the binding by C57BL/6 hyperimmune plasma to each antigen as 1 U (see Section 2.30). Each symbol represents the IgG level in units from an individual mouse and the lines represent the corresponding geometric mean. The upper and lower sets of panels are on different scales. Plasma samples were analysed for 19 mice (1 month, bottom panels), 2 mice (4.5 months, bottom left panel), 4 mice (6.5 months, bottom left panel) or 5 mice (all other time points).

Crude malaria extract

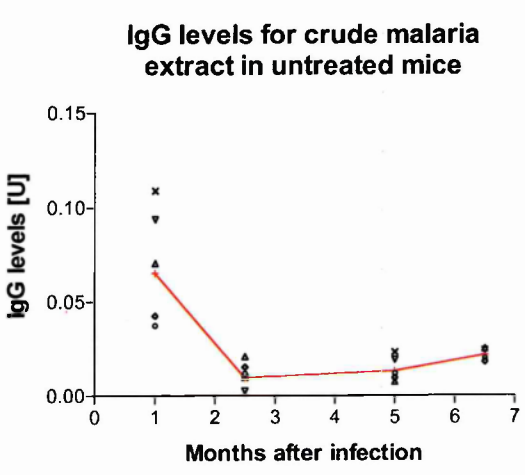

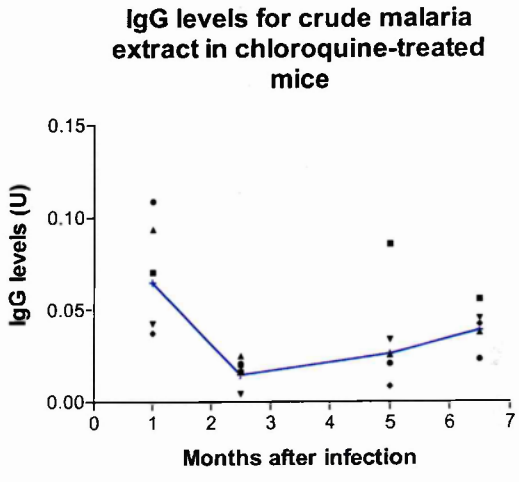

MSP-1_{21}

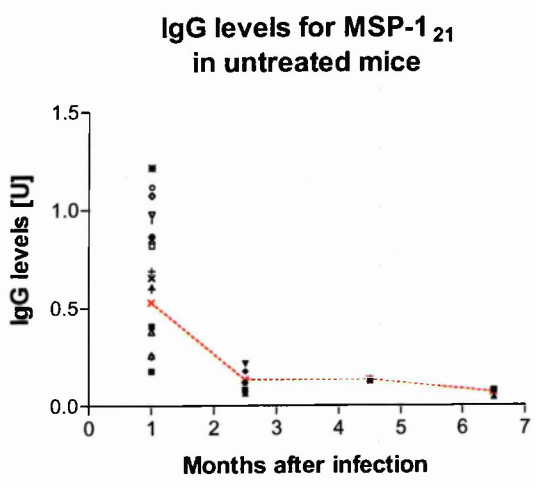

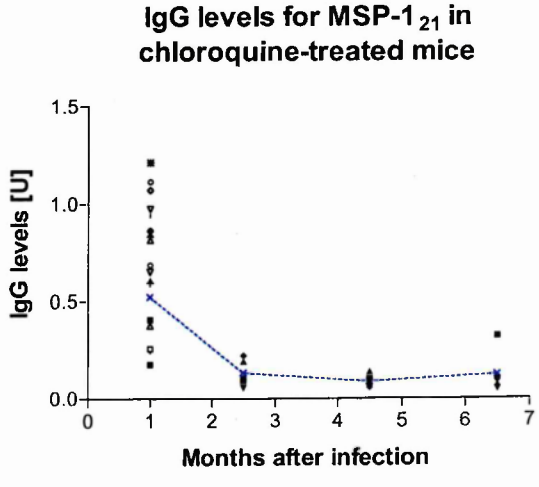

For crude malarial extract, the highest measured IgG amount (at 1 month past infection) is 0.11 U and the mean for all sera at this time point is 0.07 U, as compared with an IgG level of 1 U for hyperimmune serum for the same antigen. The highest MSP-1_{21}-specific measurement is 0.87 U with a mean of 0.36 U compared with a value of 1 U for the hyperimmune serum standard. It is not possible to compare the relative units between antigens, but these results do show that the amount of IgG produced after a single infection is closer to the amount detected after multiple infections for the MSP-1_{21} specificity than for crude malarial extract. This implies that B cells directed against the full spectrum of malarial antigens respond more strongly to repeated boosting than the subpopulation of B cells recognising MSP-1_{21}.

6.2.3 Changes in MSP-1_{21}-specific antibody levels during reinfection

Three sets of mice were infected twice with an interval of either 2.5, 4.5 or 6.5 months between the primary and secondary infections. Plasma samples were taken before reinfection and at weekly intervals for 4 weeks (see Fig. 6.1) and MSP-1_{21}-specific IgG levels determined by ELISA. Each infection set consisted of three groups of mice as described in Section 5: untreated mice infected twice, mice which were infected, chloroquine treated and then reinfected and age-matched controls undergoing primary infection at the same time as the other groups were given the second infections. All plasma samples belonging to the three groups of the same infection series were analysed simultaneously to maximise comparability. The geometric means for all three infection series are summarised in Fig. 6.3. The IgG levels from individual mice and the corresponding geometric means are shown in more detail for the reinfected groups in Fig. 6.4 along with the corresponding parasitaemias, as determined in Section 5.

Figure 6.3 Comparison of MSP-1_{21}-specific IgG levels between the three treatment groups.

The geometric means of MSP-1_{21}-specific IgG levels are shown for mice reinfected at the stated time points after an untreated primary infection (a) or after a chloroquine-treated infection (b). These two panels represent a summary of Fig. 6.4a-c and d-f, respectively, with the inclusion of a primary infection shown in black for comparison. Panel c shows IgG levels in primary infections for the age-matched control mice from these three experiments. All levels are given in arbitrary units calculated by defining the binding by C57BL/6 hyperimmune serum as 1 U. Lines represent the geometric from three to eight mice (four to five being the usual number).

(a)

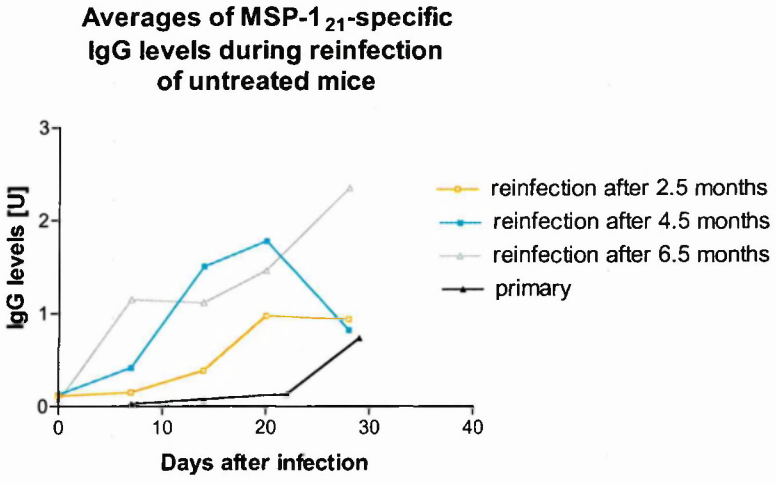
Averages of MSP-1 21-specific IgG levels during reinfection of untreated mice
IgG levels [U]
0
1
2
3
0
10
20
30
40
Days after infection
reinfection after 2.5 months
reinfection after 4.5 months
reinfection after 6.5 months
primary

(b)

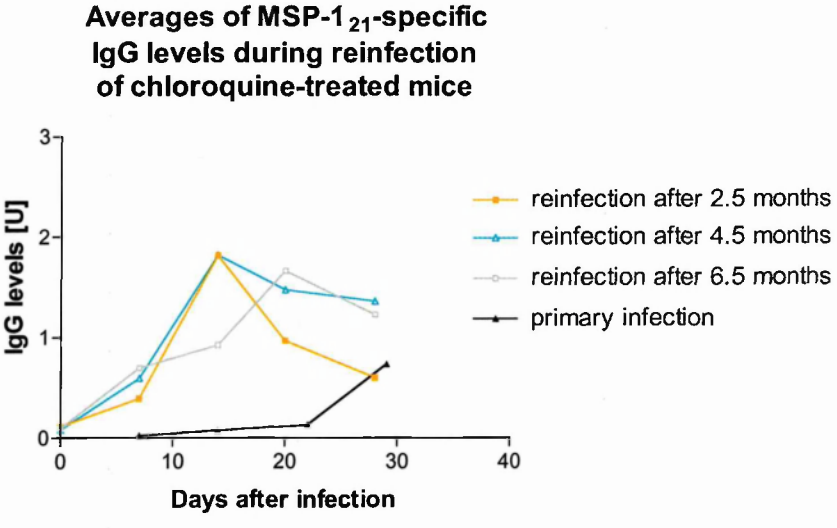
Averages of MSP-1 21-specific IgG levels during reinfection of chloroquine-treated mice
IgG levels [U]
0
1
2
3
0
10
20
30
40
Days after infection
reinfection after 2.5 months
reinfection after 4.5 months
reinfection after 6.5 months
primary infection

(c)

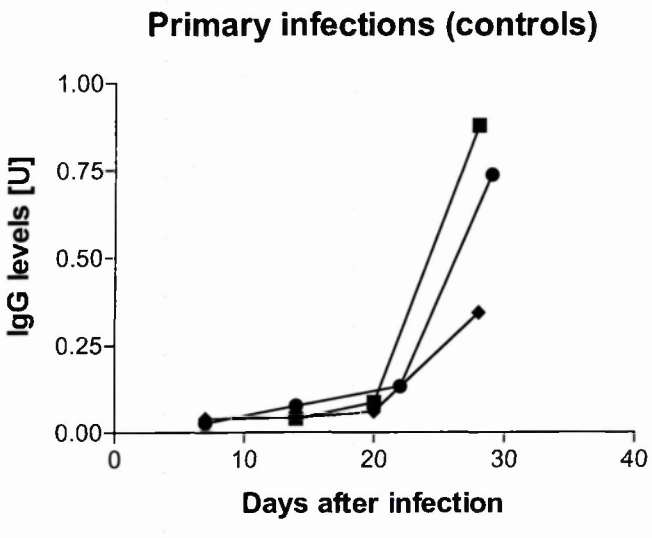
Primary infections (controls)
IgG levels [U]
0.00
0.25
0.50
0.75
1.00
0
10
20
30
40
Days after infection

Figure 6.4 Development of MSP-1_{21}-specific IgG levels during reinfection.

The left page of the figure shows the parasitaemias (taken from Section 5) of the courses of infection whose IgG levels are shown on the right-hand page.

The levels of IgG specific for recombinant *Pichia*-expressed MSP-1_{21} are shown for mice reinfected 2.5 months (a and d), 4.5 months (b and e) or 6.5 months (a and e) after a primary infection without (a-c) or with chloroquine treatment (d-f). All levels are given in arbitrary units calculated by defining the binding by C57BL/6 hyperimmune serum as 1 U. Each symbol represents the plasma level from an individual mouse (measured in duplicate) and the lines represent the geometric mean of all plasma levels at that time point. Panel b has a break in the y axis to accommodate the highest value. Lines represent the geometric from four to eight mice (four to five being the usual number).

Untreated

Chloroquine treated

(a) Reinfection after 2.5 months (untreated mice)

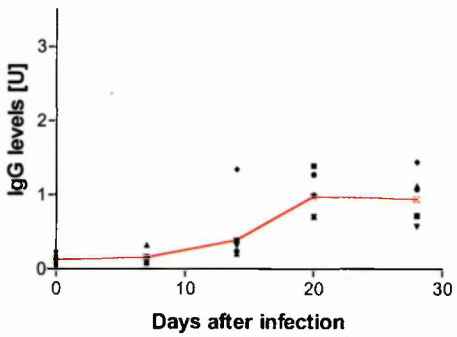

(d) Reinfection after 2.5 months (chloroquine-treated mice)

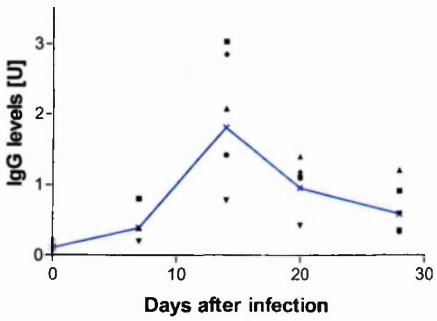

(b) Reinfection after 4.5 months (untreated mice)

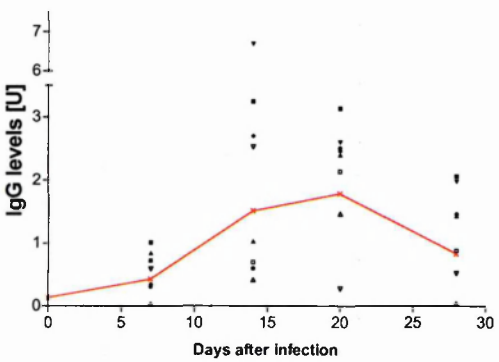

(e) Reinfection after 4.5 months (chloroquine-treated mice)

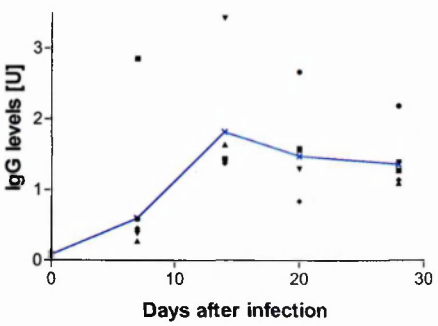

(c) Reinfection after 6.5 months (untreated mice)

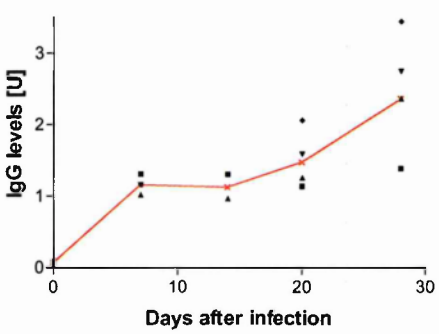

(f) Reinfection after 6.5 months (chloroquine-treated mice)

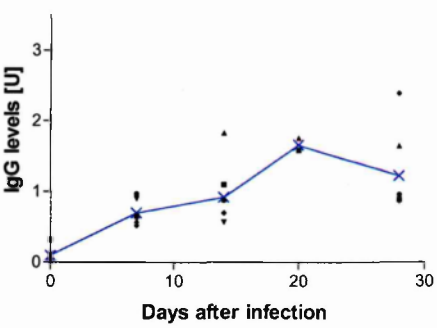

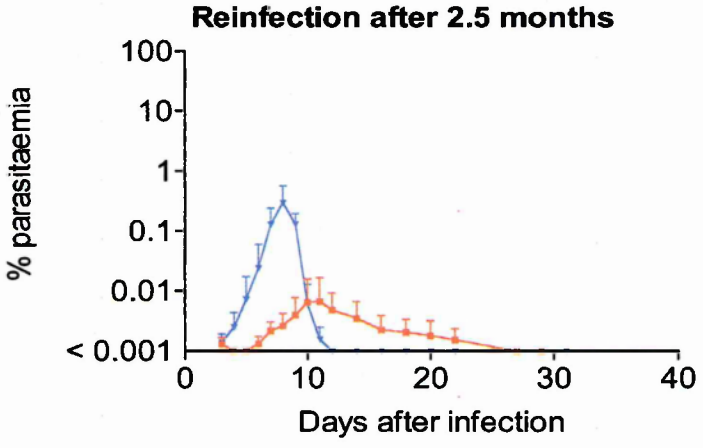
Reinfection after 2.5 months
% parasitaemia
100
10
1
0.1
0.01
< 0.001
0
10
20
30
40
Days after infection

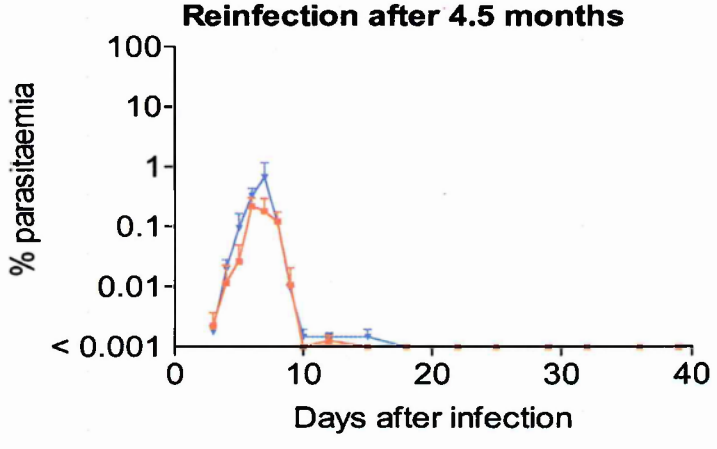
Reinfection after 4.5 months
% parasitaemia
100
10
1
0.1
0.01
< 0.001
0
10
20
30
40
Days after infection

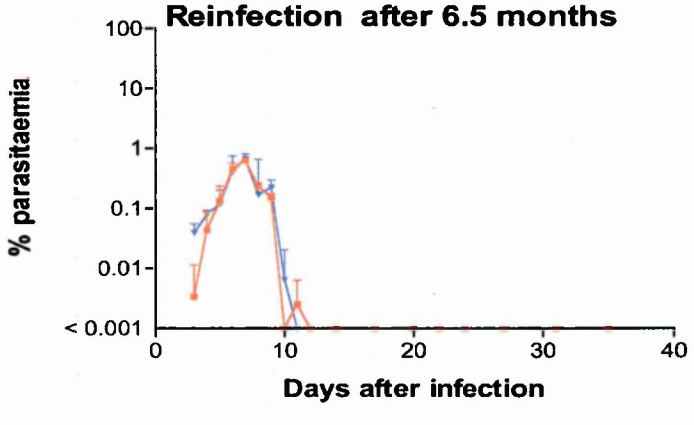
Reinfection after 6.5 months
% parasitaemia
100
10
1
0.1
0.01
< 0.001
0
10
20
30
40
Days after infection

The primary and secondary infections differ clearly in the rapidity and magnitude of the MSP-1_{21}-specific IgG response (Fig. 6.3). In the age-matched control mice undergoing primary infection, IgG levels remained low for the first 3 weeks of infection and then rose sharply in the 4th week. The variation in antibody levels at week 4 is not significant (p>0.05). In all of the secondary infections, the MSP-1_{21}-specific IgG levels rose more rapidly than in the primary infection and IgG levels are significantly higher at all secondary infection time points (p<0.05) except for week 4 of the 2.5-month drug-treated and untreated reinfected groups and for week 4 of the 6.5-month reinfected drug-treated group (Fig. 6.3a, b and c).

There is a clear difference in the development of the MSP-1_{21} IgG response between drug-treated and untreated mice at 2.5 months but not at either of the later time points (Fig. 6.4). The specific IgG levels in the 2.5 month untreated group are significantly lower than those in the drug-treated groups at weeks 2 and 3 of infection (p=0.0159 and 0.0079, respectively). At 4.5 and 6.5 months there are no statistically significant differences between the drug-treated and untreated groups (except for week 1 at 6.5 months with p=0.0159). There are also no statistically significant differences between the 4.5- or 6.5-month reinfected groups (apart from the 1 week value) or between the 4.5- or 6.5-month drug-treated groups (p>0.05 for all time points). However, the specific IgG levels in the 2.5-month reinfected group are significantly different from those measured at 4.5 and 6.5 months for the first 3 weeks or weeks 1 and 4, respectively. In summary, IgG levels develop similarly in all reinfections except in untreated mice reinfected 2.5 months after the primary infection. As discussed in Section 5, this is the only reinfection regimen in the study when parasites from the primary infection would still be present. Comparison with the parastaemias shown in Fig. 6.4 shows that the 2.5-month untreated group was also displays a course of parasitaemia deviating from that observed in the other

reinfection groups. This suggests that the presence of parasites at the time of reinfection affects both the degree of protection and the development of MSP-1_{21}-specific IgG.

6.2.4 Determination of antibody affinity

The relative affinity of the MSP-1-specific IgG antibodies was measured by chaotropic ion-induced dissociation of antibody binding in ELISA (described in Section 2.31) and Fig. 6.5 depicts how the data is interpreted. The top image shows an example comparing antibody affinities between different days of infection, with the percentage of bound antibodies displayed in relationship to the concentration of sodium thiocyanate. It is very difficult to interpret the data in this format, so the data was converted into other more easily comparable measures. A standard measure in this type of assay is the affinity index, which is the salt concentration required to reduce the amount of binding antibody by 50%. The decadic logarithm of the percentage of bound antibody is plotted against the salt concentration. A curve is fitted by linear regression. If the fitted curve has a correlation coefficient (R^2) greater than 0.8, the affinity index is measured as shown in Fig. 6.5.

Although the affinity index is a useful and comparable way of summarising information from chaotopic ion elution assays, it is not a satisfactory measure on its own. Many unrelated changes may happen in a polyclonal mixture of antibodies and a given affinity index can represent numerous different combinations of antibody affinities, especially as changes within the high-affinity populations do not affect the affinity index. Therefore, affinity distribution profiles were generated according to a method modified from (Ferreira and Katzin, 1995) as delineated in Fig. 6.5. The distribution profiles show how much antibody is dissociated by each 0.5-molar increase in salt concentration and thereby allow shifts in low or high affinity antibody populations to be recognised.

Figure 6.5 Calculation of the affinity index and affinity distribution.

The top image is a typical graph of the arithmetically meaned antibody affinities at different time points of an infection.

The left-hand branch shows how these values are used to calculate the average affinity index (AI), which is the molar concentration of sodium thiocyanate required to reduce the OD representing bound antibody to 50%. The affinity curves from duplicate measurements of each plasma sample were linearised by plotting the decadic logarithm against the molar chaotropic ion concentration. The affinity index (AI) is the concentration of sodium thiocyanate corresponding to 1.70, the decadic logarithm of 50. Only curves with a correlation coefficient (R^2) greater than 0.8 were used to calculate the average affinity index for each time point. The arithmetic mean of the affinity indices was plotted with error bars representing the SEM.

The affinity distribution was calculated by defining the amount of antibody bound in the absence of sodium thiocyanate as 100% and determining the percentage of that amount bound at each salt concentration by OD measurement. The percentage of antibody dissociated by each 0.5-M increase in salt concentration was calculated, with the value > 3 M representing the antibody still bound at the highest salt concentration. These values were plotted in the affinity distribution graph with each bar representing the arithmetic mean from all sera at that time point and salt concentration and error bars representing the SEM.

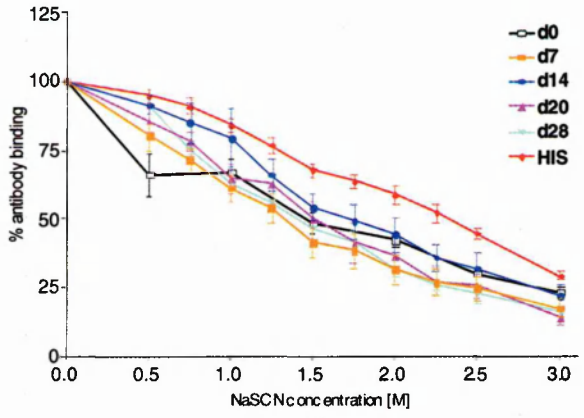

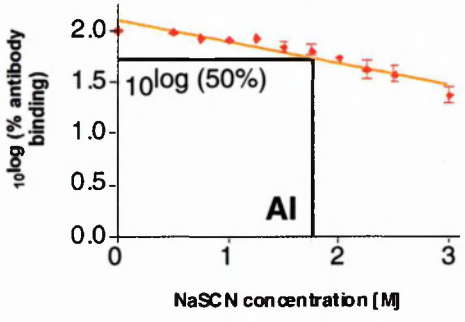

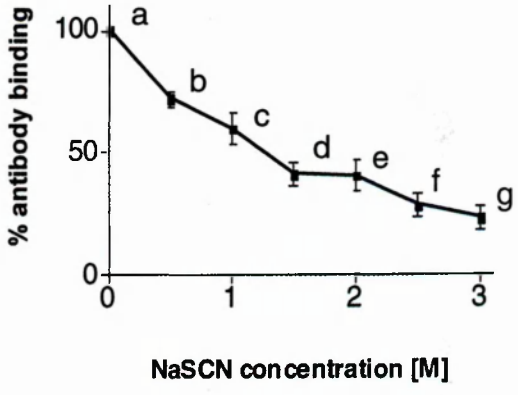

Affinity index (AI) averages from curves with $R^2 > 0.8$

Calculation of antibody dissociated by each 0.5-M increase in salt concentration

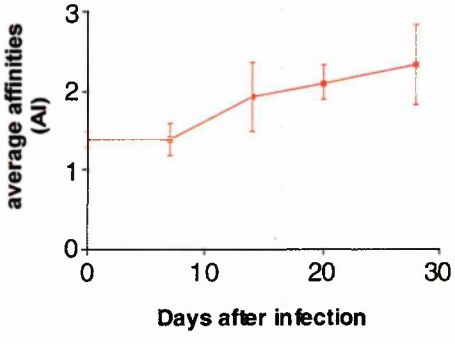

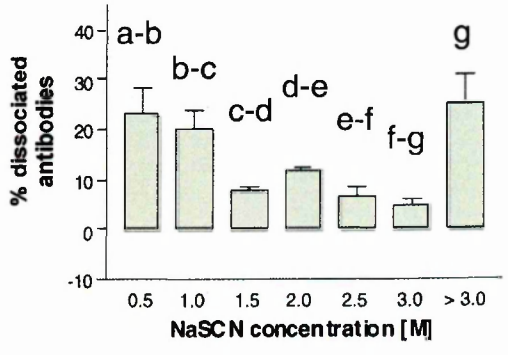

Average affinity of the sera

Affinity distribution in the sera

6.2.5 Affinity indices after primary infections

The affinity of MSP-1_{21}-specific IgG was measured in the sera whose levels were determined in Section 6.2.2 (Fig. 6.6). The mean affinity index between 1 and 6.5 months after a primary infection was 1.33 M in the untreated group and 1.29 M in the chloroquine-treated mice and the indices did not change significantly (p>0.05) during this interval. Furthermore, the difference between the affinity indices of chloroquine-treated and untreated groups had no statistical significance either (p>0.05). At all times, the affinity index was lower than that measured in hyperimmune plasma, whose arithmetic mean in the three experiments was 2.21 M. This difference was statistically significant until 4.5 months after infection (p< 0.007), but at 6.5 months the difference between the primary infected and hyperimmune affinity indices was no longer significant (p= 0.063).

6.2.6 Affinity distribution after primary infection

The affinity distribution after primary infection (Fig. 6.7a and b) was determined from the same set of measurements as the affinity indices calculated in the previous section. In all of the graphs, the increase of salt concentration from 1.5 M to 2 M causes little antibody dissociation, suggesting that this concentration step represents a kind of boundary between the low and high affinity categories of antibody. (This effect is also seen in many of the affinity distributions shown in Figs. 6.9-6.11). For all of the plasma samples taken after primary infection, the amount of antibodies falling into these low and high affinity categories is roughly equal, whereas the balance is shifted towards the high affinity group in hyperimmune plasma. All sera contain a population of antibodies which does not dissociate even at the highest thiocyanate concentration (labelled > 3.0 M in the figures). This population represents about 30% of the total MSP-1_{21}-specific antibodies in hyperimmune plasma but only 10-25% in the plasma samples taken after primary infection. Together with the affinity index calculations, this demonstrates clear affinity differences between singly and multiply infected mice.

Figure 6.6 Development of the affinity index after primary infection.

The average affinity indices are shown at different time points after a primary infection without or with chloroquine treatment. No chloroquine-treated samples were taken 1 month after infection, because the drug treatment occurs then. The average affinity indices determined for hyperimmune plasma in the three individual experiments are included as orange lines. Each bar represents the arithmetic mean from duplicates of four or five mice and error bars show the SEM.

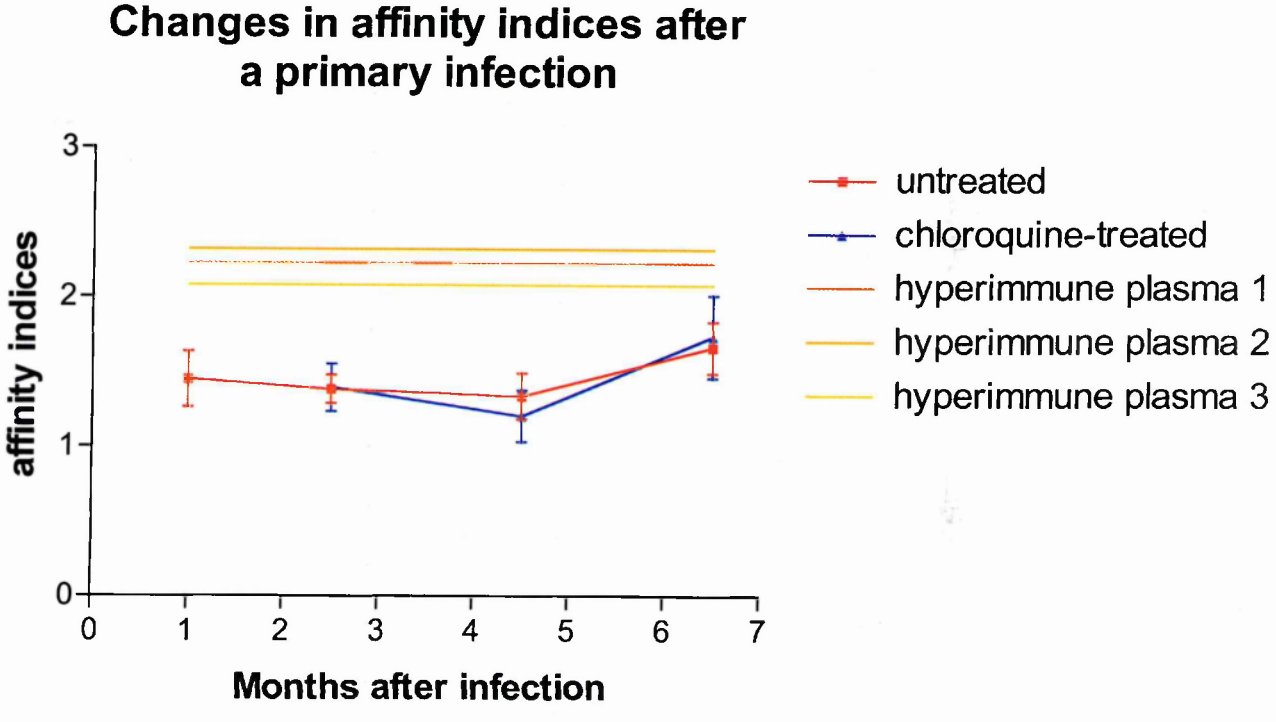
Changes in affinity indices after a primary infection
affinity indices
3
2
1
0
0
1
2
3
4
5
6
7
Months after infection
untreated
chloroquine-treated
hyperimmune plasma 1
hyperimmune plasma 2
hyperimmune plasma 3

Figure 6.7 Changes in affinity distribution after primary infection.

The affinity distribution of MSP-1_{21}-specific IgG is shown for several time points after a primary infection without (a) or with drug treatment (b). Each bar represents the arithmetic mean from duplicates of four or five mice and error bars show the SEM.

(a)

Affinities after primary infection (untreated mice)

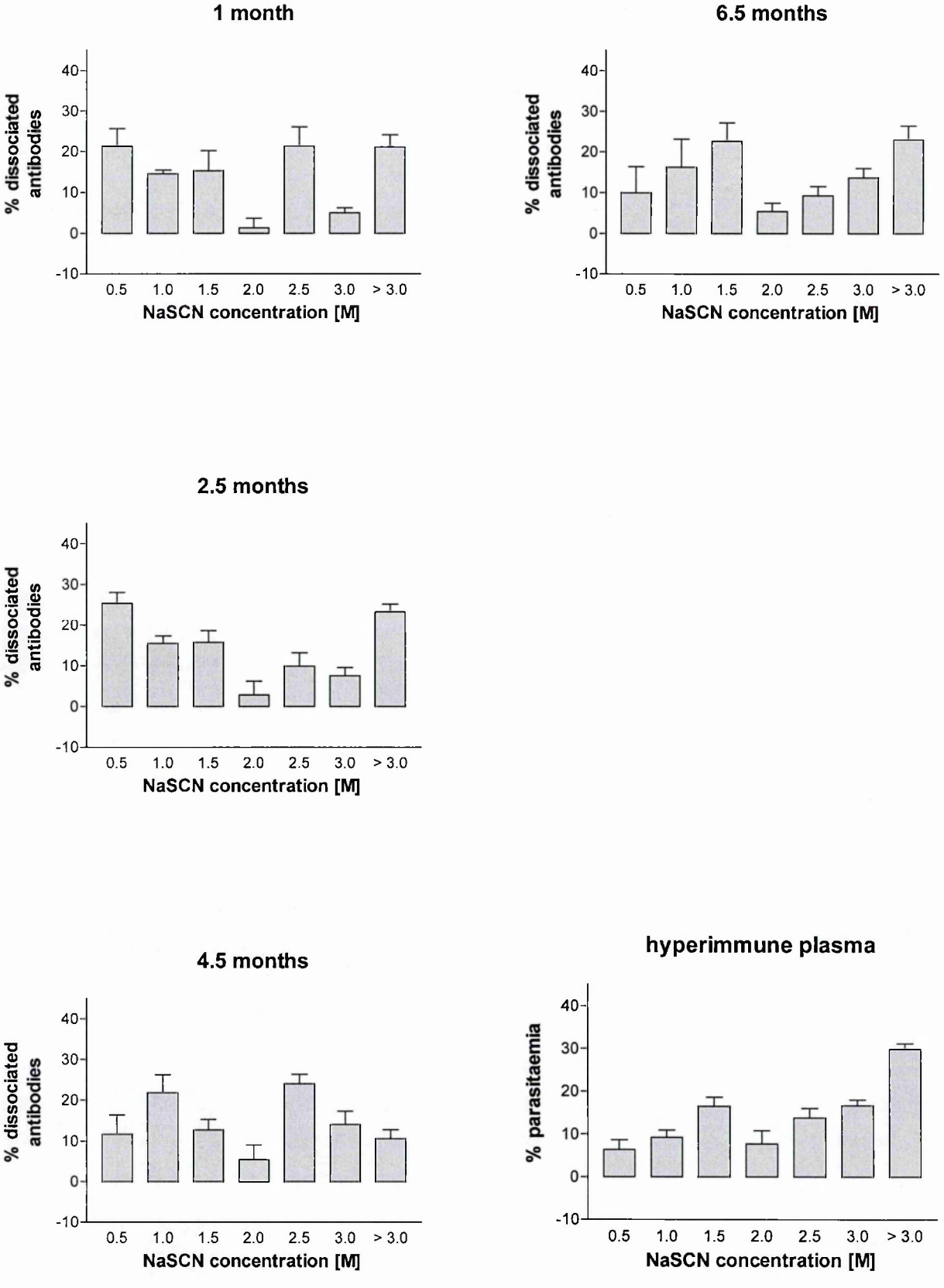

(b) Affinities after primary infection (chloroquine treated mice)

mice are being drug treated at 1 month

6.5 months

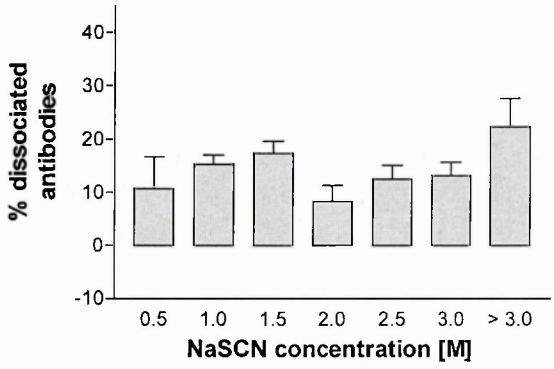

2.5 months

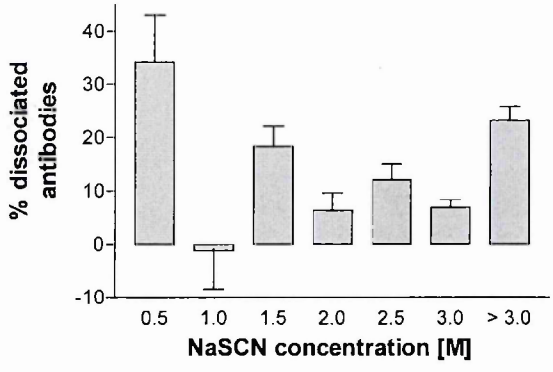

4.5 months

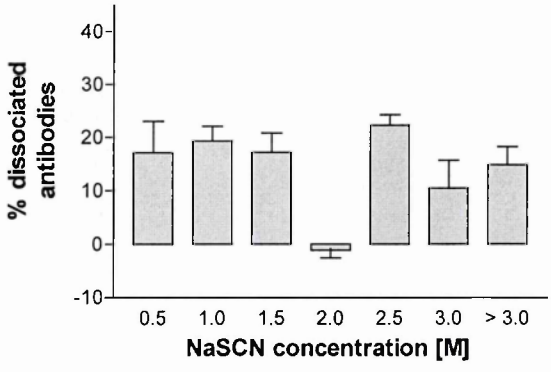

hyperimmune serum not done in chloroquine-treated mice

The following changes in affinities are shared by the sera taken from untreated (Fig. 6.7a) and drug-treated mice (Fig. 6.7b) between 2.5 and 6.5 months after infection: The clearest individual change in affinities can be seen between 2.5 and 4.5 months when the lowest affinity group shrinks by over 15% in the untreated mice and 35% in the drug-treated mice. This set of antibodies appears to dissociate first one and then two concentrations steps higher at 4.5 and 6.5 months, respectively. An overall shift towards higher affinity can be observed within both the low and high affinity categories with increasing distance from the primary infection. At 6.5 months, this culminates in a pattern of two sets of rising affinities interrupted by the 2.0-M value, a pattern also seen in hyperimmune plasma. These shifts clearly demonstrate affinity maturation of MSP-1_{21}-specific antibodies after a primary infection although none was detected by studying the affinity index.

There is hardly any difference in the affinity distribution patterns of the respective untreated and drug-treated groups at 4.5 and 6.5 months after infection (Fig. 6.7a and b). At 2.5 months, the proportion of antibodies in the lowest affinity step is noticeably higher in the drug-treated than in the untreated group, but the negative value for 1.0 M salt concentration in the drug-treated group indicates that this measurement is at least partially distorted. This distortion could be attributed to variations in the degree of influence of drug treatment in individual plasma samples. However, together with the affinity indices calculated in Section 6.2.5, the affinity distributions do not support a strong role for parasite persistence in the shaping of serum antibody affinities.

6.2.7 Affinity indices during reinfection

The affinity indices were determined from sera taken at weekly intervals during reinfection after 2.5, 4.5 or 6.5 months. The untreated and drug-treated reinfected mice were compared with age-matched mice undergoing primary infection (Fig. 6.8). Affinity indices are not shown at some time points because the curve fits were too poor for measuring these values.

Figure 6.8 Changes in the affinity index during reinfection.

The average affinity indices are shown during reinfection 2.5 (a), 4.5 (b) or 6.5 months (c) after a primary infection without (red) or with chloroquine treatment (blue). The average affinity index determined for hyperimmune serum in each experiment is included as an orange line. The affinity indices during a primary infection of age-matched controls are shown in black. All lines represent arithmetic means from three to five mice and the error bars show the SEM.

(a)

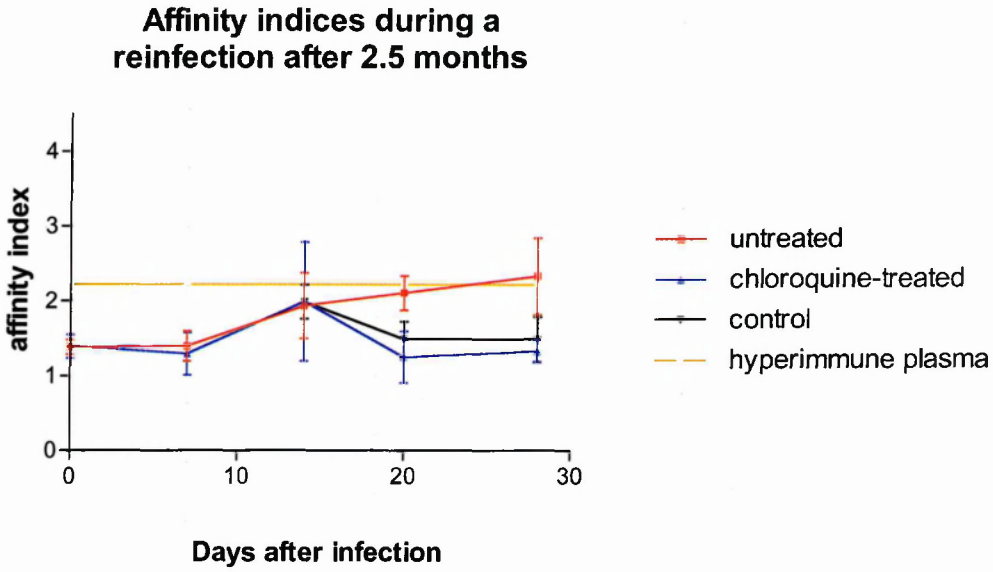
Affinity indices during a reinfection after 2.5 months
affinity index
0
1
2
3
4
0
10
20
30
Days after infection
untreated
chloroquine-treated
control
hyperimmune plasma

(b)

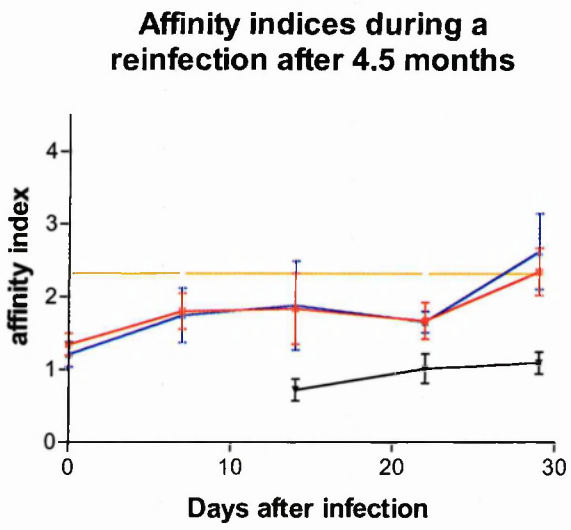
Affinity indices during a reinfection after 4.5 months
affinity index
0
1
2
3
4
0
10
20
30
Days after infection

(c)

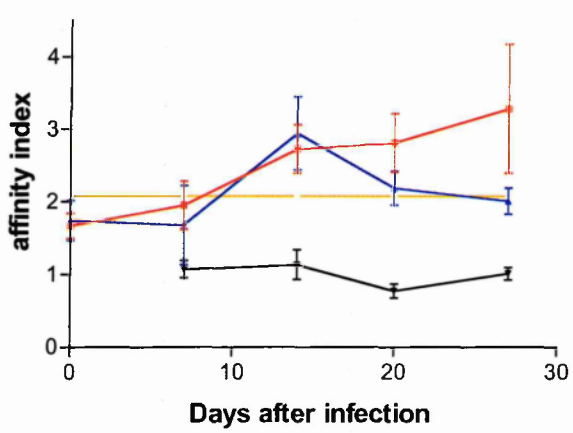
Affinity indices during a reinfection after 6.5 months
affinity index
0
1
2
3
4
0
10
20
30
Days after infection

No serum samples were tested for day 7 of the primary infection shown in panel a and the affinity index could not be calculated for day 7 of the primary infection shown in panel b.

The affinity indices in the primary infections (black lines in Fig. 6.8) are consistently lower than the affinity index of hyperimmune plasma, generally by a factor of about twofold. This difference is statistically significant for the primary infections shown in Figs. 6.8b and c (p=0.0007-0.0198), but was only significant at 3 weeks in Fig. 6.8a (p<0.05).The affinity index does not change much during the course of a primary infection, apart from the 2-week time point in the control for the 2.5-month reinfection (Fig. 6.8a). Since there is no rise at this time point in the other two primary infections (Fig. 6.8b and c), the most probable explanation is experimental error.

For all of the secondary infections, the affinity indices of the untreated and drug-treated groups are very closely matched for the first 2 weeks. In the 2.5- and 6.5-month reinfections, the affinity index in the untreated group continues to the rise, whereas the affinity index in the drug-treated group peaks at 2 weeks and then drops again (Figs. 6.8a c). However, the differences betweeen the affinity indices of the drug-treated and the untreated groups are not statistically significant for either the 2.5 or the 6.5-month reinfections (p=0.8413 or 0.1143, respectively). In addition, in the 4.5-month reinfection, the affinity indices of the untreated and drug-treated groups remain well matched through to the 4th week, making it questionable whether the affinity index in secondary infection is affected by parasite persistence.

The average affinity indices of all reinfected groups except for the 2.5-month drug-treated rise over the course of 4 weeks. In the 6.5-month reinfection, which already commences with a higher affinity index than the other two reinfections, the level of hyperimmune plasma is already exceeded in the 2nd week of infection. However, the difference betweem the affinity index of the 6.5-month reinfection samples and of hyperimmune plasma is not significant (p=0.0798). In general, the data described in this section shows mainly

trends rather than statistically significant differences. Even the difference between the affinity indices of the primary and secondary infections is only significant for a few time points. As can been seen by the size of the standard error, there is considerable variation in the affinity index between individual mice, which is not surprising in a polyclonal antibody response. However, in order to ascertain whether any of the observed trends are relevant, it would be necessary to repeat these experiments using larger groups of samples, more replicates per sample or both.

6.2.8 Affinity distributions during reinfection

The changes in affinity distribution are shown during reinfection after 2.5 months (Fig. 6.9), 4.5 months (Fig. 6.10) or 6.5 months (Fig. 6.11) for untreated mice (a), drug-treated mice (b) or primary infection in age-matched controls (c). The affinity distribution of hyperimmune serum is included in each figure as a comparison. At the bottom of each page, the corresponding course of parasitaemia from Section 5 is shown for reference.

In all three groups of untreated reinfected mice, the population of antibodies requiring more than 3.0 M salt concentration for dissociation becomes the most prominent group within the first 1-2 weeks (Figs. 6.9a, 6.10a and 6.11a). At 2.5 months (Fig. 6.9a), the affinity distributions look almost identical for days 0 and 7 of reinfection and the shift into the > 3.0 M affinity category is not seen until day 14. At 4.5 and 6.5 months, (Figs. 6.10a and 6.11a) where the peak parasitiaemia is 10-fold higher and occurs 3 days earlier, the change in the distribution pattern and the increase in the highest affinity category can be observed 1 week earlier. The highest affinity category increases most at 6.5 months, where it contains about half of the MSP-1_{21}-specific antibodies on day 20 of reinfection, a higher proportion than that found in hyperimmune plasma. In fact, the size of the >3.0 M population in hyperimmune plasma is surpassed in all reinfected groups except the 2.5-month drug-treated mice. It is interesting that the affinity patterns of all four of the groups reinfected at 4.5 and 6.5 months develop similarly, despite different initial distributions at day 0 of reinfection.

Figure 6.9 Changes in affinity distribution during reinfection after 2.5 months.

The affinity distribution of MSP-1_{21}-specific IgG is shown for plasma samples taken at weekly intervals during reinfection 2.5 months after a primary infection without (a) or with drug treatment (b). The affinity distributions during a primary infection of age-matched controls are shown for comparison (c) .Each bar represents the arithmetic mean from duplicates of four to five mice and error bars show the SEM.

At the bottom of each page, the parasitaemia for this course of infection is shown (taken from Fig. 3.2).

(a)

Reinfection after 2.5 months (untreated group)

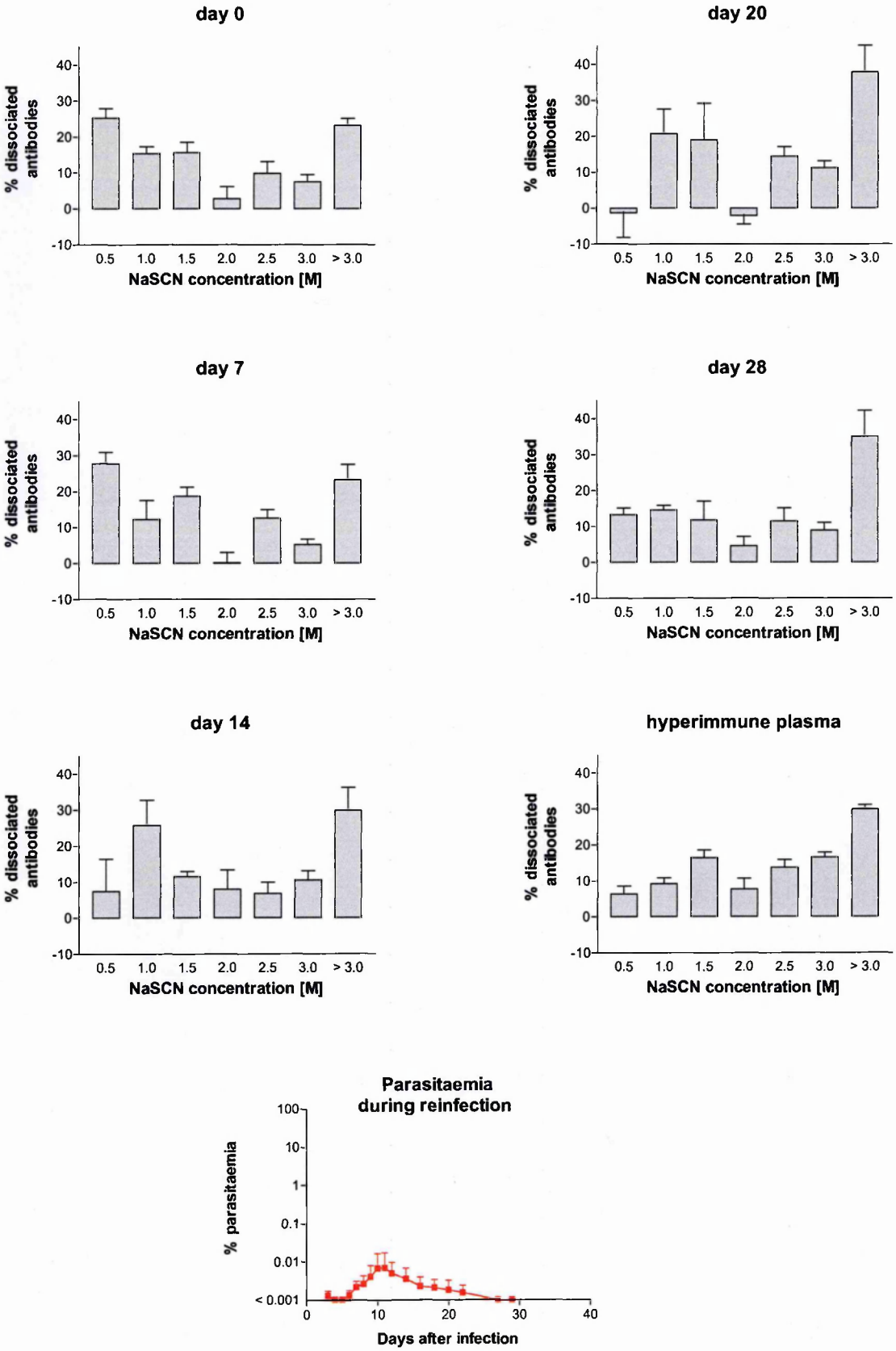

(b) Reinfection after 2.5 months (chloroquine-treated group)

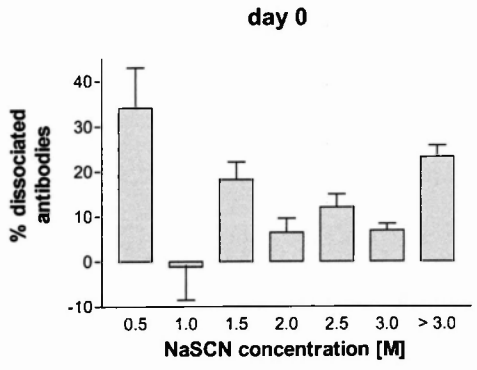

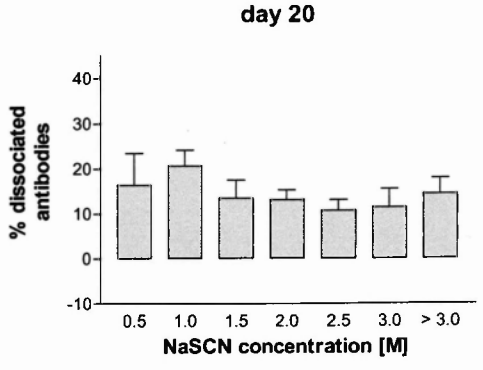

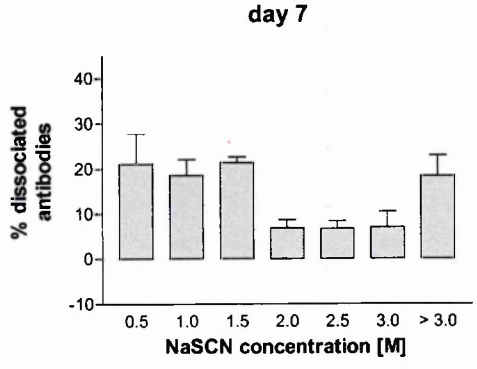

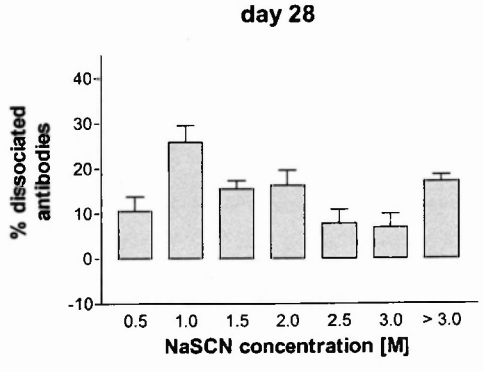

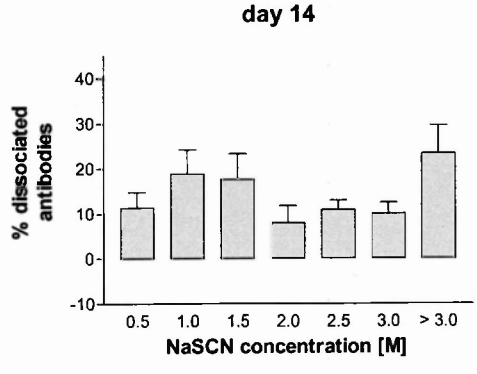

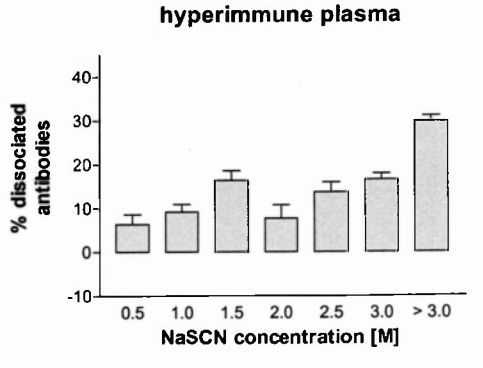

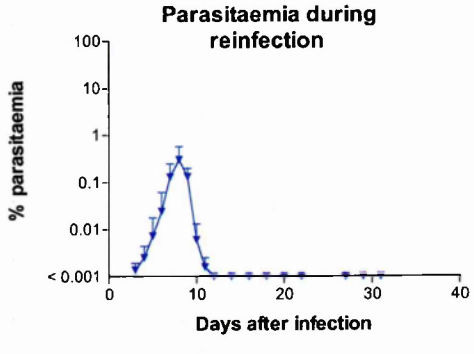

(c) Primary infection (control for 2.5-month reinfection)

day 7
not done

day 14

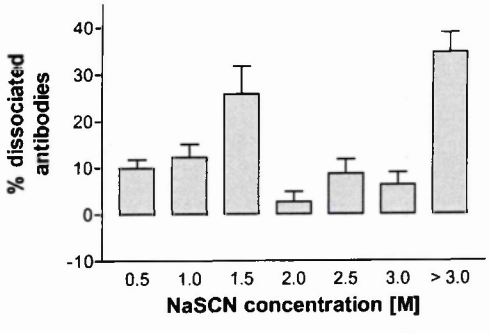

day 20

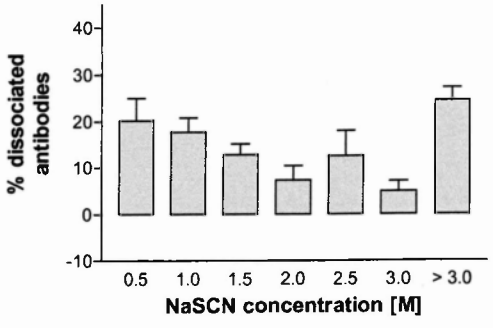

day 28

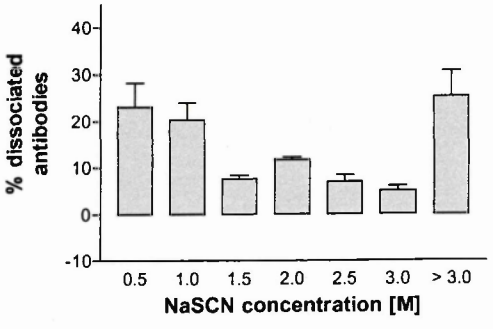

hyperimmune plasma

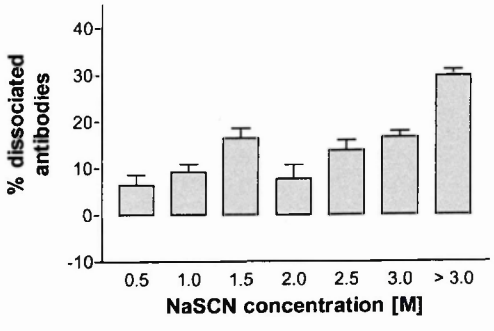

Parasitaemia during primary infection

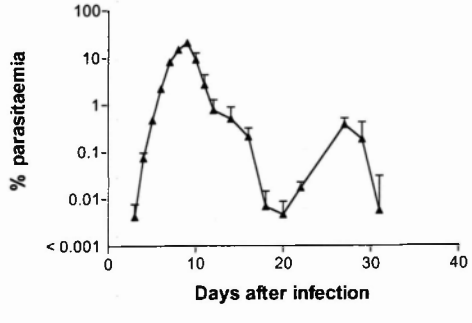

Figure 6.10 Changes in affinity distribution during reinfection after 4.5 months.

The affinity distribution of MSP-1_{21}-specific IgG is shown shown for plasma samples taken at weekly intervals during reinfection 4.5 months after a primary infection without (a) or with drug treatment (b). The affinity distributions during a primary infection of age-matched controls are shown for comparison (c). Each bar represents the arithmetic mean from duplicates of four to five mice and error bars show the SEM.

At the bottom of each page, the parasitaemia for this course of infection is shown (taken from Fig. 3.2).

(a)

Reinfection after 4.5 months (untreated group)

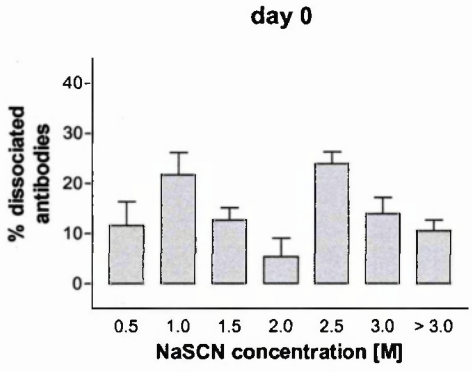

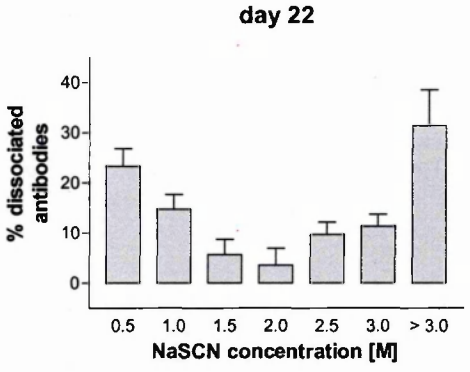

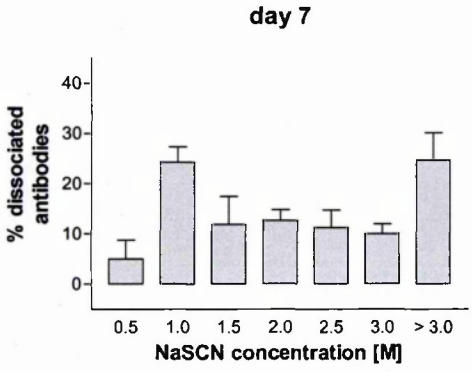

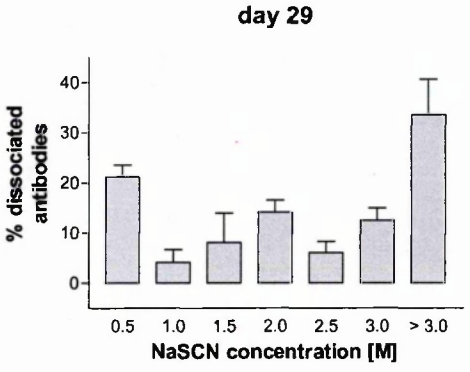

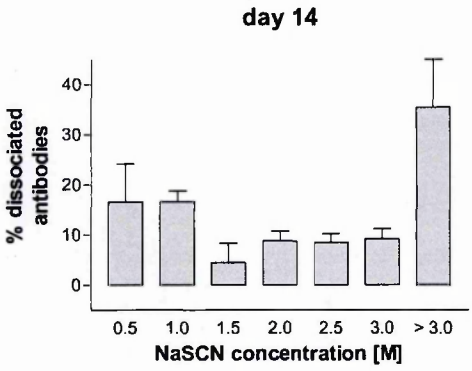

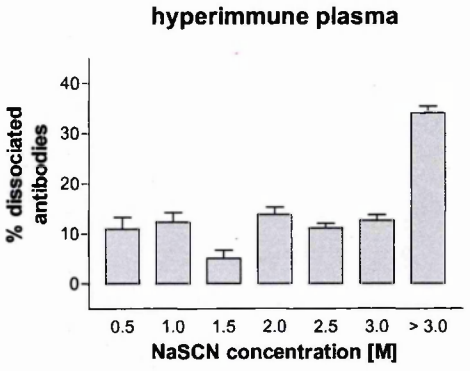

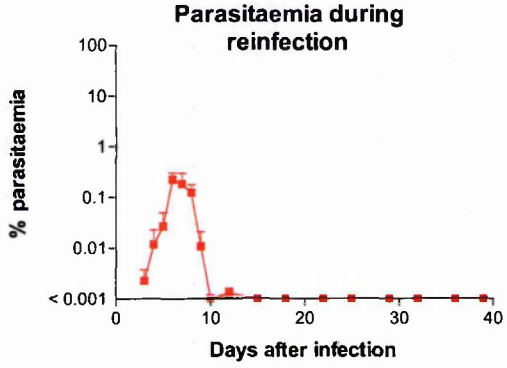

(b) Reinfection after 4.5 months (chloroquine-treated group)

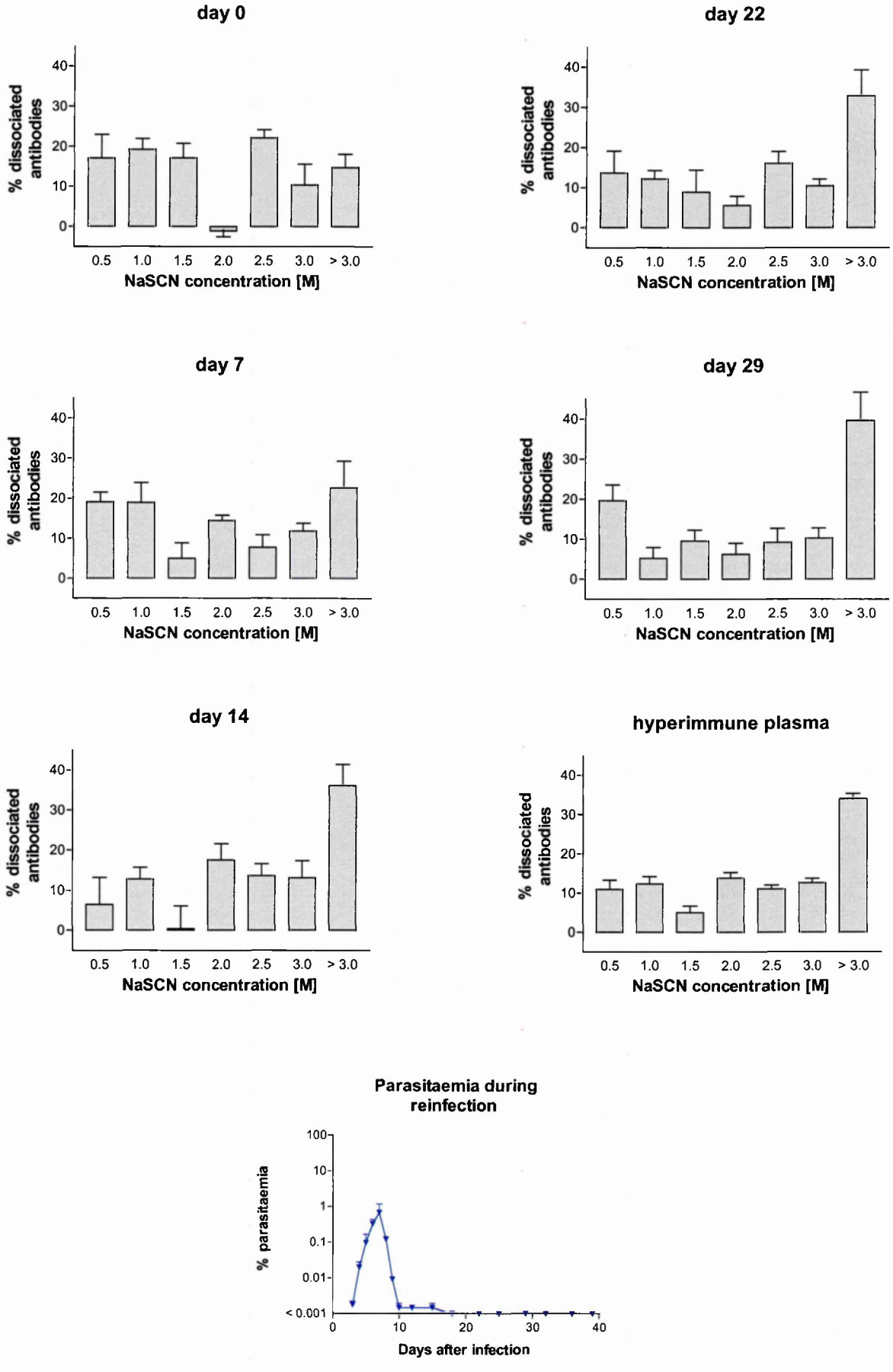

(c)

Primary infection (controls for 4.5 months reinfection)

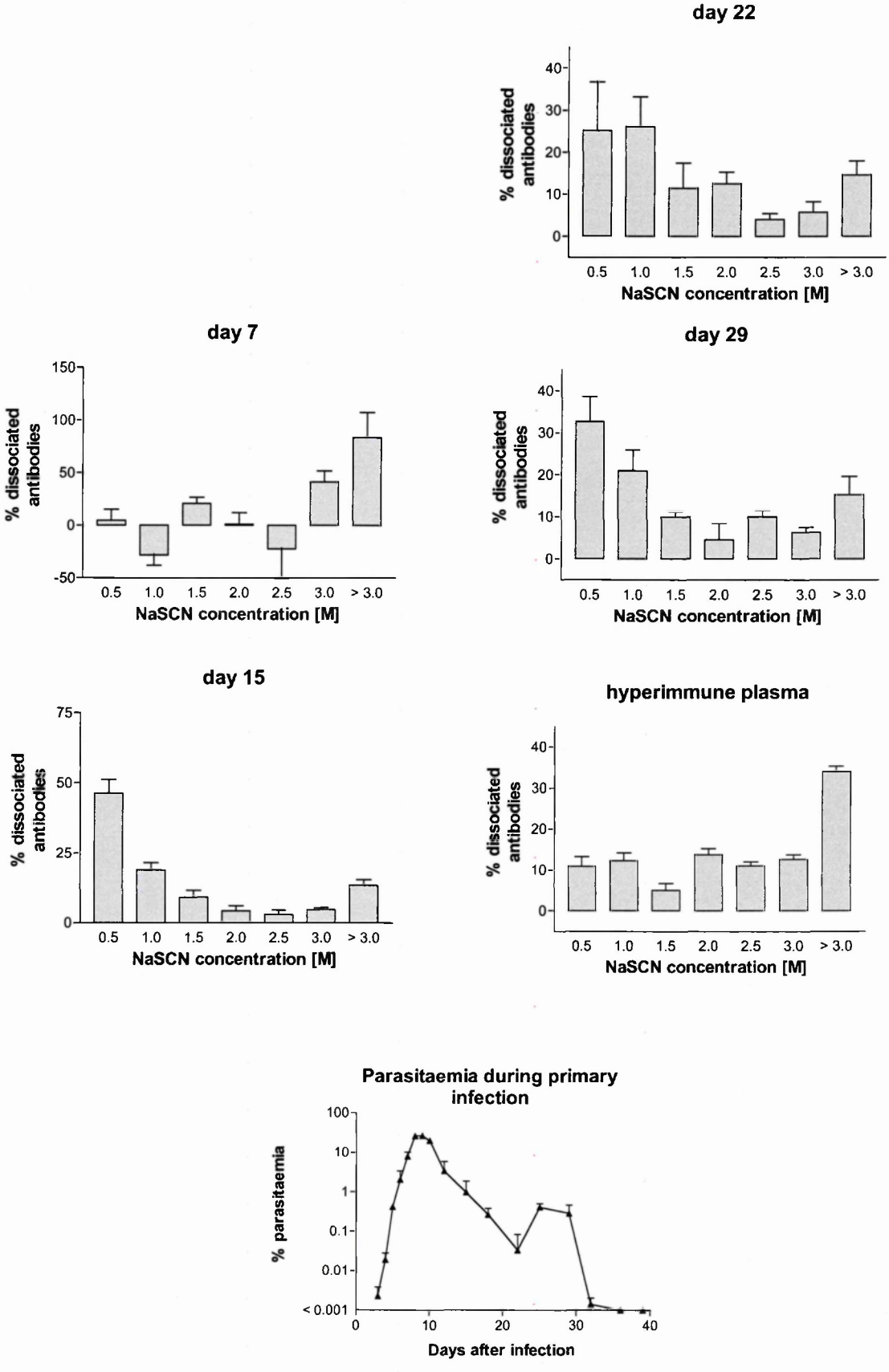

Figure 6.11 Changes in affinity distribution during reinfection after 6.5 months.

The affinity distribution of MSP-1_{21}-specific IgG is shown shown for plasma samples taken at weekly intervals during reinfection 6.5 months after a primary infection without (a) or with drug treatment (b). The affinity distributions during a primary infection of age-matched controls are shown for comparison (c). Each bar represents the arithmetic mean from duplicates of three to five mice and error bars show the SEM.

At the bottom of each page, the parasitaemia for this course of infection is shown (taken from Fig. 3.2).

(a)

Reinfection afer 6.5 months (untreated group)

day 0

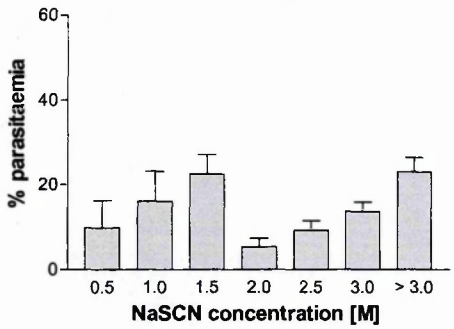

day 20

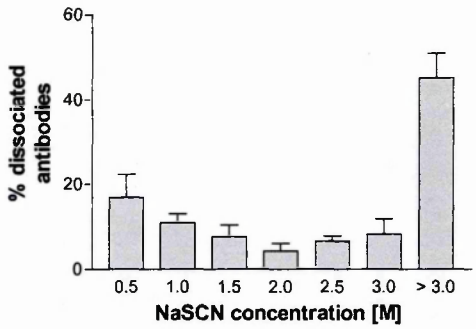

day 7

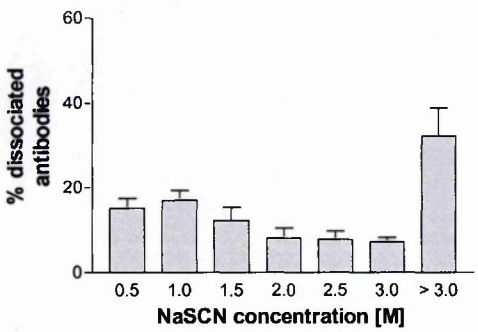

day 27

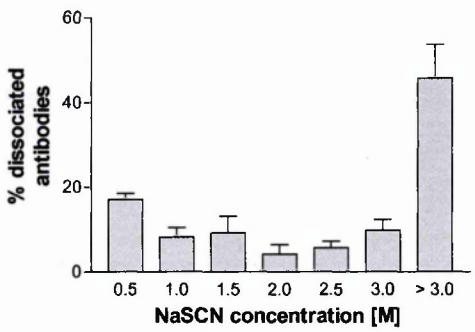

day 14

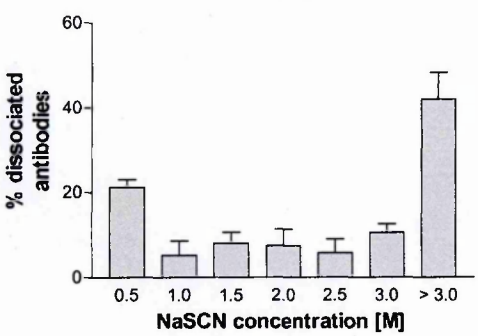

hyperimmune plasma

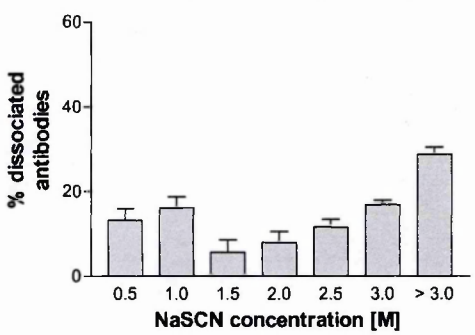

Parasitaemia during reinfection

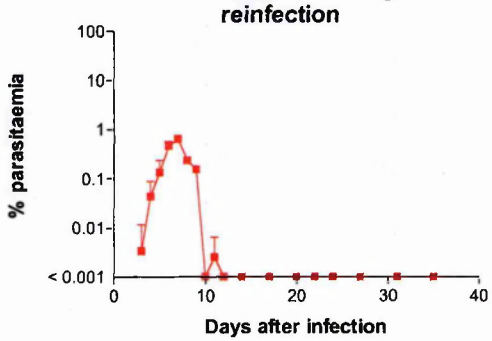

(b) Reinfection after 6.5 months (chloroquine-treated group)

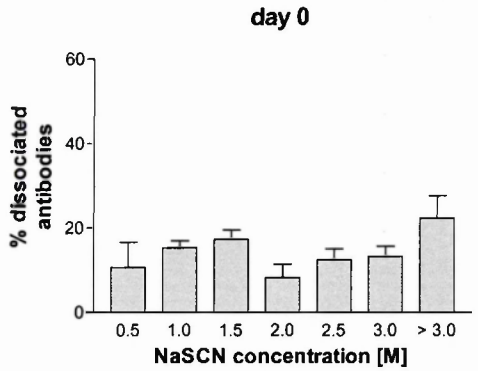

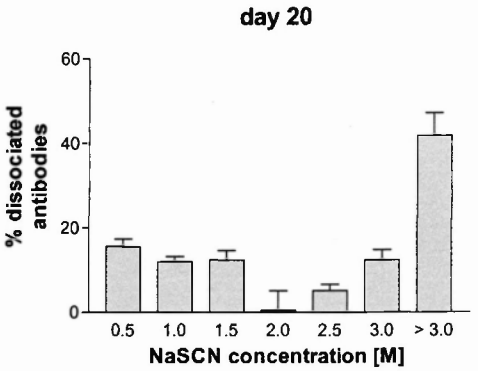

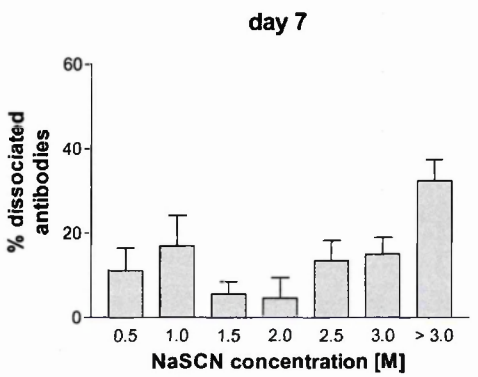

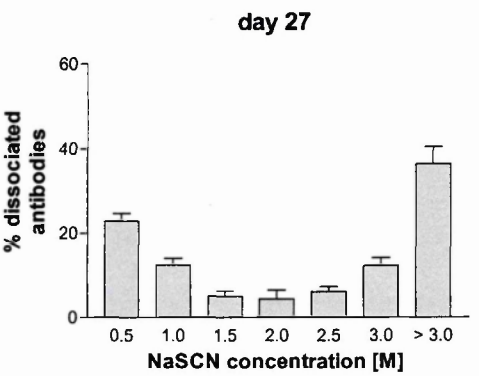

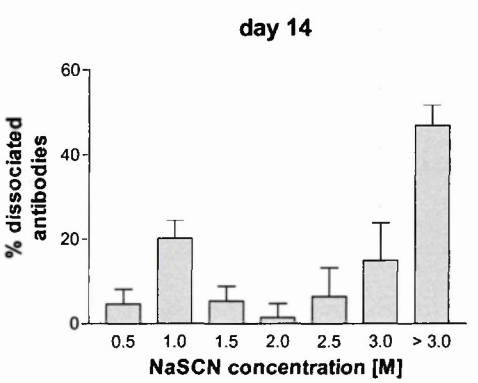

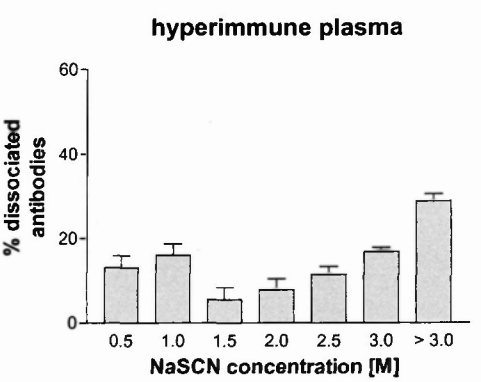

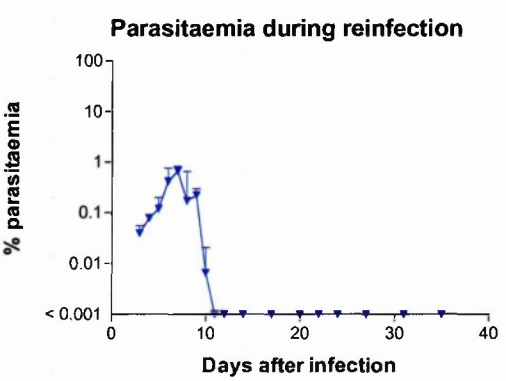

(c) Primary infection (controls for 6.5-month reinfection)

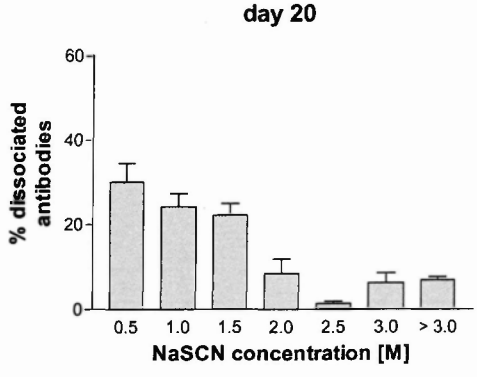

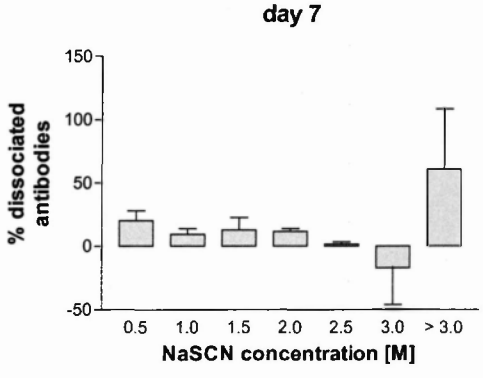

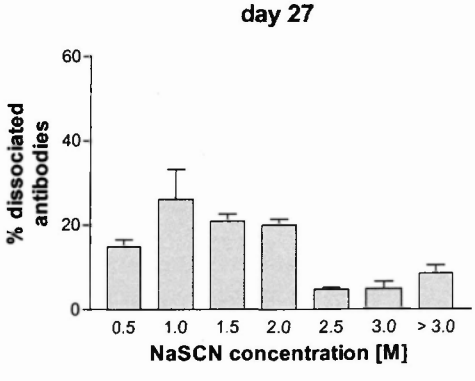

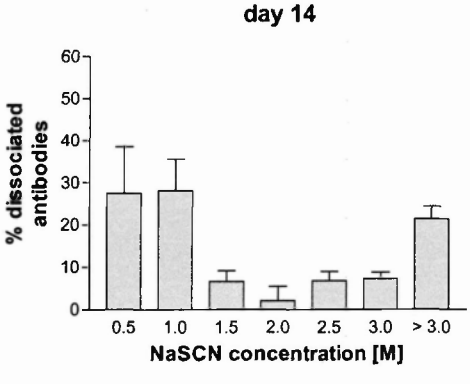

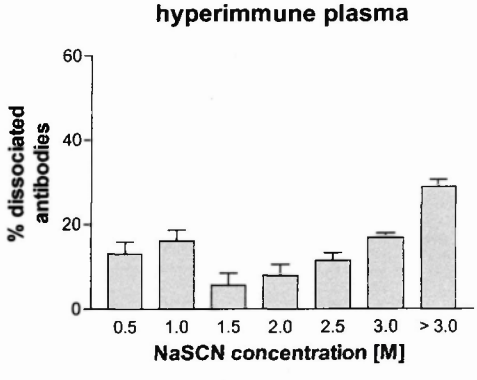

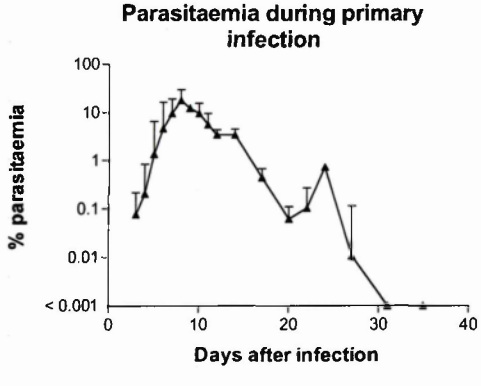

The 4.5 and 6.5-month time points of the drug-treated groups (Figs. 6.10b and 6.11b) display similar characteristics as their untreated counterparts (Figs. 6.10a and 6.11a), namely an increase of the highest affinity category visible from day 7 of infection and a higher degree of affinity maturation at 6.5 months than at 4.5 months. In contrast, the 2.5 month drug-treated group (Fig. 6.9b) differs from its untreated counterpart (Fig. 6.9a) as well as from the later reinfections of drug-treated mice (Figs. 6.10b and 6.11b). At days 7 and 14, the antibody population which is not dissociated by the 3.0 M thiocyanate concentration reaches 20 and 25%, respectively, without becoming the predominant population. At days 20 and 28 of reinfection, the population shrinks again to less than 20%. The pattern shows a fairly even distribution of affinities with the second-lowest affinity group (1.0 M) favoured slightly over the lowest affinity category when comparing with the other time points in drug-treated mice. Since the course of parasitaemia is almost identical between the three drug-treated groups, this indicates that elimination of parasites 1 month after primary infection affects the affinity distribution in temporally close reinfections but not in remote ones.

Surprisingly, there is considerable variation between the control primary infections (Figs. 6.9c, 6.10c and 6.11c). This can partially be attributed to limitations of the thiocyanate dissociation assay at low IgG levels. This can be seen in the affinity distributions calculated for the control plasma samples for the 4.5 month reinfection (Fig. 6.10c) which were eightfold more dilute than the other control samples. The inaccuracy of these measurements was reflected by the fact that the correlation coefficients (R^2) of the linear regression curves for day 7 were all too low for the affinity index calculations (Section 6.2.7) and also resulted in the two negative values in the day 7 affinity distribution graph in Fig. 6.10c. As the day-7 distribution in Fig. 6.10a is unreliable and those values are missing in Fig. 6.9a, it is not worth comparing the affinity distribution in the primary infections before day 14.

The day-14 distribution during the 2.5-month reinfection (Fig. 6.9a) should also be ignored and needs to be repeated, as some error must have occurred in that measurement. The distribution neither matches the other two affinity distributions at day 14 nor does it fit into the further affinity development during the 2.5-month reinfection. In addition, the affinity index calculated for this time point was also in contradiction with the rest of the primary infection values. Apart from that, all of the affinity distributions for the primary infections are weighted towards the low affinity categories. A slight shift to the right can be seen in the 3rd or 4th week in Figs. 6.10c and 6.11c, but this is limited to the low affinity categories The >3.0 M category of antibodies remains between 10 and 25%, which is much lower than in the secondary infections. However, the affinity distribution assays should be repeated for the primary infections at a higher plasma concentration to confirm these results.

In summary, antibody affinity does mature slightly during primary and more strongly during secondary infection, with the size of the highest affinity population increasing with the interval after the primary infection. Drug treatment with chloroquine impairs the affinity development at 2.5 months but not at the later time points.

6.3 Discussion

The results from this section are summarised in Fig. 6.12. Briefly, the persistence of MSP-1_{21}-specific IgG after primary infection even in the absence of live parasites indicates that long-lived plasma cells are generated during infection with *P. c. chabaudi* (AS). The clear differentiation of both antibody levels and affinities into primary and secondary antibody response patterns shows that MSP-1_{21}-specific memory B cells are generated as well. The discussion will focus on the quality of these responses in comparison with other infections and immunisations and the influence of drug treatment.

Figure 6.12 Summary of the results from Section 6.

Three groups:

1. reinfected mice
2. reinfected choloroquine-treated mice
3. age-matched controls

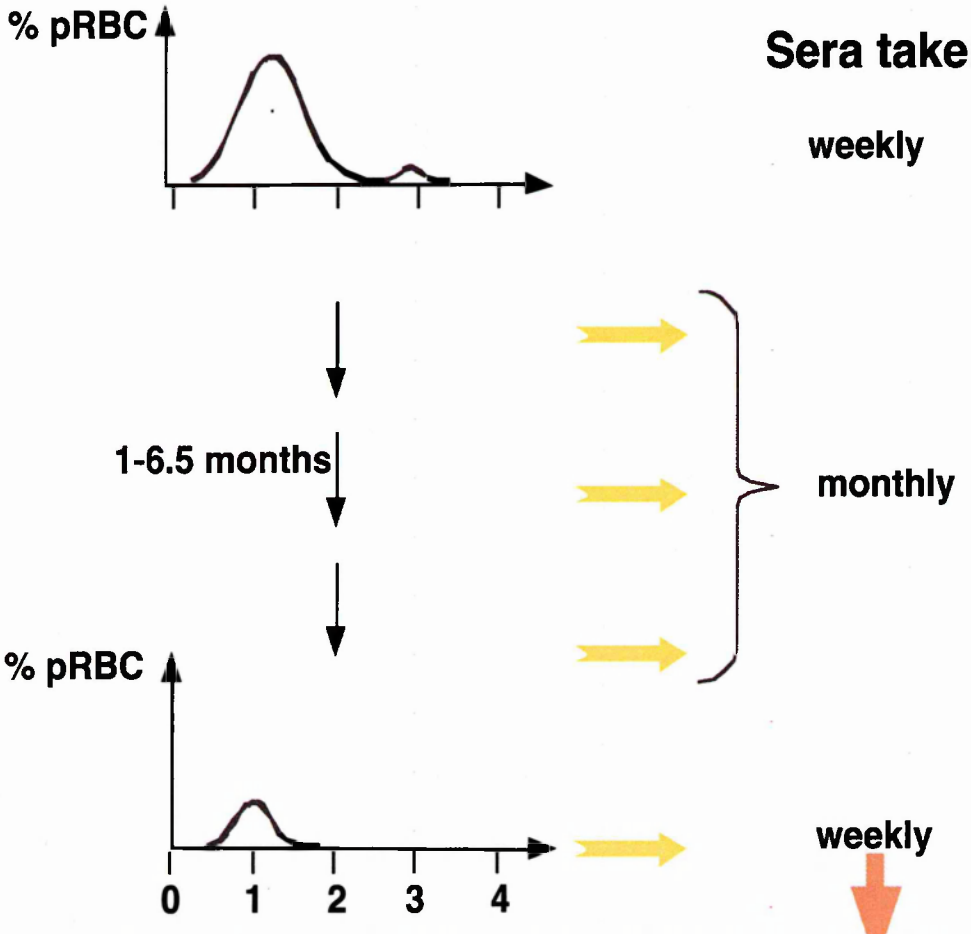

Longevity of malaria-specific antibodies:

- Levels of antibody against MSP-1_{21} and crude malarial extract drop but remain detectable irrespective of parasite presence
- Levels of antibody against MSP-1_{21} during reinfection are influenced by parasite persistence
- Clear differentiation into primary and secondary response to MSP-1_{21}

Affinity maturation of malaria-specific antibodies:

- Antibody affinity for MSP-1_{21} increases after primary infection
- Antibody affinity for MSP-1_{21} increases more strongly during secondary than during primary infection

The first part of the discussion will deal with the antibody levels against MSP-1_{21} and crude malarial extract after a single infection. Long-lived plasma cells are responsible for maintaining serum antibody levels in the absence of continued antigenic stimulation or infection. Therefore, the persistence of antibody after the end of the *Plasmodium* infection showed that long-lived plasma cells existed with specificity for both MSP-1_{21} and antigens present in the crude malarial extract. New plasma cells could be generated by activation of B cells recognising antigen presented on the follicular dendritic cells. However, it seems unlikely that this process would result in the observed steady level of serum antibody without the presence of long-lived plasma cells, since follicular dendritic cells gradually enfold the antigenic complexes they present and this would reduce the availability of antigen for stimulation of new short-lived plasma cells. Nonetheless, the definite proof for long-lived plasma cells - direct detection in the bone marrow - must still be performed.

The elimination of parasites did not affect the amount by which antibody levels against MSP-1_{21} and crude malarial extract dropped between 1 and 2.5 months after infection. This fits in with the theory that long-lived plasma cells are generated early in the germinal centre response (Smith *et al.*, 1997; Tarlinton and Smith, 2000) so that all long-lived plasma cells would already have been generated by the time the mice were treated with chloroquine, making the size of the pool independent of parasite persistence later than 1 month. The peak MSP-1_{21}-specific antibody levels at 1 month can be mainly attributed to short-lived plasma cells, whereas the antibody detected at 2.5 months would be produced by the long-lived population.

The drop in IgG levels observed for MSP-1_{21} and crude malarial extract is larger than that observed in other immunisation and infection systems. After immunisation with the NP hapten, IgG levels drop only 1.5-fold between 20 and 80 days after immunisation

(Takahashi *et al.*, 1998). The drop in *Plasmdodium*-specific antibody levels differs even more strongly from that observed in B-lymphotrophic gammaherpesvirus infection. The virus causes life-long latent infections of B cells and macrophages and in this rodent model, virus-specific IgG levels remained constant from the peak of infection until at least day 90 (Sangster *et al.*, 2000), a time frame in which the *P. c. chabaudi*-infected mice also harbour parasites. The differing influence of parasite persistence could be due to the choice of host cells, with cells of the immune system stimulating a better response than the malaria parasites which spend the majority of their time in the immune-privileged environment of the red blood cell. Alternatively, differences in the numbers of persisting pathogens in the two infections could be important. It would be necessary to determine whether the strong extrafollicular plasma cell response, which is mainly short lived, seen in malaria also exists in other diseases to determine the reason for these differences.

The next issue is the development of MSP-1_{21}-specific antibody levels during infection. The MSP-1_{21}-specific IgG levels during the primary and secondary infections with *P. c. chabaudi* exhibit a differentiation into a slow primary response with low antibody levels and a faster secondary response with higher peak levels. The slow rise of antibody levels during primary infection has also been observed in *P. c. chabaudi* infection of BALB/c mice (with the peak 5 weeks after infection) (Quin and Langhorne, 2001a).However, comparison with other infection and immunisation models shows that the change in MSP-1_{21}-specific IgG levels differs from other primary antibody responses. NP-specific IgG levels peak 8-12 days after immunisation and MMTV-specific IgG levels reach their highest levels 5 days after infection (Luther *et al.*, 1997; Takahashi *et al.*, 1998). In B-lymphotrophic gammaherpesvirus and *Neisseria meningitidis* primary infections, IgG levels begin to rise sharply from day 8 of infection and reach maximal levels at day 20-25 or day 10, respectively (Colino and Outschoorn, 1998; Sangster *et al.*,

2000). These results are in contrast with the slow development of MSP-1_{21}-specific IgG in the primary response, where levels only begin to rise between 3 and 4 weeks after infection and peak at or after the 1-month time point.

IgG responses in secondary infection can be compared with the mouse infection model of *Neisseria meningitidis* where mice were infected with bacteria expressing a modified capsular polysaccharide, which acts as a thymus-dependent antigen (Colino and Outschoorn, 1998). Bacteraemia was usually controlled within 8 h and mice were reinfected after 3 weeks. IgG levels against the polysaccharide peak 10 days after reinfection, reaching levels about ten times higher than the peak in primary infection. In the *P. c. chabaudi* secondary infection, the peak in MSP-1_{21}-specific IgG levels is not quite fivefold higher than in the primary infection. This increase is smaller than the one in *N. meningitidis* infection, but it is on the same order of magnitude. However, as in the primary infection, the MSP-1_{21}-specific IgG levels take longer to peak during the secondary infection, with a delay of 0.5 to 2.5 weeks compared to the *N. meningitidis* model.

There are several possible explanations for the slow rise in MSP-1_{21}-specific IgG levels. One explanation could be low levels of antigen. As the merozoite surface is coated with MSP-1 and the parasite can infect up to 30% of circulating erythrocytes at the peak of infection, this explanation does not sound very plausible. Another possible reason for the low IgG measurements is that a large proportion of the plasma cell output binds to antigen within the mouse and is therefore not accessible for detection by ELISA. This would be especially relevant during the primary infection, when large amounts of parasitic antigen are available to absorb specific antibodies. However, two observations make this an unlikely explanation for slow level development. First, parasite numbers have dropped strongly by days 14 and 21 of primary infection, but the MSP-1_{21}-specific

IgG levels do not begin to rise noticeably until after day 21. Second, in the secondary infections at 2.5 months, the IgG levels are lower in untreated than in the drug-treated groups, although the parasitaemia is tenfold lower in the former. This argues against antibody absorption as a major obscuring factor in the measurements.

There is evidence for poor immunogenicity of MSP-1_{21} which could explain the slow increase in antibody levels. Comparison within the MSP-1 molecule shows that the B cell response to MSP-1_{21} is no worse than that against other portions of the molecule. In BALB/c mice infected with *P. c. chabaudi*, IgG levels against the N-terminal portions of the MSP-1 molecule also develop slowly over 4-5 weeks (Quin and Langhorne, 2001a). However, this just shows that the antibody response to the entire MSP-1 molecule is slow compared to other immunisations or infections. It is likely that low levels or slow development of T cell help are partially responsible, as it has been shown that antigenic processing of MSP-1_{21} for presentation to T cells is slow and that T cell help to the molecule is slow to develop (Quin and Langhorne, 2001a; Quin *et al.*, 2001b). Analysis of IgG levels after immunisation with different concentrations of MSP-1_{21} would reveal how much of the slow rise in IgG levels can be attributed to the poor immunogenicity of the molecule itself.

Finally, it is possible that the slow MSP-1_{21}-specific IgG response is part of a general phenomenon of immune suppression in malaria. There is some evidence that immune suppression occurs during malaria infection in both mice and humans (Greenwood *et al.*, 1972; Weidanz and Rank, 1975). This immune suppression affects both the primary and secondary responses to non-malarial antigens such as bovine serum albumin (McBride and Micklem, 1977; Strambachova-McBride and Micklem, 1979). Recently, several studies have been published showing that the immunosuppression may be occurring at the stage of dendritic cells (Ocaña-Morgner *et al.*, 2003; Urban *et al.*, 1999; Urban and

Roberts, 2003). The immunisation with MSP-1_{21} mentioned above would also help to answer the question of the degree to which general immunosuppression is involved in the slow MSP-1_{21}-specific IgG response. Furthermore, the experiments where the immune response to a non-malarial antigen is studied during malaria infection should be repeated in order to analyse the results in the context of the additional knowledge on B cell development which has been gathered during the last 25 years.

One of the most interesting results from this section is the effect of the presence or absence of parasites on the development of IgG levels during reinfection. The impaired development of MSP-1_{21}-specific IgG levels at 2.5 months in untreated mice (as compared to the corresponding drug-treated mice and later time points) can be explained in two ways. First, the generation of memory B cells could be reduced in the presence of parasites. Second, the lower parasitaemia in the untreated mice results in a diminished antigenic stimulus, which could elicit a lower MSP-1_{21}-specific B cell response. To determine whether parasite number may explain the lower response, a further infection experiment should be carried out, where a secondary infection at 2.5 months is initiated with 10^5, 10^6 or 10^7 parasitised red blood cells in untreated mice and 10^4 or 10^5 parasitised red blood cells in drug-treated mice. These studies were in progress at the time of writing. Hopefully, these different doses will result in at least one combination where the untreated and drug-treated groups have comparable peaks of parasitaemia in the secondary infection. Determination of MSP-1_{21}-specific IgG levels in these groups will reveal whether the specific IgG level depends on the amount of antigen in the secondary infection or the persistence of parasites from the primary infection. Another ongoing experiment is the measurement of IgG levels specific for crude malarial extract or MSP-1_{33} in the plasma samples from the drug-treated and untreated mice reinfected at 2.5 months. This experiment is essential to determine whether the influence of persistent

parasites on the development of IgG levels during secondary infection extends to other malarial antigens or is unique to MSP-1_{21}.

The next part of the discussion will deal with the method of affinity measurement, summarise the results and their implications and then make comparisons with affinity measurements in other systems and finally draw conclusions for disease management. Chaotropic ion dissociation in the ELISA has been established as a method for determining avidities of polyclonal antibodies for some time (Pullen *et al.*, 1986). Using panels of monoclonal antibodies, it has been shown that results are comparable to those obtained by the equilibrium dialysis and biospecific interaction analysis (BIA) methods (Macdonald *et al.*, 1988; McCloskey *et al.*, 1997). There have been two reports of artefacts in the thiocyanate elution method (Gray and Shaw, 1993; Hall and Heckel, 1988) and it therefore appears that some combinations of antibodies and antigens are not suited for thiocyanate elution analysis. However, the type of curve skewing observed by Gray and Shaw does not appear with the samples studied in this chapter and no problems have been reported for polyclonal antibody mixtures. Therefore, the thiocyanate elution method should give accurate representations of the relative affinity of MSP-1-specific antibodies. This method does not allow the determination of the Michaelis-Menten dissociation constant K_D, but that could be determined by measuring real-time binding of selected plasma samples by biospecific interaction analysis.

Affinity maturation can be observed with increasing intervals after primary infection by assessing the affinity distribution, but not from the affinity indices. This affinity maturation appears to be independent of drug treatment and can presumably be attributed to selection processes among long-lived plasma cells (Smith *et al.*, 1997; Tarlinton and Smith, 2000). As will be discussed in terms of the affinity index, affinity maturation after infection is seen in several other systems as well. From 2.5 to 6.5 months after primary

infection, antibody levels against MSP-1_{21} are similar, so that the relative population sizes of the different affinity categories also represent the absolute sizes of those populations. Comparison of primary and secondary infections shows that the affinities change differently for these situations. The shifts during the primary infection are subtle and only visible by affinity distribution, occurring mainly in the low affinity populations. This is consistent with the majority of the serum antibody stemming from short-lived plasma cells of the extrafollicular foci which do not undergo affinity maturation. In the secondary infections, affinity maturation is much more pronounced with a large proportion of the antibodies attaining the highest affinity category. This effect can be attributed to restimulation of memory B cells, as it is rapid and follows the same pattern for all of the reinfections except the chloroquine-treated 2.5-month reinfection -even though the affinity distribution patterns at day 0 differ for the different reinfection time points. This is a clear indication that the serum antibody seen before reinfection stems from a different source than the majority of the antibody produced during reinfection (i.e. long-lived plasma cells versus memory B cells). Newly activated B cells also contribute to serum antibody during secondary infection as can be seen by the continued presence of low affinity antibody. The contribution of these cells is likely to be quite high, as the levels of MSP-1_{21}-specific antibodies change strongly during reinfection, leading to altered sizes as well as the proportions of the affinity categories.

In the long run, drug treatment has no effect on how antibody affinities develop during reinfection. There are no major differences between the untreated and drug-treated groups at 4.5 and 6.5 months post infection. However, there is a clear difference during the 2.5 - month reinfection when chloroquine treatment determines whether low numbers of parasites are still present at the beginning of reinfection. Antibody affinity develops less stongly in the chloroquine-treated mice. This result stands in contrast to the higher

MSP-1_{21}-specific IgG levels observed in the drug-treated group. This represents an unexpected duality in the response of memory B cells to the presence or absence of parasites at a reinfection time point of 2.5 months; parasite persistence appears to interfere with memory B cell generation or reactivation while resulting in increased affinity of these cells. Further experiments must be performed to clarify this issue and the easiest option would be to measure the antibody affinities in the plasma samples from the mice reinfected with different doses of parasite (described above).

Affinity indices have been measured by the thiocyanate elution method in a number of immunisation and infection systems. Immunisation of toddlers with conjugate vaccines used to improve the antibody response to poorly immunogenic capsular polysaccharides from *Haemophilus influenzae* type b resulted in maximal mean affinity indices of 0.55 or 0.104 M, even after boosting (Goldblatt *et al.*, 1999; Goldblatt *et al.*, 1998). Mouse monoclonal antibodies generated after immunisation with nitrophenyl haptens had affinity indices ranging from 0.45 to over 8 M (Macdonald *et al.*, 1988; McCloskey *et al.*, 1997). Immunisation of two seronegative women with attenuated rubella virus led to maximal affinity indices of 4.5 M (Pullen *et al.*, 1986). After periodontitis (infections at the tooth root), maximal affinity indices of 1.38 M and 0.67 M were measured for the two responsible pathogens (Mooney *et al.*, 1995). Chronic infection of up to 11 years resulted in constant affinity indices of around 3 M and 2 M for two of the antigens of *Pseudomonas aeruginosa* (Ciofu *et al.*, 1995)

Therefore, the affinity index value of around 1.5 M seen after primary infection seems to represent a normal degree of antibody affinity. In a rabbit immunisation study with a peptide containing four of the RESA (ring-infected erythrocyte surface antigen) tandem repeats, the maximal affinity index of 1.7 M was achieved with Freund's complete adjuvant and a 0.5 M affinity index was generated by peptide-transfected vaccinia virus

(Lew *et al.*, 1988). Thus, the affinity index for MSP-1_{21} in infection is almost as high as that generated against another malarial protein by immunisation under optimal conditions. Affinity indices against whole parasitised red blood cell extract in humans ranged from 0.04-0.45 M during acute *Plasmodium falciparum* infection and from 0.01-0.75 in convalescent patients protected from reinfection for 63 days after drug treatment (Ferreira and Katzin, 1995). However, these results cannot be compared with the response to MSP-1_{21}, as each antigen found in the malarial extract will have its own pattern of antibody affinity resulting in too many variables.

It has been shown in NP-immunised mice that affinity maturation of serum antibodies continues after germinal centres become undetectable, with a steady increase of antibody affinity up to day 119 post immunisation (Takahashi *et al.*, 1998). This was measured by comparing the ratio of antibodies against a carrier protein with two degrees of haptenation: one which would be recognised by all antibodies of that specificity (NP_{26}) and one which could only be recognised by high affinity antibodies (NP_5). In contrast, the affinity index of MSP-1_{21}-specific antibodies was shown to remain constant after the termination of the acute infection. Comparison with the affinity indices measured in several other immunisation systems reveals a mixed picture. Toddlers and young children vaccinated with polysaccharide conjugate vaccines show increases 10-100% in antibody avidity in the interval between 1 and 6-7 months after the last immunisation (Borrow *et al.*, 2001; Borrow *et al.*, 2002; Goldblatt *et al.*, 1998; Richmond *et al.*, 2001). However, a comparable polysaccharide vaccination in adults did not lead to avidity maturation (Goldblatt *et al.*, 2002).

Affinity measurements made during or after infections with other pathogens also give mixed results: Samples taken from cystic fibrosis patients with chronic *Pseudomonas aeruginosa* infections of up to 11 years duration showed no development of antibody

avidity in this time period (Ciofu *et al.*, 1999). On the other hand, the avidity of rubella-specific antibodies increased up to sixfold over a period of 15 weeks after infection (Böttiger and Jensen, 1997). The avidity of pathogen-specific antibodies can increase up to 14-fold between 4 and 30 weeks after *Toxoplasma gondii* infection. Some caution must be retained in making these comparisons, as the affinities in the last two examples were determined using a variation of the thiocyanate elution method or antibody dissociation with urea in infection system. The affinity index has also been measured in a set of *P. falciparum*-infected, patients, once right after drug treatment and again 63 days later (with patients protected from mosquito exposure during that time period) (Ferreira and Katzin, 1995). In 11 out of 20 patients, the index rose (with increases of 50-350%) in 7 of those patients and fell in 9 patients.

Taken together, this shows that affinity index measurements often do not give a sufficiently clear picture of what is happening in a polyclonal response. However, the affinity distributions of plasma samples taken after primary infection do show that affinity maturation is taking place, even when this is not revealed by the affinity index. This discrepancy is caused by the fact that the affinity index does not register shifts between neighbouring affinity categories and is not affected by changes in the high affinity categories. The affinity maturation after primary infection can be attributed to two causes. One is the selection of higher affinity plasma cells in the bone marrow (Takahashi *et al.*, 1998). Another possibility is generation of additional plasma cells from B cells which have to compete with high affinity serum antibody to bind to malarial antigen presented on follicular dendritic cells. It is not possible to distinguish between these options with a strictly serological approach and therefore, more detailed analysis of the MSP-1_{21}-specific B cells themselves is required.

There is little data in human malaria infections with which to compare these results. The affinity measurements by Falanga et al. examined antibody directed against whole parasite antigen whereas the MSP-1_{21} studies lack information on the infection history. Nevertheless, some conclusions can be drawn for human malaria. If long-lived plasma cells and memory B cells with specificity for an epitope of proven protectivity are generated in malaria infection, why does this not lead to sterile immunity upon reinfection in humans? One possibility is that drug treatment is begun too early for full-scale development of the immune response. It has been shown in mice that a minimum time of parasite exposure before drug treatment is necessary for protection against reinfection with a lethal parasite strain to develop (Favila-Castillo *et al.*, 1999). The slow development of the MSP-1_{21}-specific antibody response suggests that the length of exposure to primary infection may be relevant for the development of long-lived plasma cells or memory B cells In addition, the results showed that the presence of parasites at the time point of reinfection could impair the B cell memory response. This could be a deciding factor in highly endemic areas, where both multiple and chronic infections are common. If these observations are confirmed, it would mean that patients must be drug treated before vaccination to avoid interference with the memory B cell response.

Further analysis of the precise mechanisms of long-lived plasma cell and memory B cell development would be greatly aided by the aid of a mouse carrying a rearranged immunoglobulin transgene specific for a malarial antigen. This gene would have to be "knocked in" to the immunoglobulin location so that all normal steps of B cell development can take place. It would then be possible to observe affinity maturation, isotype switching and memory generation in greater detail.

7 Summary

The results have been discussed individually in Sections 3-6 and further experiments have been suggested. This section summarises how the separate sections fit together and considers some of the implications for future work. Sections 3 and 4 revealed that both the follicular and the extrafollicular pathway are represented in the general as well the specific B cell responses to *Plasmodium* antigens during primary infection, showing that the potential exists for long- and short-lived B cell responses. The existence of long-lived immune responses (although not necessarily in the B cell compartment) was demonstrated by the reinfection studies in Section 5. These data also showed that the presence of parasites at the time of reinfection may result in synergistic cooperation between activated effector cells and long-lived cells of the immune system. Section 6 showed that the presence of parasites at the time point of reinfection affects the B cell response differentially. Persistence of parasites beyond day 30 of infection appears to have no effect on long-lived plasma cell development and maintenance. However, persisting parasites may slow down the memory B cell response while simultaneously leading to an increase of memory B cell affinity.

One remarkable aspect of these results is the parallel occurrence of reduced anti-MSP-1_{21}-specific IgG levels during the 2.5-month reinfection of untreated mice and reduced parasitaemias. Along with the slow kinetics of the MSP-1_{21}-specific IgG response as compared to other infections and immunizations, this raises the possibiliy that MSP-1_{21}-specific antibodies and perhaps the anti-malarial antibody response *per se* may not be as important for protection against malaria as generally assumed. It has been shown that an effective immune response can be mounted against AMA-1 without strong antibody involvement [Xu *et al.*, 2000] and these data could be interpreted in a similar light. However, although mice lacking B cells are able to counter an infection with *Plasmodium*, they are not immune to reinfection, indicating that antibody is important for the development

of immunological memory. Furthermore, it is unclear what quantity of MSP-1-specific antibody would be required to mediate protection. Studies with vesicular stomatitis virus infection have shown increases of antibody levels and affinities beyond a certain level do not further increase the level of protection [Bachmann *et al.*, 1997] and it is unknown at what level such a threshold might exist for the MSP-1-specific immune response.

Another consideration when studying antibody responses to MSP-1 is that the antibodies detected by ELISA may contain non-protective blocking antibodies (discussed in Section 4.1.2) as well as protective processing-inhibitory antibodies. The existence of these types of MSP-1_{21}-specific antibodies has not yet been shown for mice, but the possibility of an MSP-1_{21}-specific pool of mixed protectivity must be kept in mind. Therefore, it is crucial to examine the B cell responses to further *Plasmodium* antigens and determine whether other malarial antibody responses develop according to the same pattern as the MSP-1_{21}-specific antibody response.

The combination of cell-based examination methods during primary infection and serological analyses during primary and secondary infection in these experiments has been very useful in analysing B cell development during malaria infection. However, further analyses must be performed at the antigen-specific level to avoid studying the nonspecific polyclonal response elicited by malaria infection which is probably not part of the long-lived B cell response. Generating a knock-in mouse with an MSP-1_{21}-specific rearranged immunoglobulin heavy chain, as suggested in Section 6.3, would avoid the problem of how to detect the low numbers of MSP-1_{21}-specific B cells. Ideally, the rearranged gene would also include a reporter gene such as green fluorescent protein under the same promoter. This would allow direct detection by immunohistology or flow cytometry. The existence of a large pool of B cells with identical receptors would also make it possible to follow the development of B cells in the germinal centers and allow tracking of migration patterns

afterwards by single cell analysis of somatic hypermutation in the rearranged immunoglobulin genes.

A final consideration in this project is that all infections were performed solely with the erythrocytic stage of the parasite. Evidence is accumulating that *Plasmodium*-infected erythrocytes can affect the maturation of dendritic cells [Ocaña-Morgner *et al.*, 2003, Urban *et al.*, 1999, Urban and Roberts, 2003] and thereby in turn influence immune response against the hepatic stages of the parasite. It is therefore conceivable that sporozoites or hepatic merozoites could influence the immune response against the erythrocytic stages of the parasite as well. Therefore, if further studies confirm that the presence of parasites from a previous infection affect the memory B cell response, it would be important to examine the situation in infections initiated by sporozoite inoculation.

8 References

Ahlborg, N., Ling, I. T., Howard, W., Holder, A. A. and Riley, E. M. (2002) Protective immune responses to the 42-kilodalton (kDa) region of *Plasmodium yoelii* merozoite surface protein 1 are induced by the C-terminal 19-kDa region but not by the adjacent 33-kDa region. Infect. Immun. **70**, 820-825

Ahmed, R. and Gray, D. (1996) Immunological memory and protective immunity: understanding their relation. Science **272**, 54-60

Alves, H. J., Weidanz, W. and Weiss, L. (1996) The spleen in murine *Plasmodium chabaudi adami* malaria: stromal cells, T lymphocytes, and hematopoiesis. Am. J. Trop. Med. Hyg. **55**, 370-378

Anders, R. F. (1986) Multiple cross-reactivities amongst antigens of *Plasmodium falciparum* impair the development of protective immunity against malaria. Parasite Immunol. **8**, 529-539

Arese, P., Turrini, F., Bussolino, F., Lutz, H. U., Chiu, D., Zuo, L., Kuypers, F. and Ginsburg, H. (1991) Recognition signals for phagocytic removal of favic, malaria-infected and sickled erythrocytes. Adv. Exp. Med. Biol. **307**, 317-327

Aribot, G., Rogier, C., Sarthou, J. L., Trape, J. F., Balde, A. T., Druilhe, P. and Roussilhon, C. (1996) Pattern of immunoglobulin isotype response to *Plasmodium falciparum* blood-stage antigens in individuals living in a holoendemic area of Senegal (Dielmo, west Africa). Am. J. Trop. Med. Hyg. **54**, 449-457

Askonas, B. A., Williamson, A. R. and Wright, B. E. (1970) Selection of a single antibody-forming cell clone and its propagation in syngeneic mice. Proc. Natl. Acad. Sci. USA **67**, 1398-1403

Ayala, F. J., Escalante, A. A., Lal, A. A. and Rich, S. M. (1998) Chapter 20: Evolutionary relationships of human malaria parasites. In Malaria: parasite biology, pathogenisis and protections (Sherman, I. W., ed.), pp. 285-300, American Society for Microbiology, Washington, D.C.

Bachmann, M. F., Kalinke, U., Althage, A., Freer, G., Burkhart, C., Roost, H., Aguet, M. , Hen gartner, H. and Zinkernagel, R. M. (1997) The role of antibody concentration and avidity in Science **276**, 2024-2027.

Baird, J. K. (1998) Age-dependent characteristics of protection *v.* susceptibility to *Plasmodium falciparum*. Ann. Trop. Med. Parasitol. **92**, 367-390

Baird, J. K., Jones, T. R., Danudirgo, E. W., Annis, B. A., Bangs., M. J., Basri, H., Purnomo and Masbar, S. (1991) Age-dependent acquired protection against *Plasmodium falciparum* in people having two years exposure to hyperendemic malaria. Am. J. Trop. Med. Hyg. **45**, 65-76

Baird, J. K., Purnomo, Basri, H., Bangs, M. J., Andersen, E. M., Jones, T. R., Masbar, S., Harjosuwarno, S., Subianto, B. and Arbani, P. R. (1993) Age-specific prevalence of *Plasmodium falciparum* among six populations with limited histories of exposure to endemic malaria. Am. J. Trop. Med. Hyg. **49**, 707-719

Barker, L. R. (1971) Acquired immunity to *Plasmodium berghei yoelii* in mice. Trans. R. Soc. Trop. Med. Hyg. **65**, 586-590

Blackman, M. J. and Holder, A. A. (1992) Secondary processing of the *Plasmodium falciparum* merozoite surface protein-1 (MSP1) by a calcium-dependent membrane-bound serine protease: shedding of $MSP1_{33}$ as a noncovalently associated complex with other fragments of the MSP1. Mol. Biochem. Parasitol. **50**, 307-315

Blackman, M. J., Fujioka, H., Stafford, W. H., Sajid, M., Clough, B., Fleck, S. L., Aikawa, M., Grainger, M. and Hackett, F. (1998) A subtilisin-like protein in secretory organelles of *Plasmodium falciparum* merozoites. J. Biol. Chem. **273**, 23398-23409

Blackman, M. J., Heidrich, H. G., Donachie, S., McBride, J. S. and Holder, A. A. (1990) A single fragment of a malaria merozoite surface protein remains on the parasite during red cell invasion and is the target of invasion-inhibiting antibodies. J. Exp. Med. **172**, 379-382

Blackman, M. J., Ling, I. T., Nicholls, S. C. and Holder, A. A. (1991) Proteolytic processing of the *Plasmodium falciparum* merozoite surface protein-1 produces a membrane-bound fragment containing two epidermal growth factor-like domains. Mol. Biochem. Parasitol. **49**, 29-33

Blackman, M. J., Scott-Finnigan, T. J., Shai, S. and Holder, A. A. (1994) Antibodies inhibit the protease-mediated processing of a malaria merozoite surface protein. J. Exp. Med. **180**, 389-393

Bluestone, J. A. and Abbas, A. K. (2003) Natural versus adaptive regulatory T cells. Nat. Rev. Immunol. **3**, 253-257

Bordessoule, D., Gaulard, P. and Mason, D. Y. (1990) Preferential localisation of human lymphocytes bearing γδ T cell receptors to the red pulp of the spleen. J. Clin. Pathol. **43**, 461-464

Borrow, R., Goldblatt, D., Andrews, N., Richmond, P., Southern, J. and Miller, E. (2001) Influence of prior meningococcal C polysaccharide vaccination on the response and generation of memory after meningococcal C conjugate vaccination in young children. J. Infect. Dis. **184**, 377-380

Borrow, R., Goldblatt, D., Andrews, N., Southern, J., Ashton, L., Deane, S., Morris, R., Cartwright, K. and Miller, E. (2002) Antibody persistence and immunological memory at age 4 years after meningococcal group C conjugate vaccination in children in the United kingdom. J. Infect. Dis. **186**, 1353-1357

Böttiger, B. and Jensen, I. P. (1997) Maturation of rubella IgG avidity over time after acute rubella infection. Clin. Diagn. Virol. **8**, 105-111

Bottomly, K. (1988) A functional dichotomy in $CD4^+$ T lymphocytes. Immunol. Today **9**, 268-274

Bouharoun-Tayoun, H. and Druilhe, P. (1992) *Plasmodium falciparum* malaria: evidence for an isotype imbalance which may be responsible for delayed acquisition of protective immunity. Infect. Immun. **60**, 1473-1481

Bouharoun-Tayoun, H., Attanath, P., Sabchareon, A., Chongsuphajaisiddhi, T. and Druilhe, P. (1990) Antibodies that protect humans against *Plasmodium falciparum* blood stages do not on their own inhibit parasite growth and invasion *in vitro*, but act in cooperation with monocytes. J. Exp. Med. **172**, 1633-1641

Bouharoun-Tayoun, H., Oeuvray, C., Lunel, F. and Druilhe, P. (1995) Mechanisms underlying the monocyte-mediated antibody-dependent killing of *Plasmodium falciparum* asexual blood stages. J. Exp. Med. **182**, 409-418.

Braga, E. M., Barros, R. M., Reis, T. A., Fontes, C. J., Morais, C. G., Martins, M. S. and Krettli, A. U. (2002) Association of the IgG response to *Plasmodium falciparum*

merozoite protein (C-terminal 19 kD) with clinical immunity to malaria in the Brazilian Amazon region. Am. J. Trop. Med. Hyg. **66**, 461-466

Braga, E. M., Fontes, C. J. F. and Krettli, A. U. (1998) Persistence of humoral response against sporozoite and blood-stage malaria antigens 7 years after a brief exposure to *Plasmodium vivax*. J. Infect. Dis. **177**, 1132-1135

Brake, D. A., Long, C. A. and Weidanz, W. P. (1988) Adoptive protection against *Plasmodium chabaudi adami* malaria in athymic nude mice by a cloned T cell line. J. Immunol. **140**, 1989-1993

Brinkman, V., Kaufmann, S. H. E. and Simon, H. H. (1985) T-cell mediated immune response in murine malaria: differential effects of antigen-specific Lyt cell subsets in recovery from *Plasmodium yoelii* in normal and T cell-deficient mice. Infect. Immun. **47**, 737-743

Brögger, L. C., Mathews, H. M., Storey, J., Ashkar, T. S. and Molineaux, L. (1978) Changing patterns in the humoral immune response to malaria before, during, and after the application of control measures: a longitudinal study in the West African savanna. Bull. World Health Organ. **56**, 579-600

Bull, P. C., Lowe, B. S., Kortok, M. and Marsh, K. (1999) Antibody recognition of *Plasmodium falciparum* erythrocyte surface antigens in Kenya: evidence for rare and prevalent variants. Infect. Immun. **67**, 733-739

Bull, P. C., Lowe, B. S., Kortok, M., Molyneux, C. S., Newbold, C. I. and Marsh, K. (1998) Parasite antigens on the infected red cell surface are targets for naturally acquired immunity to malaria. Nat. Med. **4**, 358-360

Burghaus, P., Wellde, B., Hall, T., Richards, R., Egan, A., Riley, E., Ballou, W. R. and Holder, A. (1996) Immunization of *Aotus nancymai* with recombinant C terminus of *Plasmodium falciparum* merozoite surface protein 1 in liposomes and alum adjuvant does not induce protection against a challenge infection. Infect. Immun. **64**, 3614-3619

Butcher, G. A., Mitchell, G. H. and Cohen, S. (1978) Antibody mediated mechanisms of immunity to malaria induced by vaccination with *Plasmodium knowlesi* merozoites. Immunology **34**, 77-86

Calame, K. L. (2001) Plasma cells: finding new light at the end of B cell development. Nat. Immunol. **2**, 1103-1108

Calvo, P. A., Daly, T. M. and Long, C. A. (1996) Both epidermal growth factor-like domains of the merozoite surface protein-1 from *Plasmodium yoelii* are required for protection from malaria. Ann. N Y Acad. Sci. **797**, 260-262

Camacho, S. A., Kosco-Vilbois, M. H. and Berek, C. (1998) The dynamic structure of the germinal center. Immunol. Today **19**, 511-514

Cariappa, A., Tang, M., Parng, C., Nebelitskiy, E., Carroll, M., Georgopoulos, K. and Pillai, S. (2001) The follicular versus marginal zone B lymphocyte cell fate decision is regulated by Aiolos, Btk, and CD21. Immunity **14**, 603-615

Carter, R. and Walliker, D. W. (1975) New observations on the malaria parasite of the Central African Republic: *Plasmodium vinckei petteri* subsp. nov. and *Plasmodium chabaudi*. Ann. Trop. Med. Parasitol. **69**, 187-196

Cavacini, L. A., Long, C. A. and Weidanz, W. P. (1986) T-cell immunity in murine malaria: adoptive transfer of resistance to *Plasmodium chabaudi adami* in nude mice with splenic T cells. Infect. Immun. **52**, 637-643

Cavanagh, D. R., Dobano, C., Elhassan, I. M., Marsh, K., Elhassan, A., Hviid, L., Khalil, E. A., Theander, T. G., Arnot, D. E. and McBride, J. S. (2001) Differential patterns of human immunoglobulin G subclass responses to distinct regions of a single protein, the merozoite surface protein 1 of *Plasmodium falciparum*. Infect. Immun. **69**, 1207-1211

Cavanagh, D. R., Elhassan, I. M., Roper, C., Robinson, V. J., Giha, H., Holder, A. A., Hviid, L., Theander, T. G., Arnot, D. E. and McBride, J. S. (1998) A longitudinal study of type-specific antibody responses to *Plasmodium falciparum* merozoite surface protein-1 in an area of unstable malaria in Sudan. J. Immunol. **161**, 347-359

Chang, S. P., Case, S. E., Gosnell, W. L., Hashimoto, A., Kramer, K. J., Tam, L. Q., Hashiro, C. Q., Nikaido, C. M., Gibson, H. L., Lee-Ng, C. T., Barr, P. J., Yokota, B. T. and Hut, G. S. (1996) A recombinant baculovirus 42-kilodalton C-terminal fragment of Plasmodium falciparum merozoite surface protein 1 protects *Aotus* monkeys against malaria. Infect. Immun. **64**, 253-261

Ciofu, O., Giwercman, B., Walter-Rasmussen, J., Pressler, T., Pedersen, S. S. and Hoiby, N. (1995) Antibodies against *Pseudomonas aeruginosa* chromosomal beta-lactamase inpatients with cystic fibrosis are markers of the development of resistance of *P. aeruginosa* to beta-lactams. J. Antimicrob. Chemother. **35**, 295-304

Ciofu, O., Petersen, T. D., Jensen, P. and Hoiby, N. (1999) Avidity of anti-*P. aeruginosa* antibodies during chronic infection in patients with cystic fibrosis. Thorax **54**, 141-144

Ciuca, M., Ballif, L. and Chelarescu-Vieru, M. (1934) Immunity in malaria. Trans. R. Soc. Trop. Med. Hyg. **27**, 619-622

Clark, I. A. and Schofield, L. (2000) Pathogenesis of malaria. Parasitol. Today **16**, 451-454

Clark, I. A., al Yaman, F. M. and Jacobson, L. S. (1997) The biological basis of malarial disease. Int. J. Parasitol. **27**, 1237-1249

Cohen, S., McGregor, I. A. and Carrington, S. (1961) Gamma-globulin and acquired immunity to human malaria. Nature **192**, 733-737

Colino, J. and Outschoorn, I. (1998) Dynamics of the murine humoral immune response to *Neisseria meningitis* group B capsular polysaccharide. Infect. Immun. **66**, 505-513

Collins, W. E. (1988) Major animal models in malaria research: simian. In Malaria: principles and practice of malariology, vol. 2 (Wernsdorfer, W. H. and McGregor, I., eds.), pp. 1473-1502, Churchill Livingstone, New York

Conway, D. J., Cavanagh, D. R., Tanabe, K., Roper, C., Mikes, Z. S., Sakihama, N., Bojang, K. A., Oduola, A. M., Kremsner, P. G., Arnot, D. E., Greenwood, B. M. and McBride, J. S. (2000) A principal target of human immunity to malaria identified by molecular population genetic and immunological analyses. Nat. Med. **6**, 689-692

Cox, F. E. (1966) Acquired immunity to *Plasmodium vinckei* in mice. Parasitology **56**, 719-732

Cox, J., Semoff, S. and Hommel, M. (1987) *Plasmodium chabaudi*: a rodent malaria model for *in vivo* and *in vitro* cytoadherence of malaria parasites in the absence of knobs. Parasite Immunol. **9**, 543-561

Daly, T. M. and Long, C. A. (1995) Humoral response to a carboxyl-terminal region of the merozoite surface protein-1 plays a predominant role in controlling blood-stage infection in rodent malaria. J. Immunol. **155**, 236-243

Daly, T. M. and Long, C. A. (1996) Influence of adjuvants on protection induced by a recombinant fusion protein against malarial infection. Infect. Immun. **64**, 2602-2608.

De Souza, J. B., Ling, I. T., Ogun, S. A., Holder, A. A. and Playfair, J. H. (1996) Cytokines and antibody subclass associated with protective immunity against blood-stage malaria in mice vaccinated with the C terminus of merozoite surface protein 1 plus a novel adjuvant. Infect. Immun. **64**, 3532-3536

del Portillo, H. A., Fernandez-Becerra, C., Bowman, S., Oliver, K., Preuss, M., Sanchez, C. P., Schneider, N. K., Villalobos, J. M., Rajandream, M.-A., Harris, D., Pereira da Silva, L. H., Barrell, B. and Lanzer, M. (2001) A superfamily of variant antigens encoded in the subtelomeric region of *Plasmodium vivax*. Nature **410**, 839-842

Diallo, T. O., Spiegel, A., Diouf, A., Lochouarn, L., Kaslow, D. C., Tall, A., Perraut, R. and Garraud, O. (2002) Short report: differential evolution of immunoglobulin G1/G3 antibody responses to *Plasmodium falciparum* MSP1(19) over time in malaria-immune adult Senegalese patients. Am. J. Trop. Med. Hyg. **66**, 137-139

Dodoo, D., Theander, T. G., Kurtzhals, J. A., Koram, K., Riley, E., Akanmori, B. D., Nkrumah, F. K. and Hviid, L. (1999) Levels of antibody to conserved parts of *Plasmodium falciparum* merozoite surface protein 1 in Ghanaian children are not associated with protection from clinical malaria. Infect. Immun. **67**, 2131-2137

Druilhe, P. and Pérignon, J. L. (1994) Immune mechanisms underlying the premunition against *Plasmodium falciparum* malaria. Mem. Inst. Oswaldo Cruz **89**, 51-53

Druilhe, P. and Pérignon, J. L. (1997) A hypothesis about the chronicity of malaria infection. Parasitol. Today **13**, 353-357

Druilhe, P., Pradier, O., Marc, J. P., Miltgen, F., Mazier, D. and Parent, G. (1986) Levels of antibodies to *Plasmodium falciparum* sporozoite surface antigens reflect malaria transmission rates and are persistent in the absence of reinfection. Infect. Immun. **53**, 393-397

Egan, A. F., Chappel, J. A., Burghaus, P. A., Morris, J. S., McBride, J. S., Holder, A. A., Kaslow, D. C. and Riley, E. M. (1995) Serum antibodies from malaria-exposed people recognize conserved epitopes formed by the two epidermal growth factor motifs of MSP1(19), the carboxy-terminal fragment of the major merozoite surface protein of *Plasmodium falciparum*. Infect. Immun. **63**, 456-466

Egan, A. F., Morris, J., Barnish, G., Allen, S., Greenwood, B. M., Kaslow, D. C., Holder, A. A. and Riley, E. M. (1996) Clinical immunity to *Plasmodium falciparum* malaria is associated with serum antibodies to the 19-kDa C-terminal fragment of the merozoite surface antigen, PfMSP-1. J. Infect. Dis. **173**, 765-769

Eisen, D. P., Saul, A., Fryauff, D. J., Reeder, J. C. and Coppel, R. L. (2002) Alterations in *Plasmodium falciparum* genotypes during sequential infections suggest the presence of strain specific immunity. Am. J. Trop. Med. Hyg. **67**, 8-16

Eling, W. and Jerusalem, C. (1977) Active immunization against the malaria parasite *Plasmodium berghei* in mice: sulfathiazole treatment of a *P. berghei* infection and development of immunity. Tropenmed. Parasitol. **28**, 158-174.

Eling, W. M. C. (1980) *Plasmodium berghei*: premunition, sterile immunity, and loss of immunity in mice. Exp. Parasitol. **49**, 89-96

Engwerda, C. R., Ato, M., Cotterell, S. E., Mynott, T. L., Tschannerl, A., Gorak-Stolinska, P. M. and Kaye, P. M. (2002) A role for tumor necrosis factor-α in remodeling the splenic marginal zone during *Leishmania donovani* infection. Am. J. Pathol. **161**, 429-437

Engwerda, C. R., Mynott, T. L., Sawhney, S., De Souza, J. B., Bickle, Q. D. and Kaye, P. M. (2002) Locally up-regulated lymphotoxin α, not systemic tumor necrosis factor α, is the principle mediator of murine cerebral malaria. J. Exp. Med. **195**, 1371-1377

Falanga, P. B. and Pereira da Silva, L. (1989) Acute virulent infection with *Plasmodium chabaudi* does not impair the generation of a protective immune response. Parasite Immunol. **11**, 603-613

Falanga, P. B., D'Imperio Lima, M. R., Coutinho, A. and Pereira da Silva, L. (1987) Isotypic pattern of the polyclonal B cell response during primary infection by *Plasmodium chabaudi* and in immune-protected mice. Eur. J. Immunol. **17**, 599-603

Falanga, P. B., Franco da Silveira, J. F. and Pereira da Silva, L. (1984) Protective immune response to *Plasmodium chabaudi*, developed by mice after drug controlled infection or vaccination with parasite extracts: analysis of stage specific antigens from the asexual blood cycle. Parasite Immunol. **6**, 529-543

Favila-Castillo, L., Monroy-Ostria, A. and Garcia-Tapia, D. (1999) *Plasmodium chabaudi chabaudi*: effect of low parasitemias on immunity in CB6F1 mice. Exp. Parasitol. **92**, 73-80

Favila-Castillo, L., Monroy-Ostria, A., Kobayashi, E., Hirunpetcharat, C., Kamada, N. and Good, M. F. (1996) Protection of rats against malaria by a transplanted immune spleen. Parasite Immunol. **18**, 325-331

Ferreira, M. U. and Katzin, A. M. (1995) The assessment of antibody affinity distribution by thiocyanate elution: a simple dose-response approach. J. Immunol. Methods **187**, 297-305

Fonjungo, P. N., Elhassan, I. M., Cavanagh, D. R., Theander, T. G., Hviid, L., Roper, C., Arnot, D. E. and McBride, J. S. (1999) A longitudinal study of human antibody responses to *Plasmodium falciparum* rhoptry-associated protein 1 in a region of seasonal and unstable malaria transmission. Infect. Immun. **67**, 2975-2985

François Bach, J. (2003) Regulatory T cells under scrutiny. Nat. Rev. Immunol. **3**, 189-198

García de Vinuesa, C., Cook, M. C., Ball, J., Drew, M., Sunners, Y., Cascalho, M., M. Wabl, G. G. B. K. and MacLennan, I. C. M. (2000) Germinal centers without T cells. J. Exp. Med. **191**, 485-493

García de Vinuesa, C., O'Leary, P., Sze, D. M., Toellner, K. M. and MacLennan, I. C. (1999) T-independent type 2 antigens induce B cell proliferation in multiple splenic sites, but exponential growth is confined to extrafollicular foci. Eur. J. Immunol. **29**, 1314-1323

Garnham, P. C. C. (1988) Malaria parasites if man: life-cycles and morphology (excluding ultrastructure). In Malaria: principles and practices of malariology, vol. 1 (Wernsdorfer, W. H. and McGregor, I., eds.), pp. 61-96, Churchill Livingstone, New York

Garraud, O., Diouf, A., Holm, I., Perraut, R. and Longacre, S. (1999) Immune responses to *Plasmodium falciparum*-merozoite surface protein 1 (MSP1) antigen, II. Induction of

parasite-specific immunoglobulin G in unsensitized human B cells after in vitro T-cell priming with $MSP1_{19}$. Immunology **97**, 497-505

Garraud, O., Perraut, R., Diouf, A., Nambei, W. S., Tall, A., Spiegel, A., Longacre, S., Kaslow, D. C., Jouin, H., Mattei, D., Engler, G. M., Nutman, T. B., Riley, E. M. and Mercereau-Puijalon, O. (2002) Regulation of antigen-specific immunoglobulin G subclasses in response to conserved and polymorphic *Plasmodium falciparum* antigens in an *in vitro* model. Infect. Immun. **70**, 2820-2827

Giha, H. A., Staalsoe, T., Dodoo, D., Elhassan, I. M., Roper, C., Satti, G. M., Arnot, D. E., Theander, T. G. and Hviid, L. (1999) Nine-year longitudinal study of antibodies to variant antigens on the surface of *Plasmodium falciparum*-infected erythrocytes. Infect. Immun. **67**, 4092-4098

Gilks, C. F., Jarra, W., Harvey-Wood, K., McLean, S. A. and Schetters, S. (1989) Host diet in experimental rodent malaria: a variable which can compromise experimental design and interpretation. Parasitology **98**, 175-177

Gilks, C. F., Walliker, D. W. and Newbold, C. I. (1990) Relationships between sequestration, antigenic variation and chronic parasitism in *P.chabaudi chabaudi* - a rodent malaria model. Parasite Immunol. **12**, 45-65

Godson, G. N. (1985) Molecular approaches to malaria vaccines. Sci. Am. **252**, 52-59

Goldblatt, D., Borrow, R. and Miller, E. (2002) Natural and vaccine-induced immunity and immunologic memory to *Neisseria meningitidis* serogroup C in young adults. J. Infect. Dis. **185**, 397-400

Goldblatt, D., Richmond, P., Millard, E., Thornton, C. and Miller, E. (1999) The induction of immunologic memory after vaccination with *Haemophilus influenzae* type b conjugate and acellular pertussis-containing diphtheria, tetanus, and pertussis vaccine combination. J. Infect. Dis. **180**, 538-541

Goldblatt, D., Vaz, A. R. and Miller, E. (1998) Antibody avidity as a surrogate marker of successful priming by *Haemophilus influenzae* type b conjugate vaccines following infant immunization. J. Infect. Dis. **177**, 1112-1115.

Gonzalez-Aseguinolaza, G., Van Kaer, L., Bergmann, C. C., Wilson, J. M., Schmieg, J., Kronenberg, M., Nakayama, T., Taniguchi, M., Koezuka, Y. and Tsuji, M. (2002)

Natural killer T cell ligand α-galactosylceramide enhances protective immunity induced by malaria vaccines. J. Exp. Med. **195**, 617-624

Gozar, M. M., Price, V. L. and Kaslow, D. C. (1998) *Saccharomyces cerevisiae*-secreted fusion proteins Pfs25 and Pfs28 elicit potent *Plasmodium falciparum* transmission-blocking antibodies in mice. Infect. Immun. **66**, 59-64

Gray, B. M. and Shaw, D. R. (1993) Artifacts with the thiocyanate elution method for estimating relative antibody avidity. J. Immunol. Methods **157**, 269-271

Gray, D. and Skarvall, H. (1988) B-cell memory is short-lived in the absence of antigen. Nature **336**, 70-73

Gray, D., Bergthorsdottir, S., van Essen, D., Wykes, M., Poudrier, J. and Siepmann, K. (1997) Observations on memory B-cell development. Semin. Immunol. **9**, 249-254

Gray, D., Dullforce, P. and Jainandunsing, S. (1994) Memory B cell development but not germinal center formation is impaired by *in vivo* blockade of CD40-CD40 ligand interaction. J. Exp. Med. **180**, 141-155

Gray, D., Kumararatne, D. S., Lortan, J., Khan, M. and MacLennan, I. C. (1984) Relation of intra-splenic migration of marginal zone B cells to antigen localization on follicular dendritic cells. Immunology **52**, 659-669

Gray, D., MacLennan, I. C., Bazin, H. and Khan, M. (1982) Migrant μ^+ δ^+ and static μ^+ δ^- B lymphocyte subsets. Eur. J. Immunol. **12**, 564-569

Greenwood, B. M. (1974) Possible role of a B-cell mitogen in hypergammaglobulinaemia in malaria and trypanosomiasis. Lancet **1**, 435-436

Greenwood, B. M., Bradley-Moore, A. M., Bryceson, A. D. and Palit, A. (1972) Immunosuppression in children with malaria. Lancet **1**, 169-172

Groeneveld, P. H., Erich, T. and Kraal, G. (1985) *In vivo* effects of LPS on B lymphocyte subpopulations. Migration of marginal zone-lymphocytes and IgD-bast formation in the mouse spleen. Immunobiology **170**, 402-411.

Groux, H. and Gysin, J. (1990) Opsonization as an effector mechanism in human protection against asexual blood stages of *Plasmodium falciparum*: functional role of IgG subclasses. Res. Immunol. **141**, 529-542

Guevara Patiño, J. A., Holder, A. A., McBride, J. S. and Blackman, M. J. (1997) Antibodies that inhibit malaria merozoite surface protein-1 processing and erythrocyte invasion are blocked by naturally acquired human antibodies. J. Exp. Med. **186**, 1689-1699

Guinamard, R., Okigaki, M., Schlessinger, J. and Ravetch, J. V. (2000) Absence of marginal zone B cells in Pyk-2-deficient mice defines their role in the humoral response. Nat. Immunol. **1**, 31-36

Gupta, S., Snow, R. W., Donnelly, C. A., Marsh, K. and Newbold, C. (1999) Immunity to non-cerebral severe malaria is acquired after one or two infections. Nat. Med. **5**, 340-343.

Hall, T. J. and Heckel, C. (1988) Thiocyanate elution estimation of relative antibody affinity. J. Immunol. Methods **115**, 153-155

Hamilton, R. G. and Mohan, C. (1998) The human IgG subclasses, Calbiochem, San Diego

Han, S., Zheng, B., Dal Porto, J. and Kelsoe, G. (1995) In situ studies of the primary immune response to (4-hydroxy-3-nitrophenyl)acetyl. IV. Affinity-dependent, antigen-driven B cell apoptosis in germinal centers as a mechanism for maintaining self-tolerance. J. Exp. Med. **182**, 1635-1644

Han, S., Zheng, B., Takahashi, Y. and Kelsoe, G. (1997) Distinctive characteristics of germinal center B cells. Semin. Immunol. **9**, 255-260

Hansen, D. S., Siomos, M. A., Buckingham, L., Scalzo, A. A. and Schofield, L. (2003) Regulation of murine cerebral malaria pathogenesis by CD1d-restricted NKT cells and the natural killer complex. Immunity **18**, 391-402

Hargreaves, D. C., Hyman, P. L., Lu, T. T., Ngo, V. N., Bidgol, A., Suzuki, G., Zou, Y. R., Littman, D. R. and Cyster, J. G. (2001) A coordinated change in chemokine responsiveness guides plasma cell movements. J. Exp. Med. **194**, 45-56

Hayday, A. and Tigelaar, R. (2003) Immunoregulation in the tissues by γδ T cells. Nat. Rev. Immunol. **3**, 233-242

Heidrich, H. G., Danforth, H. D., Leef, J. L. and Beaudoin, R. L. (1983) Free-flow electrophoretic separation of *Plasmodium berghei* sporozoites. J. Parasitol. **69**, 360-367

Helmby, H., Jonsson, G. and Troye-Blomberg, M. (2000) Cellular changes and apoptosis in the spleens and peripheral blood of mice infected with blood-stage *Plasmodium chabaudi chabaudi* AS. Infect. Immun. **68**, 1485-1490

Hirunpetcharat, C., Stanisic, D., Liu, X. Q., Vadolas, J., Strugnell, R. A., Lee, R., Miller, L. H., Kaslow, D. C. and Good, M. F. (1998) Intranasal immunization with yeast-expressed 19 kD carboxyl-terminal fragment of *Plasmodium yoelii* merozoite surface protein-1 (yMSP119) induces protective immunity to blood stage malaria infection in mice. Parasite Immunol. **20**, 413-420

Hirunpetcharat, C., Tian, J. H., Kaslow, D. C., van Rooijen, N., Kumar, S., Berzofsky, J. A., Miller, L. H. and Good, M. F. (1997) Complete protective immunity induced in mice by immunization with the 19-kilodalton carboxyl-terminal fragment of the merozoite surface protein-1 (MSP1[19]) of Plasmodium yoelii expressed in *Saccharomyces cerevisiae*: correlation of protection with antigen-specific antibody titer, but not with effector $CD4^+$ T cells. J. Immunol. **159**, 3400-3411

Hirunpetcharat, C., Vukovic, P., Liu, X. Q., Kaslow, D. C., Miller, L. H. and Good, M. F. (1999) Absolute requirement for an active immune response involving B cells and Th cells in immunity to *Plasmodium yoelii* passively acquired with antibodies to the 19-kDa carboxyl-terminal fragment of merozoite surface protein-1. J. Immunol. **162**, 7309-7314

Ho, F., Lortan, J. E., MacLennan, I. C. and Khan, M. (1986) Distinct short-lived and long-lived antibody-producing cell populations. Eur. J. Immunol. **16**, 1297-1301

Holder, A. A. and Freeman, R. R. (1982) Biosynthesis and processing of a *Plasmodium falciparum* schizont antigen recognized by immune serum and a monoclonal antibody. J. Exp. Med. **156**, 1528-1538

Holder, A. A., Blackman, M. J., Burghaus, P. A., Chappel, J. A., Ling, I. T., McCallum-Deighton, N. and Shai, S. (1992) A malaria merozoite surface protein (MSP1)-structure, processing and function. Mem. Inst. Oswaldo Cruz **87**, 37-42

Holder, A. A., Guevara Patino, J. A., Uthaipibull, C., Syed, S. E., Ling, I. T., Scott-Finnigan, T. and Blackman, M. J. (1999) Merozoite surface protein 1, immune evasion, and vaccines against asexual blood stage malaria. Parassitologia **41**, 409-414

Hollingdale, M. R. and Krzych, U. (2002) Immune responses to liver-stage parasites: implications for vaccine development. Chem. Immunol. **80**, 97-124

Israeli, A., Shapiro, M. and Ephros, M. A. (1987) *Plasmodium falciparum* malaria in an asplenic man. Trans. R. Soc. Trop. Med. Hyg. **81**, 233-234

Jacob, J. and Kelsoe, G. (1992) In situ studies of the primary immune response to (4-hydroxy-3-nitrophenyl)acetyl. II. A common clonal origin for periarteriolar lymphoid sheath-associated foci and germinal centers. J. Exp. Med. **176**, 679-687

Jacob, J., Kassir, R. and Kelsoe, G. (1991a) In situ studies of the primary immune response to (4-hydroxy-3-nitrophenyl)acetyl. I. The architecture and dynamics of responding cell populations. J. Exp. Med. **173**, 1165-1175

Jacob, J., Kelsoe, G., Rajewsky, K. and Weiss, U. (1991b) Intraclonal generation of antibody mutants in germinal centres. Nature **354**, 389-392

Jacob, J., Przylepa, J., Miller, C. and Kelsoe, G. (1993) In situ studies of the primary immune response to (4-hydroxy-3-nitrophenyl)acetyl. III. The kinetics of V region mutation and selection in germinal center B cells. J. Exp. Med. **178**, 1293-1307

Jakobsen, P. H., Bate, C. A., Taverne, J. and Playfair, J. H. (1995) Malaria: toxins, cytokines and disease. Parasite Immunol. **17**, 223-231

Janeway, C. A., Travers, P. and Walport, M. (2001) Immunobiology: the immune system in health and disease, Churchill Livingstone, New York

Jarra, W. and Brown, K. N. (1985) Protective immunity to malaria: studies with cloned lines of *Plasmodium chabaudi* and *P. berghei* in CBA/Ca mice. I. The effectiveness and inter- and intra-species specificity of immunity induced by infection. Parasite Immunol. **7**, 595-606

Jarra, W., Hills, L. A., March, J. C. and Brown, K. N. (1986) Protective immunity to malaria. Studies with cloned lines of *Plasmodium chabaudi chabaudi* and *P. berghei* in CBA/Ca mice. II. The effectiveness and inter- or intra-species specificity of the passive transfer of immunity with serum. Parasite Immunol. **8**, 239-254

Jayawardena, A. N., Targett, G. A., Leuchars, E., Carter, R. L., Doenhoff, M. J. and Davies, A. J. S. (1975) T-cell activation in murine malaria. Nature **258**, 149-151

Jenum, P. A., Stray-Pedersen, B. and Gundersen, A.-G. (1997) Improved diagnosis of primary Toxoplasma gondii infection in early pregnancy by determination of antitoxoplasma immunoglobulin G avidity. J. Clin. Microbiol. **35**, 1972-1977

Jongwutiwes, S., Tanabe, K. and Kanbara, H. (1993) Sequence conservation in the C-terminal part of the precursor to the major merozoite surface proteins (MSP1) of *Plasmodium falciparum* from field isolates. Mol. Biochem. Parasitol. **59**, 95-100

Kaneko, A. (1999) Malaria on islands: human and parasite diversities and implications for malaria control in Vanuatu. PhD Thesis, Department of Medicine, Unit of Infectious Diseases, Karolinska Institutet, Karolinska Hospital, Stockholm

Kaneko, A., Taleo, G., Kalkoa, M., Yamar, S., Kobayakawa, T. and Björkman, A. (2000) Malaria eradication on islands. Lancet **356**, 1560-1564

Kang, Y., Calvo, P. A., Daly, T. M. and Long, C. A. (1998) Comparison of humoral immune responses elicited by DNA and protein vaccines based on merozoite surface protein-1 from *Plasmodium yoelii*, a rodent malaria parasite. J. Immunol. **161**, 4211-4219

Karrer, U., Lopez-Macias, C., Oxenius, A., Odermatt, B., Bachmann, M. F., Kalinke, U., Bluethmann, H., Hengartner, H. and Zinkernagel, R. M. (2000) Antiviral B cell memory in the absence of mature follicular dendritic cell networks and classical germinal centers in $TNFR1^{-/-}$ mice. J. Immunol. **164**, 768-778

Kaslow, D. C. (2002) Transmission-blocking vaccines. Chem. Immunol. **80**, 287-307

Klein, U., Kuppers, R. and Rajewsky, K. (1997) Evidence for a large compartment of IgM-expressing memory B cells in humans. Blood **89**, 1288-1298

Klein, U., Rajewsky, K. and Kuppers, R. (1998) Human immunoglobulin $(Ig)M^{+}IgD^{+}$ peripheral blood B cells expressing the CD27 cell surface antigen carry somatically mutated variable region genes: CD27 as a general marker for somatically mutated (memory) B cells. J. Exp. Med. **188**, 1679-1689

Knight, K. L. (1996) Chapter 22: Overview: immunoglobulin isotypes and allotypes. In Weir's Handbook of Experimental Immunology, vol. 1 (Herzenberg, L. A., Weir, D. M.,

Herzenberg, L. A. and Blackwell, C., eds.), Blackwell Science, Cambridge, Massachusetts, USA

Knight, K. L. (1996) Chapter 22: Immunoglobulin isotypes and allotypes. In Weir's Handbook of Experimental Immunology, Volume I: Immunochemistry and Molecular Immunology, vol. I, pp. 22.1-22.3, Blackwell Science, Cambridge, MA, USA

Kosco-Vilbois, M. H., Bonnefoy, J.-Y. and Chvatchko, Y. (1997) The physiology of murine germinal center reactions. Immunol. Rev. **156**, 127-136

Kosco-Vilbois, M. H., Zentgraf, H., Gerdes, J., Bonnefoy and J.Y. (1997) To 'B' or not to 'B' a germinal center? Immunol. Today **18**, 225-230

Kraal, G. (1992) Cells in the marginal zone of the spleen. Int. Rev. Cytol. **132**, 31-74

Kumar, N. and Zheng, H. (1998) Evidence for epitope-specific thymus-independent response against a repeat sequence in a protein antigen. Immunology **94**, 28-34

Kumar, S., Good, M. F., Dontfraid, F., Vinetz, J. M. and Miller, L. H. (1989) Interdependence of $CD4^+$ T cells and malarial spleen in immunity to *Plasmodium vinckei vinckei*. Relevance to vaccine development. J. Immunol. **143**, 2017-2023

Kumararatne, D. S. and MacLennan, I. C. (1981) Cells of the marginal zone of the spleen are lymphocytes derived from recirculating precursors. Eur. J. Immunol. **11**, 865-869.

Kumararatne, D. S. and MacLennan, I. C. (1982) The origin of marginal-zone cells. Adv. Exp. Med. Biol. **149**, 83-90

Kumararatne, D. S., Gagnon, R. F. and Smart, Y. (1980) Selective loss of large lymphocytes from the marginal zone of the white pulp in rat spleens following a single dose of cyclophosphamide. A study using quantitative histological methods. Immunology **40**, 123-131

Kumararatne, D. S., Phillips, R. S., Sinclair, D., Parrott, M. V. and Forrester, J. B. (1987) Lymphocyte migration in murine malaria during the primary patent parasitaemia of *Plasmodium chabaudi* infections. Clin. Exp. Immunol. **68**, 65-77

Ladel, C. H., Blum, C., Dreher, A., Reifenberg, K. and Kaufmann, S. H. E. (1995) Protective role of $\gamma\delta$T cells and $\alpha\beta$T cells in tuberculosis. Eur. J. Immunol. **25**, 2877-2881

Langhorne, J. and Simon, B. (1989) Limiting dilution analysis of the T cell response to *Plasmodium chabaudi chabaudi* in mice. Parasite Immunol. **11**, 545-559

Langhorne, J., Cross, C., Seixas, E., Li, C. and von der Weid, T. (1998) A role for B cells in the development of T cell helper function in a malaria infection in mice. Proc. Natl. Acad. Sci. USA **95**, 1730-1734

Langhorne, J., Evans, C. B., Asofsky, R. and Taylor, D. W. (1984) Immunoglobulin isotype distribution of malaria-specific antibodies produced during infection with *Plasmodium chabaudi adami* and *Plasmodium yoelii*. Cell Immunol. **87**, 452-461

Langhorne, J., Gillard, S., Simon, B., Slade, S. and Eichmann, K. (1989) Frequencies of $CD4^+$ T cells reactive with *Plasmodium chabaudi chabaudi*: distinct response kinetics for cells with Th1 and Th2 characteristics during infection. Int. Immunol. **1**, 416-424

Langhorne, J., Kim, K. J. and Asofsky, R. (1985) Distribution of immunoglobulin isotypes in the nonspecific B-cell response induced by infection with *Plasmodium chabaudi adami* and *Plasmodium yoelii*. Cell Immunol. **90**, 251-257

Langhorne, J., Mombaerts, P. and Tonegawa, S. (1995) $\alpha\beta$ and $\gamma\delta$ T cells in the immune response to the erythrocytic stages of malaria in mice. Int. Immunol. **7**, 1005-1011

Langhorne, J., Quin, S. J. and Sanni, L. A. (2002) Mouse models of blood-stage malaria infections: immune responses and cytokines involved in protection and pathology. Chem. Immunol. **80**, 204-228

Langhorne, J., Simon-Haarhaus, B. and Meding, S. J. (1990) The role of $CD4^+$ T cells in the protective immune response to *Plasmodium chabaudi in vivo*. Immunol. Lett. **25**, 101-107

Laszlo, G., Hathcock, K. S., Dickler, H. B. and Hodes, R. J. (1993) Characterization of a novel cell-surface molecule expressed on subpopulations of activated T and B cells. J. Immunol. **150**, 5252-5262

Lew, A. M., Anders, R. F., Edwards, S. J. and Langford, C. J. (1988) Comparison of antibody avidity and titre elicited by peptide as a protein conjugate or as expressed in vaccinia. Immunology **65**, 311-314

Li, C. (1999) An analysis of Plasmodium chabaudi chabaudi (AS) infection in interleukin-10 deficient mice. PhD Thesis, University of London, London

Li, C., Seixas, E. and Langhorne, J. (2001) Rodent malarias: the mouse as a model for understanding immune responses and pathology induced by the erythrocytic stages of the parasite. Med. Microbiol. Immunol. **189**, 115-126

Ling, I. T., Ogun, S. A. and Holder, A. A. (1995) The combined epidermal growth factor-like modules of *Plasmodium yoelii* Merozoite Surface Protein-1 are required for a protective immune response to the parasite. Parasite Immunol. **17**, 425-433

Liu, Y. J., Oldfield, S. and MacLennan, I. C. (1988) Memory B cells in T cell-dependent antibody responses colonize the splenic marginal zones. Eur. J. Immunol. **18**, 355-362

Liu, Y. J., Zhang, J., Lane, P. J., Chan, E. Y. and MacLennan, I. C. (1991) Sites of specific B cell activation in primary and secondary responses to T cell-dependent and T cell-independent antigens. Eur. J. Immunol. **21**, 2951-2962

Luther, S. A., Gulbranson-Judge, A., Acha-Orbea, H. and MacLennan, I. C. (1997) Viral superantigen drives extrafollicular and follicular B cell differentiation leading to virus-specific antibody production. J. Exp. Med. **185**, 551-562.

Macdonald, R. A., Hosking, C. S. and Jones, C. L. (1988) The measurement of relative antibody affinity by ELISA using thiocyanate elution. J. Immunol. Methods **106**, 191-194

MacLennan, I. C. (1995) B cells. Avoiding autoreactivity. Nature **375**, 281

MacLennan, I. C. M. (1998) B-cell receptor regulation of peripheral B cells. Curr. Opin. Immunol. **10**, 220-225

MacLennan, I. C. M., Garcia de Vinuesa, C. and Casamayor-Palleja, M. (2000) B-cell memory and the persistence of antibody response. Phil. Trans. R. Soc. Lond. **355**, 345-350

MacLennan, I. C., Gulbranson-Judge, A., Toellner, K. M., Casamayor-Palleja, M., Chan, E., Sze, D. M., Luther, S. A. and Orbea, H. A. (1997) The changing preference of T and B cells for partners as T-dependent antibody responses develop. Immunol. Rev. **156**, 53-66

MacLennan, I. C., Liu, Y. J., Oldfield, S., Zhang, J. and Lane, P. J. (1990) The evolution of B-cell clones. Curr. Top. Microbiol. Immunol. **159**, 37-63

Maizels, N. and Bothwell, A. (1985) The T-cell-independent immune response to the hapten NP uses a large repertoire of heavy chain genes. Cell **43**, 715-720

Manz, R. A. and Radbruch, A. (2002) Plasma cells for a lifetime? Eur. J. Immunol. **32**, 923-927

Manz, R. A., Thiel, A. and Radbruch, A. (1997) Lifetime of plasma cells in the bone marrow. Nature **388**, 133-134

Maple, P. A., Jones, C. S., Wall, E. C., Vyseb, A., Edmunds, W. J., Andrews, N. J. and Miller, E. (2000) Immunity to diphtheria and tetanus in England and Wales. Vaccine **19**, 167-173

Marsh, K., Otoo, L., Hayes, R. J., Carson, D. C. and Greenwood, B. M. (1989) Antibodies to blood stage antigens of *Plasmodium falciparum* in rural Gambians and their relation to protection against infection. Trans. R. Soc. Trop. Med. Hyg. **83**, 293-303

Martin, F. and Kearney, J. F. (2000) B-cell subsets and the mature preimmune repertoire. Marginal zone and B1 B cells as part of a "natural immune memory". Immunol. Rev. **175**, 70-79

Martin, F. and Kearney, J. F. (2001) B1 cells: similarities and differences with other B cell subsets. Curr. Opin. Immunol. **13**, 195-201

Martin, F., Oliver, A. M. and Kearney, J. F. (2001) Marginal zone and B1 B cells unite in the early response against T-independent blood-borne particulate antigens. Immunity **14**, 617-629

Martin, R. M., Brady, J. L. and Lew, A. M. (1998) The need for IgG2c specific antiserum wehn isotyping antibodies from C57BL/6 and NOD mice. J. Immunol. Methods **212**, 187-192

Martin, S. and Goodnow, C. (2000) Memory needs no reminders. Nature **407**, 576-577

Martin, S. W. and Goodnow, C. C. (2002) Burst-enhancing role of the IgG membrane tail as a molecular determinant of memory. Nat. Immunol. **3**, 182-188

Maruyama, M., Lam, K. P. and Rajewsky, K. (2000) Memory B-cell persistence is independent of persisting immunizing antigen. Nature **407**, 636-642

McBride, J. S. and Micklem, H. S. (1977) Immunosuppression in murine malaria. II. The primary response to bovine serum albumin. Immunology **33**, 253-259

McCloskey, N., Turner, M. W. and Goldblatt, T. D. (1997) Correlation between the avidity of mouse-human chimeric IgG subclass monoclonal antibodies measured by solid-phase elution ELISA and biospecific interaction analysis (BIA). J. Immunol. Methods **205**, 67-72

McKean, P. G., O'Dea, K. and Brown, K. N. (1993a) Nucleotide sequence analysis and epitope mapping of the merozoite surface protein 1 from *Plasmodium chabaudi chabaudi* AS. Mol. Biochem. Parasitol. **62**, 199-209

McKean, P. G., O'Dea, K. and Brown, K. N. (1993b) A single amino acid determines the specificity of a monoclonal antibody which inhibits *Plasmodium chabaudi* AS in vivo. Mol. Biochem. Parasitol. **62**, 211-222

McLean, S. A., Pearson, C. D. and Phillips, R. S. (1982) *Plasmodium chabaudi*: antigenic variation during recrudescent parasitaemias in mice. Exp. Parasitol. **54**, 296-302

Meding, S. J. and Langhorne, J. (1991) $CD4^+$ T cells and B cells are necessary for the transfer of protective immunity to *Plasmodium chabaudi chabaudi*. Eur. J. Immunol. **21**, 1433-1438

Meding, S. J., Cheng, S. C., Simon-Haarhaus, B. and Langhorne, J. (1990) Role of gamma interferon during infection with *Plasmodium chabaudi chabaudi*. Infect. Immun. **58**, 3671-3678

Migot, F., Chougnet, C., Henzel, D., Dubois, B., Jambou, R., Fievet, N. and Deloron, P. (1995) Anti-malaria antibody-producing B cell frequencies in adults after a *Plasmodium falciparum* outbreak in Madagascar. Clin. Exp. Immunol. **102**, 529-534

Miller, L. H. (1988) Genetically determined human resistance factors. In Malaria: principles and practice of malariology, vol. 1 (Wernsdorfer, W. H. and McGregor, I., eds.), pp. 487-501, Churchill Livingstone, New York

Minoprio, P., Itohara, S., Heusser, C., Tonegawa, S. and Coutinho, A. (1989) Immunobiology of murine *T. cruzi* infection: the predominance of parasite-nonspecific responses and the activation of TCRI T cells. Immunol. Rev. **112**, 183-207

Mohan, K., Sam, H. and Stevenson, M. M. (1999) Therapy with a combination of low doses of interleukin 12 and chloroquine completely cures blood-stage malaria, prevents severe anemia, and induces immunity to reinfection. Infect. Immun. **67**, 513-519

Molineaux, L., Muir, D. A., Spencer, H. C. and Wernsdorfer, W. H. (1988) The epidemiology of malaria and its measurement. In Malaria: principles and practice of malariology, vol. 2 (Wernsdorfer, W. H. and McGregor, I., eds.), pp. 999-1090, Churchill Livingstone, New York

Mooney, J., Adonogianaki, E., Riggio, M. P., Takahashi, K., Haerian, A. and Kinane, D. F. (1995) Initial serum antibody titer to *Porphyromonas gingivalis* influences development of antibody avidity and success of therapy for chronic periodontitis. Infect. Immun. **63**, 3411-3416

Morgan, W. D., Birdsall, B., Frenkiel, T. A., Gradwell, M. G., Burghaus, P. A., Syed, S. E., Uthaipibull, C., Holder, A. A. and Feeney, J. (1999) Solution structure of an EGF module pair from the *Plasmodium falciparum* merozoite surface protein 1. J. Mol. Biol. **289**, 113-122

Mosmann, T. R., Cherwinski, H., Bond, M. W., Giedlin, M. A. and Coffman, R. L. (1986) Two types of murine helper T cell clone. I. Definition according to profiles of lymphokine activities and secreted proteins. J. Immunol. **136**, 2348-2357

Mota, M. M., Brown, K. N., Holder, A. A. and Jarra, W. (1998) Acute *Plasmodium chabaudi chabaudi* malaria infection induces antibodies which bind to the surfaces of parasitized erythrocytes and promote their phagocytosis by macrophages *in vitro*. Infect. Immun. **66**, 4080-4086

Müller, G. and Lipp, M. (2003) Concerted action of the chemokine and lymphotoxin system in secondary lymphoid-organ development. Curr. Opin. Immunol. **15**, 217-224

Murphy, K. M. (2003) In search of the CTD. Nat. Immunol. **4**, 645

Murray, C. J. L. and Lopez, A. D. (1997) Mortality by cause for eight regions of the world: Global Burden of Disease Study. Lancet **349**, 1269-1276

Neuberger, M. S., Ehrenstein, M., Rada, C., Sale, J., Batista, F. D., Williams, G. and Milstein, C. (2000) Memory in the B-cell compartment: antibody affinity maturation. Phil. Trans. R. Soc. Lond. **355**, 357-360

Nikcevich, D. A., Young, M. R., Ellis, N. K., Newby, M. and Wepsic, H. T. (1986) Stimulation of hematopoiesis in untreated and cyclophosphamide treated mice by the inhibition of prostaglandin synthesis. J. Immunopharmacol. **8**, 299-313

Noelle, R. J., Roy, M., Shepherd, D. M., Stamekovic, I., Ledbetter, J. A. and Aruffo, A. (1992) A 39-kDa protein in activated helper T cells binds CD40 and transduces the signal for cognate activation of B cells. Proc. Natl. Acad. Sci. USA **89**, 6550-6554

Nossal, G. J. (1996) Clonal anergy of B cells: a flexible, reversible, and quantitative concept. J. Exp. Med. **183**, 1953-1956

Nwuba, R. I., Sodeinde, O., Anumudu, C. I., Omosun, Y. O., Odaibo, A. B., Holder, A. A. and Nwagwu, M. (2002) The human immune response to *Plasmodium falciparum* includes both antibodies that inhibit merozoite surface protein 1 secondary processing and blocking antibodies. Infect. Immun. **70**, 5328-5331

O Gor, D., Rose, N. R. and Greenspan, N. S. (2003) T_H1-T_H2: a procrustean paradigm. Nature Immunol. **4**, 503-50

Ocaña-Morgner, C., Mota, M. M. and Rodriguez, A. (2003) Malaria blood stage suppression of liver stage immunity by dendritic cells. J. Exp. Med. **197**, 143-151

O'Dea, K. P., McKean, P. G., Harris, A. and Brown, K. N. (1995) Processing of the *Plasmodium chabaudi chabaudi* AS merozoite surface protein 1 in vivo and in vitro. Mol. Biochem. Parasitol. **72**, 111-119

O'Donnell, R. A., de Koning-Ward, T. F., Burt, R. A., Bockarie, M., Reeder, J. C., Cowman, A. F. and Crabb, B. S. (2001) Antibodies against merozoite surface protein (MSP)-1(19) are a major component of the invasion-inhibitory response in individuals immune to malaria. J. Exp. Med. **193**, 1403-1412

O'Donnell, R. A., Saul, A., Cowman, A. F. and Crabb, B. S. (2000) Functional conservation of the malaria vaccine antigen MSP-1_{19} across distantly related *Plasmodium* species. Nat. Med. **6**, 91-95

Oeuvray, C., Bouharoun-Tayoun, H., Gras-Masse, H., Bottius, E., Kaidoh, T., Aikawa, M., Filgueira, M. C., Tartar, A. and Druilhe, P. (1994) Merozoite surface protein-3: a malaria protein inducing antibodies that promote *Plasmodium falciparum* killing by cooperation with blood monocytes. Blood **84**, 1594-1602

O'Garra, A. and Barrat, F. J. (2003) *In vitro* generation of IL-10-producing regulatory $CD4^+$ T cells is induced by immunosuppressive drugs and inhibited by Th1- and Th2-inducing cytokines. Immunol. Lett. **85**, 135-139

Ogun, S. A., Scott-Finnigan, T. J., Narum, D. L. and Holder, A. A. (2000) *Plasmodium yoelii*: effects of red blood cell modification and antibodies on the binding characteristics of the 235-kDa rhoptry protein. Exp. Parasitol. **95**, 187-195

Oliver, A. M., Martin, F. and Kearney, J. F. (1999) $IgM^{high}CD21^{high}$ lymphocytes enriched in the splenic marginal zone generate effector cells more rapidly than the bulk of follicular B cells. J. Immunol. **162**, 7198-7207

Oliver, A. M., Martin, F., Gartland, G. L., Carter, R. H. and Kearney, J. F. (1997) Marginal zone B cells exhibit unique activation, proliferative and immunoglobulin secretory responses. Eur. J. Immunol. **27**, 2366-2374

Pachebat, J. A., Ling, I. T., Grainger, M., Trucco, C., Howell, S., Fernandez-Reyes, D., Gunaratne, R. and Holder, A. A. (2001) The 22 kDa component of the protein complex on the surface of *Plasmodium falciparum* merozoites is derived from a larger precursor, merozoite surface protein 7. Mol. Biochem. Parasitol. **117**, 83-89

Parrott, D. M. V., de Sousa, M. A. B. and East, J. (1966) Thymus-dependent areas in the lymphoid organs of neonatally thymectomized mice. J. Exp. Med. **123**, 191-217

Pasparakis, M., Alexopoulou, L., Episkopou, V. and Kollias, G. (1996) Immune and inflammatory responses in TNF α-deficient mice: a critical requirement for TNF α in the formation of primary B cell follicles, follicular dendritic cell networks and germinal centers, and in the maturation of the humoral immune response. J. Exp. Med. **184**, 1397-1411

Pearson, C. D., McLean, S. A., Tetley, K. and Phillips, R. S. (1983) Induction of secondary antibody responses to *Plasmodium chabaudi in vitro*. Clin. Exp. Immunol. **52**, 121-128

Petersen, E., Hogh, B., Marbiah, N. T. and Hanson, A. P. (1992) The effect of splenectomy on immunity to *Plasmodium malariae* and *P. falciparum* in a malaria immune donor. Trop. Med. Parasitol. **43**, 68-69

Podoba, J. E. and Stevenson, M. M. (1991) $CD4^+$ and $CD8^+$ T lymphocytes both contribute to acquired immunity to blood-stage *Plasmodium chabaudi* AS. Infect. Immun. **59**, 51-58

Pulendran, B., Kannourakis, G., Nouri, S., Smith, K. G. and Nossal, G. J. (1995) Soluble antigen can cause enhanced apoptosis of germinal-centre B cells. Nature **375**, 331-334

Pullen, G. R., Fitzgerald, M. G. and Hosking, C. S. (1986) Antibody avidity determination by ELISA using thiocyanate elution. J. Immunol. Methods **86**, 83-87.

Quin, S. J. and Langhorne, J. (2001a) Different regions of the malaria merozoite surface protein 1 of *Plasmodium chabaudi* elicit distinct T-cell and antibody isotype responses. Infect. Immun. **69**, 2245-2251

Quin, S. J., Seixas, E. M. G., Cross, C. A., Berg, M., Lindo, V., Stockinger, B. and Langhorne, J. (2001b) Low $CD4^+$ T cell responses in the C-terminal region of the malaria merozoite surface protein-1 may be attributed to processing within distinct MHC class II pathways. Eur. J. Immunol. **31**, 72-81

Reif, K., Ekland, E. H., Ohl, L., Nakano, H., Lipp, M., Forster, R. and Cyster, J. G. (2002) Balanced responsiveness to chemoattractants from adjacent zones determines B-cell position. Nature **416**, 94-99

Richmond, P., Borrow, R., Goldblatt, D., Findlow, J., Martin, S., Morris, R., Cartwright, K. and Miller, E. (2001) Ability of 3 different meningococcal C conjugate vaccines to induce immunologic memory after a single dose in UK toddlers. J. Infect. Dis. **183**, 160-163

Ridderstad, A. and Tarlinton, D. M. (1998) Kinetics of establishing the memory B cell population as revealed by CD38 expression. J. Immunol. **160**, 4688-4695

Riley, E. M. (1996) The role of MHC- and non-MHC-associated genes in determining the human immune response to malaria antigens. Parsitology **112**, S39-S51

Riley, E. M., Allen, S. J., Wheeler, J. G., Blackman, M. J., Bennett, S., Takacs, B., Schonfeld, H. J., Holder, A. A. and Greenwood, B. M. (1992) Naturally acquired cellular

and humoral immune responses to the major merozoite surface antigen (PfMSP1) of *Plasmodium falciparum* are associated with reduced malaria morbidity. Parasite Immunol. **14**, 321-337

Riley, E. M., Wagner, G. E., Ofori, M. F., Wheeler, J. G., Akanmori, B. D., Tetteh, K., McGuinness, D., Bennett, S., Nkrumah, F. K., Anders, R. F. and Koram, K. A. (2000) Lack of association between maternal antibody and protection of African infants from malaria infection. Infect. Immun. **68**, 5856-5863

Roberts, D. J., Craig, A. G., Berendt, A. R., Pinches, R., Nash, G., Marsh, K. and Newbold, C. I. (1992) Rapid switching to multiple antigenic and adhesive phenotypes in malaria. Nature **357**, 689-692

Rosenberg, Y. J. (1978) Autoimmune and polyclonal B cell responses during murine malaria. Nature **274**, 170-172

Rotman, H. L., Daly, T. M. and Long, C. A. (1999) *Plasmodium*: immunization with carboxyl-terminal regions of MSP-1 protects against homologous but not heterologous blood-stage parasite challenge. Exp. Parasitol. **91**, 78-85

Rotman, H. L., Daly, T. M., Clynes, R. and Long, C. A. (1998) Fc receptors are not required for antibody-mediated protection against lethal malaria challenge in a mouse model. J. Immunol. **161**, 1908-1912

Sanchez-Torres, L., Rodriguez-Ropon, A., Aguilar-Medina, M. and Favila-Castillo, L. (2001) Mouse splenic $CD4^+$ and $CD8^+$ T cells undergo extensive apoptosis during a *Plasmodium chabaudi chabaudi* AS infection. Parasite Immunol. **23**, 617-626

Sangster, M. Y., Topham, D. J., D'Costa, S., Cardin, R. D., Marion, T. N., Myers, L. K. and Doherty, P. C. (2000) Analysis of the virus-specific and nonspecific B cell response to a persistent B-lymphotropic gammaherpesvirus. J. Immunol. **164**, 1820-1828

Schmieg, J., Gonzalez-Aseguinolaza, G. and Tsuji, M. (2003) The role of natural killer T cells and other T cell subsets against infection by the pre-erythrocytic stages of malaria parasites. Microbes Infect. **5**, 499-506

Schofield, L. and Uadia, P. (1990) Lack of Ir gene control in the immune response to malaria. I. A thymus-independent antibody response to the repetitive surface protein of sporozoites. J. Immunol. **144**, 2781-2788

Schofield, L., Hewitt, M. C., Evans, K., Siomos, M. A. and Seeberger, P. H. (2002) Synthetic GPI as a candidate anti-toxic vaccine in a model of malaria. Nature **418**, 785-789

Schofield, L., McConville, M. J., Hansen, D., Campbell, A. S., Fraser-Reid, B., Grusby, M. J. and Tachado, S. D. (1999) CD1d-restricted immunoglobulin G formation to GPI-anchored antigens mediated by NKT cells. Science **283**, 225-229

Seixas, E., Cross, C., Quin, S. and Langhorne, J. (2001) Direct activation of dendritic cells by the malaria parasite, *Plasmodium chabaudi chabaudi*. Eur. J. Immunol. **31**, 2970-2978

Shakib, F. (1990) The human IgG subclasses: molecular analysis of structure, function and regulation, Pergamon Press, Oxfor

Shokat, K. M. and Goodnow, C. C. (1995) Antigen-induced B-cell death and elimination during germinal-centre immune responses. Nature **375**, 334-338.

Siddiqui, W., Tam, L., Kramer, K., Hui, G., Case, S., Yamaga, K., Chang, S., Chan, E. and Kan, S. (1987) Merozoite surface coat precursor protein completely protects Aotus monkeys against Plasmodium falciparum malaria. Proc. Natl. Acad. Sci. USA **84**, 3014-3018

Siepmann, K., Skok, J., van Essen, D., Harnett, M. and Gray, D. (2001) Rewiring of CD40 is necessary for delivery of rescue signals to B cells in germinal centres and subsequent entry into the memory pool. Immunology **102**, 263-272

Simon-Haarhaus, B., Langhorne, J. and Meding, S. (1991) $CD4^{+}$T cell-dependent effector mechanisms important in the immune response to the erythrocytic stages of *Plasmodium chabaudi chabaudi* (AS). Behring Inst. Mitt., 94-98

Sinnis, P. and Nardin, E. (2002) Sporozoite antigens: biologz of the circumsporozoite protein and thrombospondin-related anonymous protein. Chem. Immunol. **80**, 70-96

Slade, S. J. and Langhorne, J. (1989) Production of interferon-γ during infection of mice with *Plasmodium chabaudi chabaudi*. Immunobiology **179**, 353-365

Slifka, M. K. and Ahmed, R. (1996) Long-term humoral immunity against viruses: revisiting the issue of plasma cell longevity. Trends Microbiol. **4**, 394-400

Slifka, M. K., Antia, R., Whitmire, J. K. and Ahmed, R. (1998) Humoral immunity due to long-lived plasma cells. Immunity **8**, 363-372

Slifka, M. K., Matloubian, M. and Ahmed, R. (1995) Bone marrow is a major site of long-term antibody production after acute viral infection. J. Virol. **69**, 1895-1902

Smelt, S. C., Engwerda, C. R., McCrossen, M. and Kaye, P. M. (1997) Destruction of follicular dendritic cells during chronic visceral leishmaniasis. J. Immunol. **158**, 3813-3821

Smith, K. G. C., Light, A., O'Reilly, L. A., Ang, S.-M., Strasser, A. and Tarlinton, D. (2000) *bcl-2* transgene expression inhibits apoptosis in the germinal center and reveals differences in the selection of memory B cells and bone marrow antibody-forming cells. J. Exp. Med. **191**, 475-484

Smith, K. G., Hewitson, T. D., Nossal, G. J. and Tarlinton, D. M. (1996) The phenotype and fate of the antibody-forming cells of the splenic foci. Eur. J. Immunol. **26**, 444-448

Smith, K. G., Light, A., Nossal, G. J. and Tarlinton, D. M. (1997) The extent of affinity maturation differs between the memory and antibody-forming cell compartments in the primary immune response. EMBO J. **16**, 2996-3006

Snapper, C. M. (1990) The cellular and molecular biology of cytokine-directed murine Ig isotype production. In The human IgG subclasses: molecular analysis of structure, function and regulation (Shakib, F., ed.), Pergamon Press, Oxford

Snapper, C. M. and Finkelman, F. D. (1993) Chapter 22: Immunoglobulin class switching. In Fundamental Immunology (Paul, W. E., ed.), pp. 837-846, Raven Press, New York

Snounou, G., Jarra, W. and Preiser, P. R. (2000) Malaria multigene families: the price of chronicity. Parasitol. Today **16**, 28-30

Soares, I. S., da Cunha, M. G., Silva, M. N., Souza, J. M., Del Portillo, H. A. and Rodrigues, M. M. (1999) Longevity of naturally acquired antibody responses to the N- and C-terminal regions of *Plasmodium vivax* merozoite surface protein 1. Am. J. Trop. Med. Hyg. **60**, 357-363

Spencer Valero, L. M., Ogun, S. A., Fleck, S. L., Ling, I. T., Scott-Finnigan, T. J., Blackman, M. J. and Holder, A. A. (1998) Passive immunization with antibodies against

three distinct epitopes on *Plasmodium yoelii* merozoite surface protein 1 suppresses parasitemia. Infect. Immun. **66**, 3925-3930

Spitalny, G. L., Rivera-Ortiz, C. I. and Nussenzweig, R. S. (1976) *Plasmodium berghei*: the spleen in sporozoite-induced immunity to mouse malaria. Exp. Parasitol. **40**, 179-188.

Steiniger, B. and Barth. (2000) Microanatomy and function of the spleen

Stevenson, M. M. and Kraal, G. (1989) Histological changes in the spleen and liver of C57/BL6 and A/J mice during *Plasmodium chabaudi* AS infection. Exp. Mol. Pathol. **51**, 80-95

Stevenson, M. M. and Kraal, G. (1989) Histological changes in the spleen and liver of C57/BL6 and A/J mice during *Plasmodium chabaudi* AS infection. Exp. Mol. Pathol. **51**, 80-95

Stevenson, M. M. and Tam, M. F. (1993) Differential induction of helper T cell subsets during blood-stage *Plasmodium chabaudi* AS infection in resistant and susceptible mice. Clin. Exp. Immunol. **92**, 77-83

Strambachova-McBride, J. and Micklem, H. S. (1979) Immunosuppression in murine malaria. IV. The secondary response to bovine serum albumin. Parasite Immunol. **1**, 141-157

Su, X. Z., Heatwole, V. M., Wertheimer, S. P., Guinet, F., Herrfeldt, J. A., Peterson, D. S., Ravetch, J. A. and Wellems, T. E. (1995) The large diverse gene family var encodes proteins involved in cytoadherence and antigenic variation of *Plasmodium falciparum*-infected erythrocytes. Cell **82**, 89-100

Süss, G., Eichmann, K., Kury, E., Linke, A. and Langhorne, J. (1988) Roles of CD4- and CD8-bearing T lymphocytes in the immune response to the erythrocytic stages of *Plasmodium chabaudi*. Infect. Immun. **56**, 3081-3088

Sze, D. M., Toellner, K. M., Garcia de Vinuesa, C., Taylor, D. R. and MacLennan, I. C. (2000) Intrinsic constraint on plasmablast growth and extrinsic limits of plasma cell survival. J. Exp. Med. **192**, 813-821

Takahashi, Y., Dutta, P. R., Cerasoli, D. M. and Kelsoe, G. (1998) I*n situ* studies of the primary immune response to (4-hydroxy-3-nitrophenyl)acetyl. V. Affinity maturation develops in two stages of clonal selection. J. Exp. Med. **187**, 885-895

Tangye, S. G., Liu, Y. J., Aversa, G., Phillips, J. H. and de Vries, J. E. (1998) Identification of functional human splenic memory B cells by expression of CD148 and CD27. J. Exp. Med. **188**, 1691-1703

Tarlinton, D. M. and Smith, K. G. (2000) Dissecting affinity maturation: a model explaining selection of antibody-forming cells and memory B cells in the germinal centre. Immunol. Today **21**, 436-441

Taylor, P. R., Seixas, E., Walport, M. J., Langhorne, J. and Botto, M. (2001) Complement contributes to protective immunity against reinfection by *Plasmodium chabaudi chabaudi* parasites. Infect. Immun. **69**, 3853-3859

Taylor, R. R., Egan, A., McGuinness, D., Jepson, A., Adair, R., Drakely, C. and Riley, E. (1996) Selective recognition of malaria antigens by human serum antibodies is not genetically determined but demonstrates some features of clonal imprinting. Int. Immunol. **8**, 905-915

Taylor, R. R., Smith, D. B., Robinson, V. J., McBride, J. S. and Riley, E. M. (1995) Human antibody response to *Plasmodium falciparum* merozoite surface protein 2 is serogroup specific and predominantly of the immunoglobulin G3 subclass. Infect. Immun. **63**, 4382-4388

Tian, J. H., Miller, L. H., Kaslow, D. C., Ahlers, J., Good, M. F., Alling, D. W., Berzofsky, J. A. and Kumar, S. (1996) Genetic regulation of protective immune response in congenic strains of mice vaccinated with a subunit malaria vaccine. J. Immunol. **157**, 1176-1183

Tkachuk, M., Bolliger, S., Ryffel, B., Pluschke, G., Banks, T. A., Herren, S., Gisler, R. H. and Kosco-Vilbois, M. H. (1998) Crucial role of tumor necrosis factor receptor 1 expression on nonhematopoietic cells for B cell localization within the splenic white pulp. J. Exp. Med. **187**, 469-477

Toellner, K. M., Gulbranson-Judge, A., Taylor, D. R., Sze, D. M. and MacLennan, I. C. (1996) Immunoglobulin switch transcript production in vivo related to the site and time of antigen-specific B cell activation. J. Exp. Med. **183**, 2303-2312

Toellner, K. M., Luther, S. A., Sze, D. M., Choy, R. K., Taylor, D. R., MacLennan, I. C. and Acha-Orbea, H. (1998) T helper 1 (Th1) and Th2 characteristics start to develop

during T cell priming and are associated with an immediate ability to induce immunoglobulin class switching. J. Exp. Med. **187**, 1193-1204.

Trucco, C., Fernandez-Reyes, D., Howell, S., Stafford, W. H., Scott-Finnigan, T. J., Grainger, M., Ogun, S. A., Taylor, W. R. and Holder, A. A. (2001) The merozoite surface protein 6 gene codes for a 36 kDa protein associated with the *Plasmodium falciparum* merozoite surface protein-1 complex. Mol. Biochem. Parasitol. **112**, 91-101

Turk, J. L. (1973) Morphological changes in the thymus-dependent lymphoid system associated with pathological conditions in animals and man: their functional significance. Contemp. Top. Immunobiol. **2**, 137-150

Udhayakumar, V., Anyona, D., Kariuki, S., Shi, Y., Bloland, P., Branch, O., Weiss, W., Nahlen, B., Kaslow, D. and Lal, A. (1995) Identification of T and B cell epitopes recognized by humans in the C-terminal 42kDa domain of the *Plasmodium falciparum* merozoite surface protein 1. J. Immunol. **154**, 6022-6030

Unkeless, J. C. (1979) Characterization of a monoclonal antibody directed against mouse macrophage and lymphocyte Fc receptors. J. Exp. Med. **150**, 580-596

Urban, B. C. and Roberts, D. J. (2003) Inhibition of T cell function during malaria: implications for immunology and vaccinology. J. Exp. Med. **197**, 137-141

Urban, B. C., Ferguson, D. J., Pain, A., Willcox, N., Plebanski, M., Austyn, J. M. and Roberts, D. J. (1999) *Plasmodium falciparum*-infected erythrocytes modulate the maturation of dendritic cells. Nature **400**, 73-77

van der Heyde, H. C., Huszar, D., Woodhouse, C., Manning, D. D. and Weidanz, W. P. (1994) The resolution of acute malaria in a definitive model of B cell deficiency, the J_HD mouse. J. Immunol. **152**, 4557-4562

Vieira, P. and Rajewsky, K. (1990) Persistence of memory B cells in mice deprived of T cell help. Int. Immunol. **2**, 487-494

Voigt, I., Camacho, S. A., de Boer, B. A., Lipp, M., Forster, R. and Berek, C. (2000) CXCR5-deficient mice develop functional germinal centers in the splenic T cell zone. Eur. J. Immunol. **30**, 560-567

von der Weid, T., Honarvar, N. and Langhorne, J. (1996) Gene-targeted mice lacking B cells are unable to eliminate a blood stage malaria infection. J. Immunol. **156**, 2510-2516

Weibel, E. R. (1963) Principles and mehtods for the moprhometric study of the lung and other organs. Lab. Invest. **12**, 131-155

Weidanz, W. P. and Rank, R. G. (1975) Immunosuppressive effects of experimental infection with *Plasmodium gallinaceum*. Proc. Soc. Exp. Biol .Med. **148**, 725-728

Weiss, L. (1990) The spleen in malaria: the role of barrier cells. Immunol. Lett. **25**, 165-172

White, W. I., Evans, C. B. and Taylor, D. W. (1991) Antimalarial antibodies of the immunoglobulin G2a isotype modulate parasitemias in mice infected with *Plasmodium yoelii*. Infect. Immun. **59**, 3547-3554

Wipasa, J., Hirunpetcharat, C., Mahakunkijcharoen, Y., Xu, H., Elliott, S. and Good, M. F. (2002a) Identification of T cell epitopes on the 33-kDa fragment of *Plasmodium yoelii* merozoite surface protein 1 and their antibody-independent protective role in immunity to blood stage malaria. J. Immunol. **169**, 944-951

Wipasa, J., Xu, H., Makobongo, M., Gatton, M., Stowers, A. and Good, M. F. (2002b) Nature and specificity of the required protective immune response that develops postchallenge in mice vaccinated with the 19-kilodalton fragment of *Plasmodium yoelii* merozoite surface protein 1. Infect. Immun. **70**, 6013-6020

Wykes, M., Poudrier, J., Lindstedt, R. and Gray, D. (1998) Regulation of cytoplasmic, surface and soluble forms of CD40 ligand in mouse B cells. Eur. J. Immunol. **28**

Wyler, D. J. (1974) Letter: B-cell mitogen in hypergammaglobulinaemia in malaria and trypanosomiasis. Lancet **1**, 742

Wyler, D. J., Herrod, H. G. and Weinbaum, F. I. (1979) Response of sensitized and unsensitized human lymphocyte subpopulations to *Plasmodium falciparum* antigens. Infect. Immun. **24**, 106-110

Wyler, D. J., Miller, L. H. and Schmidt, L. H. (1977) Spleen function in quartan malaria (due to *Plasmodium inui*): evidence for both protective and suppressive roles in host defense. J. Infect. Dis. **135**, 86-93

Xu, H., Hodder, A. N., Yan, H., Crewther, P. E., Anders, R. F. and Good, M. F. (2000) CD4+ T cells acting independently of antibody contribute to protective immunity to

Plasmodium chabaudi infection after apical membrane antigen 1 immunization. J Immunol **165**, 389-396.

Yap, G. S. and Stevenson, M. M. (1994) Differential requirements for an intact spleen in induction and expression of B-cell-dependent immunity to *Plasmodium chabaudi* AS. Infect. Immun. **62**, 4219-4225

Young, F., Ardman, B., Shinkai, Y., Lansford, R., Blackwell, T. K., Mendelsohn, M., Rolink, A., Melchers, F. and Alt, F. W. (1994) Influence of immunoglobulin heavy- and light-chain expression on B-cell differentiation. Genes Dev. **8**, 1043-1057

Ziegner, M., Steinhauser, G. and Berek, C. (1994) Development of antibody diversity in single germinal centers: selective expansion of high-affinity variants. Eur. J. Immunol. **24**, 2393-2400